UNIVERSITY OF SOUTHAMPTON

REGULATION OF THE SYNTHESIS OF TISSUE INHIBITORS OF METALLOPROTEINASE-1 AND –2 BY HEPATIC AND PANCREATIC STELLATE CELLS

Dr Peter Raymond McCrudden

B.Sc.(Hons) MBBS FRCP

Submitted for the degree of MD

Faculty of Medicine, Health and Biological Sciences

June 2010

For Ute, Nicolas, Katia and India

UNIVERSITY OF SOUTHAMPTON

ABSTRACT

FACULTY OF MEDICINE, HEALTH AND LIFE SCIENCES (MHLS)
SCHOOL OF MEDICINE
DIVISION OF INFECTION, INFLAMMATION AND IMMUNITY

Doctor of Medicine

REGULATION OF THE SYNTHESIS OF TISSUE INHIBITORS OF METALLOPROTEINASE-1 AND –2 BY HEPATIC AND PANCREATIC STELLATE

By Dr Peter Raymond McCrudden

Hepatic stellate cells (HSC) play a central role in fibrosis development by production of extracellular matrix and also by secretion of matrix metalloproteinases (MMPs) and Tissue inhibitors of metalloproteinases (TIMPs) including TIMP-2 and MMP-2. TIMP-2 has been shown to interact with Gelatinase A in conjunction with MT1-MMP (MMP-14). TIMP-2 has been traditionally considered to be constitutively expressed. There is some evidence that TIMP-2 expression is slightly enhanced in fibrotic disease and activation in tissue culture. Little is known in terms of TIMP-2 expression in the recently described pancreatic stellate cells (PSC). HSC were cultured on plastic having been isolated from rat and human liver resections. After culture on plastic northern analysis was performed for TIMP-2 mRNA expression. TIMP-2 promoter activity was examined in rat pancreatic stellate cells (PSC) and rat hepatic stellate cells. Early work led to subcloning the promoter into a different vector though subsequent promoter studies were unsuccessful. In vivo work in immunohistochemistry studies suggest there is increased TIMP-2 expression in evaluation of rat pancreas and liver in addition to human liver and pancreas specimens. By ribonuclease protection assay TIMP-2 was noted to be upregulated in human fibrotic liver compared to normal human liver tissue. In conclusion there is some evidence that TIMP-2 regulation may be altered in fibrotic liver states as well as in pancreatic inflammatory disease.

LIST OF CONTENTS

LIST OF FIGURES

LIST OF TABLES

ACKNOWLEDGEMENTS

During the three years spent doing the work in this thesis there are a number people who merit acknowledgment. Firstly, I want to thank Professor John Iredale and Professor Derek Mann for their expert supervision throughout my period of research in the liver unit. Secondly, I want to thank Professor Michael Arthur his help, advice and support. Thirdly, I would like to thank and acknowledge the help and hard work of Julie Trim & Marianna Gaca who both helped supervise me on a day to day level with certain techniques such as Northern Blotting, DNA sequencing, transfection techniques etc. Fourthly Penny Johnson for her help in the histopathology and staining laboratory. Special thanks must go to Dr Christopher Benyon for unflinching support in my delayed write up.

This work was also supported by a number of collaborations. Firstly, Professor Yves De Klerck who supplied the promoter constructs; Dr Jill Normal of University College London for work in hypoxia. Secondly, Professor John Primrose of Southampton University Surgical Unit and Dr Harry Milward Sadler of the Southampton University Histopathology department for their help in the provision of human liver specimens for cell extractions, and Dr Adrian Bateman (Southampton University Hospitals Trust) and Dr Simon Rasbridge (Royal Bournemouth and Christchurch Foundation Trust) for review of histology specimens. Finally, I would also like to thank the Wellcome Research Group, the Royal College of Physicians (BUPA fellowship) and the Wessex Medical Liver Trust for all their generous sponsorship.

DECLARATION

The immunohistochemistry work was only possible through the meticulous supervision and hard work by Mrs Penelope Johnson. The work on the CCL_4 recovery model in rats was carried out be Prof John Iredale. Grading and assessment of the slides for immunohistochemical assessment was performed by Professor John Iredale and Dr Adrian Batemen. Digital photography pictures of my immunostaining on pancreatic tissue was provided by Dr Fanny Shek as were her methods on pancreatic cell isolation.

I declare that the work presented in the thesis is wholly mine except as acknowledged above. This work was carried out while registered as a postgraduate candidate in University of Southampton.

During and after the completion of the research work I had an invited review published on Hepatic stellate cells (1) and was a secondary author on subsequent papers (2;3).

LIST OF ABBREVIATIONS

αSMA	alpha smooth muscle actin
AP-1	activator protein-1
Bcl-2	B cell lymphoma-2
bp	base pairs
BTEB1	basic transcription element binding protein 1
CCL_4	carbon tetrachloride-4
CCN2	cysteine-rich connective tissue growth factor
cDNA	complimentary DNA
CTGF	connective tissue growth factor;
DDRs	discoidin domain receptors
DDR-2	discoidin domain receptor–2
DEPC	diethyl pyrocarbonate
DI water	de-ionised water
DMEM	Dulbecco Modified Eagles' Media
DNA	deoxyribonucleic acid
DNase	deoxyribonuclease
E coli	Escherichia coli
EC	endothelial cell
ECE	endothelin converting enzyme
ECM	extracellular matrix
EGF	endothelial cell growth factor
ESB	electrophoresis sample buffer
ET1	endothelin-1
ETB	Endothelin-1 receptor subtype B
FGF	fibroblast growth factor
g	grams
GFAP	glial fibrillary acid protein
GFAP	glial fibrillary acidic protein
HBSS	Hanks Balanced Salt Solution (+/- Calcium)
HBV	hepatitis B Virus
HCV	hepatitis C Virus
HGF	hepatocyte growth factor
HSC	hepatic stellate cell

ICAM-1	adhesion molecule ICAM-1
IFNγ	interferon gamma
IGF	insulin-like growth factor
IGF-1	insulin like growth factor-1
IL-1	interleukin-1
IL-10	interleukin-10
IL-1α	interleukin-1-alpha
IL-6	interleukin-6
IL-8	interleukin-8
kb	kilobases
KC	Kupffer cell
kDa	kilo Dalton
KLF	krupel-like factor
KLF6	krupel-like factor zinc finger gene
l	litres
LB	Luria Bertani medium or LB broth
MAPK	mitogen activated protein kinase
MCP-1	monocyte chemotactic peptide
mg	milligrams
min	minute
ml	millilitres
MLP-1	macrophage inflammatory protein-1
MMP	matrix metalloproteinase
MMP-1	matrix metalloproteinase-1
MMP-2	matrix metalloproteinase-2 (gelatinase)
MOPS	morpholino propanoic-sulfonic acid
mRNA	messenger ribonucleic acid
MT1-MMP	membrane type 1 matrix metalloproteinase
NF κB	nuclear factor kappa B
ng	nanograms
NGF	nerve growth factor
NKT cells	natural killer T cells
nm	nanometres
OD	optical density

PBS	phosphate buffered saline
PCR	polymerase chain reaction
PDGF	platelet derived growth factor
PEA3	an ETS family transcription factor
pM	pico Moles
PSC	pancreatic stellate cell
PSG	Penicillin, Streptomycin & Gentamicin
RNA	ribonucleic acid
RNase	ribonuclease
ROI	reactive oxygen intermediates
rpm	revolutions per minute
RTK	receptor tyrosine kinase
SDS PAGE	sodium dodecyl sulphate poly acrylamide gel
SMA	smooth muscle actin
Sp1	Sp1 human transcription factor, (1^{st} member of the KLF family)
STAT	signal transducer and activator of transcription
TGFα	transforming growth factor α (alpha)
TGFβ	transforming growth factor β (beta)
TGFβ1	transforming growth factor beta-1
TIMP	tissue inhibitor of metalloproteinase
TIMP-1	tissue inhibitor of metalloproteinase-1
TIMP-2	tissue inhibitor of metalloproteinase-2
TIMP-3	tissue inhibitor of metalloproteinase-3
TIMP-4	tissue inhibitor of metalloproteinase-4
TNF	tumour necrosis Factor
UV	ultra violet light
TNFα	Tumour necrosis factor alpha
U	units
UPA	Urokinase plasminogen activator
v/v	volume for volume
VEGF	vascular endothelial cell growth factor
w/v	weight per volume
μg	micrograms

CHAPTER 1
INTRODUCTION

1. Introduction

1.1 Background to liver disease and hepatic fibrosis

Chronic injury, which can lead to fibrosis in the liver, occurs in response to a variety of insults including viral hepatitis (especially hepatitis B and C), alcohol abuse, drugs, metabolic diseases due to overload of iron or copper, autoimmune attack of hepatocytes (autoimmune hepatitis) or of the bile duct (primary biliary cirrhosis), and finally to certain congenital abnormalities (4-6).

The injury is typically present months or years before a significant scar develops although the time course may be accelerated in congenital liver disease. Evidence is accumulating that liver fibrosis is reversible, whereas cirrhosis, the end stage consequence of fibrosis, has until recently been held to be generally irreversible.

Research into the understanding of fibrosis is therefore focussed primarily on events that lead to the early accumulation of scar in the hope of identifying therapeutic targets to slow its progression. The prevalence of chronic liver insults imposes a significant health care burden. For example, the prevalence of hepatitis C virus (HCV) infection in the United States is estimated at 1.8% of the country's population (an estimated 3.9 million persons infected nationwide) (7)**;** an estimated 250 million people are infected worldwide with hepatitis B virus (HBV) and here in the United Kingdom 6,000 deaths annually are attributable to liver cirrhosis (8;9).

Hepatic fibrogenesis is proving to be an important biological and clinical context for emerging concepts in molecular biochemistry that is relevant for many other tissues.

1.2 Anatomy of the liver

Positioned beneath the right hemi-diaphragm the classical division of the large right lobe and small left lobe bears no relation to the true functional division on the basis of blood supply into almost equal right and left lobes. The liver has a dual blood supply from the hepatic artery, which is usually a branch from the coeliac axis and from the portal vein formed from the confluence of the mesenteric and splenic veins. The hepatic artery supplies 25% of the

blood supply but 50% of the oxygen; the remainder is delivered by the low-pressure portal supply.

At the microanatomical level the liver essentially consists of a series of channels or sinusoids, running between plates of hepatocytes. These are lined by endothelial cells, which contain unusually large fenestration, allowing the sinusoid part of each hepatocyte surface to have free access to almost all the constituents in plasma. Hepatic stellate cells and Kupffer cells are also present in the sinusoids. Biliary canaliculi form between the contiguous surfaces of the hepatocytes, and here, and on the sinusoid surface, there are extensive microvilli in the cell membrane to increase the capacity for transmembrane transfer. Branches of the hepatic artery, portal vein and bile ducts within the liver are carried in portal tracts. The smallest of these, carrying terminal branches, supply groups of sinusoids, which together form a functional unit, the acinus. Blood from each acinus then passes into a number of different efferent veins (Figure 1.1).

Figure 1.1 (a-c) structure of the liver sinusoid

(ADAPTED FROM (10)

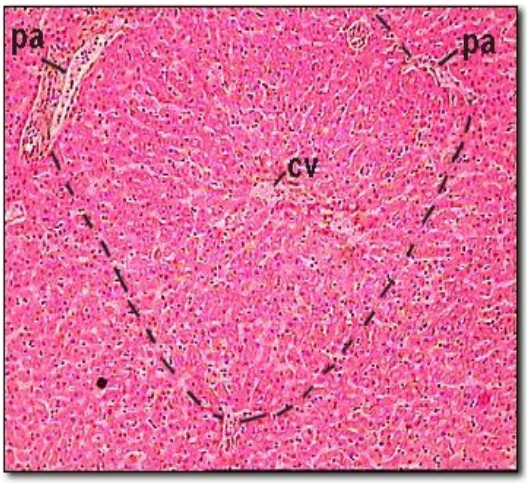

Figure 1. 1a Low power view of human liver, pa= portal space containing Portal venule, bile ductile and portal venule CV=central vein

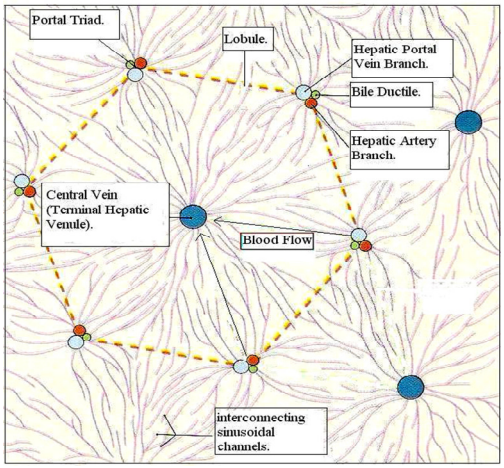

Figure 1.1b Schematic diagram of the liver acinus. Blood passes from hepatic portal vein (light blue) and hepatic artery (red) towards a central vein (darker blue).

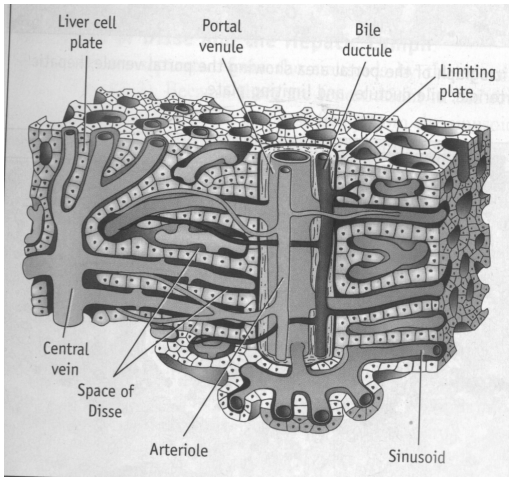

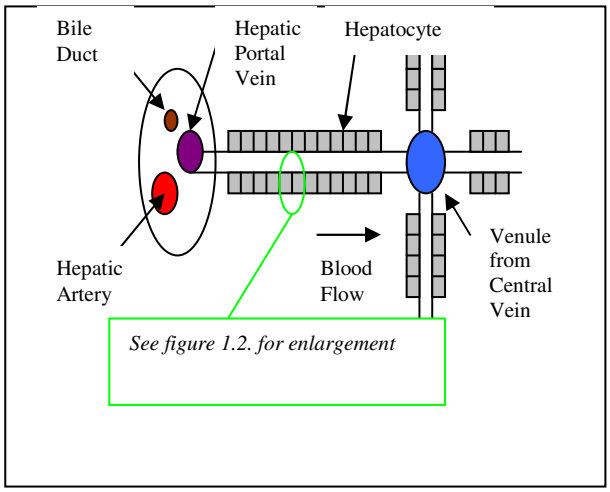

Figure 1.1c Hepatocytes are arranged in a 'sheet' like manner, radiated from a central vein located centrally in every lobule.

1.3 Structure of the normal liver sinusoid

Traditionally the basic unit of the liver structure has been the lobule. This is based on anatomical criteria, indeed in some species eg the pig, there is a distinct fibrous capsule surrounding each lobule. It is defined as the parenchyma surrounding a central vein, bordered peripherally by 3-6 portal tracts (Figure 1.1a-c). This does not describe the functional unit of the liver, which is the acinus. The acinus is defined as the parenchymal mass supplied by a single terminal portal tract (11). Blood flows from the portal vein and hepatic artery into the sinusoids from which the surrounding parenchyma is supplied. Blood then drains into the peripheral efferent veins (the central veins of the lobule) thence to the hepatic artery. One efferent vein supplies several acini. The hepatocytes of the acinus can be divided into 3 zones, these reflect both heterogeneity of the hepatocyte function, and pattern of injury in disease (12). Zone 1 hepatocytes are closest to the portal tracts and zone 3 to the efferent vein.

The sinusoids are wide vascular channels that have a unique structure. This is believed to derive from the necessity to allow efficient and controlled interaction of substances between the blood and the hepatocytes. The sinusoid is lined by a specialized fenestrated endothelium. Kupffer cells (tissue specific hepatic macrophages) are distributed sporadically through the sinusoid, but are most dense peripherally (13). These cells play a central role in host defence; they are phagocytic and have receptors for endotoxin. Pit cells are similarly distributed and are granular lymphocytes with natural killer activity. Between the endothelium and the palisades of hepatocytes lies the 'space of Disse'. This term is in some respects a misnomer because although there is no electron dense basement membrane it contains a loosely woven matrix consisting of types I, III and IV collagens, lamins, proteoglycans and fibronectin, i.e. the components of a basement membrane-like matrix (14-19). In addition the hepatic lipocytes are located within the Space of Disse, and may project into the recess between adjacent hepatocytes (20;21). When visualized in 3 dimensions HSC can be considered to encircle the sinusoid with cellular processes (22). The role of the HSC as a source of matrix components and a regulator of matrix turnover will be considered below. There is accumulating evidence that the normal basement membrane-like matrix within the space of Disse is important in determining the phenotype of these sinusoidal cells (23-26). The portal tracts consist of a stroma rich in type I and III collagen that is in continuation with the liver

capsule (27). The vascular bundles contain lymphatics and nerves and are the only site of fibroblasts in the normal liver (cf lipocyte activation below) (28).

1.4 The extracellular matrix of normal and diseased liver

The extracellular matrix (ECM) is the insoluble substance of the mesenchyme and basement membrane matrices. ECM is tissue specific and is important in tissue structure, repair and wound healing. The ECM has traditionally been viewed as an inert tissue scaffolding providing structural support for tissue but recently this view has been challenged by the demonstration of complex cell matrix interactions which will be discussed below. On the basis of this evidence ECM is now considered to be a dynamic modulator of tissue phenotype and function in addition to its structural role. During the process of wound repair the composition of ECM becomes altered to fulfill repair needs. In certain situations matrix synthesis is accelerated leading to accumulation of matrix with associated changes in relative composition. In the liver this results from chronic injury in response to diverse aetiologies such as infection (hepatitis B and C, human immunodeficiency coinfection with hepatitis C etc) and toxins (eg alcohol) etc. Liver fibrosis can be viewed as the final common pathway of most chronic liver disease. The accumulation of matrix leads to structural changes and to changes in cell matrix interactions giving rise to the disease picture so familiar to clinicians. The changes of ECM seen in liver injury and fibrosis will be described. Basic changes are depicted in Figure 1.2

Figure 1.2 normal and fibrotic liver: how the distribution of collagen changes in fibrosis

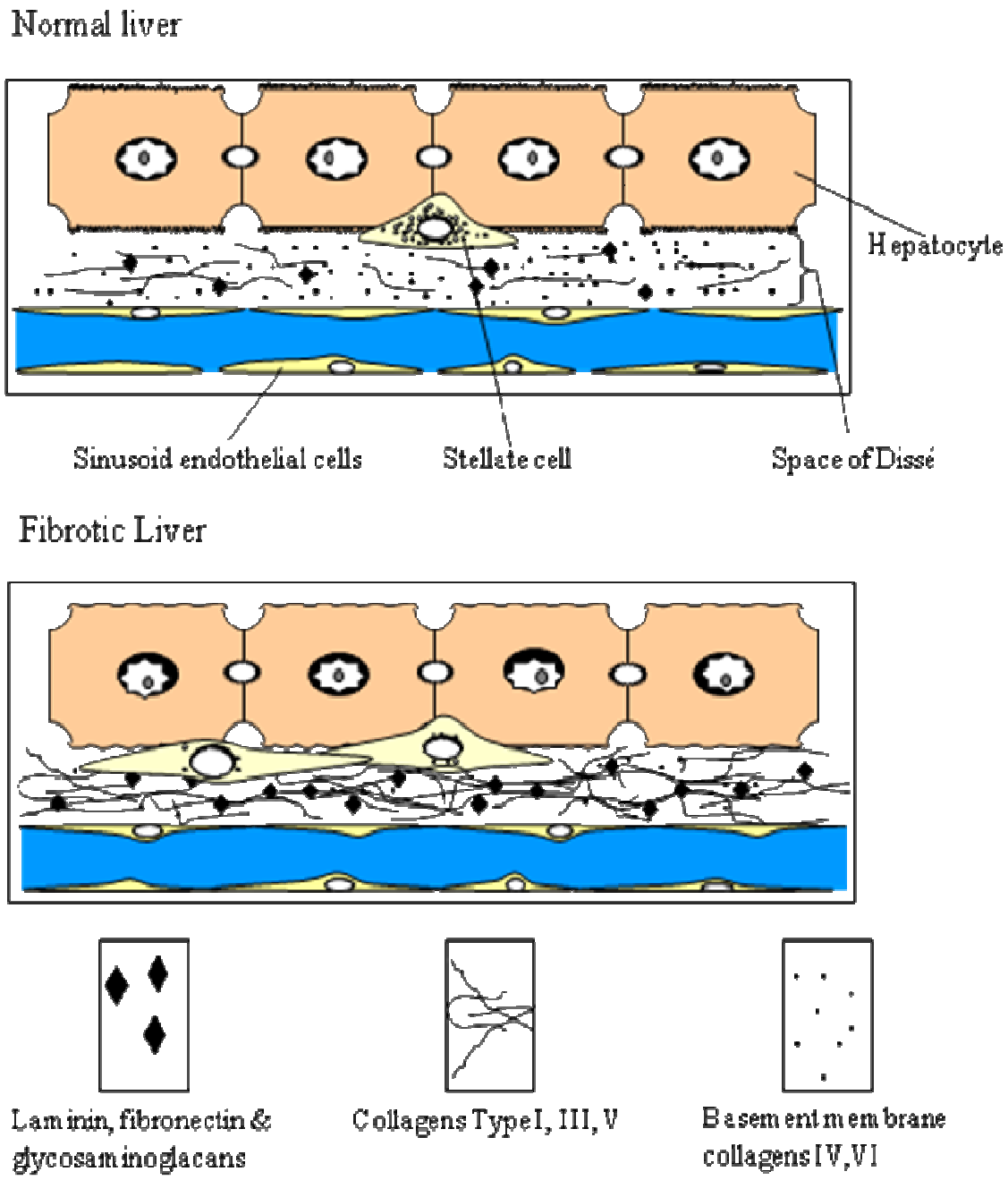

Figure 1.2 Comparisons between normal and fibrotic liver demonstrate differential changes in collagen especially collagens types I, III and V. (This Powerpoint slide was donated by Dr David Smart).

In this section components of the liver ECM (collagens, glycoproteins and proteoglycans) will be described.

1.4.1 Collagens are a group of proteins that are widely distributed through the body representing about one third of the total protein (29). In the normal liver collagens account for 5-10% of the total protein, however this proportion may increase to as much as 50% in advanced fibrosis/cirrhosis. A total of 14 collagens have been described to date, of these collagens I, III, IV, V and VI have been identified in the liver (29). Structurally collagens are composed of a triplet of similar or identified polypeptide subunits. These polypeptides are folded into a left handed triple helix, permitted by the presence of the repetitive amino acid sequence (Gly-X-Y)n where one third of the X and Y positions are hydroxyproline and proline respectively (30;31). This structure allows helix formation by virtue of the comparatively small hydrogen side chains of glycine which permits folding. The triple helix is subjected to post translational modifications before secretion. Classification of the collagen macromolecules is made according to their resulting configuration after assembly post secretion. Banded collagen (fibrillar or interstitial) are so termed because they are arranged in quarter staggered overlap, side to side. This alignment results in the presence of alternate light and dark bands on electron microscopy. Types I, III and V are fibrillar collagens. This structure confers a high strength to fibrillar collagens, which comprise the body's major structural proteins. The predominant collagens in both normal and fibrotic liver are types I and III (32;33), however there are changes in both the amount and relative composition such that type I collagen accounts for over 70% of total liver collagen which is increased at least six fold in fibrotic liver compared to normal (29;32;33). This reflects the change in collagen expression which occurs as HSC becomes activated. The biosynthesis of types I and III collagens are similar and relatively well understood, less is known for type V.

1.4.2 Type I collagen is normally formed from two alpha-1 chains and a single alpha-2 chain. Following translation, the peptides are subjected to considerable post translational modification. Within the endoplasmic reticulum lysine and proline residues are hydroxylated. Hydroxylases which mediate this are themselves up regulated in experimental fibrosis (34;35). At this stage, hydroxy-lysine residues become glycosylated and inter-chain cross links are formed. Collagens are secreted from an insoluble cell membrane (36) bundles and fibres are formed by the serial fusion of cell membrane compartments, which may arise from more than one cell (37). The length and alignment of collagens may result from the sequence

of terminal pro peptides and other non-helical domain cleavage and degradation (29;38;39). After assembly, further tensile strength is conferred on fibrils by the formation of cross links (29).

1.4.3 Type V collagen has a broadly similar structure to types I and III. It is not subjected to the same level of extracellular processing and retains a non-helical globular unit (29). Type V collagen has a broadly similar structure to types I and III. It is not subjected to the same level of extracellular processing and retains a non-helical globular unit (29). The function of type V collagen may be as a nidus for fibril formation (29). The presence of heterotrophic collagen fibrils containing types I and II have been demonstrated in the liver (40). The expression of the gene for collagen is regulated by a variety of cytokines. Transforming growth factor beta (TGFβ) up regulates mRNA expression (41-43), and stabilizes procollagen mRNA (44). The cytokine has been demonstrated to be a key mediator in several fibrotic disorders and there is accumulating evidence of a central role in liver fibrosis. Both acetaldehyde (45) and enhanced HSC activation increase expression of procollagen I.

1.4.4 Collagen expression is down regulated by interferon-gamma (46) and dexamethasone (47;48). Two other important collagens are present in normal liver: types IV and VI both of which are non-fibril forming. They represent 1 and 0.1% of total liver collagen respectively. Collagen IV and VI are more flexible than I and III by virtue of their relatively large non-helical domain and the interruptions of the triplet sequence through the length of the molecule (29). Type IV collagen is composed of three polypeptide chains with a globular N-terminal domain and carboxy terminals which are not cleared during processing. These moieties are important in the assembly and structure of the basement membrane matrix, for which type IV collagen forms the major structural protein (29). Type IV collagen will form a three dimensional tetrameric framework, via disulphide bonding between adjacent carboxy terminal and hydrophobic grouping of the globular amino termini (49-51). Lateral associations of type IV collagen have been demonstrated in human and murine tissues. Onto this framework, other basement membrane components become laid down. Indeed, type IV collagen incorporates structural features which mediate interactions with other matrix components (proteoglycans and glycoproteins) and cell receptors (52). Type IV collagen is found in small quantities in the space of Disse. Although fibrosis is associated with an increase in the rate of deposition of type IV collagen, it remains a minor component, in comparison to the fibrillar collagens. Type VI collagen is not a component of basement membrane. Like type IV it has

large non-helical domains, and has a dumb bell shape of two globular regions joined by a short helical domain (29). It has repetitive A domains of von Willebrand factor which mediate homotypic assembly via lateral alignment into macromolecule chains, and heterotypic associations with fibrillar collagens (53). When aggregated it is stabilized by the formation of disulphide bonds. In addition, the presence of the Arg-Gly-Asp sequence in the helical region suggests that this component may have a significant role in integrin mediated cell matrix interaction (54). As type VI collagen is found in greatest abundance in close proximity to blood vessels it may have a role in anchoring the vessel to its surrounding matrix. Type IV collagen is found in the space of Disse in health and its deposition is upregulated in fibrosis (29).

Glycoproteins are a heterogeneous group of molecules which comprise, by weight, the major substance of the ECM, in both health and fibrosis. They are complex molecules which sub serves as cytokine binding reservoirs and cell receptor ligands in addition to fulfilling structural functions. They comprise laminin, entactin, fibronectin, tenascin, undulin and elastin.

Laminin is composed of three polypeptide chains that inter link to form an asymmetric cross structure (29;54). There is some heterogeneity of laminin as a result in variation of chain length and content, with specific tissue isoforms (52;55). Laminin has, together with other matrix components, biological activity. In the case of specific cell receptor sequences the interaction may be important in the maintenance of differentiated parenchymal cell function. Eight cell adhesive recognition sequences that bind to cellular receptors, including hepatocytes (56) have been described in laminin (54). Binding sites also exist for other matrix components such as type IV collagen, entactin and heparan sulphate proteoglycan (29). Laminin also contains 25 endothelial cell growth factor (EGF) like repeats (57) which may become biologically active during degradation.

Entactin, also known as nidogen, is a ubiquitous component of basement membranes. It is a 150 kilo Dalton (kDa) glycoprotein which is dumb-bell shaped (29) and binds, non-covalently to lamina to type IV collagen (29). Entactin is expressed by activated HSCs (53). Fibronectins are V shaped proteins, formed of two 220kDa subunits (56). They exist in two major forms in the body, the plasma and basement membrane types, derived from alternative splicing of the single fibronectin gene (58). Fibronectins bind, via specific domains, to

fibrillar collagens, heparin, fibrinogen, syndecan and integrin tenascin receptors (29). Fibronectins are important in wound healing and clot organization (29). Their deposition is increased in liver injury with a concomitant change towards increased proportion of cellular fibronectin (29). Fibronectin may also be important in cell matrix interactions that maintain a differential cell phenotype.

Tenascins are six armed proteins (54). Within each arm there are EGF-like and fibronectin-like domains (54;59). Tenascin appear to be important in interfering with cell fibronectin interactions. They are expressed transiently during certain stages of development and injury (54). In addition certain isoforms, generated by alternative splicing, are expressed in specific tissues or developmental stages (54;60). By interfering with cell adhesion to fibronectin, tenascin like thrombospondin and osteonectin are part of a group of glycoproteins which modulate cell-matrix interactions to enhance cellular motility (54). Tenascin has been localized to the margins of healing wounds, and the space of Disse during hepatic fibrosis (61).

Undulin shares some sequence homology with tenascin, and is present in matrix when tenascin is absent (62). It is found in association with type I collagen fibres, and binds to collagens I, III, V and VI (29), in addition to cell membrane receptors. For those reasons it is believed that undulin is important in the maintenance of collagen (and matrix) structure (29). The distribution of undulin within the liver is in association with collagen bundles in the portal tract, and single collagen filaments in the space of Disse.

Whilst elastin is a prominent component of cirrhotic matrix (63) its role in the liver matrix is undetermined.

1.5 Identification of Hepatic Stellate Cells (HSCs) as the primary source of Extracellular Matrix

Hepatic Stellate Cells (HSCs) were first recognized in 1876 by the anatomist von Kupffer. He described star shaped cells identified using a gold chloride staining procedure (64). They were described as phagocytic and their cytoplasmic droplets were thought to be due to fatty degeneration (65). Ito described in 1952 a population of cells distinct from liver macrophage cells (Kupffer cells); these cells were termed Ito cells (66). In 1980 Wake noted that the cells would convert glycogen to lipid rather than acquire lipid by phagocytosis – he then termed them "fat storing cells" (65). (Figure 1.3)

Figure 1.3The Hepatic Sinusoids in Cross section and changes in the sinusoid during fibrotic liver injury

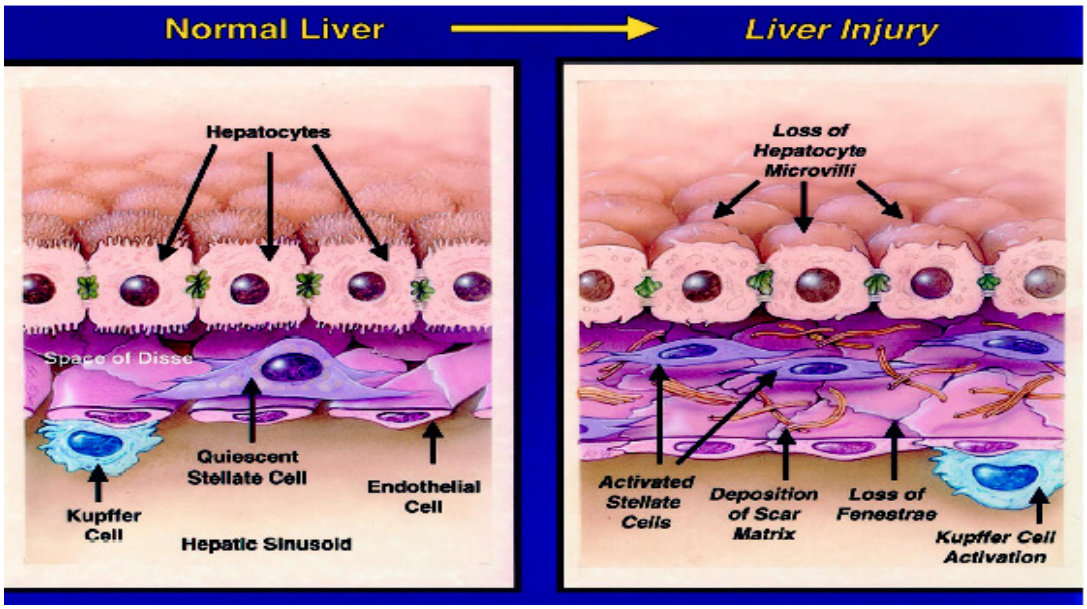

Figure 1.3: The changes that occur in the subepithelial space of Disse include changes in cellular and matrix components. HSC activation to a fibrogenic phenotype leads to accumulation of scar tissue (predominantly fibrillar collagens). This change in extracellular matrix contributes to alterations in other cell types including hepatocyte necrosis, the loss of hepatocyte microvilli and endothelial fenestrae. Overall the change from a low density to higher density matrix in the space of Disse and the loss of hepatocyte villi and endothelial fenestrae compromise molecular exchange between hepatocytes and sinusoidal lumen causing deterioration in liver functions in toto. Figure taken from (67).

Figure 1.4 Hepatic stellate cell activation

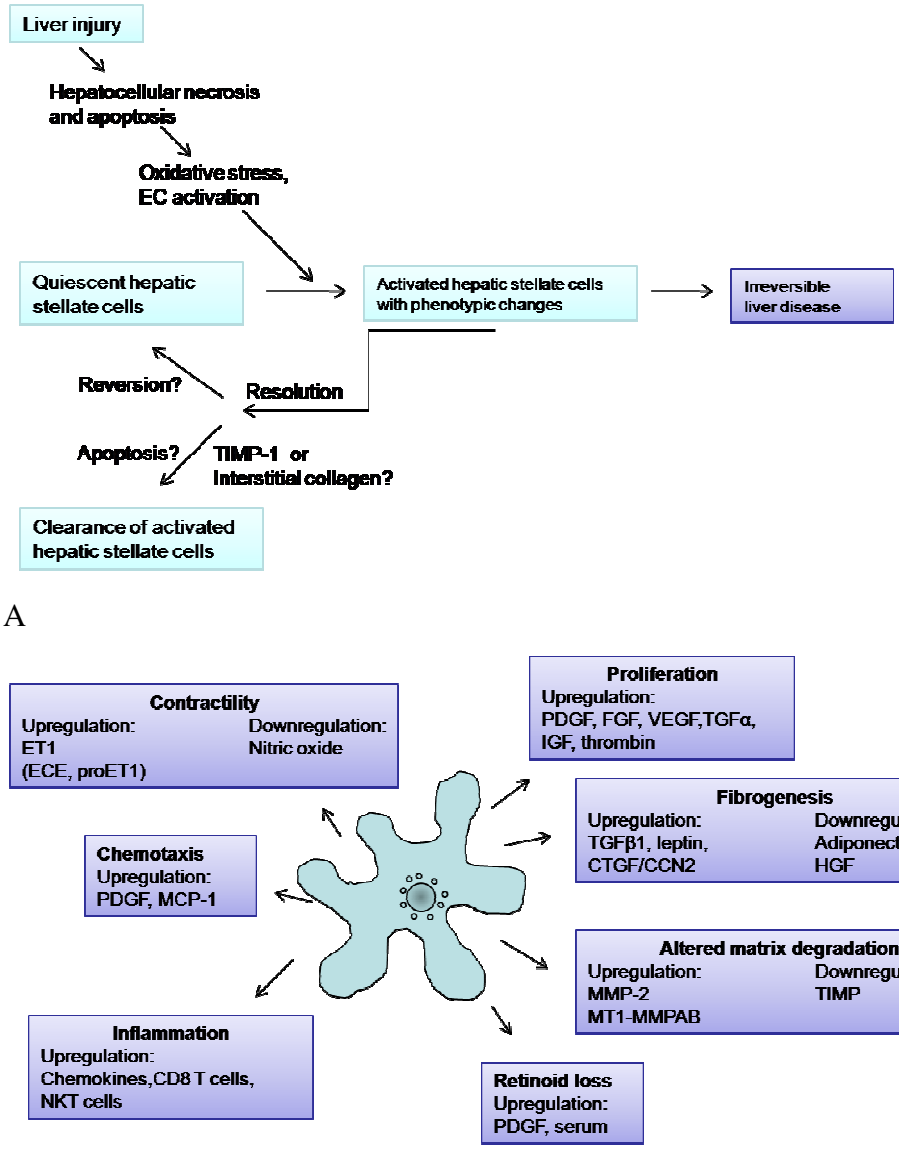

Figure 1.4 Hepatic stellate cell activation. (**A**) As a result of liver injury, quiescent vitamin-A-rich hepatic stellate cells undergo 'activation' towards proliferative, fibrogenic and contractile myofibroblasts. During resolution of liver injury, hepatic stellate cells might revert to a quiescent phenotype and/or be selectively cleared by apoptosis. (**B**) The major phenotypic changes seen after activation of hepatic stellate cells are illustrated, along with the key mediators involved (both up regulators and down regulators). CCN2, cysteine-rich connective tissue growth factor; CTGF, connective tissue growth factor; EC, endothelial cell; ECE, endothelin converting enzyme; ET1, endothelin-1; FGF, fibroblast growth factor; HGF, hepatocyte growth factor; IGF, insulin-like growth factor; MCP-1, monocyte chemotactic peptide; MMP-2, matrix metalloproteinase-2; MT1-MMP, membrane type 1 matrix metalloproteinase; NKT cells, natural killer T cells; PDGF, platelet-derived growth factor; VEGF, vascular endothelial cell growth factor; TGFα, transforming growth factor α; TGFβ, transforming growth factor β; TIMP, tissue inhibitor of metalloproteinase.

1.6 Cellular sources of Extracellular Matrix (ECM)

HSC comprise up to 15% of the total number of resident liver cells (5;67). In normal liver they are the principal storage site for retinoids (68;69). Stellate cells constitute a heterogenous group of cells that are functionally and anatomically similar but different in their expression of cytoskeletal filaments, their retinoid context, and their potential for ECM production (70;71). Studies using electron microscopy, immunohistochemistry, *in situ* hybridization and cell isolation techniques have established the stellate cells as the key effector cell in hepatic fibrogenesis. Figure 1.4 above summarizes some of the features of stellate cell activation. With progressive fibrosis HSCs proliferate and transform into a cell with a prominent rough endoplasmic reticulum. This facility to increase protein production prompted the suggestion that HSCs might be the source of the concurrently observed increase in collagen production seen in fibrosis with repeated liver injury (72;73). Stellate cells become spindle shaped with microfilament bundles with a typical appearance of alpha smooth muscle actin (αSMA) taking on a myofibroblast appearance, a phenotype associated in other cells with matrix production (64;74;75). The synthesis of collagen was originally thought to be from the liver parenchymal cells (hepatocytes) but in 1989 *in situ* hybridization studies on an experimental model of liver fibrosis confirmed that type I, type III and type IV procollagen expression takes place predominantly in non parenchymal cells (76). With immunocytochemistry the intracellular collagens fibronectin and laminin were located in HSCs (77).

Subsequently different liver cells types were examined for their respective potential in matrix production (78) lending further evidence that HSC are the cells responsible for matrix production in the liver. Recent studies have underscored the heterogeneity of mesenchymal populations in liver ranging from classic stellate cells to portal fibroblasts (79), with the variable expression of neural (80), angiogenic (81), contractile (75), and even bone marrow derived markers (82). Moreover, experimental genetic 'marking' of stellate cells by expressing fluorescent proteins downstream of either fibrogenic or contractile gene promoters, illustrates the plasticity of fibrogenic cell populations *in vivo* (83). In view of this capacity for 'trans differentiation' between different mesenchymal cell lineages and possibly even epithelial cells (84), the key issue is not necessarily where fibrogenic cells arise from, but rather whether they express target molecules such as receptors or cytokines in sufficient concentrations *in vivo* to merit their targeting by diagnostic agents or anti-fibrotic compounds.

Freshly isolated HSCs contain type III and IV collagen and laminin transcripts but no type I collagen or fibronectin (24;85). In contrast cultured HSCs contain high levels of type I, III and IV collagen and fibronectin transcripts (85). The mRNA transcripts of collagen purified from parenchymal cells almost certainly result from HSC contamination (86). Endothelial cells contain small amounts of type IV collagen mRNA; Kupffer cells do not contain any of these transcripts (78).

HSCs are the principal source of (non collagenous) glycosaminoglycans and proteoglycans in normal and fibrotic liver (87). Variations in synthesis of these proteins are observed between normal and fibrotic liver, and between fresh and cultured HSCs (87).

1.7 Cellular features of Quiescent HSCs

The phenotypic features of the hepatic stellate cell differ according to the level of activation. In normal liver HSCs make up 5-15% of the total liver cell population (88;89). HSCs lie in the space of Disse between the specialized hepatic sinusoidal endothelium and the palisades of hepatocytes (90). Recent work on their embryological origin suggests that they are neural crest derived because they express glial fibrillary acidic protein, nestin and synaptophysin (91). A neural crest origin is further supported by studies in rat neural crest stem cells which differentiate into myofibroblasts that express smooth muscle alpha actin, a marker of activated stellate cells (92).

These observations raise the possibility of using neural crest – specific promoters to drive transgene expression selectively in stellate cells *in vivo* and the prospect of reconstituting stellate cells from the neural crest precursor as part of efforts to repopulate liver.

The perivascular orientation and long cytoplasmic processes of stellate cells facilitate their interactions with neighbouring cell types. These processes are adjacent to hepatic nerves, which can respond to alpha-adrenergic stimulation with an influx of cytosolic calcium and release of osmolytes (93).

Ultrastructurally, HSCs are characterized by the presence of cytoplasmic fat droplets, well developed rough endoplasmic reticulum, a Golgi complex, multi-vesicular bodies, one or two

centrioles and few rather small lysosomes. These lysosomes are sometimes associated with fat droplets. Fat storing cells are the main storage sites for retinal esters (vitamin A) in the mammalian body (94).

The size and quantity of lipid droplets vary between individual HSCs (87;95). As well as retinol esters, the lipid droplets contain smaller quantities of triglycerides, cholesterol esters, cholesterol and phospholipid (95).

1.8 Cellular features of HSC activation

Following liver injury of any aetiology HSCs undergo a process known as "activation"; which is a term denoting the transition of quiescent cells into proliferative , fibrogenic and contractile myofibroblasts (96-98). Sources of mediators causing injury may be circulating (i.e. endocrine), transferred between cells (paracrine) or act within the same cell (i.e. autocrine). In particular, oxidant-stress-mediated necrosis leading to stellate cell activation may underlie various liver diseases, including hemochromatosis, alcoholic liver disease, viral hepatitis and non-alcoholic steatohepatitis (NASH) (99-101). See Table 1.1

Table 1.1 The characteristics of quiescent and activated HSCs

	Quiescent HSCs (qHSCs) in culture	Activated HSCs (aHSCs) in culture
Morphology	Rounded	Star-shaped / spread out
Proliferation	Low	High
Retinoid storage	High content	Reduced
Matrix synthesis	Low levels	Enhanced production due to increased - collagen-I, III and IV mRNA and - increased protein synthesizing capacity
Collagen secreted	Collagen III > I	Collagen I > III > IV
Activation Markers	None	↑alpha Smooth Muscle Actin (αSMA) ↑Platelet Derived Growth Factor (PDGF) receptor and cytokine expression ↑ Transforming growth factor-beta (TGF-β1)

Table 1.1 HSCs are compared between the quiescent and activated state.

Adapted from (10;71;102).

HSCs accumulate in areas of liver necrosis and their numbers appear to correlate with the stage of necroinflammation (103;104). Ultrastructurally, activated HSCs show increased cytoplasmic volume surrounded by abundant collagen bundles and contain characteristic bundles of microfilaments with focal condensations, hypertrophied rough endoplasmic reticulum suggesting increased protein synthesis, and a prominent Golgi apparatus (105). The intracytoplasmic lipid droplets usually decrease with HSC activation although intracytoplasmic lipid accumulation is seen in HSC activation associated with hypervitaminosis A, extrahepatic cholestasis and early alcoholic liver injury (106;107).

1.8.1 Mechanism of HSC activation

Studies of the role of the hepatic stellate cell in liver fibrogenesis have been enhanced by the demonstration that the process of activation can be modeled by plating primary HSC cultures onto uncoated tissue culture plastic, glass or collagen (24;108-110). The ultrastructural changes and associated increased collagen synthetic capabilities are similar to the changes observed in vivo, leading to the suggestion that primary cultures of HSCs are a valuable tool for studying their role in chronic liver disease (111). The process of stellate cell activation occurs in a reproducible sequence and can be placed into a discrete biologic context. Early events have been termed initiation (also referred to as the "pre-inflammatory" stage) (67). Initiation includes the rapid changes in gene expression and phenotype that render the cells responsive to cytokines and other local stimuli. Initiation is associated with transcriptional events and induction of immediate early genes. It results from paracrine stimulation due to rapid, disruptive effects of liver injury on the homeostasis of neighbouring cells and from early changes in ECM composition (67). Once initiation has been set in process by paracrine stimulation, transcriptional events begin a cascade of cellular responses. HSC activation is initiated from stimuli originating from injured hepatocytes, neighbouring endothelial cells and Kupffer cells in addition to rapid, subtle changes in ECM composition (112;113). Perpetuation incorporates those cellular events that amplify the activated phenotype through enhanced cytokine expression and responsiveness; this component of activation results from autocrine and paracrine stimulation, as well as from accelerated ECM remodeling. Some of these changes are summarized in Figure 1.5.

Figure 1.5 Phenotypic features of hepatic stellate cell activation

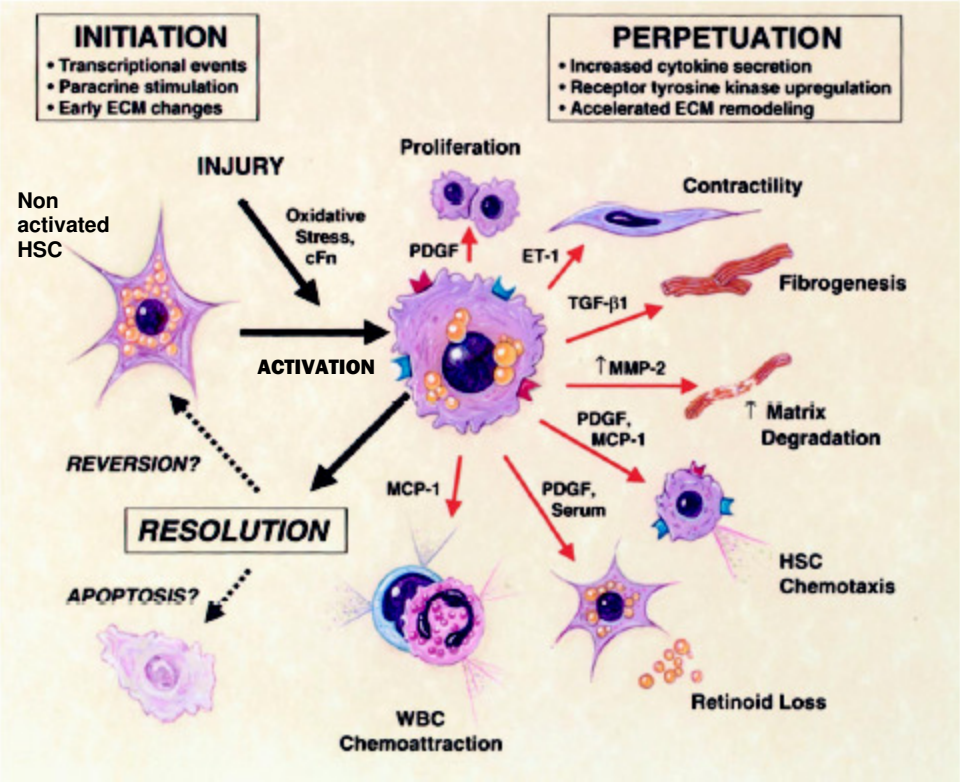

Figure 1.5 Phenotypic features of hepatic stellate cell activation during liver injury and resolution. During liver injury quiescent HSC undergo a phenotypic transformation termed 'activation' which encompasses the change to a myofibroblast-like phenotype. Reproduced from (67).

Hepatocytes and Kupffer cells are a potent source of reactive oxygen intermediates (ROI) (114). These compounds exert paracrine stimulation of stellate cells. Moreover, their activity is amplified *in vivo* by depletion of anti oxidants as typically occurs in diseased liver. When conditioned medium from hepatocytes undergoing oxidative stress is added to cultured stellate cells their proliferation and collagen synthesis is increased (115). Over expression in stellate cells of the enzyme cytochrome P4502E1, which generates ROI, stimulates collagen I gene expression; this effect is attenuated by antioxidants (116). Endothelial cells also play an important role in early cell activation. Injury to sinusoidal endothelial cells stimulates production of a splice variant of cellular fibronectin (EIIIA isoform) which has an activating effect on stellate cells (117). Endothelial cells also convert latent transforming growth factor beta-1 (TGFβ1) to the active, fibrogenic form through the activation of plasmin (118). Using molecular approaches a number of differentially up-regulated genes have been identified

during the process of activation (119-121). These consist of a transcription factor (119), and adhesion molecule (ICAM-1) (120) and, interestingly, the prion protein (121). In an effort to identify regulatory genes during early stellate cell activation has resulted in the cloning of a Krupel-like factor (KLF) zinc finger gene (KLF6). KLF6 mRNA is rapidly induced in liver injury *in vivo* and in culture (119) and can trans-activate genes regulating ECM accumulation (121). At least two other KLF proteins also regulate stellate cell activation. Sp1, the first member of the KLF family, binds more actively to its consensus motif in activated versus quiescent stellate cells (122;123).

Basic transcription element binding protein 1 (BTEB1) mediates the increase in collagen gene expression, which occurs in response to UV radiation or expression of the transcription factor c-Jun (124).

1.8.2 Perpetuation: the Paracrine and autocrine driven cytokine activity and ECM remodeling that sustain the activated phenotype

Perpetuation of stellate cell activation involves key phenotypic response mediated by increased cytokine effects and remodeling of ECM (118). Increased cytokine responses through multiple mechanisms occur (118) and in particular increased expression of cell membrane receptors and enhanced signaling are important (125). Especially important are receptor tyrosine kinases (RTKs) which mediate many of the stellate cells responses to cytokines, and which are up-regulated during liver injury (126).

Continued ECM remodeling during this phase underlies virtually all cellular responses characterizing progressive liver injury. The low density subendothelial matrix is progressively replaced by one rich in fibril-forming collagen. This fundamental shift in ECM composition affects the behaviour of hepatocytes, sinusoidal endothelium and stellate cells.

Fibril forming ECM also accelerates stellate cell activation. These effects are mediated not only through interactions with integrins, the classic ECM receptors, but also binding to at least one RTK (receptor tyrosine kinase). Several integrins and their downstream effectors have been identified in stellate cells, including $\alpha_1\beta_1$, $\alpha_2\beta_1$, $\alpha_5\beta_1$ and $\alpha_6\beta_4$ (125). Recently, a subfamily of receptor tyrosine kinases, discoidin domain receptors (DDRs) has been

characterized, which unlike other RTKs signal in response to fibrillar collagens rather than growth factors (127;128). With the identification of discoidin domain receptor –2 (DDR-2) mRNA in stellate cells (126), a mode of matrix cell interaction in liver has emerged that may explain why fibril forming matrix (especially collagen type 1) provokes activation of stellate cells during sinusoidal fibrosis. Thus, as the subendothelial basement membrane is replaced by fibrillar collagen stellate cell activation may be perpetuated via binding of collagen to the DDR-2 receptors (126;127). Collagen breakdown products produced by the action of MMPs may also involve HSC proliferation by stimulation of $\alpha_5\beta_3$ integrin on the cell (129).

HSC proliferation is stimulated by a number of mitogens, which usually signal through receptor tyrosine kinases. Amplification of HSC proliferation is a consequence of the increased secretion of mitogens in combination with the induction of their cognate HSC tyrosine kinase receptors. Mitogens that stimulate HSC activation include platelet derived growth factor (PDGF) (130), thrombin (131), endothelin-1 (132), epidermal growth factor and TGFα (133), IL-1α (134) and recently VEGF, whose effect is synergized in vitro by the addition of fibroblast growth factors (126). Lipid peroxidation products consequent upon cellular oxidative stress have also been shown to induce HSC activation (135). HSC proliferation is inhibited by TGFβ (133) and interferon gamma (IFNγ) (136;137). The mitogenic effect of PDGF can be inhibited by retinoids (138).

Chemotaxis is another HSC activity that with proliferation, contributes to the HSC accumulation at the site of the liver injury. Chemotaxis is thought to be mediated primarily by PDGFα (139) and MCP-1 (140). HSC fibrogenesis results in net ECM accumulation. The increased fibrillar matrix synthesis is primarily and most potently mediated by TGFβ (141). The activity of TGFβ is enhanced by increased HSC production of TGFβ resulting in autocrine stimulation (142), increased activation from its latent to active form (143;144) and by increased TGFβ receptor expression on HSCs (145).

Other fibrogenic mitogens include oncostatin M (146), retinoids (144), IL-1β, IL-4 (147) and acetaldehyde (148). In contrast, TNFα (149), IFNγ (136;147) IL-10 (150) and IL-1α (134) inhibit collagen gene expression in HSCs. Increased collagen production by HSCs may also result from post transcriptional events including increased collagen mRNA stabilization (151).

1.8.3 mRNA stability

One aspect of regulation of protein synthesis that is overlooked is the rate of translation. There are several independent metabolic steps that determine the level of a protein in eukaryotic cells. The steady state level of mRNA encoding the specific proteins is determined by the rate of transcription, percentage of transcripts that are ultimately processed and transported to the cytoplasm, and the half life of the mRNA in cytoplasm (152).

1.8.3.1 Regulation of mRNA degradation

Despite the fact that most mRNAs decay via a common pathway (153) there is a wide range of half lives for different mRNAs, ranging from minutes to hours. The stability of a particular mRNA is determined by *cis* elements, which may be present in the 5` untranslated region (UTR), the coding region or in the 3` UTR (154). Regulation of the half life of mRNA is probably accomplished by alteration of factors that interact with specific sequences in the mRNA. Major strategies for degrading mRNA appear to be conserved from yeast to humans. The most common decay pathway occurs as a result of shortening of the poly(A) tail.

Efficient translation of a mRNA requires that it contains both a 5` 7 methyl guanine (7mG) cap and a poly(A) tail, both of which are critical for efficient translation initiation (155;156)**.** The poly(A) binding protein (PABP)-poly(A) is a complex found at the end of the 3` end of all mRNAs except histone mRNA (157;158)**.** This results in a circular mRNA and may form part of the physiological translation initiation complex in mammalian cells. When the poly(A) tail reaches a critical minimal length, the PABP presumably disrupts the circular mRNA structure. The mRNA is then de capped and becomes accessible to exonucleases that can degrade the mRNA 5` to 3`. There are also enzymes that can degrade the mRNA 3` to 5`.

The rate of the initial step is degradation of specific mRNAs; it can be modulated by *cis* and *trans* elements that specifically bind to regions in the mRNA and cause degradation of specific transcripts in response to certain stimuli. For example, AU-rich elements located in the 3`UTR of many mRNAs generally destabilize the mRNA by binding specific proteins (159;160)**.** Since the normal location of an mRNA is on polyribosomes on which it is being actively translocated it is not surprising that the initial steps in mRNA decay occur while the mRNA is associated with polyribosomes.

As a result many mRNAs are stabilized by inhibitors of protein synthesis. Degradation of an mRNA requires several enzymatic processes: deadenylation, de capping, and exonuclease activity. Recent results have indicated that many of these activities may be contained in a single complex, termed the exosome or degradosome (155)**.**

Type I collagen mRNA stability appears to be the best studied in liver and HSC. (161)**.** The transcriptional rate of collagen α1(I) gene was increased only threefold in activated HSC, demonstrating that most of the regulation leading to the 60-70 fold increased in collagen mRNA was post translational (151). The half life of the α1(I) mRNA was increased 16x fold in activated HSCs compared with quiescent cells (161).

1.8.4 HSC and Matrix degradation

HSCs play an important role in the regulation of matrix degradation, which then affects ECM homeostasis. Primarily SMA filaments mediate HSC contractility. Molecular studies indicate that HSC activation and SMA activation are closely linked (162). Transcription factors that regulate activation such as c-myb and NFK β, also bind to the SMA promoter, inducing SMA transcription (135). The long HSC processes wrap around and contract the sinusoids, impeding blood flow. It is possible that this decreased blood flow may have an impact on the dynamics of blood flow in the hepatic portal system and arguably may be a contributing factor to portal hypertension in patients who have cirrhosis of the liver.

In normal liver HSC contraction can be initiated by neurotransmitters released from adrenergic nerve endings. In contrast, chronic diseased liver has a depletion of intra-hepatic nerves and nerve endings (163;164). Moreover, HSCs possess endothelin receptors which are up regulated with HSC activation. Endothelin 1 (ET-1) is a key contractile stimulus toward stellate cells which in part is autocrine-derived (165). Up-regulation of ET-1 production is accompanied by increased endothelin converting enzyme-1 which activates the latent ET-1(166), in addition to its potent contractile effect, also regulates stellate cell proliferation (132;167). Endothelin receptors can be stimulated via an autocrine or paracrine mechanism (168). HSC relaxation is mediated by prostaglandin E2, iloprost, adrenomedullin and nitric oxide. HSCs produce nitric oxide, which can inhibit contractility by an autocrine mechanism (169).

At least two G protein-coupled receptors mediate the effects of ET-1. Unlike receptor tyrosine kinases which are generally induced during activation, ET receptor types A and B are expressed on both quiescent and activated stellate cells (165). However, the relative prevalence of ETA and ETB receptors changes with the cellular activation and each mediates divergent responses (132).

The proliferative effect of ET-1 in quiescent cells correlates with increased Ras/EAK activity, which is blocked with ETB agonists (132). In contrast, the growth effect of ET-1 in activated cells is mediated by the ETB receptor (170) via a prostaglandin/cAMP pathway that leads to down regulation of ERK and c-Jun kinase (JNK) (170).

Once activated, HSCs are capable of cytokine production resulting in autocrine stimulation as mentioned before. Conditioned HSC medium stimulate the proliferation, transformation and matrix synthesis of primary HSC cultures (171).

The cytokines produced by HSCs include TGFβ1 (172), PDGF (173), fibroblast growth factor and hepatocyte growth factor. HSCs can also amplify inflammation through the release of neutrophil and monocyte chemoattractants such as colony stimulation factor and MLP-1 (140). Anti inflammatory cytokines produced by HSCs have also been identified. IL-10 down regulates inflammation by inhibiting macrophage production of TNFα (150;174).

Other cells participate in and regulate the process of HSC activation, both in the initiation and perpetuation phases. Kupffer cells are an important source of cytokines involved in paracrine HSC stimulation. Kupffer cell infiltration occurs just prior to, and co-incident with, the appearance of activated HSCs (97;175). Kupffer cell conditioned medium can stimulate HSC matrix synthesis, cell proliferation and release of retinoids (130;176). Endothelial cells also participate in cytokine mediated HSC stimulation by their conversion of latent TGF beta to its active pro fibrogenic form through the activation of plasmin (144).

Upon injury endothelial cells produce a splice variant of cellular fibronectin that is able to stimulate HSC activation (117). Platelets are a potent source of paracrine HSC stimulation by their generation of PDGF, TGFβ and epithelial cell factor L1 (177). Lipid peroxides, produced by hepatocytes, also stimulate HSC activation (178). This injurious effect is

compounded in cirrhosis, as the levels of antioxidants are depleted (179) and chronic hepatitis C virus (HCV) infection (180) has been reported to increase lipid peroxide production by hepatocytes. Potentially, this initiates HSC activation and results in liver fibrosis. Ethanol induced hepatocyte lipid peroxidation also stimulates collagen production (181). Exposure of HSCs in culture to conditioned medium from hepatocytes undergoing oxidative stress increases HSC production and collagen production (115). A 60 kDa cytosolic protein has been identified and partially characterized from parenchymal cell conditioned medium that stimulates HSC proliferation (182).

Inflammatory cells particularly T - lymphocytes and natural killer cells secrete IFN gamma which inhibits HSC proliferation and collagen synthesis (136;137;147;183).

Interleukin 10 (IL-10) has recently been identified as an anti-fibrogenic cytokine, primarily produced by T-lymphocytes (150;174;184). Liver fibrosis is more severe in the IL-10 deficient mouse (174). In addition to its direct anti fibrogenic effect in HSCs, IL-10 inhibits Kupffer cell function, which may have an indirect anti-fibrogenic effect (185).

1.8.5 Phenotypic characterization of quiescent and activated HSCs

HSCs are not readily recognized in routine haematoxylin and eosin histological sections.

Quiescent rat HSCs can be recognized by toluidine blue, basic fuchsin and oil-red-o staining, which allows detection of the characteristic lipid droplets (88;186). The lipid droplets can also be detected by their unique autofluorescent properties, as the vitamin A has a characteristic rapidly fading blue green fluorescence at 328nm (187). Staining for vitamin A directly with gold chloride has been demonstrated but the results are occasionally inconsistent (188). A small proportion of HSCs have no or little lipid (95;189).

HSCs can also be identified immunohistochemically using antibodies to cytoskeletal proteins. The majority of rat HSCs are desmin positive (190). HSCs are vimentin positive but so are Kupffer and endothelial cells, thus it is not useful for phenotypic identifications (141). Rat HSCs in normal liver contain an intermediate filament, glial fibrillary acid protein (GFAP) (191;192). GFAP +ve cells are seen fairly evenly in the liver lobule.

Activated rat HSC can be identified by the expression of α-SMA (193). In chronic liver injury, GFAP expression diminishes, and is mainly detected at the margins of the fibrotic septae, less so inside the septa. GFAP expression also rapidly diminishes when primary HSCs are activated on tissue culture plastic (192). Recently, nestin has been identified as a marker of rat HSCs. Whilst nestin is not seen in normal liver parenchyma (91), nestin positive HSCs are observed in the vicinity of and inside the fibrous septa in a small proportion of the α-SMA positive and desmin positive HSCs, after prolonged carbon tetrachloride induced liver injury (6 weeks) (91). In primary culture of freshly isolated HSCs no expression of nestin was detected (91) in contrast to activation in tissue culture plastic where transient expression is noted around day 13 (91). The latter result differs from *in vivo* observations.

The expression of nestin, vimentin and GFAP by HSCs prompts a comparison with astrocytes which also by the process of gliosis, have an important role in wound healing (194). Activated rat HSCs also express neural cell adhesion molecule (NCAM) (195). In normal liver NCAM is expressed in nerve structures although in acute and chronic liver injury NCAM positive cells are present in the hepatic parenchyma.

NCAM positive cells can be seen in the fibrous septa and occasional cells of the hepatic parenchyma (195). HSC expression of NCAM, nestin and GFAP, normally expressed by cells of neural origin, lend weight to the possibility of HSCs being of neural crest origin, rather than mesenchymal origin.

Quiescent human HSCs can also be identified by their vitamin A content as described for rat HSCs above. Immunohistochemical phenotyping is less advanced in the human than the rat but despite this current research pinpoints certain differences in patterns of HSC expression of some antigens. Desmin is not expressed by human HSCs (186). In normal human liver GFAP expression is limited to a small sub-population of HSCs located at the edge of the portal tracts (105). NCAM expression is seen in normal human liver, in a predominantly periportal locations (195). Most researchers report that HSCs only rarely express α-SMA in normal human liver (196); however with different immunostaining technique, there are some reports that α-SMA is positive in the majority of HSCs in normal human liver (197;198). α-SMA is the primary marker of activation in human stellate cells (96;196). Isolated HSCs are initially α-SMA negative, and early in culture develop α-SMA expression coincident with

activation (147). α-SMA is also expressed by myofibroblasts of portal fibroblast origin (199-201). In cirrhotic human liver GFAP expression is up regulated in contrast to normal liver with positive cells lying at the edge of the regenerative nodules (105). NCAM expression in human chronic liver disease has to date not been studied.

1.9 ECM degradation: role in cirrhosis

The matrix metalloproteinase are a family of zinc and calcium dependent endopeptidases, secreted by connective tissue cells that have activity against the major constituents of matrix and non fibrillar collagens. The MMPs are considered to be the mediators of extracellular matrix turnover and there is increasing evidence of their expression by HSCs and Kupffer cells (69;202-205).

The MMPs can be grouped according to their respective enzyme substrate. The first are the collagenases which are central to the process of remodeling of fibrotic tissue as they cleave the native helix of fibrillar collagens I, II and III to render the collagen susceptible to degradation by other MMPs, to which they were previously resistant (206-208). Three types of collagenases have been described, neutrophil collagenase and the recently described human collagenase-3 (209), and interstitial collagenase or MMP-1. As noted earlier, there is a predominance of collagens Type I and III in fibrotic liver (96), and thus the expression of interstitial collagenase activity would be necessary to initiate collagen degradation. It has previously been considered that only collagenases have activity against fibrillar collagens but a member of the third group Gelatinase A has also been shown to have degradative activity against collagen I (210). See Table 1.2

Table 1.2 The metalloproteinase family

Adapted from (211)

Name	MMP	Size (kDa)	Source	Substrate Profile
COLLAGENASES				
Interstitial	MMP-1	55	connective tissue cells (CT)	collagens I, II, III, proteoglycans
Neutrophil	MMP-8	75	neutrophils	collagens VIII, X
Collagenase-3	MMP-13	65	tumour cells	collagens I,III
GELATINASES				
Gelatinase A	MMP-2	72	stromal cells, HSC	collagens I, III, IV, V, X, XI, elastin, gelatin, fibronectin
Gelatinase B	MMP-9	95	KC, CT cells	gelatin, denatured collagens, collagen IV
STROMELYSINS				
Stromelysin-1	MMP-3	57	CT, macrophages endothelial cells	proteoglycans, casein, collagens III, IV, V, gelatinase B
Stromelysin-2	MMP-10	57	macrophages	as above but less activity
Stromelysin-3	MMP-11	51	tumour stromal cells	
Matrilysin	MMP-7	28	monocytes	as MMP-3 and elastin
OTHERS				
Metalloelastase	MMP-12	57	macrophages	elastin, fibronectin
Membrane-type1	MMP-14	63	tumour stromal cells	gelatinase A, MMP-13, fibronectin, collagens I, III
Membrane-types 2-4	MMP-15 16, & 17		stromal cells	Functionally active gelatinase

The second group: the stromelysins have a large substrate profile with activity against collagens (II, IV, IX, X, XI), denatured collagens (gelatin), laminin and fibronectin. There is evidence that they may activate procollagenase (212-214).

The third MMP group are the gelatinases; gelatinase A has activity against gelatins, collagens IV, V, VII, X, and XI and elastin and may have interstitial collagenase activity (210;213-215). Gelatinase B shares the same substrate profile but has not been demonstrated to have interstitial collagenase activity.

The fourth group and most recently described is the membrane type MMP, (MT-MMP) comprising three members. Functionally these enzymes activate gelatinase (216-218).

The extracellular activity of MMPs is regulated at various levels:

1) By transcriptional activation at the level of the gene,
2) Cleavage of the pro piece, and
3) By extracellular inhibition by the specific tissue inhibitors of metalloproteinase or TIMPs, or by more general protease inhibitors such as alpha 2 macroglobulins.

MMPs are regulated at the level of the gene by a series of growth factors and cytokines (212;219-221). These include IL-1, TNF-α, PDGF and basic-FGF and EGF. MMPs are differentially regulated, in addition, by certain cytokines. TGFβ1 is a key player in liver fibrosis: it is expressed by Kupffer cells and HSC, during liver injury (142;145;176;222). Activated HSCs express TGFβ1 receptors and mannose 6 phosphate receptors, necessary for activation of the latent cytokine (223).

Moreover HSCs express TGFβ mRNA and secrete the cytokine in an autocrine manner. In response to TGFβ, fibroblasts down regulate interstitial collagenase expression while up regulating the expression of gelatinase A, TIMP-1, and collagen 1 (176;224-226). TGFβ1 occupies a central role in pre-fibrogenesis and is believed to be a pivotal cytokine in the fibrotic process.

The second level of control lies in the conversion of the pro-MMP species (the form in which all MMPs are secreted) to the active moiety, by cleavage of the pro piece (206;225;227). In vivo, this function is probably mediated by plasmin (213;215). In addition, two further special mechanisms of activation exists, membrane type matrix metalloproteinase (MT-MMP)

functions to activate 72kDa gelatinase at the cell membrane (216) while active stromelysin will further cleave activated interstitial collagenase to result in a 5-8 fold enhancement in activity (220;228).

1.10 The Tissue Inhibitors of Metalloproteinase (TIMP)

The TIMPs function as an important regulatory brake in the activity of MMPs by stabilizing the proenzyme and by inhibition of the active species. To date four TIMPs have been described, each is a separate gene product (229-233).

As a family these inhibitors share common structural features. There is 40% amino acid sequence homology between TIMP-1 and TIMP-2, and both have a three looped structure stabilized by six disulphide bonds, the result of 12 conserved cysteine residues, which are also present in TIMP-3 (212;229;231;233;234). TIMP-1 and TIMP-2 are secreted into the intracellular milieu whilst TIMP-3 is detected in association with extracellular matrix (229).

The binding of TIMPs to active MMPs is essentially irreversible under physiological conditions. Binding occurs in a stoichiometric manner and the TIMPs reportedly block the active site of the metalloproteinases (214;235;236). This binding is noncovalent however and *in vitro*, the enzyme inhibitor complexes can be separated with the TIMP retaining its inhibitory activity (237). TIMP-1 and –2 inhibit the active forms of every metalloproteinase (229). As with the four TIMPs, TIMP-3 has its own distinctive characteristics. A TIMP-3 mutation leads to Sorsby's fundus dystrophy, a retinal degenerative disease (238). Although other TIMPs are soluble upon secretion from the cell, TIMP-3 remains bound to the ECM (232;239) through sulphated preoteoglycans moietieis (240). Evidence exists that either very high TIMP-3 expression or the loss of TIMP-3 promote apoptosis (241;242). Studies using site directed mutagenesis and recombinant truncated TIMPs indicate that there are two separate functional domains to the molecule. The N-terminal of the TIMP molecule is necessary for inhibitory activity against active MMPs; indeed truncated TIMPs with intact N-terminal portions retain inhibitory activity. The C-terminal domain in contrast is key to the interaction with prometalloproteinases (243-246).

Both TIMP-1 and TIMP-2 bind to specific progellatinase species therefore preventing their activation by stromelysin (206;247), in addition TIMP-1 will inhibit the formation of gelatinase B homo dimers and interstitial collagenases and gelatinase B homo dimers (206).

Transcriptional regulation of the TIMPs is mediated by cytokines and growth factors, several of which mediate MMP expression and which have been implicated in HSC activation and synthetic functions. These effectors may coordinate and differentially regulate both the MMPs and the TIMPs. Thus, TGFβ1 will up regulate TIMP-1 and gelatinase A whilst down regulating TIMP-2, interstitial collagenase and stromelysin (225;248;249) and TNFα will co-coordinately up regulate TIMP-1 and interstitial collagenase (250). Studies mapping the gene promoters of TIMPs and MMPs show some common regulatory motifs that differ in individual TIMPs/MMPs in terms of their frequency and position in relation to the transcription start site. For example, the murine TIMP-1 and interstitial collagenase (MMP-1 promoters both have AP-1 and PEA-3 binding sites in different configurations (248;251). An AP-1 site is noted in the promoters of stromelysin and gelatinase B but not in gelatinase A (MMP-2).

The human TIMP-2 gene in chromosome 17 is flanked by 5'AP-1 and AP-2 consensus sequences and several SP-1 sites in association with a TATA box (252). The AP-1 consensus site in the TIMP-2 promoter is further upstream from the transcription start site than that found in the TIMP-1 promoter and is not associated with a PEA-3 motif. As in TIMP-1 and TIMP-2, the TIMP-3 promoter has multiple SP-1 sites which confer a high basal expression in growing cells (253). The spatial distribution and differing binding sites in the promoters of TIMP-1 and TIMP-2 may explain in part the differential expression observed in response to cytokines such as TGFβ1 and TNFα. The promoters also provide a mechanism whereby TIMPs can be co-regulated and independently regulated to inhibit MMP activity in a wide variety of physiological (eg growth and development) and pathological processes (eg arthritides and liver fibrosis). From the discussion so far it can be proposed through relatively small changes in the ratio of TIMP: MMP concentrations, alterations in matrix degradation can be effected and regulated.

1.11 Evidence for change in matrix degradation during liver fibrosis

Models of liver fibrosis have established that collagenase activity in liver tissue sections and homogenates decreases with the progression of experimental fibrosis: this would promote net collagen deposition. This may reflect a decrease in matrix remodeling as fibrosis progresses. These models have included human and primate alcoholic liver injury and carbon tetrachloride mediated rat liver injury (254-258). See Figure 1.6

Figure 1.6 Time course of MMP2 and TIMPs 1&2 with HSC culture

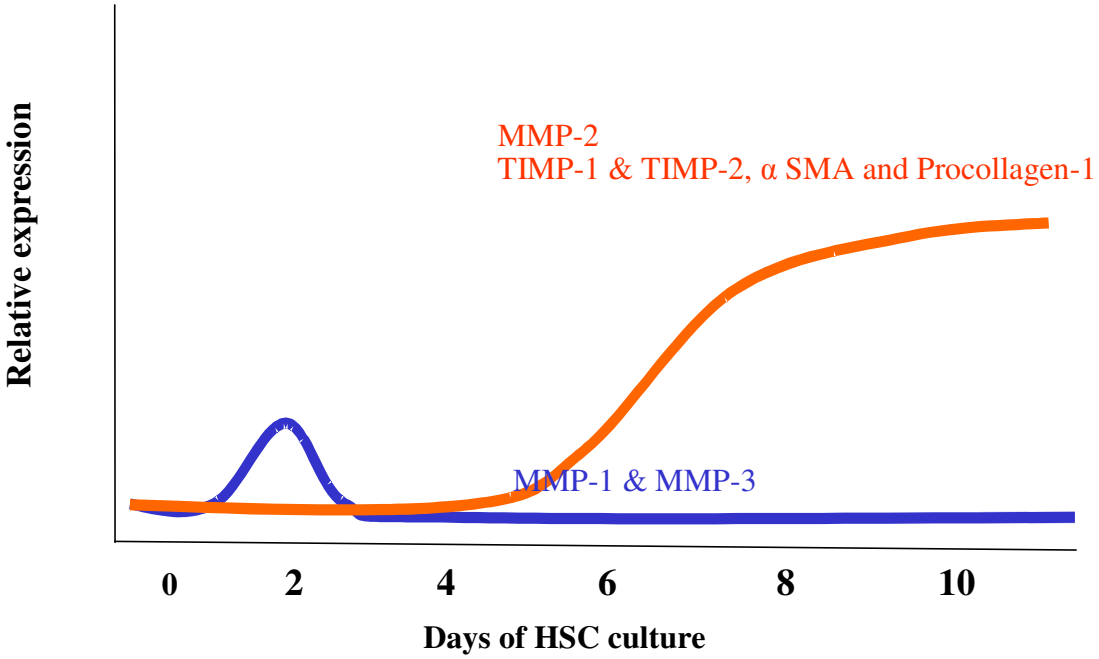

Figure 1.6 As HSC become progressively more activated their expression of MMP-2 increases. Levels of MMP-2 in the supernatant are much higher than other MMPs and coincide with phase of HSC proliferation in culture.

As indicated above, a number of detailed studies have indicated the number of MMPs expressed by HSCs during the process of activation. Both human and rat HSCs express gelatinase A and Rat HSCs express stromelysin (259-261).

Gelatinase A expression increases with activation whilst Stromelysin is transiently expressed reaching a peak at day 3-4 in cultured HSCs. In both cases the enzyme can be immuno localized to HSCs, and specific activity detected in the cell culture supernatants. There is evidence for expression of both of these enzymes during acute liver injury in perisinusoidal cells (262;263).

Interstitial collagenase has been localized to the cytoplasm of HSCs during activation by culture on plastic (264). Subsequent molecular studies have failed to demonstrate interstitial collagenase mRNA expression in fully activated HSCs although it can be detected in freshly isolated cells (262). However interstitial collagenase mRNA expression can be induced in activated HSCs by exposure to TNFα and IL-1 (265;266). In addition, cultured HSCs have been demonstrated to release interstitial collagenase activity in response to polyunsaturated lecithin (267).

There is therefore evidence from tissue culture studies to suggest that HSCs possess the ability to remodel matrix during the process of activation and specifically to mediate remodeling of interstitial collagens by expression of interstitial collagenase. HSCs may not be the only cells with the ability to do this. Kupffer cells have been shown to express gelatinase B (205), while sinusoidal endothelial cells may be a source of stromelysin (263).

1.12 Evidence for TIMP expression in progressive liver fibrosis

To address the concept that TIMP expression may promote fibrosis by reducing collagenase activity in progressive liver fibrosis, the gene expression of TIMP-1 and TIMP-2 and MMPs have been studied in HSC activation both in tissue culture and *in vivo.* When HSCs are cultured on tissue culture plastic there is an increase in the transcription of TIMP-1 mRNA in activated cells compared to quiescent (freshly isolated) cells (268). TIMP-1 can be immuno-localized to HSC and also detected extracellularly in HSC cell culture supernatants by ELISA. When HSC conditioned media is subjected to gelatin Sepharose chromatography TIMP-1 bound to gelatinase A is separated: removal of TIMP-1 is associated with a twenty fold

increase in gelatinase activity. Returning TIMP-1 to the media results in re-inhibition (268). Both TIMP-1 and TIMP-2 are found in HSC conditioned media and TIMP-2 mRNA is observed in northern analysis of activated HSC total RNA (268;269).

HSC may not be the sole source of TIMPs in the liver: TIMP-1 and TIMP-2 are detected in HepG2 hepatoma cell lines (269-271). In these studies TIMP-1 expression was found to increase in the presence of IL-6, an acute phase cytokine, suggesting that TIMP-1 may be released by hepatocytes in acute liver injury.

In a model of fibrotic liver from murine schistosomiasis expression of interstitial collagenase, detected immunologically, remains relatively constant (272-274), whilst collagenase activity decreases emphasizing the importance of expression of collagenase inhibitors during fibrogenesis. Further evidence for the important roles of TIMPs in fibrogenesis come from the analysis of serum in patients with hepatic inflammation and established cirrhosis reveals an increase in TIMP-1 levels by ELISA (275-277). In addition when TIMP-1 and TIMP-2, interstitial collagenase and gelatinase A mRNA expression in fibrotic liver compared to normal were studied by ribonuclease protection analysis TIMP 1 and TIMP 2 transcripts were increased in fibrotic liver, as are gelatinase A transcripts (266;269). In contrast interstitial collagenase transcripts were only marginally increased in primary sclerosing cholangitis and primary biliary cirrhosis (269). TIMP-1 was also immuno localized to perisinusoidal cells in fibrotic liver in 75% of biopsies positive for interstitial collagenase suggesting that co-expression of TIMP-1 with interstitial collagenases occurred (269).

The development of fibrosis entails major alterations in both the quantity and quality of hepatic ECM. Cirrhotic liver contains approximately six times more ECM overall than normal liver, and in the space of Disse collagen types III and V and fibronectin accumulate in early injury (14). Culture studies have suggested that the neo matrix laid down in the space of Disse may itself contribute to the disease associated alterations in the phenotype of HSC, sinusoidal endothelial cells, and hepatocytes (25;278;279). With progressive injury ECM spurs link the vascular structures, ultimately resulting in the architecturally abnormal nodules that characterize cirrhosis.

Complete recovery from liver fibrosis would involve remodeling and breakdown of these multiple ECM components, with degradation of the predominant component, collagen I, being particularly important for recovery of normal liver histology.

1.13 Resolution of fibrosis

In clinical circumstances, where there is a treatment available for the underlying liver disease, remodeling of the scar tissue can occur and a return towards architectural normality has been documented even in advanced fibrosis and cirrhosis. This has been noted in treatment in autoimmune disease, venesection for patients with haemochromatosis and interferon therapy for patients with hepatitis B and C (280) (110;281-283). See figure 1.7a and 1.7b.

Figure 1.7a Rat recovery model for resolution of fibrosis

6 week CCl_4 Rat Injury Model

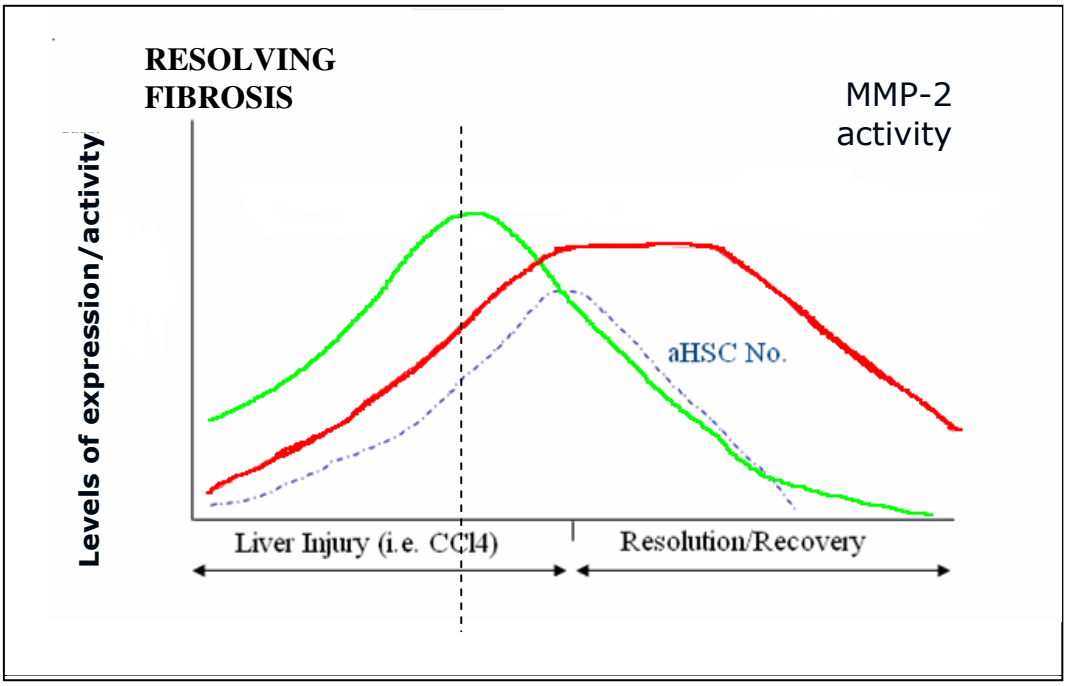

Figure 1.7b Rat recovery model for resolution of fibrosis

12 week CCl_4 Rat Injury Model

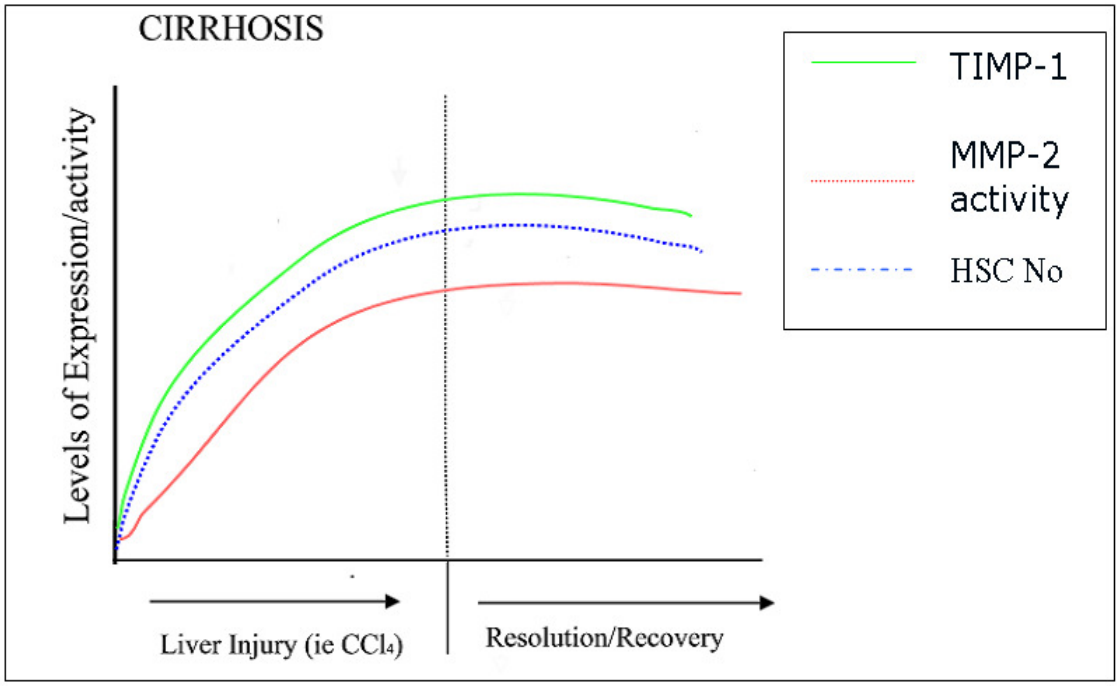

For ethical reasons, it is difficult to examine the molecular mechanisms of resolution of fibrosis in humans however recovery has been examined in a rat model which permit frequent sampling and control over the chronology and extent of the fibrotic lesion. In a model of experimentally induced cholestasis the typical features of bile duct proliferation and periportal fibrosis developed three weeks after bile duct ligation with a notable increase in hepatic mRNA for collagens I and IV. See Figure 1.7 However, following re-anastomosis of the bile duct to a jejunal loop there was resorption of periportal fibrosis and the liver ECM returned virtually to normal, except for a persistence of collagen IV in sinusoids. In addition mRNAs for collagen I and IV became virtually undetectable (284). Figure 1.8 depicts some processes that promote recovery.

Figure 1.8 Mechanisms regulating HSC survival and apoptosis

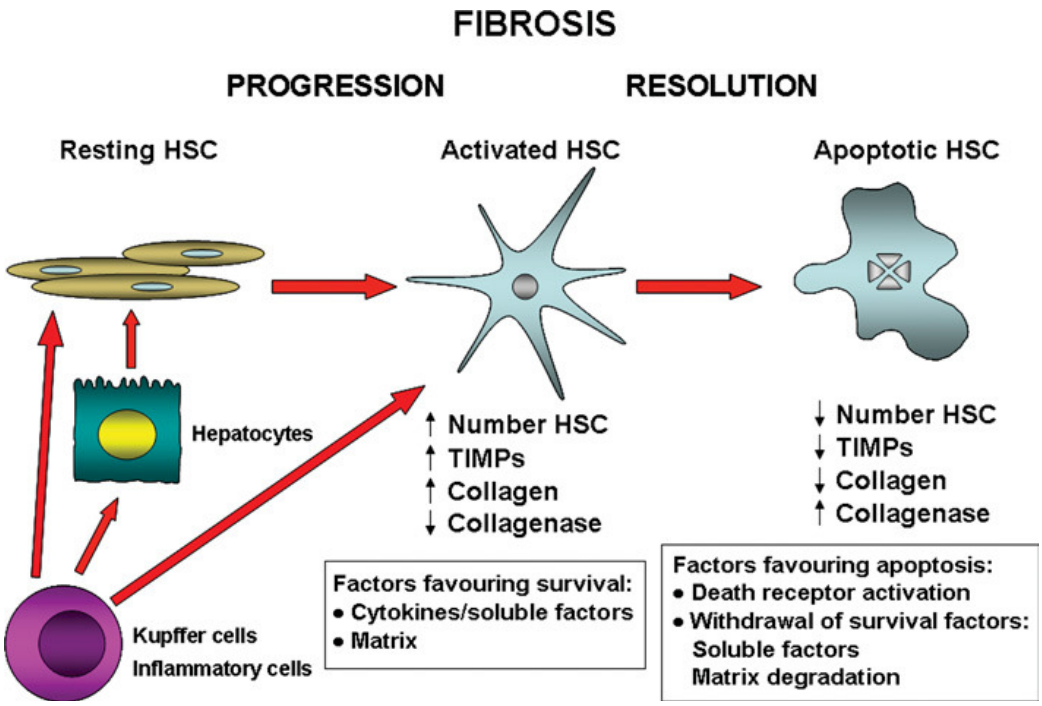

Figure 1.8 Summary of the processes mediating recovery from liver fibrosis and the mechanisms regulating HSC survival and Apoptosis (285)

In another model incorporating the use of carbon tetrachloride to induce fibrosis recovery was again examined (286). Liver fibrosis was noted after four weeks of intraperitoneal injection of carbon tetrachloride (CCL_4) with extensive intervascular bridging with collagen fibres. The liver insult was then withdrawn and livers were examined at various times up to four weeks of recovery. Histological analysis showed a noticeable dissolution of the collagenous fibrotic matrix and a return to liver structure to virtual normality. The hepatic mRNA content of TIMP-1 and TIMP-2 and procollagen-I all diminished greatly in livers the first week of recovery which coincided with the most rapid phase of collagen degradation, as assessed by hydroxyproline content. Interstitial collagenase activity increased in the liver homogenates during this time. In addition there was prominent apoptosis of activated HSC during recovery particularly in the first three days coinciding again with the largest reduction in TIMP-1 and procollagen I mRNA. Apoptosis therefore effectively removed the activated HSC, which were overproducing ECM and TIMPs. The process of programmed cell death during wound healing and resolution of fibrosis has been seen in other cell systems. Surplus mesangial cells, for example, from glomeruli during resolution of mesangial proliferative nephritis has

been noted to diminish through apoptosis (287). Myofibroblasts are also removed by apoptosis during skin wound healing.

1.14 Control of apoptosis in the liver

HSCs activated in culture undergo spontaneous apoptosis in vitro, which can be greatly increased by serum deprivation and fas ligand (286;288;289). Recent studies suggest that a further cytokine present in injured liver, nerve growth factor (NGF), induces HSC apoptosis in culture. Mast cells, which become more abundant in fibrotic liver are a rich source of NGF (290). The pro-apoptotic receptor fas and its ligand are also expressed by activated HSC (288). It is possible that persistence of HSC in fibrotic liver might therefore require undefined survival factors to offset the effects of these apoptotic stimuli, and removal of survival factors when liver injury ceases would then allow relatively rapid removal of HSC.

The role of cell-matrix interactions in regulating cell survival have most extensively been studied in epithelial cells in which deprivation of contact with the ECM is a potent pro-apoptotic mechanism, a process that has been termed anoikis (291). Preventing attachment of HSC to plastic induces apoptosis (292). When HSCs are cultured on plastic or collagen I the cells are more susceptible to apoptosis induced by serum deprivation than HSC cultured on matrigel, a basement membrane – like matrix which reduces HSC proliferation and activation. Does ECM degradation therefore result in HSC apoptosis rather than HSC apoptosis facilitate ECM degradation?

A second key question is: does liver fibrosis reach a point where it becomes irreversible?

Recovery requires degradation of the existing fibrotic matrix, but this matrix itself may be modified to resist degradation as fibrosis progresses. Newly secreted collagen fibrils can be cross- linked by both tissue transglutaminase and lysyl oxidase pathway: the activity of both pathways is increased during liver fibrogenesis (293-296). Cross linking during maturation of collagen might reduce its susceptibility to collagenase (297). Tissue transglutaminase can be released onto ECM from apoptotic hepatocytes which are found in increased numbers in fibrotic liver (298).

Recovery is unlikely if collagenolytic enzymes remain inactive following cessation of liver injury. Interstitial collagenase mRNA expression (MMP-1 in humans, MMP-13 in rats) is similar in normal compared with cirrhotic livers, but has been demonstrated to increase in a recovery model possibly due to TIMP-1 activity decreasing, (262;269;286;286). Previous studies suggest that collagenase activity becomes deficient during evolution of liver fibrosis in animal models and in humans (254;255;257;272;299), and studies described earlier suggest that this may be caused by TIMP over expression. Continued inhibition of ECM degradation by TIMPs may block the ability to recover from fibrosis, even after the removal of the injury.

As associated hepatic stellate cells are an important source of both ECM and TIMPs recovery from fibrosis might require either removal of the activated HSC population, as shown in rat models or possibly the phenotypical reversal of stellate cell activation, a process yet to be observed *in vivo*.

1.15 Pancreas Fibrosis and Pancreatic Stellate Cells

The pancreas can be functionally divided into 2 components: the endocrine gland which produces amongst other things insulin for glucose regulation and an exocrine gland for production of enzymes that aid digestion. The exocrine component consists of clusters of acinar cells (acini) that secrete the digestive enzymes. The enzymes drain from the acini via pancreatic ducts into the duodenum. A schematic is demonstrated in Figure 1.8

Figure 1.9 Schematic of the cellular components of the exocrine pancreas

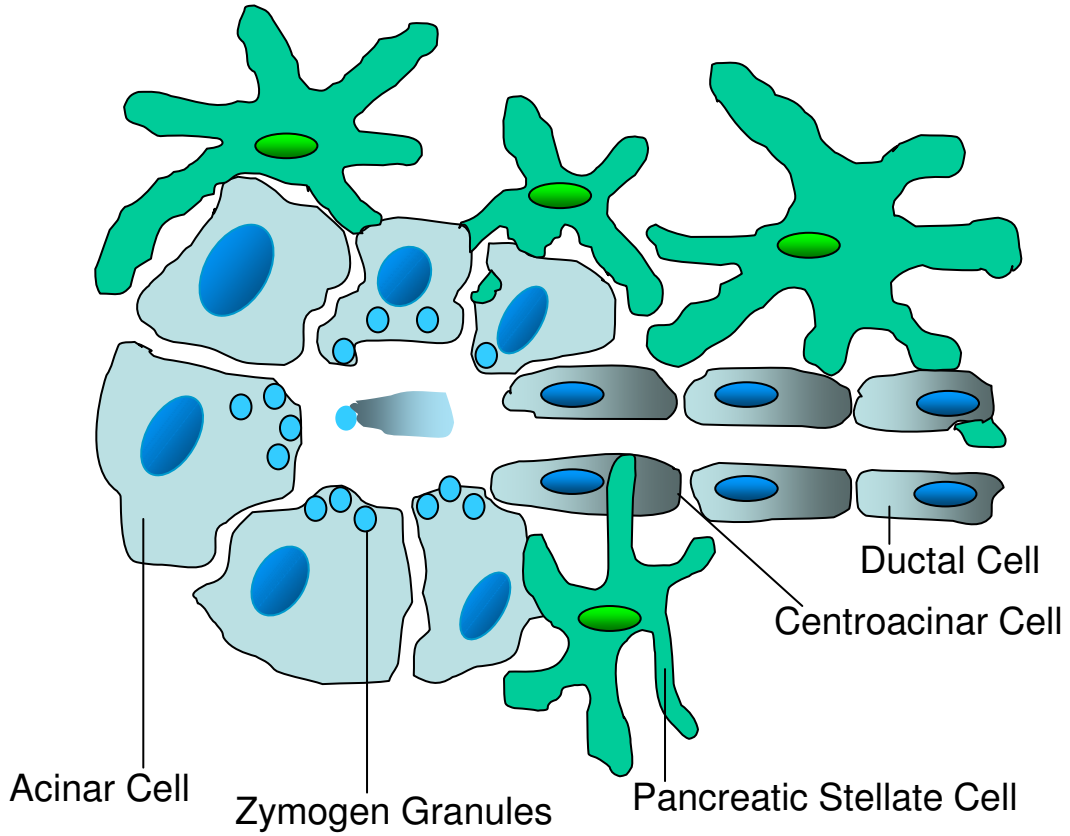

Figure 1.9 Schematic of the cellular components of the exocrine pancreas. The pancreas can be functionally divided into the exocrine and endocrine components. The exocrine component consists primarily of acini – clusters of acinar cells that feed into ductules. In normal pancreas quiescent PSCs are present in the periacinar space. These cells have long cytoplasmic processes that encircle the base of the acinus. Zymogen granules release their contents of digestive enzymes into the periacinar space into the pancreatic ductal system upon stimulation.

Pancreatic Stellate Cells (PSCs) are one of several resident cells in the exocrine pancreas. Present in the periacinar space, they have long cytoplasmic processes that encircle the base of the acinus (figure 1.9). They can also be found in perivascular and periductal regions of the pancreas and serve as key participants in the pathobiology of the major disorders of the exocrine pancreas, including chronic pancreatitis and pancreatic cancer (300-303). In these disorders PSCs participate in disease pathogenesis after transforming from a quiescent state into an "activated" state (also known as a "myofibroblastic" state). There are obvious similarities (as well as some differences) to the Hepatic Stellate Cells as will be highlighted in the subsequent discussions.

1.16 Clinical Setting of Pancreatic Disease

70-80% of all cases of chronic pancreatitis result from alcohol abuse while the remainder of cases are associated with genetic disorders such as hereditary pancreatitis and cystic fibrosis and unknown cases for example idiopathic pancreatitis (304-307). Autoimmune pancreatitis has recently been described (308).

The course of chronic pancreatitis results from repeated discrete episodes of acute pancreatitis which cause parenchymal injury and necrosis, with increasing amounts of fibrosis, chronic inflammation, and parenchymal cell loss with each successive episode. Parenchymal cells in both the exocrine pancreas and to a lesser extent the endocrine pancreas, are lost and this leads to irreversible exocrine (and eventually endocrine) insufficiency that leads to the disease known as chronic pancreatitis which can be characterised with abdominal pain, diarrhoea, weight loss, diabetes as a late presentation and ultimately an increased risk of pancreatic cancer (309;310).

This series of events which has been noted from examining human pancreatic tissue during alcohol induced acute and chronic pancreatitis has been termed the "necrosis-fibrosis" sequence – and provides a framework for understanding chronic pancreatitis (311).

Like chronic pancreatitis, adenocarcinoma of the pancreas has a remarkable fibrotic component (312-315).

1.17 Properties of PSCs

Cells in the pancreas that were similar to HSCs in that they were fat-storing cells were first observed with the use of auto-fluorescence and electron microscopy in 1982 (300). There were identified when rats were given vitamin A, because cells with cytoplasmic fat droplets, such as HSCs, became auto fluorescent when vitamin A accumulates in these droplets (300). Two reports described the isolation and initial characterization of what have henceforth been termed pancreatic stellate cells or PSCs (302;303). PSCs can be distinguished from normal fibroblasts in that they express desmin and glial fibrillary acidic protein (GFAP) and have intracellular fat droplets (302;303).

PSCs express intermediate filament proteins that usually characterise several cell types for example desmin which characterizes myocytes, GFAP - characteristic in astrocytes, vimentin seen in leukocytes/fibroblasts and endothelial cells and finally nestin seen in endothelial stem cells (316). This highlights that PSCs have a broad range of potential properties including contractility, the presence of cellular extensions to sense their environment, the potential to produce and alter ECM components and the potential to proliferate. The difference between quiescent and activated PSCs is denoted in Table 1.3. Activation of quiescent PSCs which occurs when primary PSCs are cultured and in the pancreas as a consequence of pancreatic injury is associated with several morphologic changes (302;303) including nuclear enlargement and enhanced prominence of the ER network (Table 1.3). Moreover, in situ hybridization and immunohistochemical studies indicated that activated PSCs express α-SMA and collagen type I, therefore highlighting these cells as a source of fibrosis in chronic pancreatitis and pancreatic adenocarcinoma (314;317;318).

Table 1.3 General features of quiescent versus activated PSCs

	Quiescent	Activated
Morphologic Features		
Vitamin A Auto fluorescence	+ in fat droplets	Absent or remnant
Endoplasmic reticulum	+	++
Nucleus	Basal Size	Enlarged
Molecular Markers		
Vimentin	++	++
Desmin	+	+
GFAP	+	+
Nestin	+	++
α-SMA	-	+
Properties		
ECM production	Limited	Prominent
Cell proliferation	Limited	Increased
Cell migration	Limited	Increased

Table 1.3 In isolating PSCs there appears to be some heterogeneity of marker expression that may reflect multiple states of activation or differentiation, or different pools of fibrogenic cell type. All PSCs isolated from rat pancreas express vimentin, yet only 20-40% express desmin (319).

Early efforts at PSC isolation produced cells that expressed α-SMA and collagen I, III and IV i.e. already activated (320), however with techniques used in isolation protocols for HSC studies, (especially density gradient centrifugation) quiescent PSCs could be isolated (302;303). Quiescent PSCs express desmin, GFAP and intracellular fat droplets but not α-SMA (See Table 1.3).

Primary PSCs become activated during culture and attain a myofibroblast-like phenotype characterized by the disappearance of intracellular fat droplets, and the expression of α-SMA and ECM proteins (collagen I, III and fibronectin (302;303). PSCs also increase their expression of nestin upon activation (321). On the basis of these markers PSCs are estimated to contribute 4% of total pancreatic cells as opposed to HSCs which comprise around 8% of all hepatic cells (71;302).

The early studies to date have examined the activation process of PSCs plated out on plastic. As in the study of HSCs a dilemma exists as to whether this activation model is representative of the in vivo environment (322). What is known is that PSCs cultured on plastic pass through

a series of temporal states of transformation (323). For example, rapidly proliferating PSCs in culture can either die by apoptosis or acquire a myofibroblastic differentiated state that is more resistant to apoptosis.

Immortalized PSC cell lines from rats and humans has been developed (324-326), thus providing a tool for over expression and RNA interference studies, as well as a tool for high throughput screening for compounds that affect PSC activation. Immortalized cell lines have been generated by expression of either SV40 large T antigen alone in rat PSCs or SV40 large T antigen and human telomerase in human PSCs. The resultant immortalized cell line possesses a phenotype consistent with activated PSCs, which includes expression of α-SMA and ECM proteins. DNA micro arrays have been used to compare the gene expression profile of immortalized and primary culture rat PSCs. These revealed only a few overall differences including differences in the expression of genes encoding ECM related proteins, cytokines, integrins and intermediate filament proteins (325). Both rat and human immortalized cell lines responded to TGF-β1, PDGF, and the PPARγ ligand PGJ_2 in a manner similar to that of their primary cell counterparts (325-327).

1.18 Mediators of PSC activation

Whilst initial activation could be distinguished from persistent activation, the events that cause both in PSCs are likely to be similar. Numerous growth factors, cytokines, hormones, intracellular signaling molecules and transcription factors as regulators of PSC activation have been described (328). Potential activation of PSCs in vivo included paracrine factors such as cytokines (IL-1, IL-6, IL-8 and TNF-α) growth factors (PDGF and TGF-β1) angiotensin II, and reactive oxygen species released by damaged neighbouring cells and leukocytes recruited in response to pancreatic injury (3;329-334).

Figure 1.10 Mechanisms of PSC activation

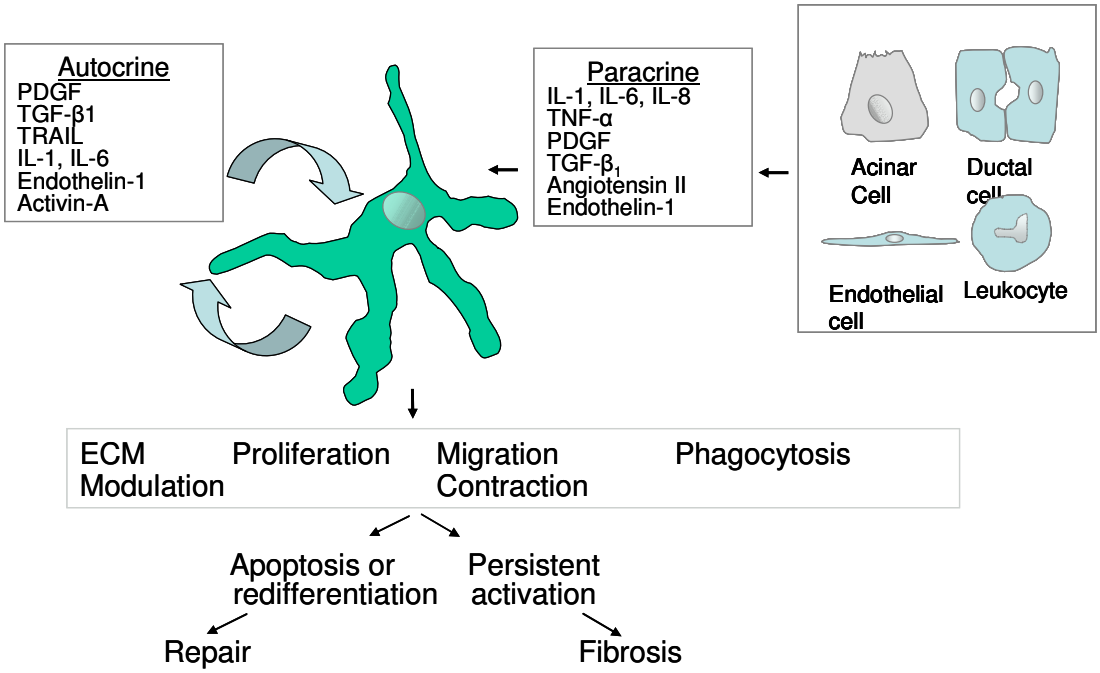

Figure 1.10 Mechanisms of PSC activation. Exposure of the pancreas to ethanol, to its metabolites, and to insults that generate ROS all result in PSC activation by autocrine and paracrine products. The paracrine factors are derived from neighbouring cells such as acinar cells, ductal cells, endothelial cells, and leukocytes. Activated PSCs can migrate to sites of tissue damage, undergo regulated contraction, proliferate, phagocytose, and generate products that modulate the ECM by facilitating repair or promoting fibrosis (335-338). Persistent activation of PSCs promotes fibrosis, while redifferentiation to a quiescent state or simulation to undergo apoptosis facilitates tissue repair.

Activated PSCs in turn can produce autocrine factors such as PDGF, TGF-β1 cytokines (IL-1, IL-6 and pro inflammatory molecules (COX-2) that can perpetuate the activated phenotype (3;333;339;340). See Figure 1.10 Activin-A, a member of the TGF-beta family of soluble factors, also functions in an autocrine manner, increasing collagen secretion and augmenting TGF-β1 expression and secretion (341).

Endothelin-1 is expressed by rat PSCs in primary culture and can stimulate their migration and contraction (342). Whilst several inflammatory mediators (that have potential to impact or regulate PSCs) are released during pancreatitis there is evidence that PDGF, TGF-β1, and angiotensin II have major roles, PDGF induces proliferation of PSCs and contributes to their migration potential; angiotensin II induces PSCs to express alpha SMA and ECM proteins (329;332;343-345).

Oxidative stress and ethanol metabolites have also been suggested as potential perpetuators of the activated PSC phenotype. Ethanol can be metabolized in pancreatic acinar cells, resulting in toxic metabolites and oxidative stress that can induce pancreatic damage (346). Cultured PSCs exhibit ethanol – induced alcohol dehydrogenase activity in vivo, suggesting that PSCs can also metabolize ethanol (346). Ethanol and acetaldehyde promote activation of rat PSCs in vitro and cause lipid peroxidation in these cells (346;347). Furthermore, vitamin E which is an antioxidant prevents ethanol and acetaldehyde induced activation of PSC, thereby suggesting that oxidative stress regulates PSC activation. 4-hydroxy-nonenal for example is a highly reactive product of lipid peroxidation and activates primary rat PSCs in culture. These in vitro findings have been supported by histological analysis of pancreatic sections from patients with chronic pancreatitis, which showed 4-hydroxy-nonenal staining localized to activated PSCs within fibrotic areas and to acinar cells adjacent to areas of fibrosis (318).

Multiple studies have identified several major signaling pathways involved in the regulation of PSC function (317;342;348-351). MAPKs are key mediators of activating signals initiated by growth factors, angiotensin II and ethanol (350;351). Other signaling pathways regulating PSC activation include P13K, RHO kinase, the JAK/STAT pathway, the activator protein-1 and NF-κB pathways and the TGF-β1/SMAD related pathways (342;349;352). PPARγ ligands have been implicated in pathways leading to down regulation (317). Characterisation of these pathways further could lead to potential therapeutic targets for the modulation of PSC function.

1.19 PSCs and pancreatic inflammation

Activated PSCs in culture express several growth factors and cytokines, as well as receptors for these molecules which are known to participate in inflammatory and fibrotic processes. Although incomplete, current knowledge of pancreatitis is thought to be initiated by damage to acinar ductal and/or mesenchymal cells in the pancreas (306;353;354). The pathological processes that follow on from damage include interstitial oedema, necrosis of parenchymal cells, intra pancreatic trypsin activation, inflammatory cell infiltration, and activation and proliferation of PSCs. In human and rodent pancreas, activated PSCs are noted in areas of extensive necrosis and inflammation where an environment rich in cytokines, growth factors and reactive oxygen species prevails (355-357). Time course studies have established that what comes first is parenchymal necrosis and inflammation followed by PSC activation

suggesting that the former is a prerequisite for the latter (358-360). Hence autocrine and paracrine mediators are probably involved in PSC activation. In turn activation facilitates PSC proliferation, migration and ECM deposition, which leads to fibrosis or ECM remodeling as part of a repair processes.

Analysis of pancreatic sections from patients with chronic pancreatitis and from experimental pancreatic fibrosis in rodents suggests PSCs play a central role in the development of pancreatic fibrosis. For example alpha SMA expressing cells are abundant in areas of fibrosis in pancreatic tissue sections from patients which chronic pancreatitis of different aetiologies (303;317;318;357). In these areas only alpha SMA expressing cells produce mRNA encoding procollagen α_1, indicating that activated PSCs are probably the predominant source of collagens during pancreatic fibrosis (317). In support of this, spontaneous chronic pancreatitis in the Wister Bonn/Kobovi (Wbn/Kob) rat is characterized by inflammation and PSC activation in areas of pancreatic fibrosis (349). Moreover, in vivo, rat studies of administration of tri nitrobenzene sulphonic acid into the pancreatic duct as well as I.V. injection of dibutyltin dichloride , induces necrosis and inflammation of the pancreas followed by PSC activation and fibrosis (317;361). In addition, mouse pancreatitis induced with the use of cerulein (a cholecystokinin analogue and pancreas secretagogue) is also accompanied by PSC activation and fibrosis (305;362).

The involvement of PSCs in the regulation of the inflammatory response during pancreatitis occurs, at least in part, through this production of chemokines and cytokines, as has been reported for myofibroblast-type cells in other tissues (363-366). PSCs have also been shown to have phagocytic activity in vivo and in cell culture (367) and therefore might also function as resident phagocytic cells during pancreatitis.

PSC phagocytic activity is regulated by PPARγ expression of CD36, a scavenger receptor that promotes phagocytosis. Interestingly, pro fibrogenic cytokines such as TGF-β1, TNFα and IL-I, decreased the phagocytic capacity of PSCs activated in culture (367). It is clear from what has been discussed that the regulation of pro fibrotic and pro inflammatory properties of PSC during pancreatic inflammation is complex.

1.20 Inflammation and PSC modulation of ECM

There is increasing evidence that PSCs have a key role in the extensive tissue fibrosis that accompanies chronic pancreatitis and leads to destruction of the pancreas and loss of exocrine function (344;355;357). Conversely, observational studies have shown that activated PSCs participate in tissue repair processes after acute necrotizing pancreatitis in humans and experimental acute pancreatitis in rodents (358-360;368). Activated PSCs, although their role is still not fully understood, appear to contribute to the provisional matrix at the site of injury that allows cell proliferation, migration, and assembly of new parenchymal cells (359;360;369). In addition PSCs can regulate ECM remodeling during pancreatic tissue repair through the production of ECM degrading proteases and their inhibitors, such as tissue inhibitor of metalloproteinase-I (TIMP-1) (3;370). In this context resolution of mouse cerulein induced pancreatitis involves transient activation of PSCs and deposition of ECM proteins as well as transient up-regulation of MMPs and TIMP-1 (360). It is likely that parallel processes of ECM remodeling by HSCs also mediate liver regeneration after experimental injury (371;372).

In most studies in which PSCs are activated after damage to the pancreas, the inflammatory process resolves and activated PSCs progressively disappear after the cessation of the injurious agent. However, repeated pancreatic damage and failure of the mechanisms regulating tissue repair can both lead to chronic inflammation, persistent activation and proliferation of PSCs and finally to fibrosis. Consistent with this hypothesis, repeated episodes of acute experimental pancreatitis produces changes that resemble those found in chronic pancreatitis (305;373). In fact, fibrosis in the pancreas and other organs can be considered the consequence of a wound healing process responding to chronic injurious stimuli. In humans, repeated damage to the pancreas is associated with chronic alcohol consumption, pancreatic duct obstruction, metabolic disorders and genetic defects (306;374). The chronic injury results in the perpetuation of the activated PSC phenotype. Furthermore chronic pancreatitis is associated with reduced production of MMPs by PSCs which probably helps promote and sustain the fibrotic phenotype (3).

In addition to the above, other mechanisms can explain the persistent activated state of PSCs during pancreatitis. For example activated PSCs express protease activated receptor-R (PAR-2) which is cleared by trypsin (a key pathogenic protease in pancreatitis) to become active.

Active PAR-2 stimulates PSC proliferation and collagen synthesis (375). Changes in the composition of the ECM during repair processes can also modulate PSC activation. For example, activated PSCs revert to a quiescent state when cultured on a basal membrane like matrix, thereby suggesting that ECM composition regulates PSC behaviour (3;376). Studies of liver fibrosis have shown that extensive ECM degradation is accompanied by apoptosis of HSCs, as a result of either increased pro-apoptotic signaling a reduced survival signals from the ECM (296) but it remains to be shown whether this is also true in the pancreas. More recently, impaired extra cellular proteolysis of the ECM in mice lacking plasminogen has been associated with persistent PSC activation and accumulation of pancreatic collagens during the recovery phase of mouse cerulein-induced pancreatitis (360). Moreover, levels of pancreatic TGF-β1 plasminogen activating inhibitor 1 and TIMP-1, factors that promote fibrosis (296;329) were elevated persistently in plasminogen-deficient mice after treatment with cerulein but only transiently in similarly treated plasminogen sufficient mice (360).

1.21 PSCs and pancreatic cancer

Ductal pancreatic adenocarcinoma is the most common form of pancreatic cancer with a five year survival of less than 5% (377). Several tumours and especially pancreatic adenocarcinoma are characterized by tumour desmoplasia, a remarkable increase in connective tissue that infiltrates and envelops the neoplasm (378). Activated PSCs in the tumour desmoplasia of human pancreatic cancers express α-SMA and co localize with mRNA encoding procollagen $alpha_1$-I (314) and are probably major contributors of the ECM proteins that constitute the desmoplasia (312;314;379-383). Of note, analysis of gene expression in human pancreatic adenocarcinoma, chronic pancreatitis, normal pancreas, and pancreatic cancer cell lines demonstrated that 107 genes predicted to be expressed in the stromal compartment were found in both pancreatic adenocarcinoma and chronic pancreatitis (380). Furthermore, isolation and characterisation of stromal cells from human pancreatic adenocarcinoma and alcohol induced chronic pancreatitis samples demonstrated that cells from both sources had the same characteristic morphology, cytofilaments expression, and capacity to synthesize ECM proteins (383). These results demonstrate that these two disorders contain common stromal elements and suggest similar mechanisms underlying the development of fibrosis in chronic pancreatitis and the desmoplasia in pancreatic adenocarcinoma.

Evidence is emerging that there is a symbiotic relationship between pancreatic adenocarcinoma cells and PSCs that results in an overall increase in the rate of growth of the tumours. E.g. culture supernatants from human pancreatic tumour cell lines stimulate PSC proliferation and production of ECM proteins (314;381-383). In addition the growth rate of tumour cells injected sub cutaneously into nude mice (mice that lack T cells and are severely immunocompromised) is markedly increased when PSC are included in inoculum (384). In contrast to the tumours that form when only both cancer cells and PSCs are used have a desmoplasia similar to that observed in human pancreatic adenocarcinoma (383). Furthermore pancreatic tumour cells induced the proliferation of PSC by secreting PDGF and include PSC production of ECM proteins by secreting TGF-β1 and FGF-2 (383). Although studies using animals indicate that pancreatic tumours cells and PSC promote each others proliferation, supporting data from human pancreatic tumours are limited and inconsistent. One report shows that more extensive intratumoural fibroblastic cell proliferation correlates with a poorer disease outcome (385). Another report shows that patients with a better outcome have increased expression of connective tissue growth factor (CTGF) in fibroblasts surrounding the human pancreatic tumours cells (386). CTGF has been implicated in the pathogenesis of fibrotic disease, and its expression is predominant in PSCs and is regulated by TGF-β. These early findings are intriguing and suggest that further work is needed to delineate the role of PSCs and their regulation in pancreatic cancer. The mechanisms by which PSCs and the desmoplasia enhance the growth of tumour cells in the adenocarcinoma are complex and only partly understood. One role of the desmoplasia is to promote survival and prevent apoptosis of the tumour cells through a direct action of ECM proteins on the tumour cells (387;388).

The pro survival effects of the ECM proteins laminin and fibronectin are mediated through their integrin receptors which are expressed by the tumour cells. In addition, the effects of fibronectin seem to be mediated through transactivation of IFG-1. Overall these interactions lead to the activation of pro survival and pro growth signaling pathways in pancreatic tumour cells (388;389). Another possible mechanism by which tumour desmoplasia might promote pancreatic adenocarcinoma cell growth is that PSCs and tumour cells produce MMPs and tissue serine proteases such as members of the plasminogen activating system, that degrade ECM proteins (360;370;390). In this context, MMPs and tissue serine proteases might promote tumour cell invasion and metastasis, as has been postulated in other cancers (390-393).

1.22 Comparison of PSCs and HSCs

Although PSCs and HSCs share several morphological and marker features, some differences exist. Unique, context-related features of HSCs include the portal perfusion and generally abundant vascular flow in the liver, and their proximity to encounter endothelial cell cross talk due to their hepatic location within the sub endothelial space (96). In addition, a genome-wide assessment of gene expression that included 21,329 genes identified 29 that were differentially expressed between cultures of primary HSCs and PSCs (394). However the fact that the overwhelming majority of genes showed no difference in expression supports the notion that these 2 cells types are very similar. Recent studies have revealed that the bone marrow is the source of 68% of HSCs and 70% of myofibroblasts in mouse models of carbon tetrachloride and thioacetamide-induced fibrosis (395). Whether the same holds true in the pancreas remains to be determined, but a common origin in the bone marrow could account for the strong similarities between HSCs and PSCs. In addition to stellate cells, other potential sources of fibrosis exist in both pancreas and liver. E.g. the hepatic myofibroblasts which are distinguished from HSCs by their location with the liver and their expression of the ECM component fibulin-2 but not GFAP (70;396), and tissue fibroblasts, which express vimentin but not GFAP and desmin represent an additional source of ECM proteins (70;82;396-398).

Subpopulations of fibroblastic cells which might reflect distinct levels of fibroblast activation can be distinguished in cirrhotic liver on the basis of differing levels of cellular retinol-binding protein-1 and alpha SMA (399), and these cells might also produce ECM proteins. The origin of these liver myofibroblast type cells and similar cells in the pancreas remains to be conclusively determined. Bone marrow transplantation on a mouse model of pancreatic insulinoma demonstrated that the bone marrow is the source of 25% of pancreatic fibroblasts and is likely to contribute to tumour associated fibrosis (400). In addition, nestin-positive and nestin-negative precursors isolated from adult mouse pancreas are able to differentiate in vitro to yield multiple lineages of the pancreas, including PSCs (401). The relative contribution of bone marrow and resident precursors to the PSC population, as well as to the other myofibroblasts and fibroblasts related cell populations, remains to be determined.

The function of quiescent PSCs is still being investigated, but clues can be gleaned from studies involving HSCs (71;371;402). For example HSCs have been implicated in several important liver physiologic roles, under basal conditions, that include vitamin A storage; production and turnover of normal ECM proteins; and communication with hepatocytes via gap junctions and the production of paracrine factors to promote hepatocyte differentiation, and to regulated ductal and vascular pressures. Similar roles can be envisioned for PSCs in the inactive state. For example, perivascular and periductal PSCs (301) might regulate the pressure within these compartments by contraction mediated by endothelin-1 (342). The functions of PSCs by analogy to HSCs should be envisioned not only in isolation but also in the context and under the influence of their microenvironment.

Although alcohol and/or its metabolites have been shown to similarly activate stellate cells of the pancreas and liver, it is unclear why substantial differences exist in an individual's susceptibility to liver and pancreas fibrosis. Potential differences between the pancreas and the liver after injury, in addition to the apparent difference in the cellular microenvironment, include oedema formation during pancreatitis; different ethanol metabolism in acinar cells and hepatocytes; and different lipid metabolism between acinar cells and hepatocytes (for example, " fatty pancreas" has not been described). Given that the stellate cell is an integral element of the onset of these diseases, microenvironment differences and other genetic and epigenetic modifiers related to stellate and/or other resident and infiltrating cells are likely to be important (Figure 5), but this hypothesis remains to be tested. For example, comparison of the response of PSCs and HSC isolated from the same animal with parallel comparative responses in different genetic backgrounds has not been reported. Furthermore, attempts at assessing genetic polymorphisms (e.g. in enzymes such as cytochrome P450 2E1 and aldehyde dehydrogenase-2) that may promote susceptibility to alcoholic chronic pancreatitis or cirrhosis have not been overly revealing (403). However an understanding of genetic polymorphisms that predispose to chronic pancreatitis (307;374) or liver fibrosis (404;405) or even protect from chronic pancreatitis (406), is being pursued. A systematic and broad based genetic screening will be needed, using well defined animal models and patient cohorts. Proteomic comparisons between PSCs and HSC, which are likely to be forthcoming, should also provide additional insights.

1.23 Hypoxia, Oxygen and genes in health and disease: an introduction

Excessive supply and reduced supply of oxygen to the tissues underlies the pathophysiology of many diseases. Excessive supply can produce toxicity; an extreme example of this is oxygen given to neonates and ultimately causes tissue death for example in myocardial or cerebral tissue. Reduced oxygen delivery, hypoxia, may lead to cell death.

Investigation into the molecular understanding of oxygen regulation began with the cloning of the erythropoietin gene (407). Although produced in the kidney and liver, a tissue culture model to investigate this physiological system was designed following the discovery that oxygen regulated erythropoietin-gene transcription occurs in the human hepatoma cell lines Hep3B and HepG2 (408). Following this, it was possible to isolate an oxygen-regulated control element in the DNA 3` to the coding sequence of the erythropoietin gene (409) (410-412). Was this control element and the mechanisms activating it specific to the erythropoietin gene and hepatoma cells, or could it operate more widely? Coupling the element to the promoter of other genes, such as alpha globin was found to confer oxygen regulation on the expression of these genes. Following transient transfection oxygen regulation of these artificial genes could occur in a wide variety of tissue culture cells. Not just those making erythropoietin, (413). Demonstrating that mechanisms impacting on the control element were expressed ubiquitously may have explained this. The generalized expression of a specific protein complex, hypoxia-induced factor-I (HIF-1) capable of binding to the erythropoietin control sequence provided support for this conclusion (414).

If this system existed in other cells not connected with erythropoietin production the inference was that the mechanism served another purpose, presumably the control of other genes in response to hypoxia. This led to speculation as to what these other genes might be. Candidates included genes involved in the angiogenesis, control of vasomotor tone and energy provision. Experiments on the glycolytic genes phosphoglycerate kinase -1 (PGK-1) and lactate dehydrogenase-A (LDH-A) provided the first clear evidence for a link with the erythropoietin system.

It was found that their mRNA accumulated in cells cultured in hypoxia conditions compared with normoxic controls. This phenomenon was dependent on specific DNA sequences

flanking these genes which were homologous to the erythropoietin control sequence and competed for binding of HIF-1 (415).

The list of oxygen genes has now expanded greatly (416) to include genes involved in glucose transport (Glut-1 and Glut-3) (417;418), gluconeogenesis (PEPCK) (419), vascular growth factor (VEGF), (420) vasomotor regulation (iNOS, endothelin) (421) (422), iron metabolism (transferrin), coagulation (tissue factor), (418), retroviral transposons, VL30 (423) and catecholamine synthesis (tyrosine hydroxylase) (424). The involvement of HIF-1 is common to many but not all of these.

Affinity purification of HIF-1 led to the cloning of two genes which encode basic helix-loop-helix PAS domain transcription factors, which dimerize to form the DNA binding complex (425). One of these proteins, HIF-1α was novel, the other was known previously as aryl hydrocarbon receptor nuclear translocator (ARNT).

Mutant hepatoma cells that fail to produce HIF-1 because of ARNT deficiency show substantially reduced hypoxic gene regulation, confirming the importance of HIF-1 in this response (426). Another protein with 48% homogeneity to HIF-1α called endothelial PAS domain protein (EPAS-1) appears to dimerize with ARNT and be regulated by hypoxia (427). This raises the possibility that a family of proteins exist that may serve similar but not identical functions in different tissues.

1.23.1 HIF-1 activation by Hypoxia

HIF-1α and ARNT mRNA levels do not change dramatically between normoxia and hypoxia culture conditions, suggesting that control is mediated at a translational or post translation level. Current evidence suggests that hypoxia relief of normoxia destabilization of HIF-1α protein may play a central role (428;429).

Other mechanism may be involved in hypoxia regulation of the complex. For example HIF-1α has been shown to bind to P300 (430), a non-DNA binding transcriptional activator, involved in a wide variety of responses. Whether this binding is itself regulated by hypoxia is unknown but it clearly has the potential to increase the power of transcriptional activation.

ATF-1 and CREB-1 may bind constitutively to the HIF-1 DNA recognition site (431) but the functional relevance of these observations is also unclear.

1.23.3 The sensor control

To elucidate what controlled these responses a haem protein sensor was proposed because hypoxia induction can be minimized by exposure to cobalt, nickel or manganese ions, can be abrogated by exposure to carbon monoxide and reduced by the haem synthesis inhibitor 4,6-dioxoheptanoic acid (432).

Hydrogen peroxide which is itself generated in an oxygen dependent manner by cells, can abolish the activation of HIF-1 and the consequent hypoxia up-regulation of erythropoietin, although whether it does so in the physiological range is not yet clear.

1.23.4 Hypoxia studies in the liver

Little has been published recently with regard to MMP and TIMP expression in the liver in hypoxia versus normoxia. Human HSCs were studied in normal oxygen condition and hypoxia (1%). Shi reported that in hypoxia the expression of HIF-1α and VEGF was induced. Western blotting demonstrated the expression of alpha SMA to increase with hyoxia stimulation. The expression of MMP-2 and TIMP-1 genes was also increased. Hyoxia also elevated the expression of collagen type-1. The analysis of TGF-B / SMAD signaling pathway showed that hypoxia potentiated the expression of TGFβ-1 and the phosphorylated status of Smad-2 (433)**.**

Brenner et al (434) documented the effects of alcohol on fibrogenesis. Although the major mechanisms of fibrogenesis are independent of the origin of liver injury, alcoholic liver fibrosis features distinctive characteristics including the pronounced inflammatory response of immune cells due to elevated gut derived endotoxin plasma levels, increased formation of reactive oxygen species (ROS), ethanol induced pericentral hepatic hypoxia or formation of cell toxins and pro-fibrogenic ethanol metabolites (eg acetaldehyde or lipid oxidation products). These factors are together responsible for increased hepatocellular cell death and activation of HSC (435).

In the knowledge that hypoxia leads to enhanced production of angiogenic factors, such as vascular endothelial growth factors (VEGF), HSC were studied in hypoxia. Low oxygen conditions led to the expression of VEGF mRNA which was dose dependent and time dependent. The expression of VEGF mRNA correlated with the secretion VEGF protein in conditioned media. VEGF mRNA expression could be enhanced by mimics of hypoxia conditions using S-Nitroso-N-acetyl-D-L, penicillamine (SNAP), nitric oxide (NO) and cobalt chloride. The hypoxic induction of VEGF may be of mechanistic importance in the pathogenesis of hepatic wound healing and hepatic carcinogenesis (436).

The expression of MMP-2 and TIMP-2 in rat cultured HSC was detected by immunocytochemistry. MMP-2 was enhanced in hypoxia while the expression of TIMP-2 was decreased. Over time the relative amount of MMP-2 was highest in the 6hr group with a contrary curve in TIMP-2. It was concluded that hypoxia promotes the expression of MMP-2 and inhibits the expression of TIMP-2 in HSC. This observation was more noticeable at early stages of hypoxia (437).

The same group repeated their work, again in hypoxia but also in hyperoxia. MMP-2 expression rose in hypoxia as before with a concomitant fall in TIMP-2 expression – the greatest changes being at 6hrs. With hypoxia the protein contents of MMP-2 and TIMP-2 were both increased at 12hrs versus control. MT1-MMP was also increased (438).

1.24 Inhibition of Tissue inhibitors of Metalloproteinases

As has been described, the inhibition of MMPs in the extracellular space represents a regulatory mechanism of matrix: the major inhibitors being the TIMPs which are capable of binding to and inhibiting the MMPs (214). In liver cirrhosis decreased collagenolytic activity has been observed along with increased levels of TIMP-1 (285). Studies by Iredale et al suggested that the decrease in collagenolytic activity during the development of liver fibrosis, in a rat model, was due to overexpression of TIMP-1 mRNA (90). TIMP-1 and TIMP-2 have been shown to be upregulated 3-7 fold in a variety of liver diseases which correlated with liver hydroxyproline content (439). Previous work by colleagues in the Southampton liver group have suggested that TIMP-2 may be increased in fibrotic liver disease in conjunction with MT1-MMP (440), yet traditionally TIMP-2 expression has been conceptually viewed as constitutive.

1.25 Hypothesis

Liver cirrhosis is characterized by increased net deposition of fibrillar and non fibrillar collagens, glycoconjutes and proteoglycans. This can occur either through excessive production, failure of degradation or a combination of the two. HSC have been shown to be the major producers of ECM and matrix metalloproteinases in the diseased liver. Activity of MMPs is tightly regulated. Gelatinase A which has actions against fibrillar and non-fibrillar collagens, has been found to be produced by activated HSC in vitro and in vivo. In liver cirrhosis its mRNA is upregulated. The activation of gelatinase A involves the complex of MT1-MMP/TIMP-2/gelatinase A at the cell surface and can be inhibited by excess TIMP-2. The hypothesis examined in this thesis is that TIMP-2 expression is upregulated during HSC activation and progressive liver fibrosis in vivo and in vitro. It is proposed that potential novel pathways exist of TIMP-2 regulation in HSC.

1.26 AIMS

The aims of this thesis were:

1. To determine the key sequences of the TIMP-2 gene promoter which regulate TIMP-2 expression during hepatic stellate cell (HSC) activation and pancreatic stellate cell (PSC) activation.

2. Determine at what level the enhanced expression of TIMP-2 mRNA observed in activated HSC and activated PSC is regulated using Nuclear Run On assays (studies of mRNA production).

3. Perform studies of the TIMP-2 promoter activity in HSC and PSC in collaborative work with Dr Yves De Clerk.

CHAPTER 2

GENERAL METHODS

2: Materials and General Methods

2.1 Materials

This chapter sets out to document the general methods used repeatedly throughout the course of this thesis including the method development for individual techniques where appropriate. Unless otherwise stated, chemicals and reagents were obtained from Sigma, Poole, UK. General solutions and buffers etc are listed in Appendix I.

2.1.1 General Methods

I would like to thank and acknowledge the help and hard work of Dr Julie Trim & Dr Marianna Gaca who both helped supervise me on a day to day level with certain techniques such as Northern Blotting, DNA sequencing, transfection techniques etc. Dr Matt Wright was an enourmous help in teaching me techniques involving plasmid DNA preparation.

2.1.2 Immunohistochemistry

This method relies on the binding of specific antibody to the antigen on the tissue and then the antigen location can be visualized using a marker to the antibody-antigen complex. Here, the primary antibody was detected using a three stage streptavidin-biotin complex technique. A biotinylated secondary link antibody binds to the primary antibody and when the tertiary layer of avidin-biotin enzyme complex finally binds to the secondary antibody an intense colour was produced when streptavidin peroxidase conjugate and DAB chromogen added. Negative controls were performed by repeating the experiments withouth the primary antibody.

Materials

Absolute Methanol, BDH, Poole, UK

Alcohol (70%, 100%)

3,3`– diaminobenzidine tetrahydrochloride (DAB), Dako

DMEM, Invitrogen Life Technologies, Paisley, UK

DPX, Poole, UK

Harris haematoxylin*

Hydrochloric acid (1%) / Alcohol (70%)

PBS

Primary Antibody: Non-immune rabbit IgG, 18140, Sigma, UK
Monoclonal Mouse anti-human Desmin (1:50) – N1526

Clone- D33 (Dako, Abingdon, Oxon, UK)

Mouse monoclonal antibody to rat α-SMA
- A5228 Clone 1A4, Sigma,
Monoclonal Mouse anti-Human Ki 67 – N1633 Clone-MIB-1 (Dako, Abingdon, Oxon, UK)

Monoclonal Mouse anti- NGF receptor p75- NCL-NGFR (Novocastra Laboratories Ltd, UK)

Rabbit Anti-Nerve Growth Factor-Beta polyclonal antibody- AB1526SP (Chemicon International, USA)

Secondary Antibody: Monoclonal antibody to biotin – 11 297 597 001 (Clone 33) (Roche Diagnostics, Mannheim, Germany)

Secondary Antibody: Polyclonal swine Anti-Rabbit immunoglobulin/Biotinylated – E0353 (Dako, Abingdon, Oxon, UK)

Strept AB Complex/HRP – K0377 (Dako, Abingdon, Oxon, UK)

The archival human chronic pancreatitis tissues used in this project were all fixed in formalin and embedded in paraffin. Formalin fixation can cause the epitopes of the antigen to undergo substantial changes and can even crosslink with other unrelated proteins. This results in the partial or complete loss of the immunoreactivity by the antigen and/or the "masking" of the antigen. Initially the attempts to improve the immunoreactivity were by the use of tryptic digestion prior to staining. However, the use of enzymes may entail the risk of destroying the epitopes. Later methods included microwave heating (441) and the use of citrate buffer (pH6.0) together with the effect of heat further improved the technique of antigen retrieval (442). More recently, it has been reported the combined use of heat and enzyme (protease) digestion produced a superior staining than when only one of the measures were used (443). Prior to antigen retrieval, the tissues have to be deparaffinized by soaking the slides in xylene

twice in 10 min each and then rehydrated through graded alcohols to 70%. Endogenous peroxidase was inhibited with 0.5% hydrogen peroxidase in methanol for 10 min.

For freshly isolated PSC studies, cells were cultured into 1 well-chambers glass slides (Lab-Tek®) at a density of 10,000 cells per well. The cells were harvested after 7 days and the slides were washed with sterile PBS. The slides were air dried and stored at -20^{0}C until immunostaining was performed. The slides were defrosted and again air dried to remove the condensation, the cells were then fixed by adding absolute methanol to denature the proteins. Once the methanol had evaporated, the primary antibody may be applied. Sections were then washed in Tris-buffered saline (TBS), pH 7.6 before the addition of the primary antibodies at optimal dilutions as follows: α-SMA (1:50) and desmin (1:50). For negative controls, the primary antibody was replaced with non-immune IgG and TBS alone. After incubation with the primary antibodies, sections were washed in TBS (3x5 min) and incubated with biotinylated anti-mouse anti-serum (Roche Diagnostics, Mannheim, Germany) for 30 min. Sections were washed as before, and then incubated with streptavidin complexed with biotinylated horseradish peroxidase (Dako, UK) for 30 min. After washing with TBS as described above, sections were exposed to 3`-3`- Diaminobenzidine (Sigma) for 8 min, followed by TBS rinse. Finally the sections were counter stained in Harris' hematoxylin, dehydrated through graded alcohol and mounted.

2.1.3 Method 1: Preparation of slides

Microscope slides were coated with 3-Aminopropyltriethoxysilane (APES) for In-Situ hybridization and immunocytochemistry according to the protocols of V.an Prooijen-Knegt et al. (444).

In brief the following equipment and reagents were required:

1. 3-Aminopropyltriethoxysilane (APES) -Sigma, cat no: A3648. Store at +4^{0}C
2. Technical grade acetone (in inflammable cupboard)
3. RO water

Slides were racked into large stainless steel units and washed on a routine cycle (65°C). Excess water was shaken off and the slides dried in the glass drying cabinet overnight. 800ml of 2% APES in acetone (16ml of APES to 800ml of acetone) was made up in the fume hood. Each rack was immersed, in the fume hood, in 800ml of each solution in the plastic staining troughs as follows:

a. 2% APES solution -5 seconds
b. Acetone (1) -5 seconds
c. Acetone (2) -5 seconds
d. RO water (1) -5 seconds
e. RO water (2) -5 seconds

Racks were then placed on absorbent paper to drain and then transferred to the glass drying cabinet overnight to dry. Slides were then stored for use.

2.1.4 Method 2: Antigen Retrieval -Proteolytic Enzyme -Pronase Pre-treatment

In fixed paraffin-embedded tissue sections demonstration of some antigens is enhanced after pre-treatment with the proteolytic enzyme pronase. The effectiveness of proteolysis for antigen retrieval is related to the length of fixation and the type of fixative used. The following reagents were used:
1. Pronase -Dako cat no S2013 2
2. TBS pH 7.6
3. 1% Pronase Stock Solution was made up by dissolving l00mg pronase in 10ml of TBS then stored in 0.1m1 aliquots at -20°C: stable for one year. Repeated freezing and thawing was avoided.

Sections were mounted on APES coated slides and dried for 24 hours at 37°C before staining. Sections were de-paraffinised and endogenous peroxidase blocked in the usual way and placed in water until required. The 0.05% Pronase working solution was prepared by thawing one vial of 0.1ml of Pronase Stock Solution, adding 1.9ml of TBS and mixing well. Slides were drained and covered with 200µl of 0.05% pronase, incubated at room temperature for approximately 15-20 min (depending on the length and type of formalin fixation). The slides

were then washed in TBS twice for 5 min before continuing with the immunostaining technique.

2.1.5 Method 3: Antigen Retrieval - heat mediated – microwave pre-treatment using citrate or EDTA buffer

In fixed paraffin-embedded tissue sections demonstration of some antigens is enhanced after pre-treatment in a microwave oven using a pre-selected buffer (citrate, EDTA or urea) (445).

The following equipment and reagents were used: microwave oven, Panasonic NN-6450 (800 watts). Solutions included the following:

I. 0.01M citrate buffer (pH6.0) prepared as follows:
Citric acid crystals 2.1g
RO water 1000m1
Adjust pH to 6.0 with 1M sodium hydroxide (approximately 25ml).

OR

EDTA 1mM pH 8.0 prepared as follows:
EDTA 0.37gm
RO water 1000 mL
Adjust to pH 8.0 with 0.1M NaOH (approximately 8ml)

The antibody register was consulted for recommended buffer to be used for each antibody. Sections were mounted on APES coated slides and dried for at least 24 hours at 37^0C before staining. Sections were de-paraffinised and endogenous peroxidase blocked in the usual way and placed in water until required. The plastic staining racks were filled with 24 slides and placed in the polythene box. Each box was filled with 330m1 of prepared buffer and covered. The microwave was set to medium power and run for 25 min. Each box was removed and filled quickly with cold running water then left in running water for 2-3 min before being returned to the staining trays and washed in TBS twice for 5 min each before continuing with the immunostaining technique.

2.1.6 Method 4: Antigen Retrieval -Heat-mediated -Pressure Cooker Pre-treatment

In fixed paraffin-embedded tissue sections demonstration of some antigens is enhanced after pre-treatment in a pressure cooker using a pre-selected buffer (citrate, EDTA or urea) (446).

The following equipment was required: Stainless steel pressure cooker (Tefal Optima, 8/13Ib pressure), hot plate, stainless steel staining racks with wide slots, 8 inch Spencer-Wells type forceps. The following solutions were made up:

I. 0.01M citrate buffer (pH6.0) prepared as follows:
Citric acid crystals 2.1g
RO water l000ml
Adjust pH to 6.0 with IM sodium hydroxide (approximately 25ml).

OR

EDTA lmM pH 8.0 prepared as follows:
EDTA 0.37gm
RO water 1000 ml
Adjust to pH 8.0 with 0.1M NaOH (approximately 8 ml)

The antibody register was consulted for recommended buffer to be used for each antibody. Sections were mounted on APES coated slides and dried for at least 24hours at 37°C before staining. Sections were de-paraffinised and endogenous peroxidase blocked in the usual way and placed in water until required. Slides were placed in stainless steel staining racks in such a way that pairs of slides were used back to back (providing larger gaps between sections and preventing bubbles from becoming lodged).
When the buffer boiled freely, slide rack(s) were placed into the pressure cooker chamber using the large forceps and fitted to the lid carefully. The regulator valve was set to 13lb pressure and pressure was allowed to build up. Timing was commenced for 2 min when a steady stream of steam escaped from the regulator. The slides were removed, placed back in staining trays and washed twice for 5min in TBS before proceeding with the immunostaining.

2.1.7 Method 5: Demonstration of Enzyme Peroxidase using Biomed Liquid DAB Substrate Kit

The peroxidase label on the final stage reacts with hydrogen peroxidase and Diaminobenzidine (DAB) to form an insoluble brown precipitate at the site of antigen/antibody reaction (447). The following reagents were obtained concentrated in kit form (Sigma) and stored between 2-8°C:

2 x 4ml of 3, 3'-diaminobenzidine chromogen solution.
20ml of l0X concentrated substrate buffer.
2 x 3ml of hydrogen peroxide substrate solution.
2.5ml of working solution (allowing 200µl per slide) was prepared as follows:

Add 0.25ml of l0X substrate solution to 2.25ml RO water
Add 2 drops of chromogen and mix
Add l drop of Hydrogen Peroxide (H_2O_2) substrate solution and mix

Enough working solution (2-5 drops) was used to entirely cover the tissue section only and slides were then incubated at room temperature for 3-10 min. In most cases, colour development was completed in 5 min. However, development time varied due to the amount of specific antigen/antibody binding in the specimen and the ambient temperature of the room.

2.1.8 Method 6: Streptavidin-Biotin Peroxidase Complex (StABCPx) immunostaining technique for fixed, paraffin embedded sections using monoclonal or polyclonal antibodies

Antigen binds to either a monoclonal or polyclonal antibody which is then detected using a three stage Streptavidin-Biotin peroxidase complex technique. The enzyme label peroxidase is then demonstrated using the chromogen diaminobenzidine (DAB) or 3-amino-9-ethyl-carbazole (AEC) (448).

The following solutions were made up:

1. Inhibitor for endogenous peroxidase (0.5% H_2O_2 in methanol)
Hydrogen peroxide (30%) 0.2m1
Methanol 11.8m1

2. TRIS buffered saline pH 7.6 (TBS):
Sodium chloride 80g
TRIS hydroxymethyl methylamine (TRIS) 6.05g
IM hydrochloric acid 38m1
RO water to 10L

3. Bovine serum albumin (BSA):
To one aliquot (mL) of 10% BSA (-20^{0}C), add 9m1 TBS.

Sections were de-paraffinised twice in low toxicity processing solvent (BDH laboratories) for 5 min each and rinsed in 100% alcohol for 1 minute followed by 70% alcohol for a further minute. Endogenous peroxidase was inhibited by treating with freshly prepared inhibitor (Reagent 1) for 10 min. Slides were then washed well in RO water. The antibody register was consulted before proceeding for recommended techniques of antigen retrieval. If antibody retrieval was not necessary, 1% BSA in TBS for 30 min (Reagent 3) was applied, the slides drained and primary antibody applied. Methods for antigen retrieval are outlined above.

The primary antibody was applied in correctly diluted in TBS and incubated either at room temperature for 30 min or at 4°C for 18-24 hours (overnight). Again the antibody register was consulted for recommended incubation time for each antibody. For slides incubated overnight at $+4^0$C a period of 15 min was incorporated to allow warming up to room temperature before washing prior to a wash in TBS three times for 5 min each.

Biotinylated sheep anti-mouse Ig (BAM) for monoclonal antibodies or biotinylated swine anti-rabbit Ig (BAR) for polyclonal antibodies were applied at the current dilution in TBS, for 30 min at room temperature. Peroxidase labeled complexes were prepared at this stage by adding the equivalent of 2µl of solution A, 2µl of solution B to 396µl of TBS making a 1:200 dilution and left on the bench to complex. Slides were washed in TBS three times for 5 min each prior to the application of the prepared Streptavidin/ Biotin peroxidase complexes for 30 min at room temperature. Slides were then washed again in TBS three times for 5 min each. DAB substrate was applied for 5 min prior to a final rinse in TBS, followed by a wash in running tap water for 2 min. Slides were then rinsed in 70% alcohol, counterstained with Harris' haematoxylin for 1-2 min, rinsed in tap water for one minute and differentiated in 1% acid alcohol for 5 seconds before being 'blued' in running tap water for at least 5 min. The slides were then dehydrated clear and mounted in DPX.

2.2 Isolation and Culture of Hepatic Cells

Appropriate home office licenses were obtained and local ethics committee approval obtained before any animal work was undertaken. In order to study the cellular origins of TIMP-2 in the liver, it was essential to obtain highly pure and functionally intact hepatic cell populations from normal liver. Parenchymal cells constitute the predominant fraction of cells (65%) in the normal mammalian liver (449), the rest being made up of endothelial cells, HSC and KC in roughly equal proportions. A number of methods for the isolation of purified populations of the different cell types in the liver have now been described, all involve sequential perfusion of the liver via the portal vein with a calcium free buffer to dissociate intercellular calcium dependent desmosomal junctions (450). This is followed by perfusion with collagenase diluted in a calcium containing buffer, to allow enzymatic activity. Collagenase digestion on its own allows isolation of both parenchymal and non-parenchymal cells from the same liver (450) but has the drawback of yielding relatively impure cultures even after subsequent purification (451). More aggressive digestion of the liver by the addition of pronase gives much purer populations of HSC and KC from a single liver (451) (452;453). The disadvantage of such aggressive digestion is that it damages membrane receptors for up to 24 hours after isolation (451).

The following methods describe the isolation technique used for rat hepatic cells; the different techniques for human hepatic cell isolation will be discussed later. The majority of the cells isolated in the first half of my stay in the liver unit were carried out by Jan Gentry MLO, in the second half rat HSC were obtained through the work of colleague researchers Matt Wright, David Smart and Julie Trim – I am extremely grateful to them all for their important work.

2.2.1 Method of Isolation of Rat Hepatic Stellate Cell

Rat hepatic cells were isolated by the method of Friedman (454) with modifications as described by Arthur (455). Male Sprague-Dawley rats (450-750g body weight) were anaesthetized by intraperitoneal injection of Hypnorm (Jansen) and midazolam. A simultaneous injection of 2500 units of heparin was also administered intraperitoneally to prevent intra portal thrombosis. The anaesthetized animal's belly was swabbed with videne scrub before a section of skin was removed and the portal vein was exposed at laparotomy. Two sterile 3.5/0 silk sutures were placed behind the portal vein in preparation to secure a 17.5G intravenous cannula (Wallace, UK) pre-primed with 2500 units of heparin. This was then inserted into the portal vein so that

the tip of the catheter was still in the main portal vein before its division to ensure an even perfusion of the liver. Perfusion was immediately commenced with sterile, calcium-free Hanks Balanced Salt Solution (HBSS) pH 7.4 (Imperial, UK) and the inferior vena cava was severed to allow resistance-free perfusion and for all the portal blood to be flushed out. Adequate perfusion was signaled by blanching of the whole liver which was then carefully removed (whilst ensuring constant perfusion was maintained) and placed in a covered, 10 cm diameter sterile Petri dish.

Perfusion of 200ml calcium-free HBSS was followed by 100ml of 0.275 % pronase (S. Griseus, Boehringer, UK) in HBSS and then 225ml 0.008 % collagenase B (Boehringer) in HBSS. All perfusions were carried out at a constant flow rate of 10ml/min and a delivery temperature of 39°C (normal rat body temperature). When the perfusion was complete the liver was transferred to a sterilized laminar flow cabinet and the capsule was opened. The digested slurry was dispersed in 100ml (total volume) 0.02% pronase/HBSS containing 2.4mg/ml deoxyribonuclease (Boehringer). After incubation for 30 min in a shaking oven at 37°C, the cell suspension was filtered through a sterile nylon gauze (125µm, John Staniar and Co., Manchester, UK) to remove fibrous and vascular remnants and washed threefold at 500g for 7 min in 200ml HBSS containing 1.2mg/ml deoxyribonuclease to prevent cell clumping in the presence of free DNA in solution from damaged cells. After the third wash, the supernatant was relatively clear of cell debris and the cell pellet was re suspended to a total volume of 44.4ml in HBSS containing 2.4mg/ml deoxyribonuclease before separation by density gradient centrifugation. Buoyant HSC were separated from the resulting cell suspension over a discontinuous 2 layer Nycoprep (Nycomed, Birmingham, UK) gradient prepared as described by Hendriks et al (456). This consisted of a 4 ml lower layer of 17.2% Nycoprep (w/v) in HBSS and a 7.4ml upper layer of cell suspension in HBSS/0.5% deoxyribonuclease containing Nycoprep (final concentration 11.5%) carefully overlaid in 15ml centrifuge tubes (Greiner) finally covered with 0.5ml of HBSS. To prepare the lower layer 16ml of HBSS was added to 24ml of a 27% Nycoprep and 4ml of this was placed in ten 15ml centrifuge tubes. The upper layer was made up by adding 29.6ml of Nycoprep to exactly 44.4ml of the filtered and washed cell suspension in HBSS/0.5% deoxyribonuclease giving a final Nycoprep density of 11.5%. After centrifugation at 1400xg for 20 min in a Beckman TJ-6 centrifuge. HSC were isolated from the top of the 11.5% layer and KC from the 11.5%/17.2% interface.

Further purification was obtained by the use of centrifugal elutriation (Beckman JE2-21 centrifuge fitted with a JE6-B rotor, Beckman Instruments, Geneva, Switzerland). Centrifugal

elutriation is a well documented method of separating particles mainly by their size. It involves circulating a suspension of cells through a specialized chamber in a centrifuge rotor flowing against the direction of centrifugal force. At a given flow rate and rotor speed, cells in the suspension will be sorted according to their size and density, with the smallest cells at the front (closest to the rotor spindle). HSC which are the lightest cells can therefore be continuously collected leaving behind heavier contaminants in the chamber. Different cell populations require specific rotor speeds and flow rates as previously described (457) (458) (459) (460-463). HSC were purified at a rotor speed of 1500rpm with a flow rate of 18ml/min in HBSS; KC at a rotor speed of 2500rpm, flow rate 45ml/min. Cells were collected in a total volume of 150ml and were then pelleted down before re suspension in Dulbecco Modified Eagles Medium (DMEM, Gibco) containing antibiotics and 16% foetal calf serum (FCS) in preparation for cell culture.

2.2.2 Preparation of Human Hepatic Stellate Cells

I am grateful to Drs Matt Wright and Julie Trim for their work in developing the isolation of human HSC in the department. This technique was adapted from the method of Pinzani (464). 12 normal human liver preparations were obtained from the resection margin of partial hepatectomies performed to resect isolated hepatic metastases (kindly provided by Professor Primrose, Professor of surgery, Southampton General Hospital). Ethics approval for this work was obtained through the local Southampton University Ethics Committee. Each patient was counselled by a member of the surgical team prior to their operation and written consent was sought on each occasion. Inclusion criteria for example consisted of a diagnosis of a primary malignant condition such as colorectal cancer with liver metastase for patients over the age of 18. For normal liver preparations exclusion criteria included diffuse parenchymal liver disease. For each patient data was available regarding their clinical condition and their concurrent medication list. Each specimen was carefully inspected for evidence of tumour involvement and rejected if any was seen. The liver was then perfused manually with calcium free HBSS until it was cleared of visible blood. The liver was then placed on a sterile Petri dish and it was perfused with 100ml of calcium containing HBSS at 37°C to which 1g pronase, 80mg collagenase and 1mg DNAse had been added. Maceration was performed by repeated cutting with sterile scalpel blades whilst the liver was still in the enzyme solution. The resulting cell suspension was purified by separating over a discontinuous 2 layer gradient and by centrifugal elutriation as above.

2.2.3 Assessment of Cell Number and Viability

The viability of all cells, immediately after isolation, was routinely determined by exclusion using 0.05% (w/v) Trypan blue dye. Viable cells stay small, round and refractile. Non-viable cells become swollen, enlarge and stain dark blue. Both the total cell count of cells/ml and percentage of viable cells were determined. Cells were counted using a hemocytometer with Neubauer ruling and total number calculated by correcting for total volume of cells and trypan blue dilution factor. Cell viability was generally good with >98% of cells viable in most isolations.

2.2.4 Cell Culture

Purified HSC and KC elutriation fractions were washed and re suspended in DMEM containing 16% foetal calf serum (FCS), penicillin (20mU/ml), streptomycin (20mg/ml) and gentamicin (20mg/ml) (PSG). Cell viability and total yield in this suspension were calculated on a hemocytometer (as above). Cells were seeded at a plating density of 1.33 $x10^6$ cells/ml on uncoated 50ml (25cm^2) plastic flasks (Greiner) in 5ml of culture medium (DMEM, 16% FCS, PSG). The cells were maintained in culture in a humidifying incubator at 37°C in 5% CO_2. The culture medium was changed every 48 hours.

2.2.5 Characterization of Hepatic Stellate Cells

Isolated hepatic stellate cells have a very characteristic morphology under phase contrast microscopy (Leitz inverted microscope). Initially in culture on uncoated plastic, they are round cells with few cytoplasmic processes for the first 24 hours after plating. During the first two days they gradually adhere to the plastic, become spindle shaped and develop cytoplasmic processes, giving them a more stellate appearance. In addition they contain abundant retinoid vesicles within their cytoplasm which permits their identification by autofluorescence under UV light. After further culture on plastic, stellate cells gradually lose their retinoid droplets. This process is widely described as characteristic of their activation into a myofibroblast-like phenotype (457;462;465-469) and is associated with expression of desmin and α-SMA (457;462;470-474). Having attained this activated phenotype, stellate cells then proliferate so that by 7-14 days in the standard culture methods used in this thesis they had reached confluence. The rate of morphological transformation in culture was consistently found to be inversely

proportional to the initial plating density of viable cells, making it imperative to standardize plating density. In order to assess purity of cell culture, HSC were identified either by vitamin A autofluorescence or by indirect immunofluorescence for desmin, whilst contaminating KC were identified by staining for endogenous peroxidase (470;472;473;475-478).

2.2.6 Cell Purity

Highly pure populations of rat HSC were obtained as assessed by vitamin A autofluorescence at day 2 (>98% n=5), and desmin staining at day 4-7 (>99% n=6) (262). The major contaminants were KC demonstrated by endogenous peroxidase staining at day 2 (<2% n=6) (205). As HSC proliferated at later time points in culture, KC had minimal influence on the purity of HSC.

2.2.7 Pancreatic Stellate Cells Isolation

Materials
Collagenase P, Roche Diagnostics
Pronase, Roche Diagnostics
Deoxyribonuclease, Roche Diagnostics
Dulbecco Modified Essential Medium (DMEM), Invitrogen Life Technologies, Paisley, UK
Foetal Calf Serum (FCS), Invitrogen Life Technologies, Paisley, UK
Hanks Balanced Salt Solution (HBSS) plus calcium (1.4g Calcium Chloride/l), Invitrogen Life Technologies, Paisley, UK
Optiprep, Invitrogen Life Technologies, Paisley, UK
Penicillin/Streptomycin PSG), Invitrogen Life Technologies, Paisley, UK
Gentamicin (PSG)
Trypan blue solution (0.4% w/v)

Rat pancreatic stellate cells extraction in our department was initially performed by Dr. David Fine using a modification of the method previously described (479) for the isolation of pancreatic acinar cells. This technique was later modified by a member of the Liver Group, Fiona Walker and then by Dr Fanny Shek to enhance the yield and purity of the preparation. Pancreata from Sprague-Dawley rats (300g plus) which were sacrificed for other experiments were used. The pancreas was dissected and finely minced and placed in a solution of HBSS (containing calcium) with digestive enzymes pronase (1mg/ml) and collagenase P (0.5mg/ml).

The pancreas in the digest solution was shaken for 30min at 37º C. The digested tissue was then filtered through nylon mesh [125u John Staniar, UK] and deoxyribonuclease (DNase-0.1%) was added. The cell suspension was centrifuged at 1500rpm for 5min to obtain a pellet which was then re suspended with Optiprep (Sigma, Poole, UK) 12%v/v in HBSS. These were then placed into a centrifuge tube and a buffering layer of HBSS (2ml) was placed on top. This was centrifuged for 20min at 2000rpm at 4°C. The stellate cells were collected from the band between the Optiprep/HBSS interface. The cells were pelleted by centrifugation (at 500g, for 5min, at 4°C) and re suspended with HBSS in order to remove any residue of Optiprep. The cell suspension was again centrifuged and the pellet obtained was re-suspended in DMEM/16% FCS/ PSG. In order to ensure that cell cultures reached the optimum level of growth it is helpful to obtain an accurate cell count and a measure of the percentage viability of cell population. Cell counting was done using a hemocytometer and cell viability assessed using trypan blue. The viable cells are round, refractive and relatively small compared to the dead cells which are larger, crenated and non-refractive. Trypan blue is a stain that can cross membranes of non-viable cells and it ensures quantitative analysis of the condition of the cells. A mixture of 75µl cell suspension and 25µl of trypan blue solution (0.4%) was slowly drawn into the chamber slide by capillarity. Using the low power of a light microscope the number of cells was counted (stained and unstained) in a $1mm^2$ area. The cell number and the viability percentage can be analyzed. The cells were then plated out onto either plastic culture flasks and onto Nunc-chamber slides (Lab-Tek®) at density of 100, 000 per ml. The cells were maintained in DMEM containing 16% foetal calf serum and 4% PSG at 37°C in a humidifying incubator with 5% CO_2. The culture medium was replaced every 48 hours. Regarding human PSC isolations, ethical approval was sought from the South West Ethics Committee. Patients undergoing pancreatic resections would be approached for consent for the pancreatic tissue in order to obtain the cells. Once consent was obtained the resected pancreatic tissues were to be used to isolate PSC in a similar fashion to rat HSC preparation.

2.2.8 Trypsinization and Passaging Of Pancreatic Stellate Cells

Materials

Cultured rat or human pancreatic stellate cells

DMEM**,** Invitrogen Life Technologies, Paisley, UK
FCS, Invitrogen Life Technologies, Paisley, UK

HBSS (calcium-free), Invitrogen Life Technologies, Paisley, UK
PSG (Penicillin, Streptavidin, Gentamicin)
10x trypsin ethylenediaminetetraacetic acid (EDTA), Santa Cruz Biotechnology, Santa Cruz, California, USA.

A confluent monolayer of PSC was harvested by trypsinization. The cells were washed at least 5ml HBSS to remove any residue serum and the cells were detached from the plastic flask by exposing the cells to TEDTA (1ml-1x) in HBSS at 37 ºC for 5 min. Once the cells were detached from the flask, TEDTA was inactivated with 1ml of 100% FCS. The detached cells were collected into 50ml conical flasks and centrifuged (1,500rpm, 7 min, 4 ºC). The pellet was then re suspended in 2ml of complete DMEM containing the concentration of cells was determined with a haemocytometer and the cells re-plated according to the required concentration.

2.2.9 Preparation of conditioned media

To obtain the serum free conditioned media required for many of the experiments described in this thesis HSC (rat and human) and PSC (rat and human) that had been cultured for varying times in serum containing media were washed three times in serum free DMEM with pre-incubation in serum free media for 1 hour following the final wash. The cells were then incubated in half of their original volume of fresh serum free media containing antibiotics (Penicillin, Streptomycin and Gentamicin or PSG) and 0.01% BSA for 24 or 48 hours. The media were then collected and clarified by centrifugation at 2,000rpm for 5 min and the cell monolayers lysed by the addition of guanidinium isothiocyanate (GIT) for RNA extraction or used for analysis of DNA content.

2.2.10 Trypsinization of adherent cells

Trypsinization of adherent cells was performed by washing the monolayer three times in calcium free HBSS before briefly exposing the cells to 1 x TEDTA in HBSS pre-warmed to 37^0C. The duration of exposure required to detach the cell monolayer was determined by light microscopy but was usually between 2 and 5 min. Once detached a small volume (approximately 5% by volume) FCS was added to the HBSS to inactivate the TEDTA and the cells were immediately pelleted by centrifugation and re suspended in DMEM supplemented

with 16% FCS and 4% PSG. The required plating density was achieved by determination of the total number of cells/ml using a haemocytometer, as described above.

2.3 Extraction, Purification and Analysis of RNA

2.3.1 Extraction of RNA

Materials
Diethyl-pyrocarbonate (DEPC) treated water*
4M GIT* containing β-mercaptoethanol
2M sodium acetate pH 4.0
Phenol
Chloroform/isoamyl alcohol (49:1 by volume)
Phenol/chloroform/isoamyl alcohol (25:24:1 by volume)
3M sodium acetate pH 6.0
Isopropanol
75% ethanol (in DEPC treated water)
Agarose
Ethidium bromide (1mg/ml) in DEPC treated water
Formaldehyde (37% volume/volume, v/v)
10 x MOPS (3-(N-Morpholino) propanesulphonic acid)*
RNA loading buffer*
20 x salt sodium citrate (SSC)*
Sodium hydroxide
Hybond-N (Amersham)

2.3.2 General precautions for working with RNA

RNA is extremely susceptible to degradation by ubiquitous ribonucleases (RNase) that are themselves comparatively resistant to degradation. To minimize this problem the following precautions were taken with all RNA work to avoid the loss of RNA integrity. Gloves were worn at all times as skin is a major source of RNase, and dedicated glassware used which had been baked for 5 hours at 200^0C. Water was pre-treated overnight with DEPC, which modifies tyrosine residues and hence inactivates any RNase present and autoclaved (to

inactivate the DEPC by degrading it to ethanol and CO_2) prior to use (480). Stock solutions were prepared from DEPC treated water and molecular biology grade reagents. Any solutions or instruments unsuitable for DEPC treatment were autoclaved and non-disposable plastic ware including electrophoresis equipment was soaked in 0.5M sodium hydroxide and rinsed in deionized (dI) water prior to use. All tips and microcentrifuge tubes were autoclaved prior to the procedure. Total RNA was extracted, purified and separated by electrophoresis on a denaturing agarose gel, after which it was transferred to a nylon membrane (Northern blotting) to permit the detection of specific messenger ribonucleic acid (mRNA) signal by hybridisation with radiolabeled complementary DNA (cDNA) probes.

2.3.3 Preparation of GIT lysate

1ml of 4M GIT containing β-mercaptoethanol was added to 75cm^2 flasks of confluent cultured HSC (with the volume being varied for sub-confluent cultures or different sizes of flasks). The cells bathed in GIT were vigorously agitated on an orbital shaker shaker (Beckman) to lyse the cells and denature proteins including RNase. To extract RNA from whole liver, approximately 0.5 grams (g) of snap frozen was rapidly homogenised in 5ml GIT using a pre-autoclaved polytron homogenizer probe. The tissue homogenates were then centrifuged to remove debris and aliquoted. The cell lysates and tissue homogenates were stored at -70^{0}C until required for RNA isolation.

2.3.4 RNA extraction by the acid phenol method

Total RNA was extracted from GIT lysates using a modification of the method described by Chomczynski and Sacchi (481). To each 900µl aliquot 90µl of 2M sodium acetate pH 4 was added at room temperature and mixed rapidly, followed by 900µl of phenol and 100µl phenol/chloroform/iso-amyl alcohol. The suspension was mixed thoroughly by inversion and incubated for 15 min on ice. This ensures separation of nucleic acids that, because of their phosphate backbone, are strongly negatively charged and will therefore accumulate into an aqueous environment where these charges are solvated. Proteins, carbohydrates and lipids contain charged and uncharged as well as hydrophobic and hydrophilic regions, and will thus accumulate in either a hydrophobic (organic) environment or at the organic/aqueous interface

After centrifugation (14,000rpm, 15 min, 4°C), the upper, aqueous phase, of the samples was transferred to a fresh tube, 700µl of phenol/chloroform/IAA added and mixed by inversion prior to a further incubation on ice for 10 min to ensure the complete removal of proteins from the RNA preparation. The supernatant obtained after aqueous/organic phase separation by centrifugation (14,000 rpm for 5 min at 4°C) was removed to a fresh micro centrifuge tube and 1/20 volume of 3M sodium acetate pH 6 was added and mixed gently. The RNA was then precipitated by addition of a 1:1 volume of ice cold isopropanol for at least 1 hour (or overnight) at -70°C.

The RNA precipitated in this reaction was recovered by centrifugation at 14,000 rpm at 4°C for 20 min, washed twice in 75% ethanol and dried at 65°C on a heater block. The pellets were re suspended in between 20-50µl DEPC treated water and dissolved by heating to 65°C for 10 min.

The yield and purity of total RNA was determined by measuring the optical density (OD) at 260 nanometres (nm) and 280nm. The integrity of the RNA samples was confirmed by electrophoresis through denaturing agarose gels of 2µg aliquots of each RNA sample and subsequent visualisation of the 28 S and 18 S ribosomal RNA bands with UV light (section 2.3.4). Once purified, any RNA not immediately used was aliquoted and stored at -70°C until needed.

2.3.5 Electrophoresis of RNA

A 1% horizontal denaturing agarose gel was prepared by dissolving the appropriate amount of agarose in 1 x MOPS/DEPC treated water by heating in a microwave oven (Panasonic). After allowing cooling, formaldehyde (to give a final concentration of 2.2M) was added and the gel cast. Formaldehyde disrupts the secondary structure of RNA and therefore allows accurate estimation of the size of RNA molecules.

10µg aliquots of RNA (calculated from the O.D. reading at 260nm), were mixed with an equal volume of RNA loading buffer and heated to 65°C for 10 min to denature the RNA. Immediately prior to loading 1µl of ethidium bromide (1mg/ml, which intercalates with the stacked bases of nucleic acids) was added to the samples to permit visualisation of the pro- and eukaryotic ribosomal RNA bands under UV light. In addition to a large increase in

fluorescence of the ethidium bromide molecule binding, which is the basis of its use as a stain of DNA in gels, the binding causes a local unwinding of the helix by around 26^{o}C. DNA/RNA is stained by the inclusion of ethidium bromide in the gel, or by soaking the gel in a solution of ethidium bromide after electrophoresis. The DNA shows up as an orange band on illumination by UV light.

The samples were subjected to electrophoresis at 100V for 1-2 hours using 1 x MOPS as electrophoresis buffer. RNA molecular weight markers (Promega) were run concurrently. After electrophoresis, the gel was viewed under UV light to check for any evidence of degradation of the ribosomal bands.

2.3.6 Northern Blotting

RNA was transferred immediately after electrophoresis to a nylon membrane by overnight capillary elution (Northern blotting). Prior to transfer the gel was rinsed in DEPC treated water for 10min to remove the formaldehyde. It was then rinsed in 50mM sodium hydroxide for 20min which improves both the speed and efficiency of transfer by partially hydrolysing the RNA. After a further rinse in DEPC treated water the gel was soaked in 10x SSC for 20min.

Transfer to a nylon membrane (Hybond-N) was achieved using a conventional gel-blotting apparatus using 10x SSC as the transfer buffer, with the objective being to draw liquid from the reservoir through the gel and the membrane so that RNA molecules were eluted from the gel and deposited on the membrane. After transfer the membranes were then air dried and exposed to low doses of UV irradiation for 5min to immobilise the nucleic acids through the formation of cross-links between a proportion of the bases in the RNA and the amine groups on the surface of the membrane.

2.3.7 Hybridisation of Northern Blots with Radiolabeled cDNA Probes

Radiolabeled, random primed cDNA probes were prepared using Amersham's MegaPrime^{TM} DNA labeling kit. The probes were hybridised overnight with membrane bound RNA on the Northern blots.

Materials

Hybridisation buffer ("Ultrahyb" Amersham)
Mega prime ^{TM} cDNA labeling kit (Amersham)
[α-^{32}P] deoxyadenosine triphosphate (dATP, Amersham)
Template DNA (Section 2.5.4 or 2.6.1.2)
DEPC treated water*
Sephadex G-50
SSC

2.3.8 Pre-Hybridisation of Northern Blots

The membrane, RNA side facing in, was pre-hybridised for 2-3 hours with hybridisation buffer at 42^{0}C in a rotating hybridisation oven (Hybaid). The inclusion of blocking reagent, herring sperm DNA and Denhardt's reagent in the buffer ensured efficient blocking of non-specific binding sites. Additionally, to maximise the rate of annealing of the probe with its target the ionic strength of the hybridisation buffer was high. In experiments where the mRNA signal of interest was suspected to be weak Ultrahyb hybridisation buffer was sometimes used.

2.3.9 Radiolabeling Of cDNA Probes By Random Priming

Random priming is an efficient and simple method to make short cDNA probes. The system uses random sequences of hexanucleotides to prime DNA synthesis onto a DNA template that has been denatured by heating, with a radioactive nucleotide being substituted into the copy. The Klenow reagent extends the primers to create multiple short length (150-200bp) complementary sequences radiolabeled with ^{32}P. 0.1µg of template DNA (Amersham, Promega) was added to 5 µl of primer and an appropriate volume of DEPC treated water, to give a final reaction volume of 50µl. The DNA was denatured by heating to 95^{0}C for 5 min, as the solution cools the primers anneal in a random fashion with the template. The following were then added to the reaction mixture: 5µl reaction buffer, 4µl of each unlabeled nucleotide (dCTP [deoxy cytosine triphosphate}, dTTP [deoxy guanine triphosphate], dGTP [deoxy thymine triphosphate]), 5µl [α-^{32}P] dATP (800Ci/mmol) and finally 2µl Klenow fragment (lacking 5`-3` exonuclease activity). After mixing, the solution was incubated for 1 hour at 37°C.

Unincorporated [α-^{32}P] dATP was separated from radiolabeled probes by centrifugation over a Sephadex G-50 column. The purified probe was collected in a microfuge tube and denatured by heating to 95^{0}C for 5 min. The heated probe was added to fresh hybridisation buffer and immediately exchanged with the pre hybridisation solution. The blot was left to hybridize, rotating overnight at 42°C. If the probe and target are 100% identical in sequence, then high stringency hybridization can be carried out. The stringency in the hybridization temperature and the salt concentration in the hybridization buffer (high temperature and low salt is more stringent as only perfectly matched hybrids will be stable). Formamide can be included in the hybridisation buffer to reduce the actual hybridization temperature by about 25^{o}C, from the more usual 68^{o}C to the more convenient 43^{o}C. Northern blots give information about the size of the mRNA and any precursors and can be useful to determine whether a cDNA clone used as a probe is full length or otherwise.

2.3.10 Stringency washing of Northern blots

After hybridisation, the membrane was washed under stringent conditions to remove unbound probe. Any unstable non-specific hybrids with few hydrogen bonds are then disrupted by high temperature, low salt conditions.

The membrane was washed for 15 min in 0.2 x SSC/0.2% sodium dodecyl sulphate (SDS) at 42^{0}C in the rotating hybridisation oven and then again washed twice for 15 min at 55°C in the same solution. Membranes that had been hybridised using Ultrahyb required stringency washing in different conditions at 42^{0}C, namely, 2 x 5 min in SSC / SDS**,** then 2 x 15 min in SSC/SDS.

2.4 Reverse Transcription- Polymerase Chain Reaction (RT-PCR) of Messenger RNA Sequences

RT-PCR was used to detect RNA. This is a very efficient reaction and is able to detect specific mRNA with a sensitivity of less than one part of 10^8. A complementary copy of the double stranded DNA (cDNA) can be synthesized from total RNA in a 5` to 3` direction using reverse transcriptase (RNA dependent DNA polymerase), together with oligo(dT)$_{15}$ primer. The cDNA was then subjected to PCR which requires 2 primers (a sense and antisense) to flank the specific DNA region to be amplified. A heat stable DNA polymerase, *Thermus*

aquatics (Taq) was used to synthesize the extension of the products which are complementary to the primers. Repeated cycles of denaturation, priming and extension caused the rapid accumulation of the target fragment.

2.4.1 Synthesis of Double Stranded DNA Copy

Materials
Deoxynucleotide triphosphate mixture (dNTP) – 100mM diluted to 10mM with DEPC water
Moloney murine leukaemia virus (M-MuLV) reverse transcriptase, Promega
Random Hexamers
Reaction buffer (5x), Promega
Ribonuclease inhibitor (RNasin), Promega
Total RNA

The total RNA (2µg) was reverse transcribed by mixing the RNA sample with the following: dNTP (10mM), random hexamers (2µl), 5x reaction buffer (4µl), M-MuLV reverse transcriptase (20units/µl- 0.1µl), Rnasin (1unit/µl) and the total volume made up to 20µl of DEPC treated water. In the negative control tube, RNA sample was replaced by DEPC treated water. The mixture was then incubated at 37°C for 60 min with the reaction terminated by heating the mixture up to 95°C for 2 min. The reaction mixture was then made up to 100µl with DEPC treated water. The cDNA sample can then be stored at -20°C until required.

2.4.2 Polymerase Chain Reaction

Contamination of PCR was avoided by preparing the process in a hood which was UV radiated prior to use. PCR dedicated pipettes and filtered tips were used at all times.

Materials

Ultra- high Quality water

Sample of cDNA

Taq polymerase, Promega, UK

10x DNA polymerase buffer, Promega, UK

dNTP mixture (100mM diluted to 10mM), Promega, UK

Magnesium Chloride (50mM)

PCR markers & Specific PCR Primers, Oswell Laboratories.

For each PCR, 25µl of "master mix" was required containing 10x DNA polymerase (2.5µl), Taq Polymerase (0.2µl), dNTP mixture (1µl), forward primers (0.5µM), reverse primer (0.5µM) and an optimum concentration of magnesium chloride. PCR reactions are very sensitive to magnesium ions and the optimum concentration (0.8-2.0mM) must be established for each pair of primers. If the magnesium concentration is too low, the primers may hybridize non-specifically leading to non-specific fragments however, if the concentration is too high the primers will form stable hybrids and no products will be seen. The tubes were placed in an automated PCR cycling apparatus (Perkin Elmer Gene Amp PCR system 2400) with a programmable incubation blocks with heated covers. The temperature, incubation time and numbers of cycle can be set accordingly. Cycling conditions for each PCR were adjusted to ensure efficient and accurate amplifications of the desired template. The following parameters were considered for each PCR reaction; the optimum temperature at which *Taq* polymerized, the annealing temperature of the primers, the temperature for the dissociation of the cDNA and finally the numbers of cycles of annealing, extension and dissociation of the strand. The products of the PCR reaction were analyzed on a 1.5% agarose/TAE gel (Section 2.5.3). A PCR molecular weight marker was included in the gel to enable the size of the amplified cDNA to be measured.

The membranes were then wrapped in cling film and exposed to either pre-flashed blue sensitive x-ray film (Genetic Research Instruments) for 24-72 hours at -70°C or to a Storm phosphor screen (Kodak) for 2-24 hours at room temperature which was then developed using a Storm phosphor screen image analyser (Molecular Dynamics). Autoradiographs and Storm images were quantified by scanning densitometry.

The membrane was kept moist at all times to enable it to be probed sequentially for a number of different mRNA transcripts; this prevented each probe from becoming too tightly bound. On completion of experiments, the hybridised probe was removed by immersing the membrane in boiling DEPC treated water for 15 min. To confirm that the probe was completely removed, the membrane was again exposed to X-ray film.

2.5 Ribonuclease Protection Assays

The ribonuclease protection assay (RPA) is a sensitive method used to detect and quantify specific mRNA transcripts in a complex mixture of total RNA or mRNA molecules (482) The procedure is straightforward in theory though demands focused attention in the laboratory. (Figure 2.1 below). An RNA probe is synthesized through an *in vitro* transcription reaction. These probes must be complementary to the gene sequence of interest and incorporate either radioactive or biotinylated nucleotides. The labeled probe is then incubated with a sample of total RNA or mRNA to facilitate hybridization of the complementary region of interest to the labeled probe. After hybridization, the mixture of single-stranded RNA and double-stranded probe-target hybrid is treated with ribonuclease (RNase), which digests all single-stranded RNA but no double-stranded RNA molecules. As a result, only the double-stranded gene target of interest remains. Usually, the sample is electrophoresed on a denaturing TBE-urea polyacrylamide gel and detected by methods specific to the label on the probe (483).

Ribonuclease protection assays (RPA) were used to detect various mRNA transcripts of interest, particularly when examining mRNA expression in whole liver as it is more sensitive than Northern analysis (484). This is partly because larger amounts of RNA can be loaded (up to 100 µg) and also because hybridisation occurs in solution thus ensuring that the maximum number of hydrogen bonds are available. RPA is not as sensitive as RT-PCR but is amenable to quantitation of mRNA expression which is not the case for PCR based methods, unless all the reactions have appropriate internal standards that are co-amplified and any quantitation measurements are restricted to the exponential phase of the reaction. The various methods can thus provide complementary information on the expression of mRNAs of interest.

The principles of the assay are that the target mRNA is hybridised in solution with a single stranded radiolabeled antisense RNA probe (riboprobe). In the presence of excess riboprobe, the number of probe-mRNA hybrids will be proportional to the amount of target mRNA in the sample. Following hybridisation, the mixture is treated with RNase to digest any single stranded RNA or redundant probe, whilst the double stranded probe-target mRNA hybrids are 'protected'. After inactivation of the RNase the protected fragments are ethanol precipitated, suspended in formamide loading buffer and separated on a denaturing polyacrylamide gel. Once the gel has been dried the relative abundance of the protected fragment can be visualised

by autoradiography and quantitated by scanning densitometry. These steps are summarised diagrammatically in Figure X above. The first step of the assay involves the transcription of antisense riboprobes that were synthesised from the relevant cDNA that had been inserted into plasmids.

Figures 2.1 Quantification of mRNA by ribonuclease protection assay

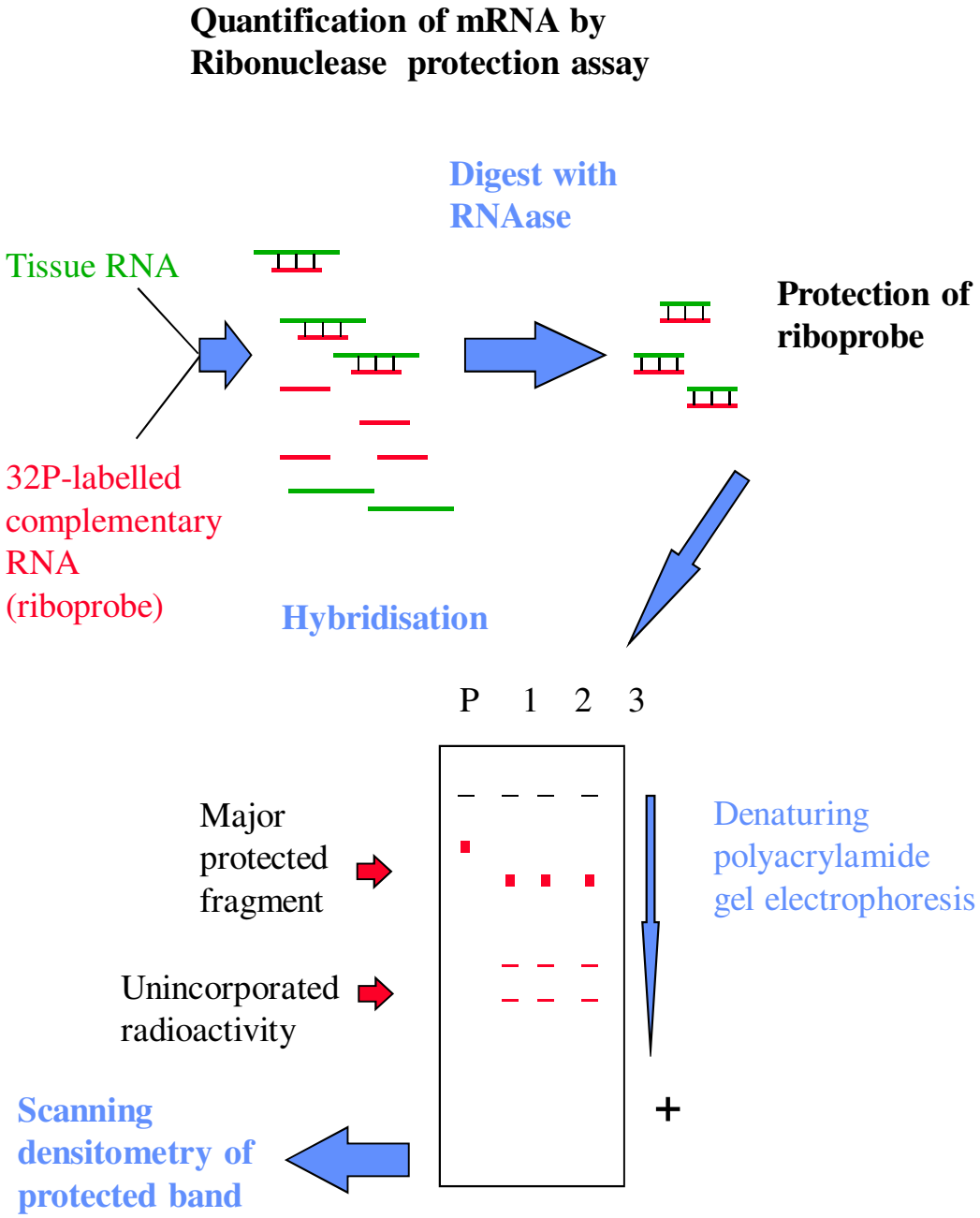

2.5.1 Preparation of Radiolabeled Antisense Riboprobe

To transcribe an antisense riboprobe, transcription must proceed from the 3` to the 5` end of the cDNA. Conversely sense riboprobes, identical to the target mRNA and hence non-complementary, are made from the 5` to the 3` end. All riboprobes were generated from cDNA in plasmids in which the target sequence was flanked by RNA polymerases. Once a RNA polymerase has bound to its recognition sequence the enzyme moves along the template synthesizing RNA until it either runs out of substrate or reaches the end of the template. Thus, to prevent the production of excessively long riboprobes, including some of the plasmid sequence, the insert must be completely linearized using restriction enzyme digests as described in section 2.6.3. Linearization was confirmed by subjecting a sample of the restriction digest to electrophoresis on an agarose/TAE gel (section 2.6.3**).**
2.5.2.2 The linearized DNA was then purified by phenol/chloroform extraction and ethanol precipitation before being used for the synthesis of riboprobes.

Materials
DEPC treated water*
Phenol/chloroform/isoamyl alcohol (49:1 by volume, pH 7.0)
3M sodium acetate (pH 7.0)
Isopropanol
75% ethanol
Riboprobe *In Vitro* Transcription Kit (Promega) [rNTP mix (0.2mM UTP, 2.5mM CTP, 2.5mM ATP and 2.5mM TTP), 100mM DTT, 5 x transcription buffer, RNA polymerases, RNasin Ribonuclease inhibitor, RNase Free DNase]
[α-32P] α-32P (Amersham)

2.5.2 Phenol chloroform extraction of cDNA templates

To 220µl of plasmid digest 300µl of DEPC treated water and 500µl of phenol/ chloroform/isoamyl alcohol were added, vortexed and incubated on ice for 5 min. After centrifugation at 14,000g for 10 min at 4^{o}C, the upper aqueous phase was transferred to a clean microfuge tube, 50µl of 3M sodium acetate and 900µl of isopropanol were added and mixed and the DNA precipitated overnight at -70^{0}C. The DNA was pelleted by centrifugation (14,000g for 15 min at 4^{0}C) and the supernatant discarded. The pellet was washed twice with

70% alcohol, dried and re suspended in DEPC treated water. The DNA was quantified by measuring the OD at 260nm and the integrity checked by running a sample on a 1% agarose / TBE gel (section 2.5.3).

2.5.3 In Vitro Transcription of Radiolabeled Antisense Riboprobe

To 1µg of linearized template 4µl of 5x transcription buffer, 2µl of 100mm DTT and 4µl of 2.5mm dNTP mix were added, mixed and heated to 65^{o}C for 10 min to enhance the inhibition of RNase by DTT. Then 1µl of the appropriate RNA polymerase (see Table 2.1), 0.5µl of RNasin Ribonuclease inhibitor and 5µl of [α-32P] dUTP were added and the mixture incubated at 30^{o}C for 1 hour to permit transcription of the RNA. RNase free DNase was then added to a concentration of 1U/µg of template DNA and the mixture heated at 37^{o}C for 45 min. This digests the template DNA, leaving radiolabeled RNA only. The mixture was then heated to 65^{0}C for 10 min to inactivate the polymerase and the volume increased to 150µl by the addition of DEPC treated water.

The riboprobes were precipitated by the addition of 500µl 0.3M sodium acetate, 500µl isopropanol with 20µg tRNA, as a carrier, and incubated at -70^{o}C for 2 hours. Samples were then centrifuged at 14000 rpm for 15 min at 4^{o}C, the pellet washed twice in 75% ethanol and dried at 65^{o}C. The riboprobe was then re suspended in 50µl DEPC water. The integrity of the riboprobe was assessed by running 5µl on a denaturing 1% agarose/MOPS gel (section 2.3.4) and autoradiography see figure 5.4. Scintillation counting (1µl probe in 4ml water) was used to determine the radioactivity of the probe.

2.5.4 Protocol for Ribonuclease Protection Assay

Materials
Ribonuclease Protection Assay Kit (Promega) (Yeast tRNA, RNase ONE)
DEPC treated water
RPA Hybridisation buffer*
RNase digestion buffer*
RPA Stop solution*
RPA Gel loading buffer*
100% / 75% ethanol
'Sequi-Gen' Vertical Sequencing apparatus (Bio-Rad)

1% SDS
Sigmacoat
Acrylamix (Promega)
10% Ammonium Persulphate (APS)
TBE
3MM filter paper (Whatmann)

2.5.5 Sample Preparation

10-50µg of sample RNA or yeast tRNA (negative control) was mixed with 30µl of hybridisation buffer and 10^5 cpm of ^{32}P-UTP radiolabeled riboprobe. The samples were heated to 95^0C for 5 min to denature the probe and target mRNA at 42^0C. Following overnight hybridisation un-hybridised probe and non-target RNA were digested by the addition of 270µl of ribonuclease digestion buffer containing 10U RNase ONE to each sample and incubated at 37^0C for 45 min. The reaction was terminated by the addition of 30µl of RPA stop solution (containing yeast tRNA as a carrier and SDS to inactivate RNase ONE) and the protected fragments precipitated by the addition of 800µl of ice cold 100% ethanol and incubation at -70^0C for 1 hour. The protected RNA-probe fragments were pelleted by centrifugation at 14,000g for 15 min at 4^0C and washed once with 75% ethanol before being re suspended in 8µl of RPA loading buffer. The samples (including 10^3 probes in RPA loading buffer) were heated to 95^oC to denature the RNA, loaded onto a 7M urea polyacrylamide gel and subjected to electrophoresis.

2.5.6 Resolution of Protected Fragments on Polyacrylamide Urea Gels

Gels were cast in 'small' (maximum 20 samples) or 'large' (maximum 40 samples) vertical sequencing apparatus. Prior to assembly the equipment was washed sequentially with 1% SDS, DEPC treated water and 100% ethanol and the back plate was sialinised with Sigmacoat to prevent the gel from sticking and make removal easier. Two gels were made, the first a sealing gel to seal the plates and the second a 5% sequencing gel, using materials as detailed in Tables 2.1 and 2.2 respectively

Table 2.1 Sealing gel materials

	small	large
Acrylamix (ml)	10	20
10% APS (µl)	80	160

Table 2.2 5% Sequencing gel materials

	small	large
Acrylamix (ml)	42	84
7M Urea (ml)	8	16
10% APS (µl)	400	800

Once the sequencing gel had polymerised the electrophoresis apparatus was assembled, pre-warmed TBE added and the gels deionised by pre-running at 50^{o}C at 1.5-1.8kV for 30 min. The prepared samples were added and separated by electrophoresis at 50-55^{o}C for approximately 60-90 min. Following electrophoresis the gel was transferred to a backing of 3MM filter paper, covered with cling film and vacuum dried. The dried gel was exposed to X-ray film at -70^{o}C or to a Storm phosphor screen and the resulting bands analysed by scanning densitometry.

2.6 Amplification, Purification and Analysis of Plasmid DNA

The full-length cDNA (rat TIMP-1, rat TIMP-2, rat α1 chain procollagen –1) used in this thesis were obtained from Professor John Iredale and Dr Chris Benyon and were contained in a variety of plasmids. All the plasmids were contained in an ampicillin resistance gene to allow for selection of successfully transformed *RNase*. Plasmid DNA can be isolated and purified for use as a template. I performed all the plasmid preparations myself in terms of amplification, purification and analysis of plasmid DNA.

Materials
Plasmid DNA (rat TIMP-1, pGem 7 containing the full length cDNA) (286)
Competent *E. coli* DH5α, Promega, Southampton, UK
Ampicillin
Luria-Bertani (LB) Medium*
Terrific Broth*
Glycerol

Sterile technique was used throughout the procedure. Plasmid DNA (2-10 ng) was added to 100µl of competent *E coli*. The cells were placed in a water bath at 42^0C for 2 min to promote the uptake of the DNA into the bacteria. The cells were then transferred to ice. This allows the repair of membranes and the cells to recover from the transformation. LB medium (100µl) was added to the cells and then it was spread onto the agar plates and left overnight at 37^0C to allow colonies to grow. The inclusion of the ampicillin allows for the selection of transformed cells.

The following day a single transformed colony was selected and placed in 10 ml of Terrific Broth (containing ampicillin 50µg/ml to maintain selection) and left overnight at 37^0C in a shaking incubator. Plasmid stocks were maintained by storing 1ml aliquot of the broth in -70^0C. A Miniprep was performed to ensure that the transformation was successful (see below) once confirmed, 1ml of the culture was added to 200ml of Terrific broth (contain ampicillin) and grown again overnight at 37^0C in a shaking incubator.

2.6.1 Purification of Plasmid DNA

Plasmids were isolated and purified using the QIAGEN Mini and Maxi Plasmid Purification Systems. Briefly the purification system is based on the modified alkaline lysis procedure. The bacteria are lysed in an alkaline buffer followed by neutralization by the addition of acidic potassium acetate and the subsequent high salt concentrate causes the SDS to precipitate with the denatured proteins, chromosomal DNA and cellular debris trapped in a salt-detergent complex, whilst the smaller plasmid DNA remains in solution. The precipitated debris is removed and washed away whilst the plasmid DNA under low salt conditions binds to the anion-exchange resin which can then be eluted in a high salt buffer and concentrated by isopropanol precipitation. The plasmids DNA for all the templates are made using the protocol described in the Qiagen Maxi prep and Miniprep manufacturer's handbook. Once the DNA pellet was obtained, the DNA was quantified by measuring the OD at 260nm and a restriction digest performed to release the required cDNA.

2.6.2 Restriction Enzyme Analysis of Plasmid DNA

The desired cDNA were isolated by using restriction enzymes digest and the digested DNA products analyzed using a gel electrophoresis.

Materials
DNase free water
10x Multicore buffer, Promega, Southampton, UK
Restriction Enzymes:

Rat TIMP-1 (648 bp) – EcoR 1, KpN

Rat α-1 procollagen (470 bp) – EcoR 1, HIND III

DNA ladder, (Promega)

For every µg of plasmid DNA, 5 units of the appropriate restriction enzymes and 0.1 x volume of multicore buffer were added and the mixture was made up to 100 µl with DNase free water. A negative control of uncut plasmid was included whereby the restriction enzymes were replaced by water. The mixture was incubated at 37°C for 16 hours. Equal aliquot of DNA digests were then separated on a 1% agarose/TAE gel (Figure 2.1). The separate desired DNA can be purified from the agarose gel using QIA quick gel extraction

kits. This kit is based on the fact that in the presence of high salt buffers and a pH<7.5, DNA are adsorbed onto a silica-gel membrane whilst the contaminants can be washed away. The purified product can be eluted from the membrane with water. The purified DNA could then be used to synthesize random prime cDNA probes (see section 2.4.4.b).

2.6.3 Preparation of Plasmid DNA for cDNA Probes, Riboprobes, Transfections, and Nuclear Run Ons

Whilst a great deal of work was performed on nuclear run ons during my research time this was unsuccessful. The methods are outlined briefly in Appendix II.

2.6.4 Amplification, Purification and Analysis of Plasmid DNA

Throughout this thesis experiments incorporated the use of full or partial-length complementary DNA (cDNA) which were obtained from a variety of sources and were contained within a variety of plasmids. Plasmids are autonomously replicating DNA incorporated, in this case, within DH5α *Escherichia coli (E. coli)* unless otherwise stated, which replicate independently from chromosomal DNA (original genome) and which form recombinant DNA. Propagation of the host organism containing the recombinant DNA forms a set of genetically identical organisms, or a clone. Subcloning described later involved the transfer of a fragment of cloned DNA from one vector to another. All the plasmids used contained an ampicillin resistance gene which facilitated the selection of *E coli* that had been successfully inserted into the relevant plasmid (transformation). The plasmid DNA was then isolated and purified for use as a template e.g. for riboprobe. All plasmid stocks were produced by the propagation of transformed competent DH5α *E. coli* – a long term frozen bacterial stock of clone obtained from Promega.

2.6.5 Production of competent cells (DH5α E. coli)

A bacterial culture of untransformed DH5α *E. coli* (Promega) was streaked out on to a fresh Lauria Bertani (LB) agar plate to incubate overnight at 37^0C. One colony was then taken and

10ml of LB media was inoculated and grown in static culture overnight at 37^0C. 1ml from this was taken to inoculate 30ml of LB media and placed in an orbital shaker at 37^0C. The incubation proceeded until the absorbance of the overnight static culture reached 0.4-0.5 at 550nm using sterile LB media as a control, 1ml samples were taken every 15-20 min (usually the total time taken was around 2hrs)

The sterile culture was then transferred to sterile centrifuge tubes and placed on ice for 15 min. All subsequent steps were carried out at 4^0C. First the cells were centrifuged at 2000g for 10 min whereupon the supernatant was discarded and the pellet re suspended in a solution of RFI equal to 1/3 the volume before the supernatant was discarded. This solution was incubated on ice for 15 min before being centrifuged at 2000g for 10 min. The supernatant was again discarded and re-suspended to 1/12.5 the original volume with RF2. These cells were then transformed and could be used directly for transformation or frozen at -70^0C. DH5α *E. coli* were tolerant to slow freezing.

2.6.6 Transformation and Amplification of competent *Escherichia coli (E coli)* with Plasmid DNA

Materials:
Plasmid DNA
Competent E Coli DH5α (Promega)
Ampicillin
Luria-Bertani (LB) Medium
Terrific Broth
Glycerol

Fresh LB plates were prepared. Ampicillin was added to give a final concentration of 50μg/ml and the media poured into sterile 90mm petri dishes and allowed to set. Sterile techniques were employed throughout the procedure. Between 2-10ng of plasmid DNA in a volume not greater than 10μl were added to 100μl of competent *E coli* and the mixture immediately placed on ice (promoting the uptake of DNA into the bacteria). The cells were temporarily permeabilized by heat shock treatment by placing in a pre-heated water bath at 42^0C for 2 min, which induces enzymes involved in the repair of DNA and other cellular components allowing the cells to recover from transformation and thus increase the efficiency

of the process. The cells were then incubated on ice for 10 min. The competent cells were then allowed to warm to room temperature over five min; an equal volume of LB was added before incubating shaking at 37^0C for one hour. It was then spread onto the agar plates and left overnight at 37^0C to allow the colonies to grow. The inclusion of ampicillin in the media allowed for the selection of transformed cells. The following day a single transformed colony was selected and placed in 10ml of LB or Terrific broth (containing ampicillin 50μg/ml) and allowed to grow to stationary phase overnight at 37^0C in a shaking incubator. Aliquots of 1ml were then removed for the preparation of bacterial stocks (see below) to be stored at -70^0C. It was possible to isolate sufficient plasmid DNA for initial manipulation from a few ml of bacterial culture for example to perform a restriction digest to confirm the identity of the plasmid. Such isolation is normally known as a mini-preparation or "Miniprep" (see below). After confirmation that transformation had been successful, the main plasmid amplification procedure was performed ("Maxi prep"). For this, 10ml of the culture was added to 100ml of LB or 30ml Terrific broth (containing ampicillin) and grown overnight at 37^oC in a shaking incubator.

2.6.7 Bacterial Propagation

Materials
90mm Petri dishes
Competent E Coli DH5α (Promega)
Ampicillin
Luria-Bertani (LB) Medium
Terrific Broth
Glycerol

Inoculants from freshly transformed DH5α *E coli* or from frozen bacterial stocks were streaked onto LB ampicillin petri dish plates before incubation overnight at 37^oC in order to obtain single colonies. A single colony (clone) from the plate was used to inoculate a sterile conical flask containing 100ml of LB or 30ml of Terrific Broth containing ampicillin. The inoculated broth was incubated overnight in an orbital shaker at 220rpm and 37^oC. *E. coli* inoculants were centrifuged at 220rpm for 30mins at 4^oC to pellet.

2.6.8 Production of Bacterial Stock

Materials
Plasmid DNA
Competent E Coli DH5α (Promega)
Ampicillin
Luria-Bertani (LB) Medium
Terrific Broth*
Glycerol

Transformed DH5α *E. coli* clones were stored frozen. One clone from a streaked plate was used to inoculate 10ml of LB with ampicillin and incubated overnight at 37^0C. The inoculant was then used to form a bacterial stock by the addition of 0.5ml of sterile 30% v/v glycerol to 0.5ml of the culture. The bacterial stock in 15% v/v glycerol was mixed before freezing at -80^0C.

2.6.9 Purification of Plasmid DNA

Plasmids were isolated and purified using the QIAGEN Mini and Maxi Plasmid Purification systems. The QIAGEN plasmid purification protocols are based on a modified alkaline lysis procedure (485;486). Briefly, the cell pellet is re suspended in a buffer solution which contains lysozyme to digest the cell wall of the bacterium. The cell lysis solution, which contains the detergent sodium dodecyl sulphate (SDS) disrupts the cell membranes and denatures the proteins; the alkaline conditions denature the DNA and begin the hydrolysis of RNA. The preparation is then neutralized with a concentrated solution of potassium acetate at pH 5.0. This has the effect of precipitating the denatured proteins, along with the chromosomal DNA and most of the detergent (potassium dodecyl sulfate is insoluble in water). The resulting high salt concentration causes SDS to precipitate and denatured proteins, chromosomal DNA and cellular debris become trapped in the salt-detergent complex, whilst the smaller covalently closed plasmid DNA remains in solution. The precipitated debris is removed and the cleared lysates applied to the QIAGEN tip. Under low salt conditions the plasmid DNA binds to the anion-exchange resin in the tip, whilst any contaminants are washed away. The plasmid DNA is then eluted in a high salt buffer and concentrated and 'desalted' by isopropanol precipitation.

Materials

Qiagen Maxi prep / Miniprep Plasmid Purification Systems (buffer P1, buffer P2, buffer P3, QIAGEN-tip 500, buffer QBT, buffer QC, and buffer QF)

Isopropanol

70% ethanol

DNase free water

The method below describes the Qiagen protocol for the larger scale Maxi prep. The Miniprep protocol was executed according to the manufacturer's instructions. The bacterial cells were harvested by centrifugation at 6,000g for 15 min at 4^0C. The cell pellet was then re suspended in 10ml of buffer P1**,** an equal volume of buffer P2 was added and the mixture allowed to incubate for 5 min at room temperature. 10 ml of chilled buffer P3 was then added, mixed by inversion and the mixture incubated on ice for 20 min, allowing the precipitation of genomic DNA, proteins and cell debris. The sample was next centrifuged at 20,000g for 30 min at 4^0C and the supernatant, containing the plasmid DNA removed and placed in a clean tube. The supernatant was re-centrifuged at 20,000g for 15 min at 4^0C and the supernatant again removed and placed immediately in a QIAGEN-tip 500, which had been pre-equilibrated by the prior addition of 10ml of buffer QBT. The column was then washed twice with buffer QC after which the DNA was eluted off by the addition of 15ml of buffer QF. The plasmid DNA was precipitated by adding 0.7 x volume of isopropanol, the mixture centrifuged at 15,000g for 30 min at 4^0C and the supernatant discarded. Both Minipreps and Maxipreps were followed according to the manufacturer's instructions except in the final steps of the Maxi prep protocol. Qiagen advises that the final pellet is spun in a single 50ml conical tube: this step was modified to increase the DNA yield by aliquoting the suspended DNA in isopropanol into several microfuge tubes (typically 16-18) and subsequent centrifuging took place in a microfuge to produce a total yield of around 1 gram of material. The DNA pellets were then washed with 5ml 70% ethanol and centrifuged at 15,00g for 10 min at room temperature. After a second wash with ethanol the DNA pellets were dried and re suspended in DI water. DNA was quantified by measuring the OD at 260nm and a restriction digest performed to confirm the presence of the cDNA in the amplified plasmid.

2.6.10 Restriction Enzyme analysis of Plasmid DNA

The plasmid DNA isolated was examined for its pattern of cleavage by restriction enzymes (restriction map) and the size of linear DNA molecules was determined by agarose gel electrophoresis using marker fragments of known sizes.

Materials

DNase free water

10 x Multicore restriction enzymes (Promega)

Restriction enzymes (Promega)

DNA ladder (Promega)

To each μg of plasmid DNA, 5 units of the appropriate restriction enzymes and 0.1 x volume of buffer were added. The volume was made up with DNAse free water, ensuring that the restriction enzyme contributed less than 10% of the final volume. A negative control of uncut plasmid that was treated in an identical way except that the restriction enzymes were replaced with water was also included. The mixture was incubated at 37^{o}C unless otherwise stated for at least one to two hours (up to 16 hours) and the resulting cut plasmid was run on a 1% agarose TAE gel with appropriate plasmid controls and DNA ladder for estimate of size of cut fragments. To isolate the bulk of the cut DNA all the product was run out in a 1% agarose TAE gel and the fragment of interest excised and gel purified.

2.6.11 Purification of DNA or PCR products from Agarose Gels

Materials

Qiagen QIA quick gel extraction kit: (buffer QG, buffer PE, QIAquick spin column, 3M sodium acetate), Isopropanol, DNAse free water

DNA subjected to a restriction digest or PCR products were isolated from non-specific amplification products by separation in a 1% TAE low melting temperature agarose gel. The band of interest was excised quickly to minimise damage to the DNA by UV light. The

agarose added to a microfuge tube along with 3 volumes of buffer QG for each volume of agarose. The agarose was melted by incubation of the mixture at 50^0C for approximately 10 min, with frequent vortexing during this period. An equal volume of isopropanol was added to the mixture which was then added to a QIAquick column which contains a silica matrix that binds DNA. The DNA was washed by adding 0.75ml of buffer PE to the column for 5 min, and then centrifuging twice at 13,000 g for 1 minute. The column was then placed in a clean microfuge tube and the DNA eluted using a 30-50µl DNase free water added to the centre of the column, followed by centrifugation at 13,000g for 1 minute. The purity of the resulting DNA fragments was examined by running a small aliquot on a TBE gel with appropriate DNA markers to check for contamination. The purified DNA could then be used for experiments such as synthesis of random primed cDNA probes.

2.7 Transfection Protocols

2.7.1 Transfection techniques: Introduction

The ability to introduce nucleic acids into cells has enabled the advancement of our knowledge of genetic regulation and protein function within eukaryotic cells, tissues and organisms (487;488). The process of inserting nucleic acids into cells by non-viral methods is known as 'transfection'. Advancements in techniques for cloning plasmid DNA now provides the means to manipulate DNA sequences and the ability to produce virtually unlimited amounts of relatively pure DNA for transfection experiments. The development of reporter gene systems and selection methods for stable gene expression of transferred DNA has greatly expanded the applications for gene transfer technology

In 1982 Curran et al, initiated the reporter gene concept with the bacterial chloramphenicol acetyl transferase (CAT) gene and associated CAT assay system (489). Using a reporter gene that is not endogenous to the cell coupled with a sensitive assay system for that gene product, allows investigators to clone regulatory sequences of interest upstream of the reporter gene to study expression of the reporter gene under various conditions. This technology, together with the availability of transfection agents provides the foundation for studying promoter and enhancer sequences, *trans*-acting proteins such as transcription factors, mRNA processing, protein/protein interactions, translation, and recombination events. Following the introduction of the CAT gene and assay system several other reporter systems have been developed for various *in vitro* and *in vivo* applications including luciferase, β-galactosidase, alkaline phosphatase and green fluorescent protein.

Figure 2.2 Reporter gene systems

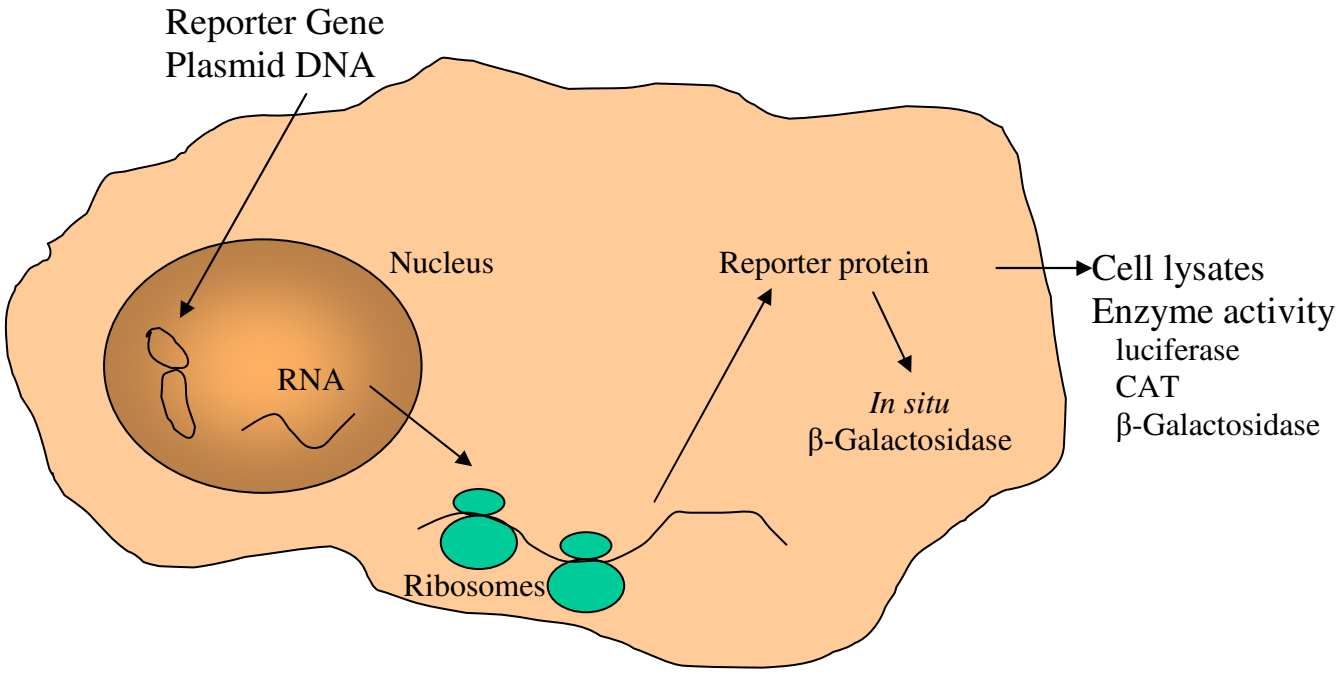

Figure 2.2 Reporter gene systems. Integration of DNA into the chromosome, or stable episomal maintenance, of reporter genes occurs with a relatively low frequency. The ability to select for these cells is made possible using genes that encode resistance to a lethal drug. In examining transient expression, cells are typically harvested 48-72 hours post transfection for studies designed to analyse transient expression of the transfected genes. Extracts are prepared using a reporter lysis buffer and can then be assayed for luciferase, CAT or β-galactosidase activity.

2.7.2 Luciferase Reporter Assay System

The reporter genes are often used as indicators of transcriptional activity in cells. Typically a reporter gene is joined to a reporter sequence in an expression vector that is transfected. Following transfer the cells are assayed for the presence of the reporter by directly measuring the amount of reporter mRNA, the reporter protein itself or the enzymatic activity of the reporter protein. A control vector can be used to normalise the transfection efficiency or cell lysate recovery between treatment or transfection experiments (490). The control reporter gene is frequently driven by a strong, constitutive promoter and is co-transfected with experimental vectors.

The luciferase enzyme used here is derived from the coding sequence of the *luc* gene cloned from the firefly *'Photinus pyralis'* (491-493). The firefly luciferase enzyme catalyses a reaction using D-luciferin and ATP in the presence of oxygen and Mg^{2+} resulting in light

emission. The total amount of light measured during a given time interval is proportional to the amount of luciferase reporter activity in the sample. This light emission can be quantified.

The 'dual luciferase reporter assay system' (Promega) combines two luciferase reporter enzymes. The firefly luciferase can be effectively quenched so that the second (derived from the sea pansy 'Renilla reniformis") can be assayed for its luminescence.

The CAT gene is derived from transposon 9 of Escherichia coli (*E.coli)* (494). CAT is a trimeric protein comprising three identical subunits of 25kDa (495).The CAT protein is relatively stable in mammalian cells, although the mRNA has a comparatively short half life, making the CAT reporter especially suited for transient assays designed to assess accumulation of expressed protein (496). CAT catalyses the transfer of the acetyl group from acetyl-CoA to the substrate, chloramphenicol. The enzyme reaction can be quantified by incubating cell lysates with [^{14}C] chloramphenicol and following product formation by physical separation with thin layer chromatography (TLC) (497).

The vectors used in these experiments from Promega (pGL3) contain a modified cDNA, designated 'Luc+' and a vector backbone that has been enhanced to provide reporter gene expression but ensuring that there is no spurious transcriptional signals. The PRL family of 'Renilla' luciferase reactions are used to co-transfect the experimental luciferase reporter gene.

The expression of Renilla luciferase can provide an internal control value to which expression of the experimental firefly luciferase reporter gene may be normalised**.** During the course of this work it became obvious that relatively small quantities of the pRL co-reporter gene were needed to provide low-level constitutive expression of Renilla luciferase control activity (to the extent that ratios of luciferase co-transfection reaction of 50:1 were used).

Figure 2.3 pGL3 Basic (promega)

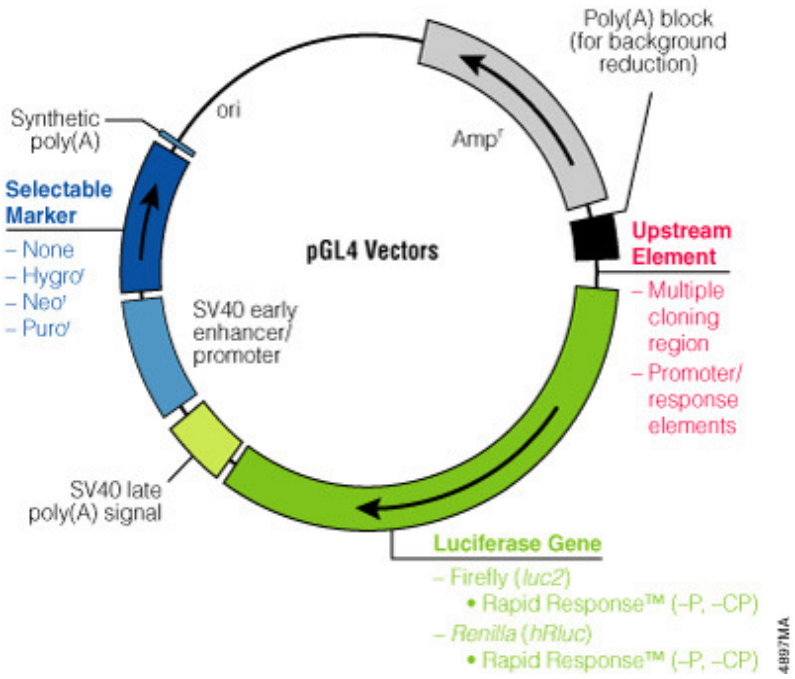

2.7.3 Transfection

Materials

Two transfection kit protocols were incorporated in the body of this work:

1. Lipofection for dual luciferase transfection

This protocol was used in accordance with a Promega Kit and carried out to the manufacturer's instructions (498;499). Cells were incubated during transfection, placed in serum-free media for at least 6 hours and transfected over a period of 72 hours following which they were harvested with a view to freezing and performing a luciferase assay at a later date.

2. Effectene for dual luciferase transfection

This system incorporated a new transfection agent 'Effectene" based on a proprietary non-liposomal lipid. Transfection was carried out according to the manufacturer's instructions (Qiagen). A serum free step was avoided with this protocol and this proved in subsequent work to be a major advantage. The 'Dual Luciferase Reporter Assay' system (Promega) allowed the dual transfection of reporter genes in a variety of cell types and required the measurement of emitted light with a manually operated luminometer (Promega). All protocols were carried out accurately to manufacturer's instructions.

2.7.4 The Chloramphenicol Acetyl Transferase (CAT) Transfection Assay

All transfection were carried out using the 'Effectene' kit by Qiagen outlined above according to the manufacturer's instructions. After incubation in fresh media transfections were carried out over a period of 24-48 hours avoiding a serum free step/ following this the cells were scraped off tissue culture plates into media, and pelleted at 1000 rpm for 5min. The supernatant was removed and the cells were re-suspended in 5ml of PBS. They were then pelleted at 1000rpm for 5min; this was then repeated. Following suspension in PBS a third time and pelleting as outlined the cells were re-suspended in 50µl of 0.25M Tris buffer pH7.9. Three cycles of freezing in liquid nitrogen for 2 min then thawing at 37^{o}C for 5min followed by vortexing was carried out. The disrupted cells were then pelleted using a microfuge at 13000 rpm for 5 min. The pellet was retained and stored at –20^{o}C. A protein assay was carried out on 2µl samples of the supernatant. (To 2µl of sample 18µl of H_2O was added; a

'blank' sample was made up with 2µl of tris and 18µl of water to give the same buffering conditions). A proprietary kit was used to perform the protein assay (DC colorimetric assay (BioRad): 100µl of Solution A and 800µl of Solution B was added and the solution was incubated at room temperature for 20 min. 5µl of the sample/supernatant was then added to 15ml of H_2O in a cuvette and a protein assay reading was taken at 750nm. Samples were then modified to 25µg in 50µl and to this a mastermix was added (the master mix represented 70µl of 1M Tris-HCl pH 7.8, 20µl of Acetyl Coenzyme A 3.25µg/µl and 1µl of 400µCi/ml [^{14}C] 35-50mCi/mmol Chloramphenicol (Amersham), for each reaction).

Each sample was 'flick spun' using a microfuge at 13000rpm and incubated at 37^{o}C for 2 hours. To each sample 0.5 ml of ethyl acetate was added and the solution vortexed for 30 seconds and microfuged at 13000 rpm for 5mins. The top layer was removed into another tube and the lower layer discarded. The top layer was speed vacuum dried and the residual precipitate was re-suspended in 15µl of ethyl acetate before being applied to a thin layer chromatography plate and allowed to dry. The plate was run in a chromatography tank containing 95% chloroform, 5% methanol. Imaging was performed by plate exposure to Blue Autoradiography X-ray film (GRI) and quantitation was determined by phosphor image analysis using a Storm scanner and an "Image Quant" software data analysis package (Molecular Dynamics).

2.8 Erase-a-Base

The Erase-a-base system by Promega is designed for the rapid construction of plasmid containing progressive unidirectional deletions of any inserted DNA. It is based on a procedure developed by Henileott (500) in which the enzyme exonuclease III (Exo III) is used to specifically digest insert RNA from a 5 prime (5`) protruding or blunt end restriction site. The adjacent primer binding site is protected from digestion by a 4-base 3` overhang restriction site. DNA fragments with a defined length are used as the starting point to obtain smaller components by successive deletion from the 5` end. Exo III works at a consistent rate and therefore defined time points are incorporated to obtain predictable lengths by simply removing timed aliquots from the digestion mix reaction.

Samples of the Exo III digestion are removed at timed intervals and added to the tubes containing S1 nuclease, which removes the remaining single stranded tails. The low pH and presence of zinc cations in the S1-nuclease buffer effectively inhibits further digesting by Exo III. After neutralisation and heat inactivation of S1 nuclease, Klenow DNA polymerase is added to flush the ends which are then ligated to circularize the deletion containing vectors. The ligation mixtures are used directly to transform competent cells. Each successive time point yields a collection of subclones containing clustered deletions extending further into the original insert.

For Erase-a-base Solutions, see Appendix 1 for Materials & Solutions.

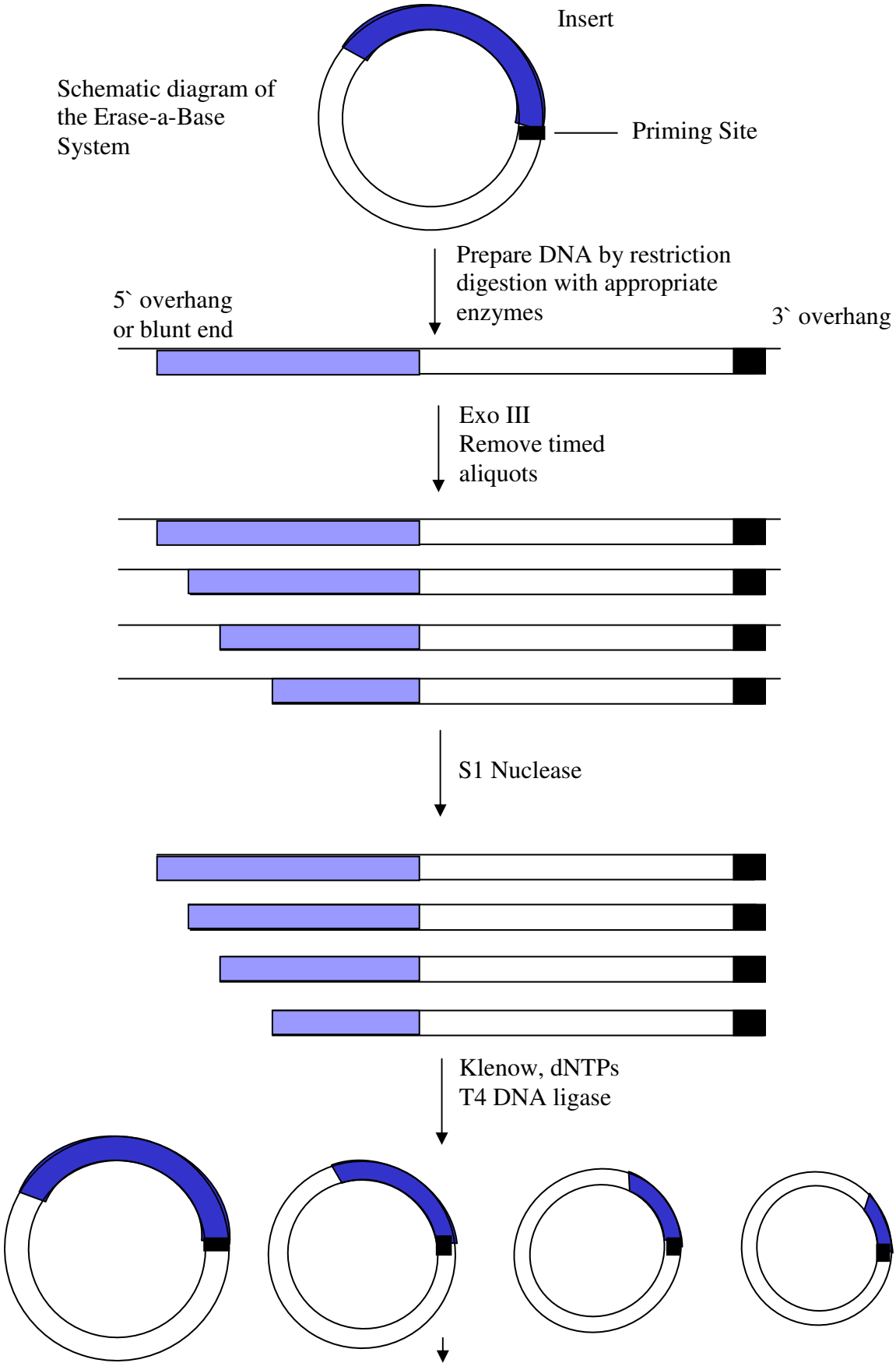

Figure 2.4 The Erase-A-Base technique

2.8.1 Erase-a-Base system for restriction digestion of plasmid DNA

A double-digest of 10µg of closed circular DNA with two different restriction enzymes was performed: one to generate a 4-base 3`-protrusion protecting the primer binding site and another to leave a 5`-protrusion or blunt end adjacent to the insert.

2.8.1.1 Protection of 5`-Protruding Ends with α-Phosphorothioate dNTP Mix

10µg of recombinant DNA was digested to completion with the enzyme chosen for the primer protecting site. This was then phenol:chloroform extracted, precipitated and spun down briefly at 13,000rpm for 1 second in a microfuge. The pellet was rinsed in 70% ethanol. The tube was drained and the pellet dried under vacuum. The pellet was re suspended in 50-100µ1 of Klenow 1x Buffer. Sufficient α-Phosphorothioate dNTP Mix was added to achieve a final concentration of 40µM each. DTT was added to a final concentration of 1mM and Klenow DNA Polymerase to 50u/ml. The mixture was incubated for 10 min at 37°C. The sample was heated for 10 min at 70°C to inactivate the Klenow DNA Polymerase. The DNA was extracted as described above and re suspended in the appropriate restriction endonuclease digestion buffer. After performing the second restriction digestion, the DNA was extracted again as above, then the main part of the experiment proceeded: Exonuclease III deletion, ligation and transformation.

2.8.2 Exonuclease III deletion, ligation and transformation

The DNA pellet was re suspended in 10µl of TE buffer or water and the concentration of the DNA estimated by gel analysis. 5µg of DNA was added to 6µ1 10x Exo III Buffer. Water was added to a total volume of 60µl. Meanwhile, for each DNA deletion series, 7.5µl of S1 nuclease mix was added to each of 24 microcentrifuge tubes and left on ice. The DNA tube was warmed to the digestion temperature in a water bath. 300-500 units of Exo III was added to the DNA and mixed rapidly. 2.5µl samples were removed at 30 second intervals into the S1 tubes on ice, with mixing achieved by pipetting.

Once all samples were taken they were incubated at room temperature for 30 min. 1µl of S1 Nuclease Stop Buffer was added to each tube and which was then heated at 70°C for 10 min followed by a brief centrifuge at 13,000rpm for 1 second in a microfuge. The extent of

digestion was determined by gel electrophoresis of 2-3µl samples (40-60ng DNA) from each time point. The samples was precipitated with 0.3 volumes of 7.5M ammonium acetate and 2 volumes of 100% ethanol and mixed well. It was then incubated at -20°C for 15 min, then centrifuged at 12,000 x g for 5 min. The supernatant was carefully removed and the pellet washed with 0.5ml of 70% ethanol. Once the tube was drained and the pellet dried the pellet was re suspended in 9µl of TE buffer. The samples were transferred to 37°C; 1µl of Klenow mix was added to each sample then incubated for 3 min. 1µl of the dNTP mix was added to each sample then they were incubated for a further 5 min at 37°C. The Klenow was heat inactivated at 65°C for 10 min. The samples were transferred to room temperature and 40µl of ligase mix was added to each sample. All samples were mixed well and incubated at room temperature for 1 hour. The resulting plasmid DNA was transformed into competent cells.

2.9 Sequencing Methods

DNA to be sequenced was denatured with 0.2M NaOH, 0.2M EDTA at 37^0C for 30 min. The denatured protein was precipitated with 3x volumes of 100% ethanol at 70^0C for 15 min. Following a centrifuge spin at 14,000 rpm for 30 min at room temperature most of the ethanol was removed and the final amount was taken off after a final 'flick' spin for 60 seconds. The pellet was dried for 2-5 min and re suspended in a reaction buffer containing water and primer.

2.9.1 Chain Termination Sequencing

The 'T7 Sequenase' version 2.0 DNA sequencing method (1,2) (Amersham Life Science) involves the *in vitro* synthesis of a DNA strand by a DNA polymerase using a specifically primed single-stranded DNA template(501;502).

DNA synthesis is carried out in two steps. The first is the labeling step in which the primer is extended using limiting concentrations of the deoxynucleoside triphosphates, including radioactively labeled dATP. This step continues to virtually complete incorporation of labeled nucleotide into DNA chains. These initial primer extensions are distributed randomly in length from several nucleotides to hundreds of nucleotides.
In the second step, the concentration of all the deoxynucleoside triphosphates is increased and a chain terminating nucleotide analogue is added. These 2`3`- dideoxynucleoside-5`-

triphosphates (ddNTPs) lack the 3`-OH group necessary for DNA chain elongation. Processive DNA synthesis occurs, with extensions on the average of only several dozen nucleotides, until all growing chains are terminated by a ddNTP. When proper mixtures of dNTPs and one of the four ddNTPs are used, enzyme catalysed polymerisation will be terminated in a fraction of the population of chains at each site where the ddNTP can be incorporated.

Four separate reactions each with a different ddNTP give complete sequence information. The sequencing reactions are terminated by the addition of EDTA and formamide, denatured by heating, separated from high resolution denaturing acrylamide gel electrophoresis and visualised by autoradiography.

Materials

For 3-dNTP protocol: α labeled dATP such as [α-^{32}P]dATP or [α-^{35}S]dATP where the specific activity should be 1000-1500Ci/mmol.

Water (only deionized, distilled water was used for the sequencing reactions).

Tris-EDTA (TE) buffer: this buffer is 10mM Tris HCl, 1mM EDTA, pH 7.5.

It is used for template preparation.

For Gel reagents sequencing gels were made only from fresh solutions of acrylamide and bis-acrylamide. Other reagents were electrophoresis grade materials.

Specialized sequencing primers

Some sequencing projects required the use of primers which are specific to the project. For all sequencing applications, 0.5-1.0pmol of primer was used for each set of sequencing reactions.

Necessary equipment:

Constant temperature bath

Sequencing required incubations at room temperature, 37°C, 65°C and 75°C. The annealing step required slow cooling from 65°C to room temperature.

Electrophoresis equipment

While standard, non-gradient sequencing gel apparatus is sufficient for most sequencing work, the use of field-gradient ('wedge') gels will allow greater reading capacity on the gel **(5)**. A power supply offering constant voltage operation at 2000V or greater was incorporated.

Gel handling

For ^{35}S or ^{32}P sequencing, a large tray for soaking the gel (to remove urea) and a gel drying apparatus was necessary. (Gels containing ^{35}S or ^{32}P must be exposed dry in direct contact with the film at room temperature).

Autoradiography

Large format autoradiography film and film cassettes, such as HyperfilmTM or BiomaxTM and HypercassettesTM, were used. Development of films was performed according to the film manufacturer's instructions.

2.9.2 Sequencing Reactions

Two sets of reactions were set up: four forward and four reverse. For each set of four sequencing lanes a single annealing (and subsequent labeling) reaction was used. Each reaction tube contained: 1µl primer, 2µl reaction buffer, 3µl of DNA insert (0.5µg/µl) and 5µl distilled water (total volume 10µl). The capped microfuge tubes were warmed to 61°C for 2 min then the whole heating block was switched off and removed from the heating filaments: the microfuge tubes were allowed to cool in the block over a period of 45 min. (Once the temperature is below 30°C annealing is complete). All tubes were then placed on ice.

2.9.3 Termination Reaction

During the cooling process above the termination reaction was prepared in advance. One set of four microfuge tubes labeled G, A, T and C were obtained for each reaction (eg one set each for the TIMP-2 human 2600 ‘forward’ and TIMP-2 human 2600 ‘reverse’ reactions), 2.5µl of ddGTP termination mix was placed in “G”, similarly the tubes labeled A, T and C were made up with ddATP, ddTTP and ddCTP termination mixes respectively.

2.9.4 Labeling Reaction

The labeling mix (dGTP) was diluted 5x fold with distilled water eg 4µl mix added to 16µl H_2O. 2µl of enzymes for the 'Sequenase' Version 2.0 Kit were added in a ratio of 1:8 in ice cold enzyme dilution buffer. To the annealed template primer the following was added (on ice): 10µl template primer, 1.0µl DTT 0.1M, 2.0µl diluted labeling mix, 0.5µl [α-^{35}S]dATP, 2.0µl diluted sequenase and thoroughly mixed. The resulting solution was incubated for 5 min at room temperature.

2.9.5 Termination Reaction

The previously prepared termination mix was warmed to 37^{0}C for 1 minute. Following completion of the incubation and labeling reaction 5µl was removed and transferred to 'G'. This was repeated for microfuge tubes labeled 'A', 'T' and 'C'. All were returned to the water bath at 37^{0}C for 5 min. 'STOP' solution was added to terminate each reaction.

2.9.6 Acrylamide Gel

This was prepared in advance and stored in the dark. The gel was pre warmed to 55^{0}C at 35 watts for 15mins and then run for 35 watts for 5mins. A gel was run 60mins prior to each experiment and loading was performed in the following sequence:

T forward	T reverse
GATC	GATC

It was then reduced to 30W and run over three hours.

2.10 Culture of cells in hypoxic condition

HSC were obtained in the usual way in the liver unit at Southampton and plated out onto plastic in order to allow cells to culture in the standard way. Cells were transferred to the Rayne Institue, UCL, London in June 1999 where a facility for tissue culture under hypoxic conditions was provided by Dr Jill Norman. Primary rat HSC, passaged rat HSC and human HSC were provided in DMEM and 16% FCS. Cells were divided into two groups and cultured for a variable time course in either control or hypoxic condition for 12, 24, 48 and 72hrs. Hypoxic conditions consisted of 1% oxygen, 5% CO_2, balanced nitrogen (specialist gas from BOC) in a humidified atmosphere at 37^0C, the control group cells normoxic controls were cultured under the routine incubator conditions ie 21% oxygen, 5% CO_2 in a humidified atmosphere at 37^0C. (These methods are described in 4.2 Methods). Cells were harvested for RNA extraction at each time point. Northern membranes were made and transferred to Southampton.

Table 2.3 Hybridisation protocols differed slightly for these membranes

Prehybridisation *(Store in -20^{0}C freezer)*		50ml
20x SSC		10ml
10% SDS		2.5ml
Denhardts 50x		5ml
$T_{50}E_{10}$:	Tris 50mM EDTA 10mM	5ml

The prehybridisation fluid was DEPC'd water to final volume.

Prehybridisation took place at 65^0C for at least 2 hours.

Hybridisation Buffer	50ml
20x SSC	10ml
10% SDS	2.5ml
Denhardt's 50x	5ml
$T_{50}E_{10}$: Tris 50mM EDTA 10mM	5ml
Dextran Sulphate *(final concentration 10%)*	5g
Poly A^+ 10mg/ml	250µl
ssDNA *boiled salmon or herring sperm*	250µl
^{32}P cDNA	-

Hybridisation then was carried out at 65^0C for at least 18 hours. Four washes were carried out using 4x SSC / 0.5% SDS 50^0C – for 20min, shaking. For the stripping blot 0.05x SSC and 0.01M EDTA (pH8.0) was incorporated and heated to boiling. SDS was added after the boiling stage to a final concentration 0.1%. The filter was immersed in hot elution buffer for 15 minutes. This was repeated with fresh boiling elution buffer. The filters were never allowed to dry between batches of elution buffer. The filters were then rinsed briefly in 0.01x SSC at room temperature. Most of the liquid was removed from filters by placing on a pad of paper towels. The filters were then wrapped in saran paper and exposed to check signal had been removed.

2.11 Statistical Analysis

Unless otherwise stated, results are expressed as mean ± standard error of the mean (SEM) with the number of independent studies shown (n). In many of the experiments, the results were normalised to the control which is set at 100%, this allows comparisons between the experiments to be made. A comparison of means evaluation was made (Anova test) for data depicted in Figure 5.4 (Table 5.2) and a paired Student's t test was performed for data shown in Figure 5.29 (Table 5.8).

CHAPTER 3

Expression of TIMP and MMP
Assessed by
Immunostaining pancreas and liver tissue

3.1 INTRODUCTION

In the liver the accumulation of extracellular matrix may result not only from increased synthesis but also from changes in degradation. The matrix degrading metalloproteinases or MMPs are a family of zinc dependent proteinases that are expressed by mesenchymal cells and are the major mediators of extracellular matrix degradation (503). Gelatinase A (MMP-2) degrades collagen I and partially degraded collagens I and III (gelatins); in addition it degrades native collagen IV, a key component of the basement membrane matrix. The activity of MMPs is regulated by transcription, proenzyme activation, or inhibition through the non-covalent binding of the tissue inhibitors of metalloproteinase or TIMP-1 and TIMP-2. In addition, TIMP-2 plays a specific role in the activation of gelatinase A by linking the pro gelatinase A with the membrane bound MMP activator membrane type metalloproteinase 1 (MTl-MMP) (504).

Increasing evidence suggests that pancreatic stellate cells (PSC) are the major mediators of fibrosis in chronic pancreatic injury and inflammation. Pancreatic stellate cells demonstrate many similar features to hepatic stellate cells and glomerular mesangial cells. These features include the acquisition of a myofibroblast like phenotype in the context of injury, a process known as activation. In the activated state PSC express alpha-smooth muscle actin (αSMA), enter the growth cycle and secrete fibrillar collagens, including collagen-1, that characterize chronic pancreatic fibrosis. As such the PSC probably represents the wound healing myofibroblasts of the pancreas.

Pancreatic fibrosis is associated with an increase in extracellular matrix, predominantly interstitial or fibrillar collagens including collagen I and III. Studies presented in abstract form suggest that, in addition to the architectural distortion mediated by the increased expression of fibrillar collagens, altered cell matrix interactions perpetuate the myofibroblast-like PSC phenotype (345). In contrast, by plating PSC onto a model basement membrane like matrix (EHS) a more quiescent phenotype develops in which expression of collage-1 and alpha SMA are down regulated. These studies suggest that the mechanism of development of pancreatic fibrosis may in part depend on critical changes in cell - matrix interactions (314).

The central role played by PSC in pancreatic fibrosis suggests that these cells may express mediators of matrix degradation. Indeed previous studies of hepatic fibrosis and renal fibrosis

suggest that it is likely that activated PSC would express MMP 2, MTl-MMP, and TIMPs-l and -2 (355). PSC have also been shown to express MMPs and TIMPs in culture (demonstrated later in this thesis) (3). However less is known about expression of MMPs and TIMPs in pancreatic disease. In this chapter I examined the expression of MMPs and TIMPs in chronic pancreatitis as compared to the normal pancreas. I also set out to co-localise the expression of α-SMA in relations to MMPS and TIMPs. If confirmed this would suggest that activated pancreatic stellate cells promote the progression of fibrosis through altering the pattern of matrix degradation.

Objectives

In this part of the thesis my intention was to show the following in human liver and pancreas:

- Perform immunohistochemistry on normal and fibrotic liver and pancreatic tissue for TIMP-1, TIMP-2, αSMA, Gel A (MMP-2) and MT1-MMP (MMP-14)
- In so doing, this will demonstrate parallel fibrotic processes in pancreatic injury in comparison to liver fibrosis such as increased expression of αSMA and TIMP-1, TIMP-2

3.2 Methods

3.2.1 Ethics Approval

Ethics approval for this research was granted through the local Southampton University Ethics Committee. Patient consent in written form prior to the time of operations was sought in order for archived tissue to be incorporated in experimental work.

3.2.2 Selection of cases - Pancreas

Formalin-fixed and paraffin wax-embedded tissue blocks from six cases of chronic pancreatitis and six normal controls were incorporated. All cases were retrieved from the histopathology database at Southampton General Hospital. The normal tissue was taken from two Whipple's' resections, for duodenal adenocarcinoma and a small ACTH-secreting neuroendocrine pancreatic tumour. Three specimens were obtained from patients undergoing resection of gastroesophageal adenocarcinoma and in which tumour extended close to, or focally into, the pancreas. One sample was an open biopsy for a suspicious pancreatic nodule, found at cholecystectomy. The last two were from pancreas removed after an oesophagogastrectomy for squamous cell carcinoma of the oesophagus and a distal pancreatectomy with colectomy for adenocarcinoma of the colon. In each of the six normal controls, in the blocks chosen for the study, there was no evidence of tumour involvement or chronic pancreatitis.

In the chronic pancreatitis cases, three specimens were resections (one resection of the head of pancreas, two distal pancreatectomies) performed for painful alcohol-related chronic pancreatitis. One specimen was an open pancreatic biopsy of a nodular pancreas found at cholecystectomy. One was a proximal resection of a symptomatic pancreatic mass (idiopathic chronic pancreatitis) and one was from an area of obstructive chronic pancreatitis above a pancreatic adenocarcinoma

Table 3.1 Selection of normal human pancreas (from archived biopsy specimens)

Details of normal human pancreas specimens		
No	Patient Initials	Operation comments, diagnosis and context of pancreas retrieval
1	LO	Normal pancreas tissue
2	BM	Pancreatic tumour, but adjacent specimen used for normal pancreas tissue
3	KO	Adeno carcinoma of stomach and esophagogastric junction. Normal pancreas tissue
4	JW	Indication for biopsy: Cushing's disease, pancreas nodule ?cause. Results show normal pancreatic tissue
5	Not Available	Esophagogastric tumour Normal pancreatic tissue
6	Not Available	Esophagogastrectomy Normal pancreatic tissue

Table 3.2 Details of diseased human pancreas (from archived biopsy specimens)

Details of diseased human pancreas specimens		
No	Patient Initials	Operation comments, diagnosis and context of pancreas retrieval
1	KD	Chronic pancreatis
2	JB	Chronic pancreatitis
3	KM	Chronic pancreatitis
4	EN	Chronic pancreatitis
5	Not Available	Chronic pancreatitis
6	Not Available	Chronic pancreatitis

3.2.3 Selection of cases – Liver

Formalin-fixed and paraffin wax-embedded tissue blocks from six cases of chronic liver disease and three normal controls were used. All cases were retrieved from the histopathology database at Southampton General Hospital. The normal tissue was taken from two liver resections, one for a bile duct tumour invading into the liver parenchyma – tissue here was taken from uninvolved tissue; the second for a possible liver mass which was finally diagnosed as a haemangioma; one for resection of metastatic colon cancer. For fibrotic liver: 2 cases were due to alcohol liver disease, one for active hepatitis C infection, one for ongoing autoimmune active hepatitis, and one case of fibrosis secondary to possible alcohol disease.

Table 3.3 Selection of diseased human livers (from archived biopsy specimens)

Fibrotic liver details		
	Initials	Diagnosis
1	GM	Alcoholic hepatitis with cirrhosis
2	RS	abnormal architecture with linking fibrosis, grade I siderosis, mixed acute/chronic inflamm.
3	MJR	Clincial: alc liver disease Micronodular cirrhosis, acute steatohepatitis, accompanying sinusoidal pericellular fibrosis supporting alc liver disease
4	AM	Clincal: HCV infection Micronodulat cirrhosis, piecemeal necrosis, (IPA score 3,3,3).
5	JW	Clin hi alc intake with signs of chronic liver disease Severe fibrosis & early cirrhosis; predominant lesion - chronic active hepatitis (no signs of alc liver disease)
6	JH	Clinical: Autoimmune hepatitis Histology: Idiopathic macronodular cirrhosis with low grade activity

Table 3.4 Selection of normal human livers (from archived biopsy specimens)

Details of normal human livers		
No	Initials	Operation comments, diagnosis and context of liver retrieval
1	CB	Normal liver tissue
2	Not available	Normal liver tissue
3	Not available	Normal liver tissue

Six proteins were chosen for study using immunohistochemistry: TIMP-1, TIMP-2, α-SMA, Gel-A and MT1-MMP. The optimum dilution of each primary antibody was determined using sections from liver known to express each of the molecules under study. After de-paraffinising for ten minutes and washing the slides in 100% through to 70% alcohol, for one minute each, the endogenous peroxidase activity was inhibited with hydrogen peroxide (Merck) for ten minutes.

In order to establish the optimum staining dilution and pre-treatment all the sections underwent a pre-treatment antigen retrieval involving either microwave irradiation in 0.01M citrate buffer (pH 6.0) (Merck) for thirty minutes at medium power; pressure cooking at 13lb pressure for two minutes in 0.01M citrate buffer; or proteolytic enzyme exposure with pronase or no treatment (applying 10% bovine serum albumin, BSA for thirty minutes). The primary antibodies were applied (at various dilutions) to all sections, except negative controls and incubated overnight at +4ºC.

On the second day after the specimens had warmed up to room temperature, secondary antibodies were applied for thirty minutes (Dako). The sections were washed in Tris-buffered saline (TBS) and pre-prepared Streptavidin-Biotin Peroxidase complexes (Dako) applied for thirty minutes. After a further wash with TBS, the sections were stained with diaminobenzidine substrate (DAB) (Biogenex) for five minutes. After a two minute wash in running tap water and a rinse with 70% alcohol, the sections were counter-stained with Harris's haematoxylin (Merck) for one to two minutes, rinsed for one minute in running tap water, differentiated in 1% alcohol for five seconds and finally, blued in running tap water for five minutes before dehydrating and mounting with coverslips.

All antibody solutions were diluted from fresh stock solutions, which were kept at $+4^0$C. All incubations were undertaken at room temperature. All negative controls were noted to be negative. At the end of each staining protocol, cells were mounted and viewed under appropriate light with a Zeiss photomicroscope. Examples of immunstained cells were photographed on Kodak Ektachrome film.

Table 3.5 Pre-treatment regimes and primary antibody concentrations for immunohistochemistry

Antibody	**Dilution**	**Type**	**Pre-treatment**	**Source**
TIMP-1	1:200	Rabbit polyclonal	Pronase	Chemicon International
TIMP-2	1:400	Goat polyclonal	Pronase	Chemicon International
αSMA	1:200	Mouse monoclonal	Pronase	Sigma
Gel A	1:400	Mouse monoclonal	Pronase	Oncogene Research Products
MT1-MMP	1:200	Mouse	Pronase	Dako

General Methods are described in Chapter 2 Methods Section 2.1.2.

3.3 Results of Immunohistochemistry

Sections from each case underwent immunohistochemical staining using the standard method for Streptavidin-Biotin immunostaining outlined in Chapter 2 Methods section 2.1.2. Negative controls were performed by omitting the primary antibody as described in 2.1.2.

Slides were initially reviewed and scored by Professor John Iredale at the time of performing the immunohistochemistry: the results depicted here are based on these scorings. Subsequent to this at the time of writing slides were again reviewed by Dr Adrian Bateman (Southampton University Hospitals Trust) and Dr Simon Rasbridge (Royal Bournemouth and Christchurch Hospitals Trust).

Table 3.6 depicts the results of staining 6 sections of normal human pancreas and 6 sections of fibrotic human pancreas. An increase in expression of MMP-2, MT1-MMP, αSMA, TIMP-1 and TIMP-2 staining was seen in fibrotic pancreas compared to normal pancreas in the perivascular stroma and periacinar stroma. Whilst expression of TIMP-1 and TIMP-2 was noted in the pancreatic islets of normal human pancreas the expression of TIMP-1 and TIMP-2 was increased in the islets of fibrotic pancreas compared to normals.

Table: 3.6 In-Vivo expression of MMP-2, MT1-MMP, αSMA, TIMP-1 and TIMP-2 in human pancreas

Normal Human Pancreas

Site	αSMA	Gel A	MT1-MMP	TIMP-1	TIMP-2
Perivascular Stroma	++ 6/6	++ 6/6	++ 6/6	++ 6/6	++ 6/6
Periacinar Stroma	+/- 2/6	absent	absent	absent	absent
Area of Fibrosis	absent	absent	absent	absent	absent
Acini	absent	absent	absent	absent	Absent
Islets	absent	absent	absent	++ 6/6	++ 4/6

Fibrotic Human Pancreas

Site	αSMA	Gel A	MT1-MMP	TIMP-1	TIMP-2
Perivascular Stroma	++ 6/6	++ 6/6	++ 6/6	++ 6/6	++ 6/6
Periacinar Stroma	++ 6/6	++ 6/6	+++ 6/6	++ 6/6	++ 6/6
Area of Fibrosis	+++ 6/6	++ 6/6	+++ 6/6	+++ 6/6	+++ 6/6
Acini	absent	absent	absent	absent	absent
Islets	absent	absent	absent	++++ 6/6	++++ 4/6

(Please note that data is not shown for MT1-MMP in the ensuing figures).

Table 3.7 In-Vivo expression of MMP-2, MT1-MMP, αSMA, TIMP-1 and TIMP-2 in human liver

Normal Human Liver

Site	αSMA	Gel A	MT1-MMP	TIMP-1	TIMP-2
Portal tracts	++6/6	++6/6	++ 6/6	++ 6/6	+6/6
Connective tissue	Weak +ve 3/6	Absent	Absent	Absent	Subtle background only +6/6
Hepatocytes	Weak +ve 3/6	Absent	Absent	Absent	absent
Sinusoids	Weak +ve 3/6	Absent	Absent	Absent	Absent
Perisinusoids	Weak +ve 3/6	absent	Absent	Absent	absent

Fibrotic Human Liver

Site	αSMA	Gel A	MT1-MMP	TIMP-1	TIMP-2
Portal tracts	++6/6	++6/6	++ 6/6	++ 6/6	+6/6
Connective tissue	+++6/6	+4/6	+4/6	++6/6	Subtle background only +6/6
Hepatocytes	+6/6	+4/6	+4/6	++6/6	+6/6
Sinusoids	++6/6	+4/6	+4/6	++6/6	++4/6
Peri-sinusoids	+6/6	+4/6	+4/6	++6/6	++4/6

Table Results of staining 6 sections of normal human liver and 6 sections of fibrotic human Liver. (Please note that data is not shown for MT1-MMP and αSMA in the ensuing figures).

Figure 3.1 TIMP-1 staining in human pancreas

A) Normal control

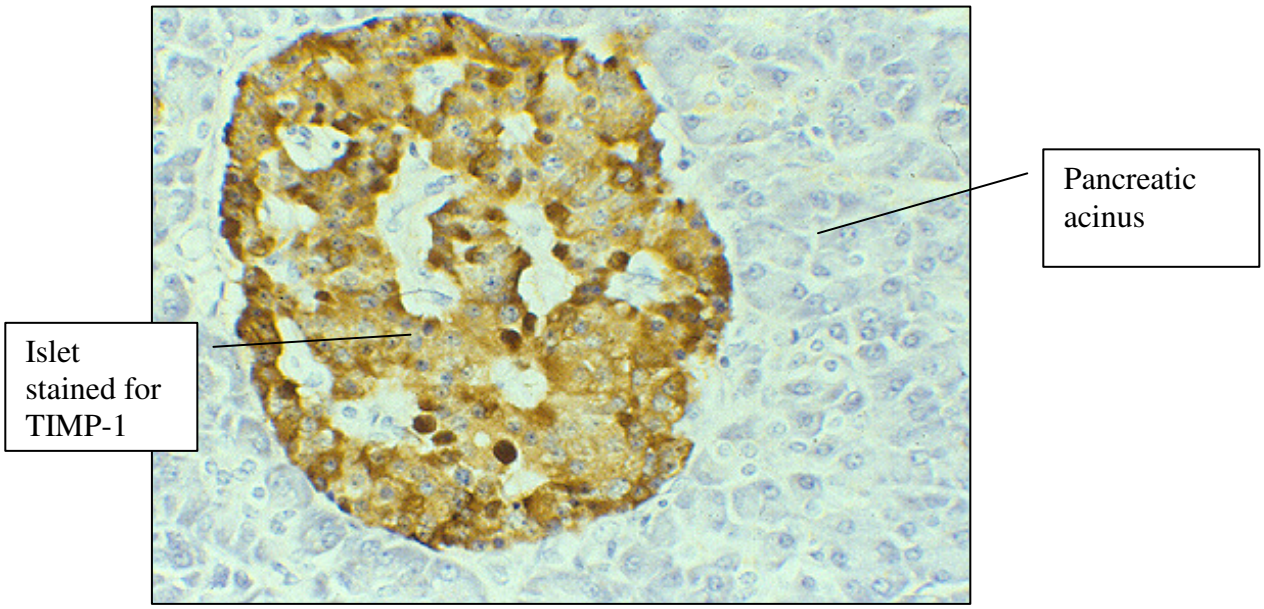

B) Fibrotic pancreas

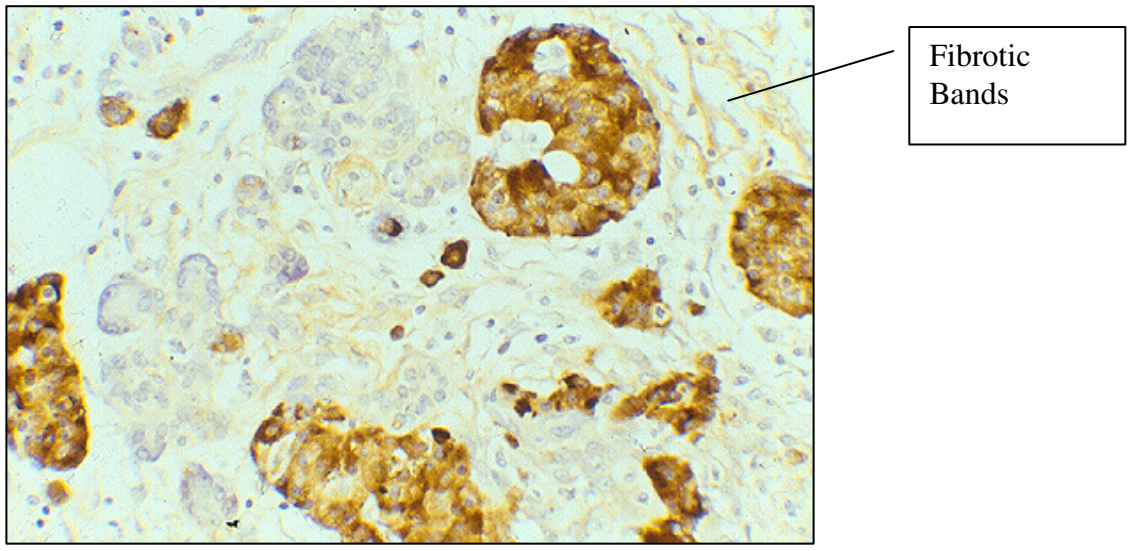

Streptavidin-biotin staining of TIMP-1 in human pancreas. There is intense cytoplasmic expression of TIMP-1 in the pancreatic islets in both A and B but in addition TIMP-1 is also localised to fibrotic bands in B. Negative controls (not shown) demonstrated a consistent negative stain). Magnification x500 A, x200 B.

Figure 3.2 TIMP-2 staining in human pancreas

A) Normal control

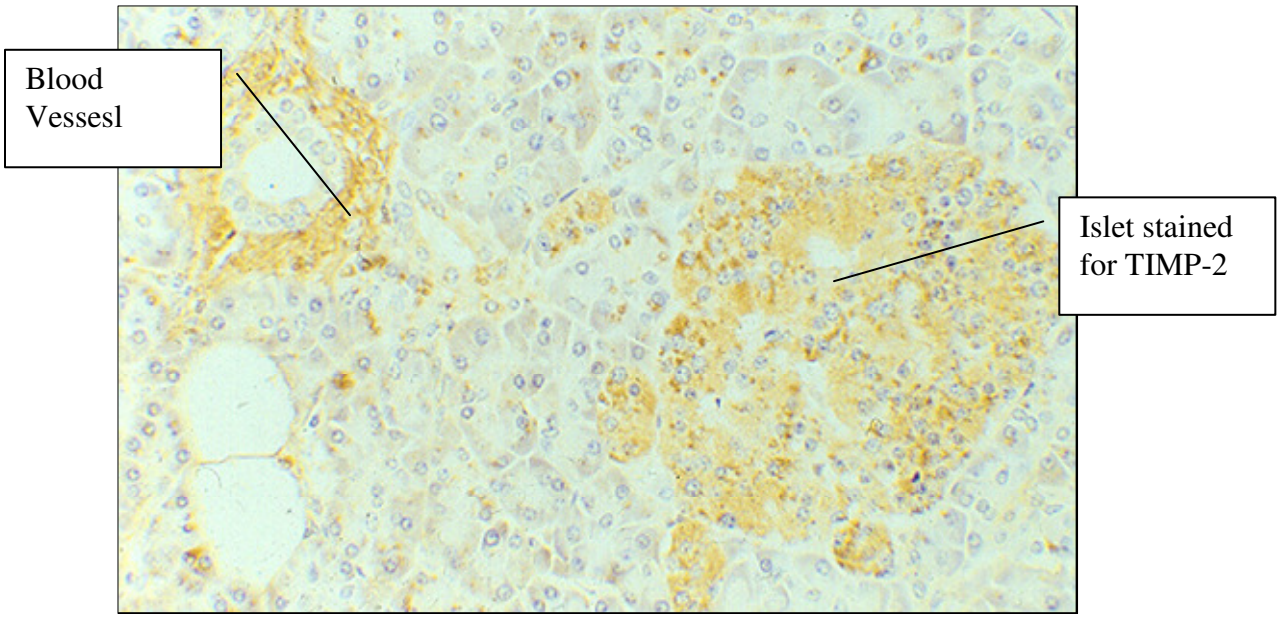

B) Fibrotic pancreas

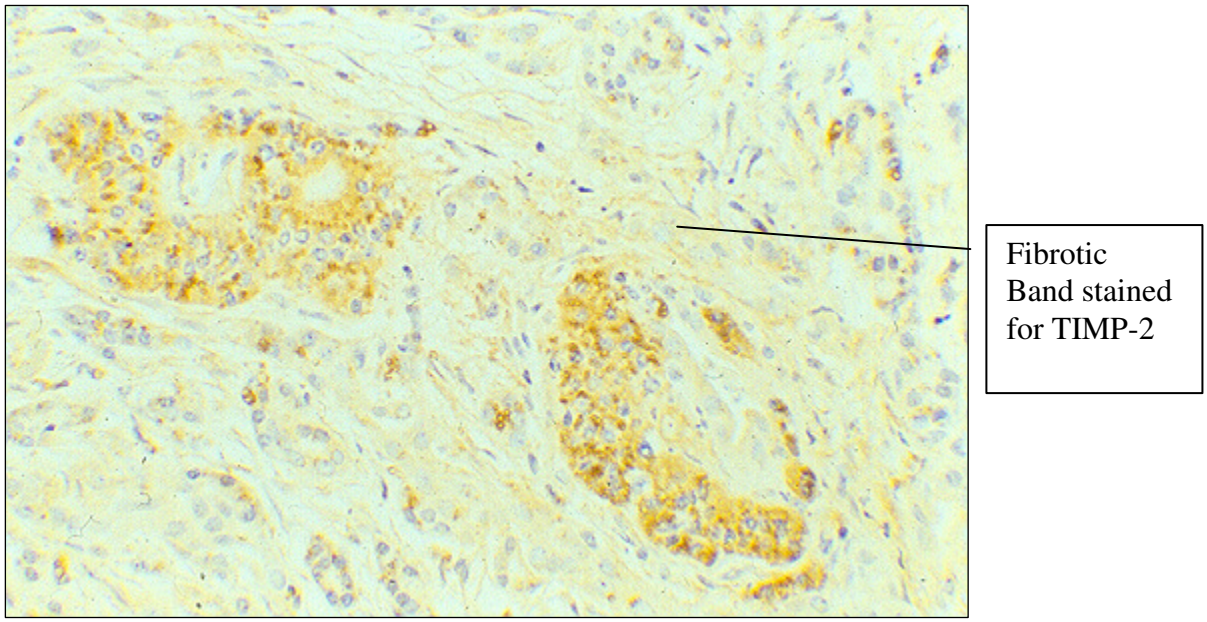

Streptavidin-biotin staining of TIMP-2 in human pancreas. Although staining was weaker in comparison to TIMP-1, again there is cytoplasmic staining of TIMP-2 in the pancreatic islets and, in addition, around blood vessels in normal and fibrotic tissue. TIMP-2 is also localised to fibrotic bands in B.. Magnification x200 A, x200 B.

Figure 3.3 Gelatinase A staining in human pancreas

A) Normal control

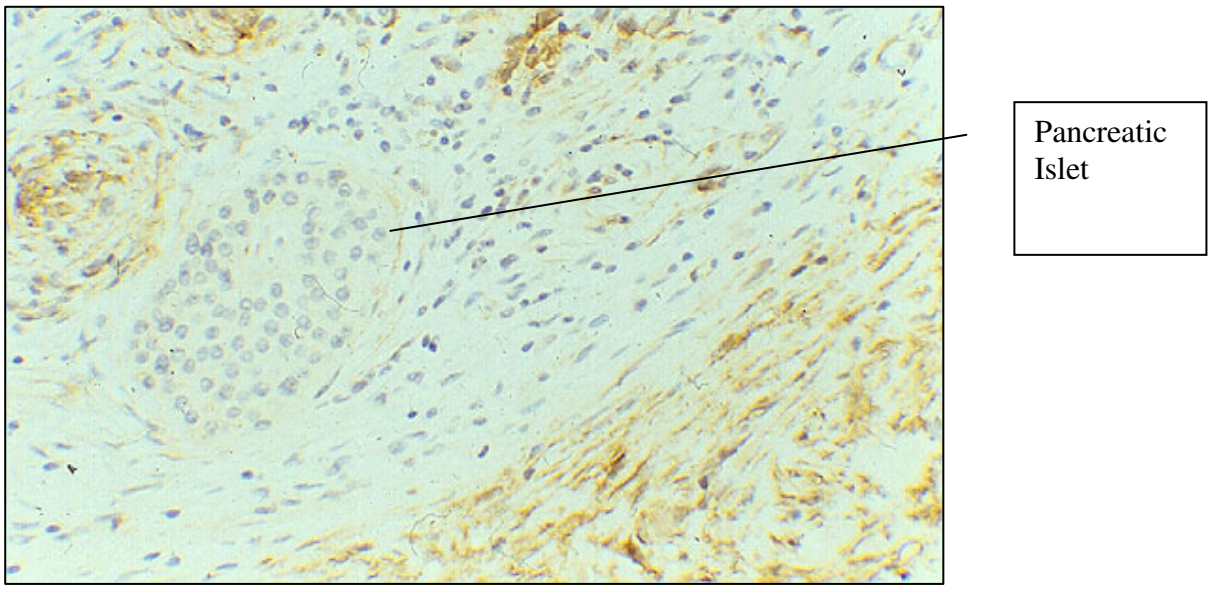

B) Fibrotic pancreas

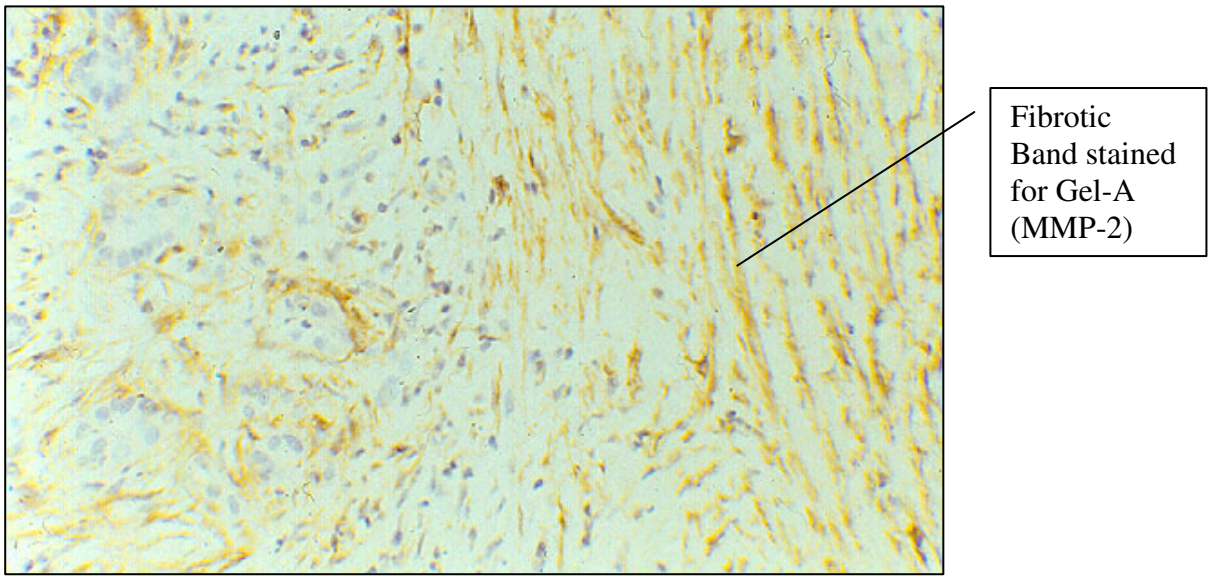

Streptavidin-biotin staining of Gelatinase A in human pancreateas. Gel A is seen predominantly in the stroma but not in the pancreatic islets in both A and B but in addition is also localised to fibrotic bands in B. MT1-MMP (MMP-14, not shown) was noted to stain for normal and fibrotic pancreas in a similar pattern to Gelatinase A (MMP-2).
Magnification x500 A, x200 B.

Figure 3.4 α-Smooth Muscle Actin (αsma) staining in human pancreas

A) Fibrotic pancreas, Low power

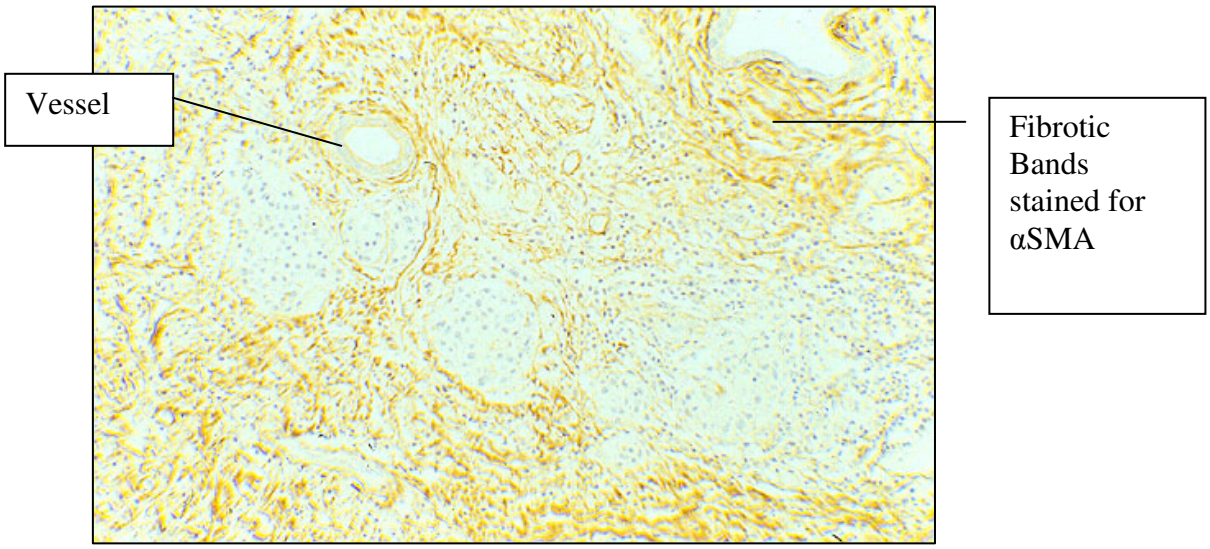

B) Fibrotic pancreas, High power

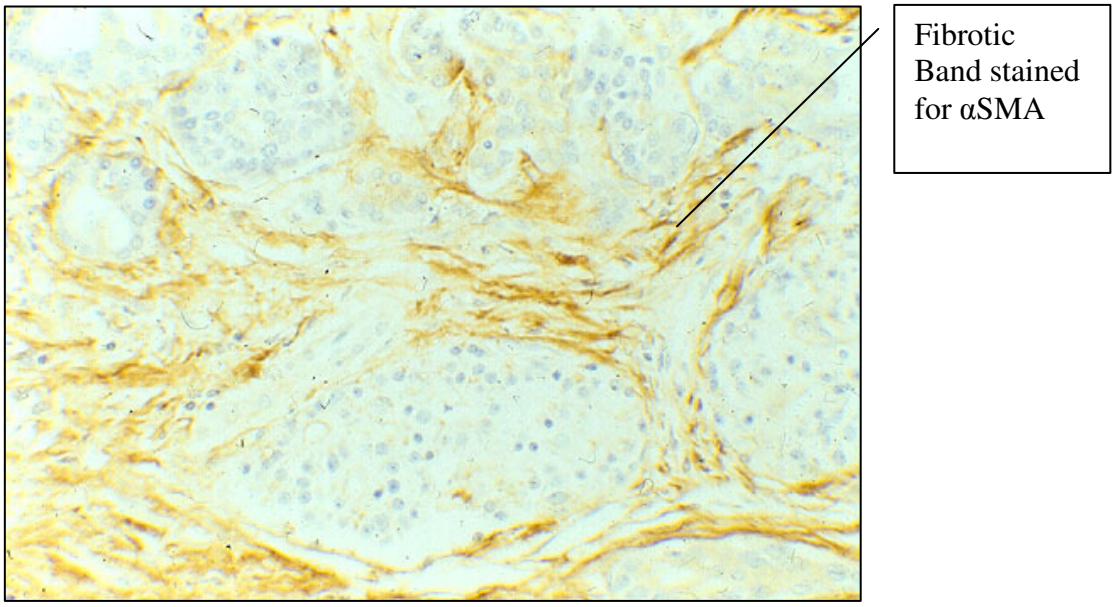

Streptavidin-biotin staining of αSMA in human pancreas. Normal pancreas is not shown. αSMA was noted in normal perivascular stroma and periacinar stroma but not the islets or normal acini. The fibrotic bands stained positively for α-SMA. Magnification x200 A, x500 B.

Figure 3.5 Gelatinase a (MMP-2) staining in fibrotic human liver

A) Normal Control stain x50

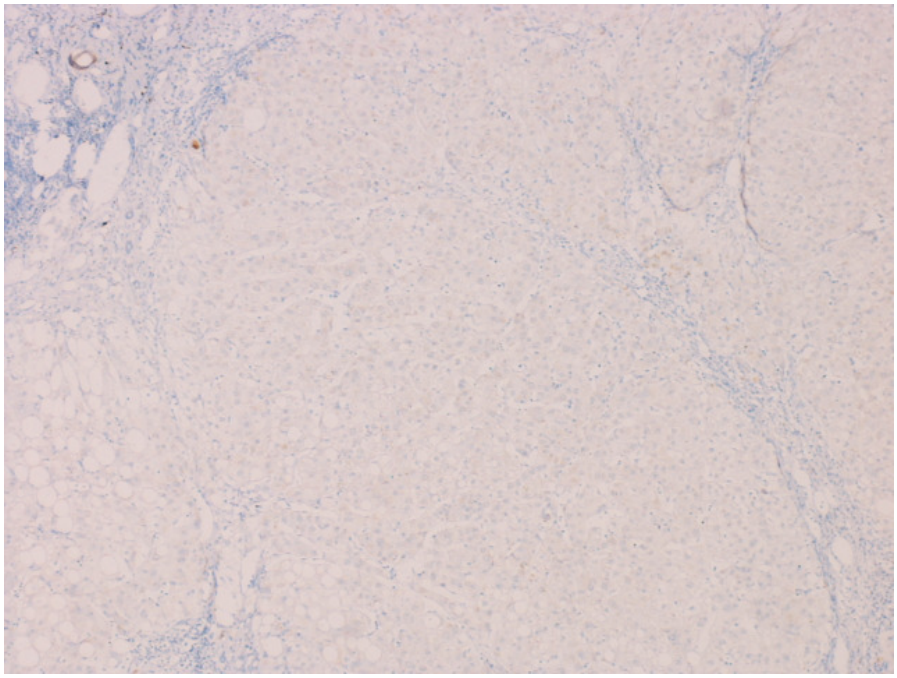

B) Fibrotic liver Low power

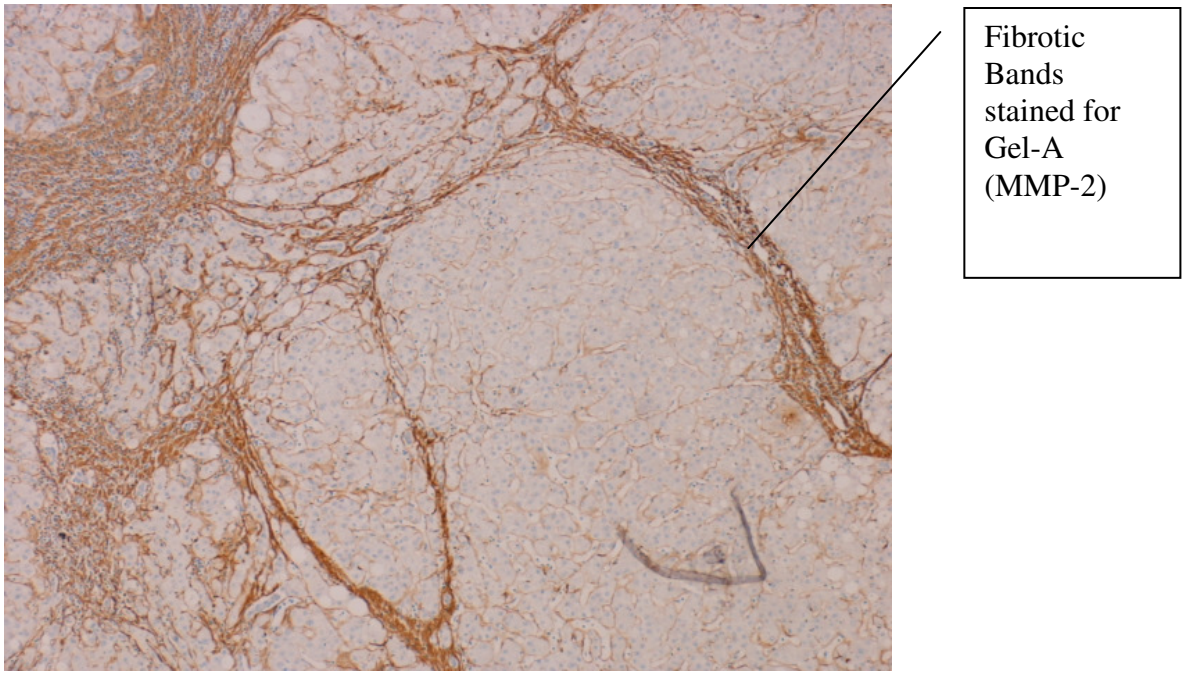

Streptavidin-biotin staining of Gelatinase A in human liver. Gel A is seen predominantly in the fibrotic bands but also in the liver sinusoids.

Magnification x50 A, x50 B.

Figure 3.6 Gelatinase a (MMP-2) staining in fibrotic human liver

A) High power

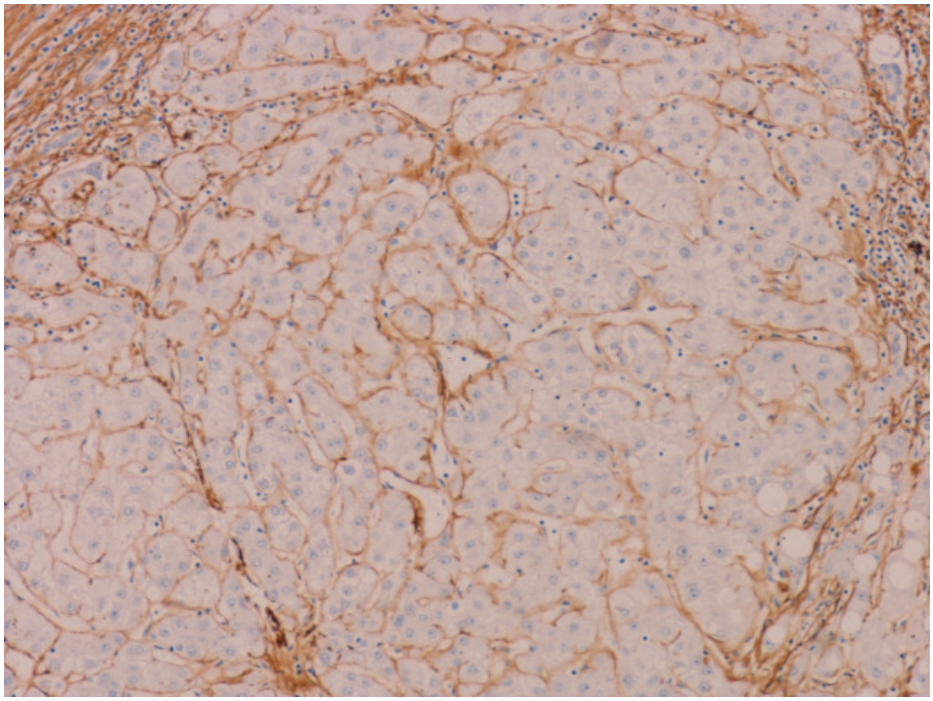

A) High power x200

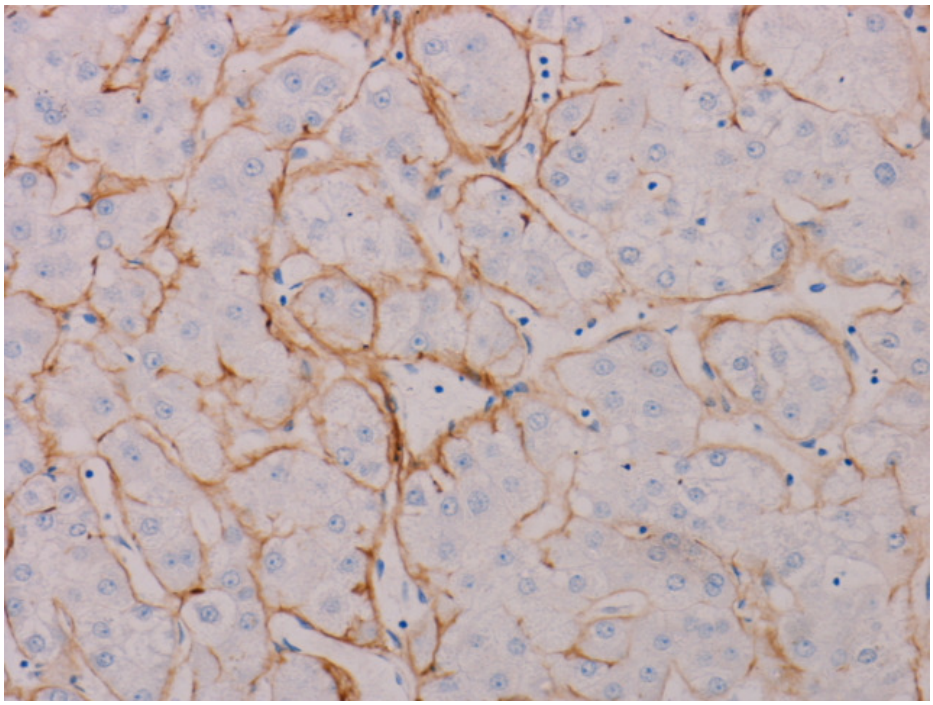

Streptavidin-biotin staining of Gelatinase A in human liver. Gel A is seen to be strongly expressed in both fibrotic bands and the liver sinusoids. MT1-MMP (MMP-14) whilst not shown here in normal or fibrotic liver had broadly a similar pattern to Gelatinase-2 (MMP-2). 1:100 Pronase staining; Magnification x100 A, x200 B.

Figure 3.7 TIMP-1 staining in fibrotic human liver

A) Staining in hepatocytes (Goat staining) Low power

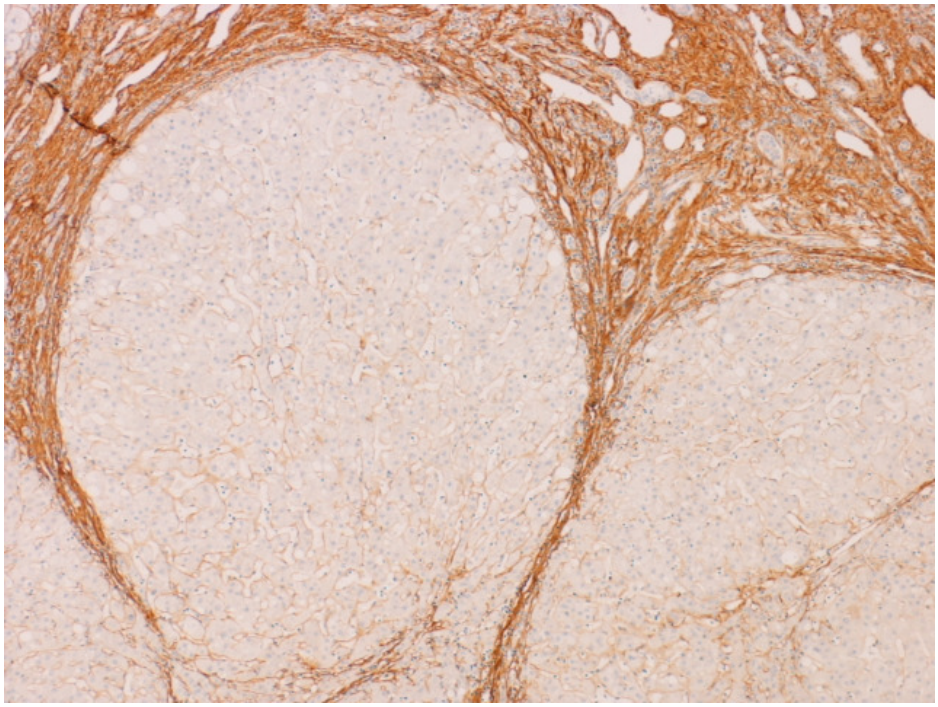

B) High power TIMP-1 staining in human fibrotic liver

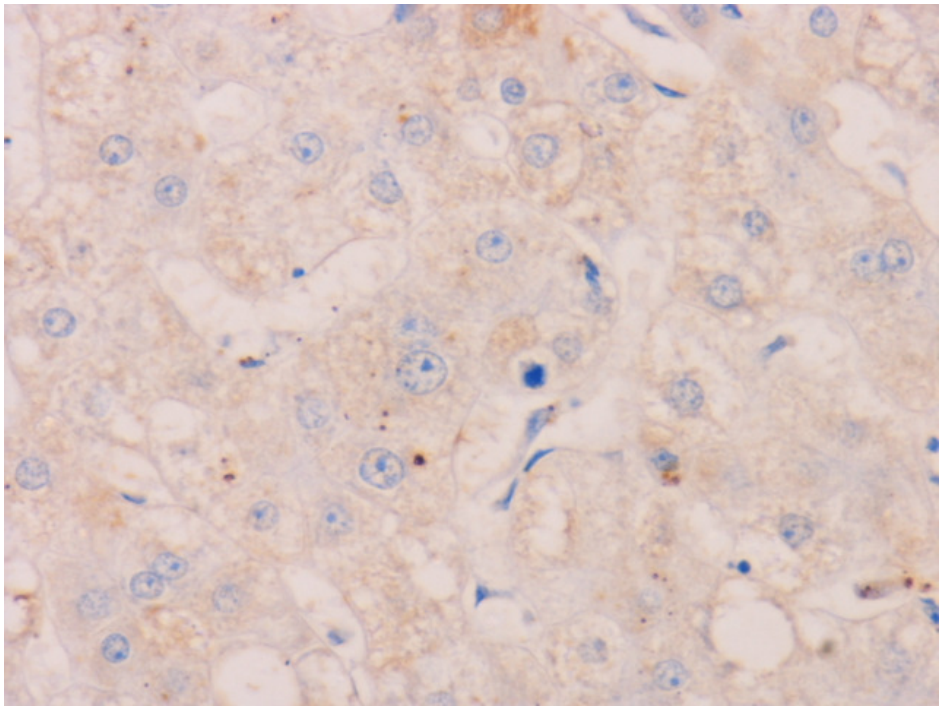

The main area of staining for TIMP-1 in fibrotic liver shown here is related to the portal tracts and the sinusoids. Pronase staining; Magnification A) x50 and B) x200.

Figure 3.8 TIMP-1 staining in fibrotic human liver

High power

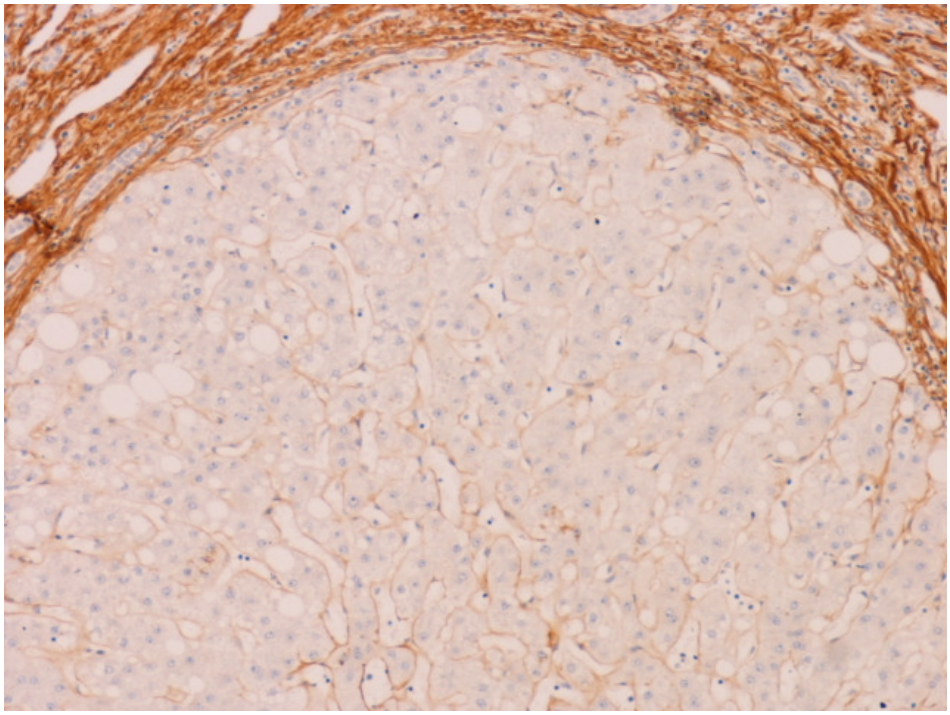

B) TIMP-1 staining in fibrotic human liver High power

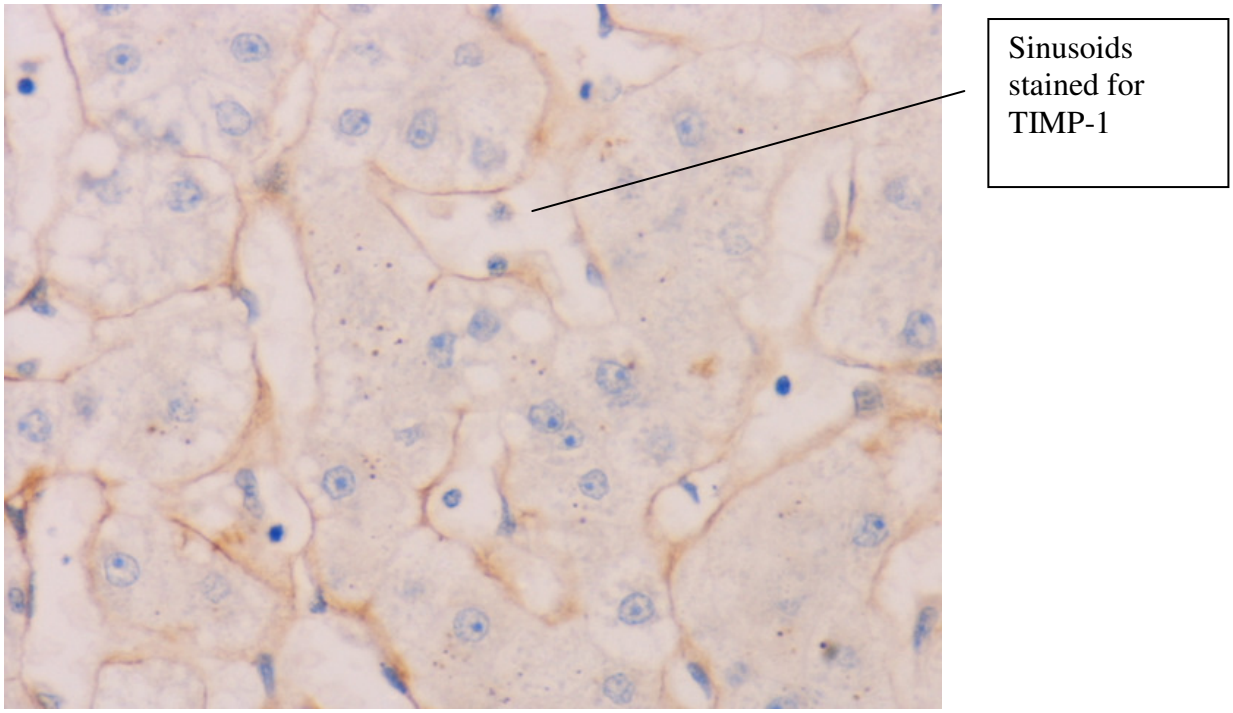

The main area of staining for TIMP-1 in fibrotic liver shown here is related to the sinusoids. There is some granular staining in the hepatocytes. In control liver there was no parenchymal staining. Pronase staining; Magnification x100 A and x400 B

Figure 3.9 TIMP-2 staining in fibrotic human liver

A) Low power TIMP-2 staining Goat 1:400

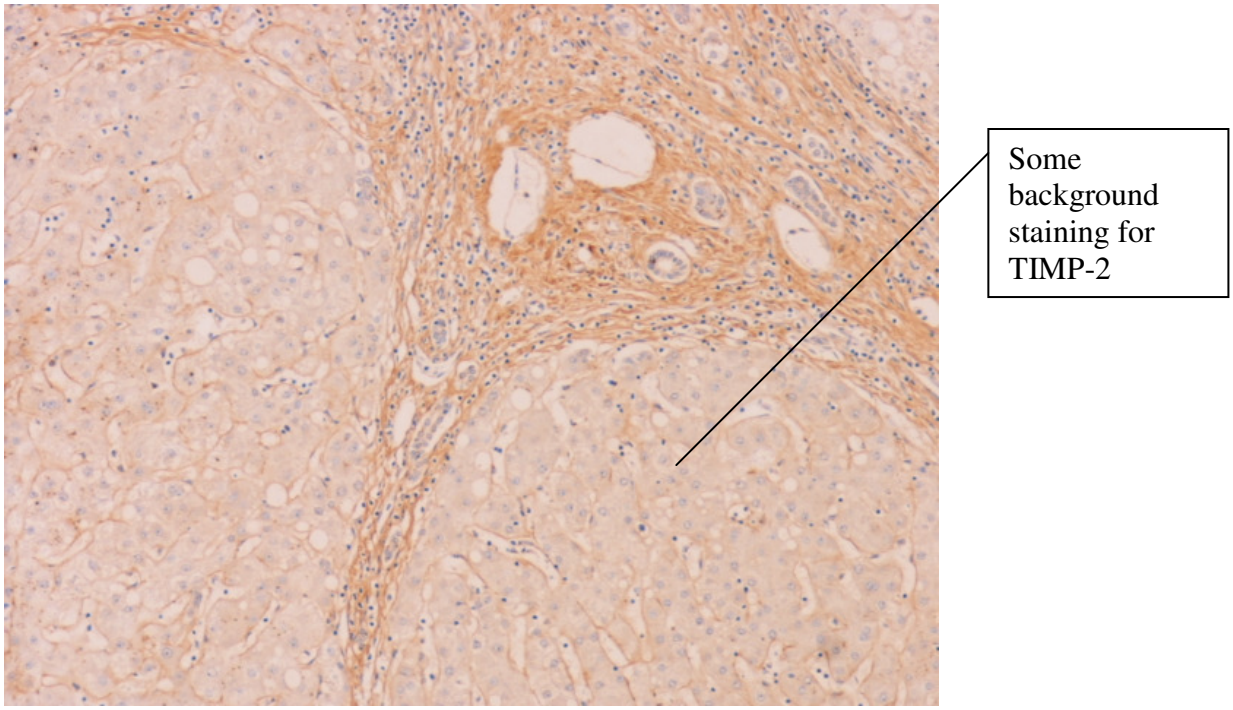

B) High power TIMP-2 staining Goat 1:400

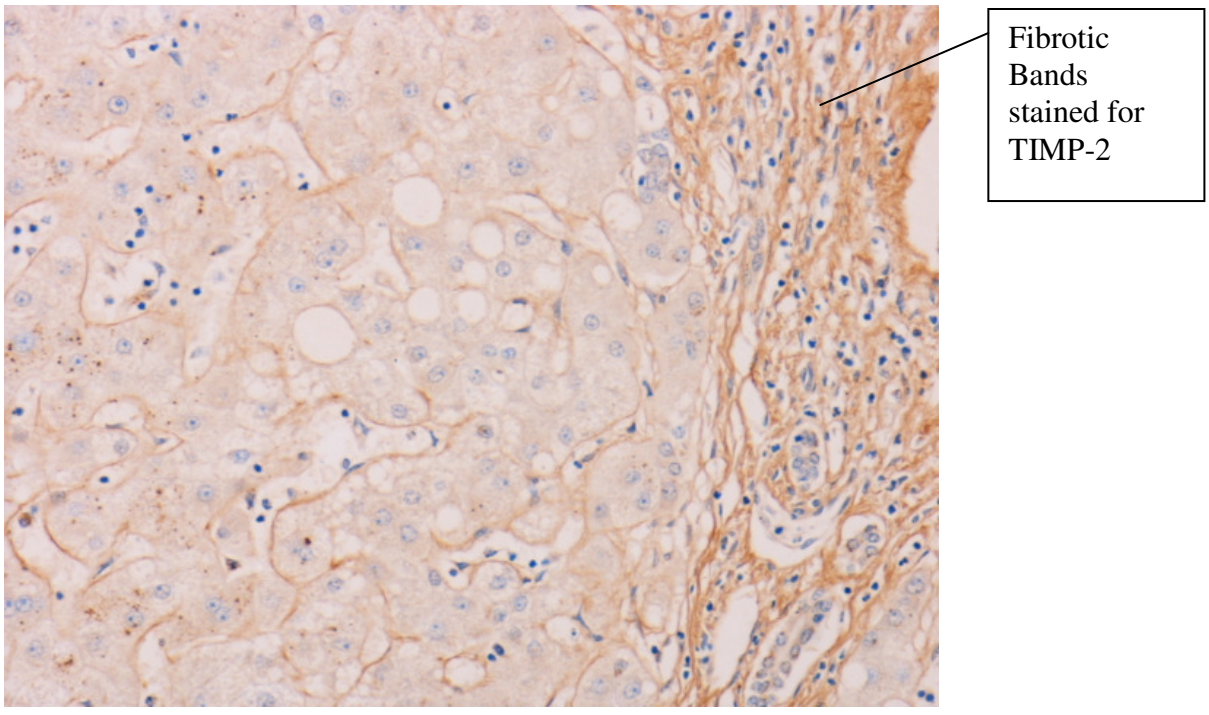

Staining of fibrotic liver with TIMP-2 Magnification A) x50 & B x100. Although there is evidence of some background staining in addition there is TIMP-2 staining in fibrotic bands. This follows a similar pattern to TIMP-1. However there is clear staining here in Figure 3.9 and Figure 3.10 of staining around the sinusoids.

Figure 3.10 TIMP-2 staining in fibrotic human liver

A) High power TIMP-2 staining Goat 1:400

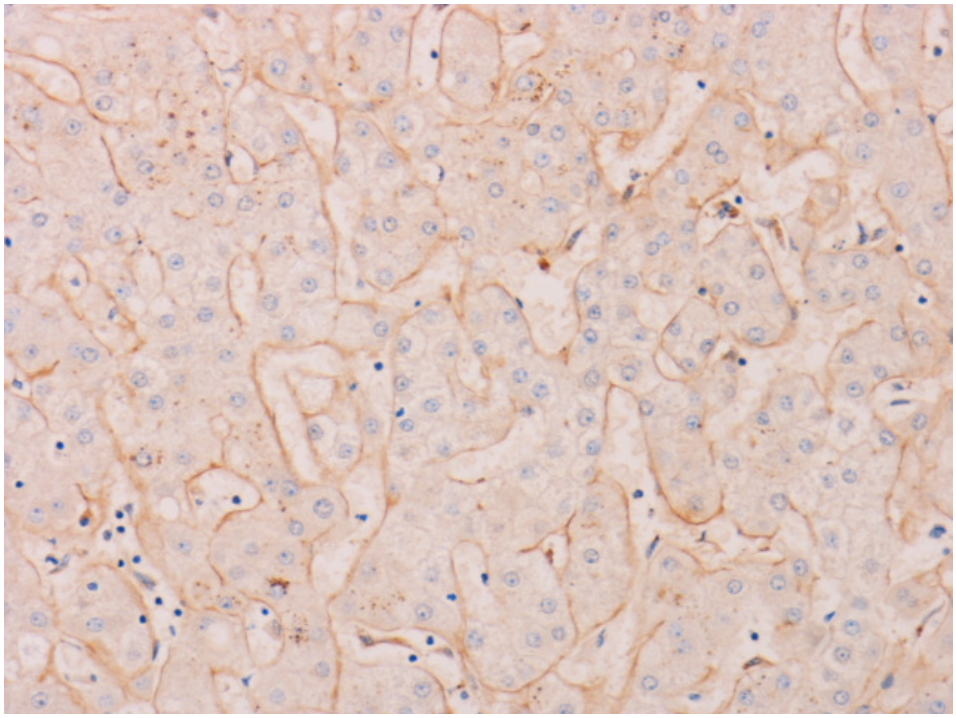

B) High power TIMP-2 staining Goat 1:400

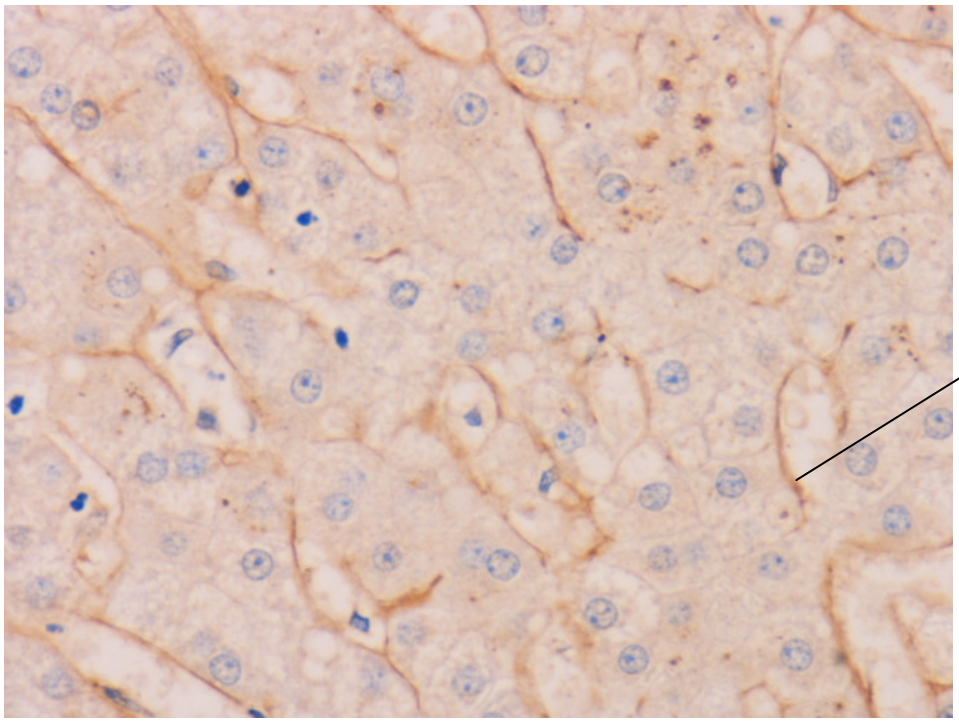

TIMP-2 staining in fibrotic liver Magnification A) x200 B) x400. Although there is some subtle background staining there is clear staining around the sinusoids seen best in Figure 3.10B.

3.4 Discussion

3.4.1 Pancreas

Six examples of normal human pancreas and six cases of chronic pancreatitis were stained for MMP-2, MT1-MMP, TIMP-1 and TIMP-2. In addition parallel examples were stained for αSMA to localize activated pancreatic stellate cells (PSCs) although this also detects vascular smooth muscle. In all 6 fibrotic samples the cell rich stroma dividing up the remnant acini and islets was strongly αSMA positive indicating the presence of activated PSCs. MMP-2 was detected and localized in the αSMA positive cell rich stroma in each of the six examples of chronic pancreatitis. No MMP-2 was detected in the islets or acini. MT1-MMP was also readily detected in the activated PSC of each specimen (please note this is not shown in the figures). In contrast to the localization of MMP-2 the distribution of MT1-MMP was more widespread with expression seen in either the islets or elements within the islets in five samples. In addition in three of the specimens staining of variable intensity was observed in the acinar cells. Expression of TIMP-1 and TIMP-2 was detected in the αSMA positive cells within the stroma. In addition, TIMP-1 was localized to the islets and in four samples TIMP-2 was also expressed by islet cells.

3.4.2 Liver

Three examples of normal human liver and six cases of fibrotic/cirrhotic liver were stained for MMP-2, MT1-MMP, TIMP-1 and TIMP-2. No cirrhotic liver had a diagnosis of inherited disease such as alpha-1 antitrypsin deficiency (as this may have explained some of the staining in diseased hepatocytes for TIMP-1 and TIMP-2 had this been the case). In addition parallel examples were stained for αSMA to localize to activated hepatic stellate cells (HSCs).

αSMA was positive in some normals which was unexpected. It is possible that in these patients they may have had unsuspected liver disease. MT1-MMP showed good staining in one or two cases only and there was increased expression in hepatocytes or increased background; the majority of needle biopsies were negative. (Please note the αSMA and MT1-MMP slides are not shown in the figures above). MMP-2 was weakly positive in some normals but strongly positive in fibrotic bands in diseased livers. TIMP-2 demonstrated some staining of hepatocytes in a granular fashion, weak staining in blood vessels, with a subtle increased background in some cases. However there was strong localization to the sinusoid

and perisinusoidal areas in fibrotic liver. TIMP-1 demonstrated some staining of fibrotic bands in addition to some stromal staining. There was some granularity in the hepatocytes only but strong staining in the sinusoids and perisinusoids.

Activated PSC in vivo during sustained (chronic) pancreatic injury express mediators of matrix degradation. Specifically MT1-MMP, Gelatinase A/MMP-2, TIMP-1, and TIMP-2 were expressed in chronic pancreatitis. These results when obtained were the first description of this facet of activated PSC phenotype and demonstrated a further aspect in which these cells behave similarly to hepatic HSC and renal mesangial cells. Fibrotic disorders in other organs including the liver and kidney are also characterized by increased expression of MMP-2. These observations have led to speculation that MMP-2 may promote the fibrotic process. This appears counter intuitive, and indeed the mechanism(s) for this are not clear, however MMP-2 has been implicated in promoting stellate cell proliferation possibly by remodelling the matrix and revealing ligands for integrin alpha v beta3 (129). In addition, in models of both hepatic and pancreatic stellate cells activation there is evidence to suggest that degradation of the normal basement membrane like matrix, which is rich in type IV collagen and replacement with a matrix rich in collagen-1 is associated with promotion and perpetuation of the activated stellate cell phenotype (296). After liver injury, the Disse space matrix remodelling might be initiated by MMPs expressed in early stages of HSC activation such as MMP-3 and MMP-13 and then perpetuated by MMP-2 which is expressed in the fully activated cells (259) (263). Thus the expression of MMP-2 may be directly pro fibrotic by altering matrix degradation in favour of a matrix relatively depleted of collagen IV and rich in collagen I. Of interest, in models of hepatic fibrosis there is a clear temporal relationship between the progression of fibrosis and expression of MMP-2 and its activator MT1-MMP, while spontaneous recovery from fibrosis is associated with a decrease expression of both (505). The role of MMPs and TIMPs in injury and fibrosis has been examined extensively in the context of liver, but there is far less information in the pancreas. My studies show activated PSC as a source of these proteins. However, my samples were limited to either normal or advanced fibrosis and only provide a snapshot of antigen expression. More detailed information of the temporal and spatial expression of the MMPs and TIMPs as injury proceeds to fibrosis will require the establishment of models of progressive fibrosis in rodents. Such models could use mice genetically deficient in the various TIMP2 and MMPs.

In addition to expression of matrix degrading MMPs, this data demonstrate that PSCs in vivo are potent sources of TIMP-1 and TIMP-2. As described previously, TIMP-2 is required for the activation of proMMP2 by MT1-MMP. However the activation model is complex and in the presence of excess TIMP-2 net matrix degradation is inhibited including MMP-2 activity. The additional expression of TIMP-1, which like TIMP-2 has a potent inhibitory effect on all activated MMPs including those with collagenase activity, suggests that matrix degradation may be significantly inhibited. Although the immunolocalization experiments were undertaken to determine the expression of MMPs and TIMPs by PSC, the data with respect to islets is particularly interesting. Islet cells were found to express TIMP-1 and 2 at a very high level. Moreover this expression was constant across all sections regardless of the extent of fibrotic change. The reason for this pattern of expression was highly speculative at that time. Nevertheless, Islet cell function is relatively well preserved even in comparatively advanced chronic pancreatitis. This suggests that islets are protected from the inflammatory and fibrotic damage that is occurring elsewhere in the organ. The expression of TIMPs 1 and 2 may represent a mechanism whereby peri-islet matrix is protected from remodeling. An alternative and potentially more intriguing possibility is that TIMP-1, which has been shown to have both cell growth and survival promoting activities, may be acting to promote the survival of islet cells surrounded by an inflammatory and fibrotic process.

CHAPTER 4

HYPOXIA AND TIMP-2 EXPRESSION

4.1 Introduction

It has been established that during the fibrogenic progression of chronic liver disease towards cirrhosis excess deposition of extracellular matrix and capillarization of sinusoids increases the resistance to blood flow and lowers oxygen delivery, thus rendering the tissue hypoxic (506). Angiogenesis itself is a hypoxia stimulated and growth factor dependent process consisting in the formation of new vascular structures from pre-existing blood vessels. Formation of new vessels is known to occur in several organs and to be critical for both growth and repair of tissues in several pathophysiological conditions (507). However it has become increasingly clear that angiogenesis occurring during chronic wound healing and fibrogenesis provides a key contribution to disease progression. Pathological angiogenesis as recently reviewed has indeed been described in chronic inflammatory/fibrotic liver diseases of different aetiologies (508).

Pathological angiogenesis is associated with fibrogenic progression of chronic liver disease (509). Experimental data suggests that hypoxia and vascular endothelial growth factor (VEGF) may stimulate proliferation and synthesis of type I collagen in activated rat HSC (510). HSC express MMPs and TIMPs under a variety of conditions and evidence discussed above indicates TIMP overexpression contributes to fibrosis. Prior to this work there was little known on the effect of hypoxia on TIMP expression in HSC.

In collaboration with Dr Jill Norman in University College Hospital (Department of Renal medicine, Rayne Institute) primary and passaged cultured rat HSC were transferred to London for study under control and hypoxic conditions. Cells were split into two populations, control and hypoxia and those in the latter group were cultured in hypoxic conditions for variable time points extending from 12, 24, 48 and 72hrs.

4.1.1 Northern Blotting for the detection of α SMA, Procollagen-1, Gelatinase A, TIMPs -1 & -2 in Activated rat pancreatic stellate cells (PSC)

In chapter 3 the expression of MMPs and TIMPs in chronic pancreatitis was investigated compared to normal controls in vivo. In this chapter the expression of pancreatic stellate cells

cultured on tissue culture plastic was studied for the expression of messenger RNA of alpha SMA, procollagen 1, Gelatinase A, Tissue inhibitor of metalloproteinase 1 & 2.

4.1.2 Ribonuclease Protection Assay in human livers for expression of TIMP-2

The ribouclease protection assay is a laboratory technique used in biochemistry and genetics to identify individual RNA molecules in a heterogeneous RNA sample extracted from cells. The technique can identify one or more RNA molecules of known sequence even at low total concentration. The extracted RNA is first mixed with antisense RNA probes that are complementary to the sequence or sequences of interest and the complementary strands are hybridized to form double-stranded RNA. The mixture is then exposed to ribonucleases that specifically cleave only *single*-stranded RNA but have no activity against double-stranded RNA. When the reaction runs to completion, susceptible RNA regions are degraded to very short oligomers or to individual nucleotides; the surviving RNA fragments are those that were complementary to the added antisense strand and thus contained the sequence of interest

Ethics approval was obtained from the local Southampton University Hospitals Trust. Written consent was obtained from all patients. Five samples of liver resection from cirrhotic liver and 3 samples from normal liver (liver resected for colorectal cancer metastases) were obtained to study the expression of human TIMP-2 mRNA in normal and diseased liver. For this experiment a ribonuclease protection assay (RPA) was chosen to detect mRNA as it has increased sensitivity over Northern Analysis (484). This is partly because larger amounts of RNA can be loaded (up to 100µg) and also hybridisation occurs in solution ensuring that the maxiumum number of hydrogen bonds are available for hybridisation. As stated above the principles of the assay are that a single stranded radiolableled antisense RNA probe is hybridised with the target mRNA in solution. In the presence of excess probe, the number of probe mRNA hybrids will be proportional to the amount of target mRNA present. After hybridisation the mixture is treated with RNAase to digest any single stranded RNA and any redundant probe. The probe-target mRNA hybrids are therefore “protected”. After inactivation of the RNAase the protected framgents are ethanol precipitated, suspended in loading buffer and separated on an RNA denaturing polyacrylamide gel. The abundance of the protected fragment can then be visualised by autoradiography of the dried gel and analysed by scanning densitometry.

Ribonuclease Protection Assays (RPAs) are described in detail in chapter 2 secton 2.5. This discusses in detail the following:

- Preparation of Radiolabeled Antisense Riboprobe
- *In Vitro* Transcription of Radiolabeled Antisense Riboprobe
- Protocol for Ribonuclease Protection Assay & Sample Preparation
- Resolution of Protected Fragments on Polyacrylamide Urea Gels

The objectives in this chapter therefore included the following:

- An examination of the role of hypoxia in the expression of TIMP-2 mRNA in rat hepatic stellate cells and if the trial protocol was successful to move onto rat pancreatic stellate cells both fresh and passaged and finally human liver and human pancreas
- To test the hypothesis that pancreatic stellate cells express messenger RNA for alpha SMA, ProCol-1, Gel-A, TIMP-1 and TIMP-2
- Examine the expression of TIMP-2 mRNA in whole liver taken during hepatic resections for patients with colorectal cancer metastases (where normal liver segments free of metastatic disease were incorporated) in comparison to expression from diseased fibrotic human liver.

4.2 Methods

Cells were cultured in hypoxic conditions ie in 1% oxygen, 5% CO_2, balanced nitrogen (specialist gas from BOC) in a humidified atmosphere at 37^0C, normoxic controls were cultured under the routine incubator conditions ie 21% oxygen, 5% CO_2 in a humidified atmosphere at 37^0C. The medium was the standard medium (DMEM) incorporated in the laboratory in Southampton for experiments. For the experiments cells were made quiescent for 48hr in reduced 0.5% serum, medium was changed to fresh reduced-serum medium immediately prior to start of hypoxia/normoxia as previously described (511). Cells were grown in dishes or 6 well plates (rather than flasks) for hypoxia culture vessels are placed in the modular incubator with the lids off (to facilitate gas exchange in the medium). The chamber was gassed for 20mins at 10L/min to ensure complete gas exchange in the modular incubator and then sealed. The incubator operating at hypoxic conditions was technically known as a Billups Rothenberg Modular Incubator (originally obtained from ICN) (512). Cells were generally incubated in the chamber for various time points up to 96 hours (ie continuous hypoxia, the chambers were not re-gassed at regular intervals) as previously described (513). Total RNA was extracted from frozen tissue sample and cells by guanidium thiocyanate based method (section 2.10).

Northern blots were obtained from rat HSC cultured in control and hypoxic conditions as described in the methods (section 2.3).

10μg of total RNA were subjected to electrophoresis through a 1.2% agarose formaldehyde gel, and blotted onto a nylon membrane filter. After prehybridization the filter was incubated overnight at 50^0C in a 50% formamide buffer with a 32P labeled probe. The northern blots were probed for β actin and TIMP-2 rat cDNA. The resulting autoradiographs were subjected to scanning densitometry. The TIMP-2 values were normalized for beta actin and expressed in an Excel spreadsheet chart.

The membranes were prehybridised at 65^0C for at least 2 hours. The cDNA probe was added in the hybridisation buffer at 65^0C for at least 18 hours (overnight). The blots were then washed with 4x SSC / 0.5% SDS for 20 minutes/ shaking on 4 occasions. The autoradiograph was exposed.

4.2.1 Methods RNA expression are described in the Methods chapter section 2.27 & 2.3

Freshly isolted HSC were taken to make Northern blots for analysis of TIMP-2 cDNA.

4.2.2 Methods RPAs are described in the Methods chapter 2 section 2.5

In brief, 10µg of each of sample RNA and the negative control RNA (yeast) was mixed with 30µl of hybridisation buffer containing 10^5 cpm of ^{32}P-UTP labelled antisense riboprobe. Sample RNA was heated to 95^0C for 5 minutes to denature RNase and then left to hybridise at 42^0C overnight. RNase one was diluted the following morning in its digestion buffer and 180µl added to each sample, mixed and incubated at room temperature for 60mins. The reaction was terminated by the addition of 30µl of stop solution and the protected fragment precipitated by the addition of 825µl of ice cold 100% ethanol and chilling at -70^0C for 60mins. All samples were centrifuged for 15mins at 1400rpm at 40^0C and the supernatants removed with a drawn out flask Pasteur pipette. The resulting pellets were then resuspended in 8µl gel loading buffer, heated to 95^0C for 5mins to denature RNA and loaded onto 8M polyacrylamide gel and subjected to electrophoresis.

Gels were then cast in a Bio-Rad vertical sequencing apparatus. Plates were first washed in ethanol and the back plate sialinised with Sigmacote (Sigma UK) to prevent the gel sticking and make removal easier. Two gels were made, the first to seal the end of the plates and a 6-8% sequencing Gel. The gels were polymerised at room temperature by the addition of TEMED and freshly prepared 10% APS, with the combs in situe. Once set the gels were then assembled in the electrophoresis apparatus. TBE was warmed then added and the gels de-ionised by being pre-run at 50^0C with 1.5kV for 30mins. The samples were then added and fractionated by electrophoresis at 50-55^{0}C for 90 mins. The gel was transferred to a backing of 3MM filter paper. Following coverage with cling film the gel was vacuum dired at 65^0C. The dried gel was then placed next to pre-flashed X ray film and left at -70^0C for 48-96 hours. After development of the autoradiographe the resultant bands were analysed by scanning densitometry.

4.3.1 Results

Northern blots were made using 10μg of total rat HSC RNA obtained from cells incubated at various time points in control and hypoxic conditions. After hybridization with the [^{32}P]-ATP cDNA for rat TIMP-2 a dual signal was noted at 3.8kb and 1.2kb which persisted after washing with 0.2SDS/0.2xSSC at 50^0C (Figure 4.1 depicts a representative of three experiments). The autoradiographs were subjected to scanning densitometry and the results plotted on an excel spread sheet. Figure 4.2 demonstrates densitometry for the two TIMP-2 species both in control and hypoxic conditions for 8, 24, 48 and 72hrs. These values are graphed in chart format in Figure 4.3.

This experiment was repeated over 3 occasions. On each occasion there was little difference between control and hypoxic conditions for the expression of TIMP-2 in rat passaged HSC. The average of the three experiments is shown in Figure 4.4 with columns showing the standard error of the mean.

Figure 4.1 Expression of TIMP-2 in rat HSC cultured in hypoxic conditions

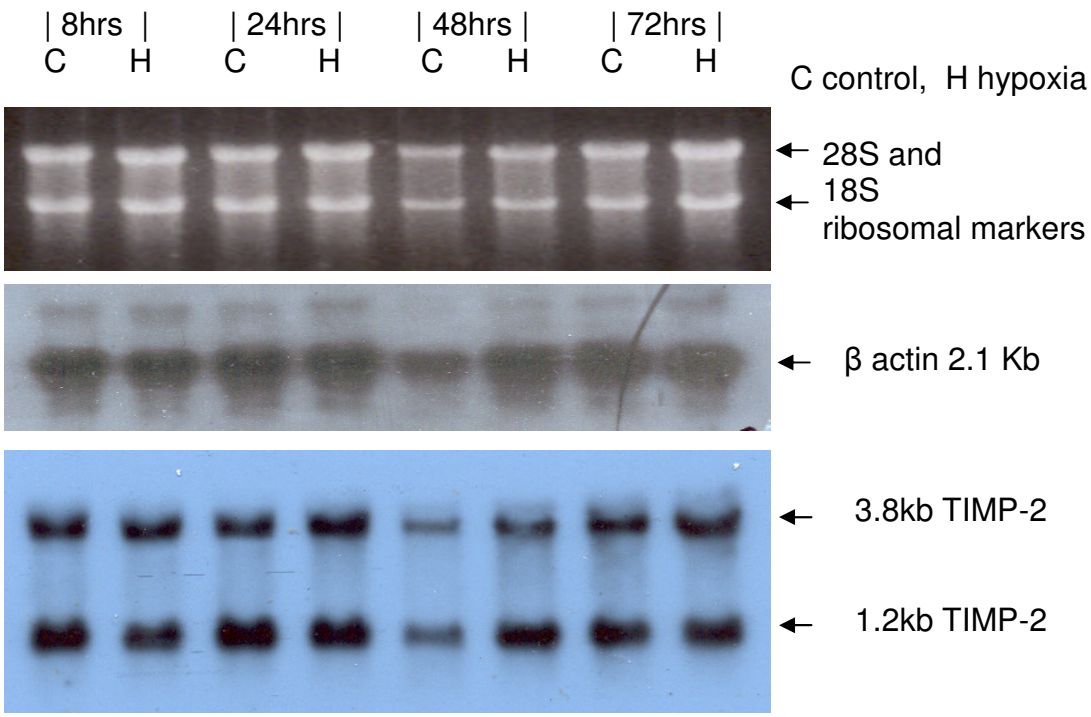

Figure 4.1 A representative northern with B actin and TIMP-2 probes. Ethidium bromide stained RNA is shown above to show loading. Northern blots were prepared from 10μg of total RNA from rat HSC cultured in control and hypoxic conditions. They were then hybridized with the cDNA of rat TIMP-2; following this the blots were subjected to stringency washes with 4x SSC / 0.5% SDS at 50^0C. This was repeated on three occasions each wash lasting for 20min washes, shaking. A beta actin probe was used as a control.

Figure 4.2 Scanning densitometry

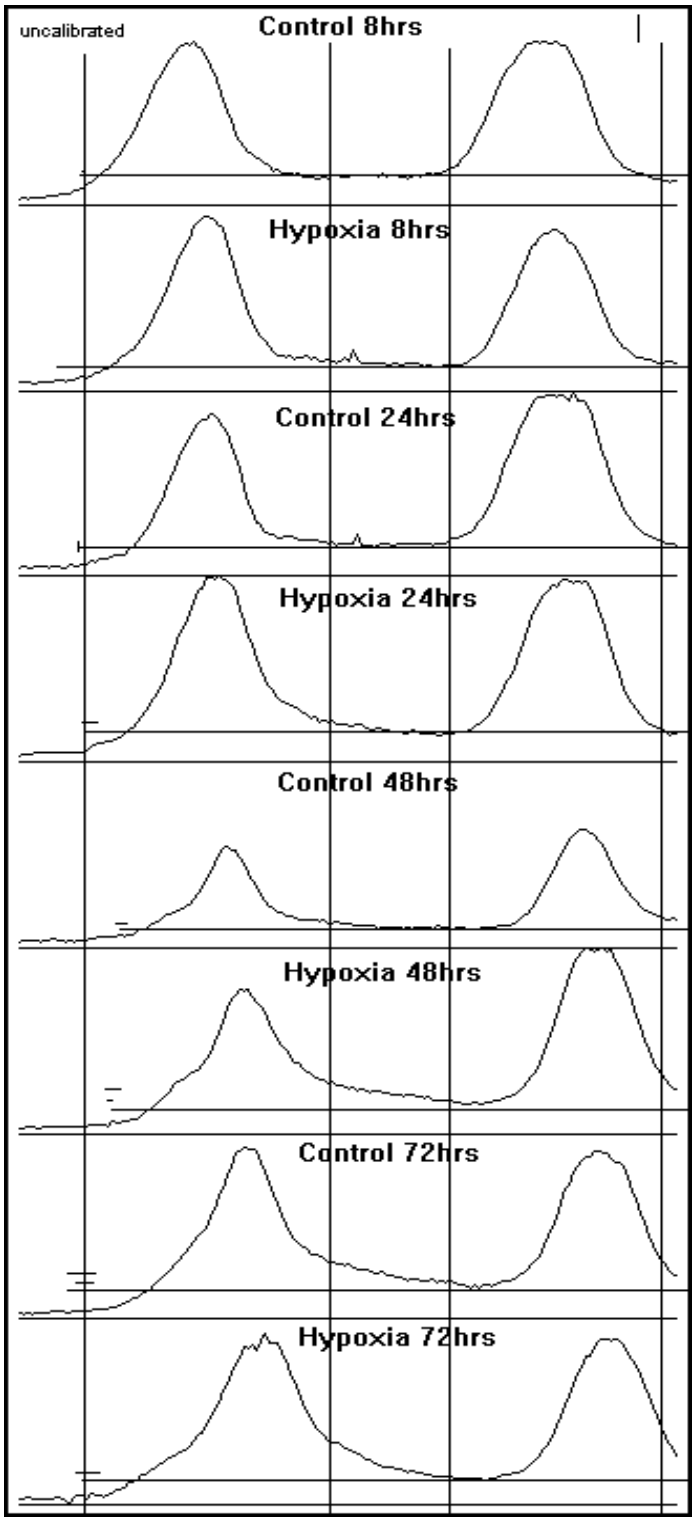

Figure 4.2 Autoradiographs were exposed to northerns probed for rat TIMP-2 cDNA for variable time points. The resulting autoradiographs were subjected to scanning densitometry. There are two peaks illustrated here representative of the 3.8kb and 1.2kb species respectively.

Table 4.1 Raw data from scanning densitometry

		Hours	densitometry		
			Timp-2	β-actin	Timp2 / β actin x 100%
1	Control	8	2912	193	1508.808
			3544	193	1836.269
2	Hypoxia	8	3240	199	1628.141
			3219	199	1617.588
3	Control	24	2638	200	1319
			4321	200	2160.5
4	Hypoxia	24	3591	179	2006.145
			3818	179	2132.961
5	Control	48	1463	169	865.6805
			1970	169	1165.68
6	Hypoxia	48	2679	181	1480.11
			3880	181	2143.646
7	Control	72	3162	186	1700
			3249	186	1746.774
8	Hypoxia	72	3561	188	1894.149
			3199	188	1701.596

Table 4.1 Raw data from scanning densitometry. Density values for TIMP-2 were normalized with B actin for each of the 3.8kb and 1.2kb species at each of the control and hypoxia time points.

Figure 4.3 TIMP-2 mRNA expression in rat HSC cultured in hypoxic conditions

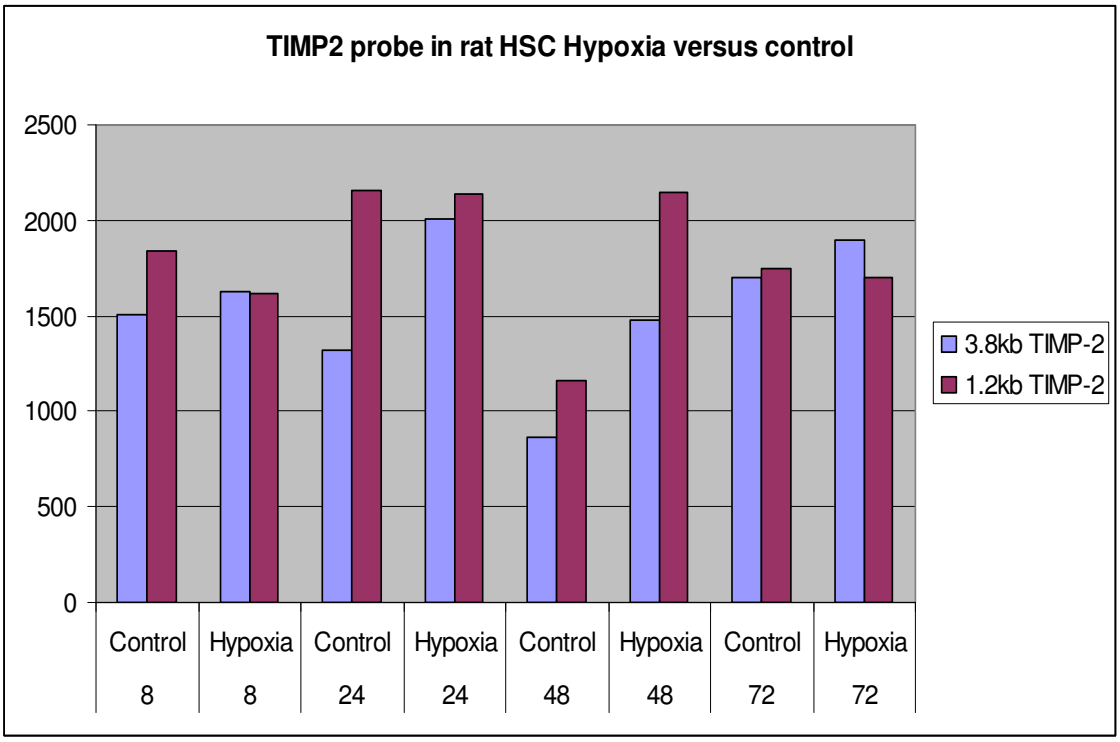

Figure 4.3 Graph of data from a single experiment. Both species of TIMP-2 are graphed together from the raw data presented earlier. Y axis is in arbitrary units, the X axis denotes the experimental conditions and the various time points in hours. No consistent trend is noted from this data.

Figure 4.4 Mean of 3 experiments: TIMP-2 expression in hypoxia

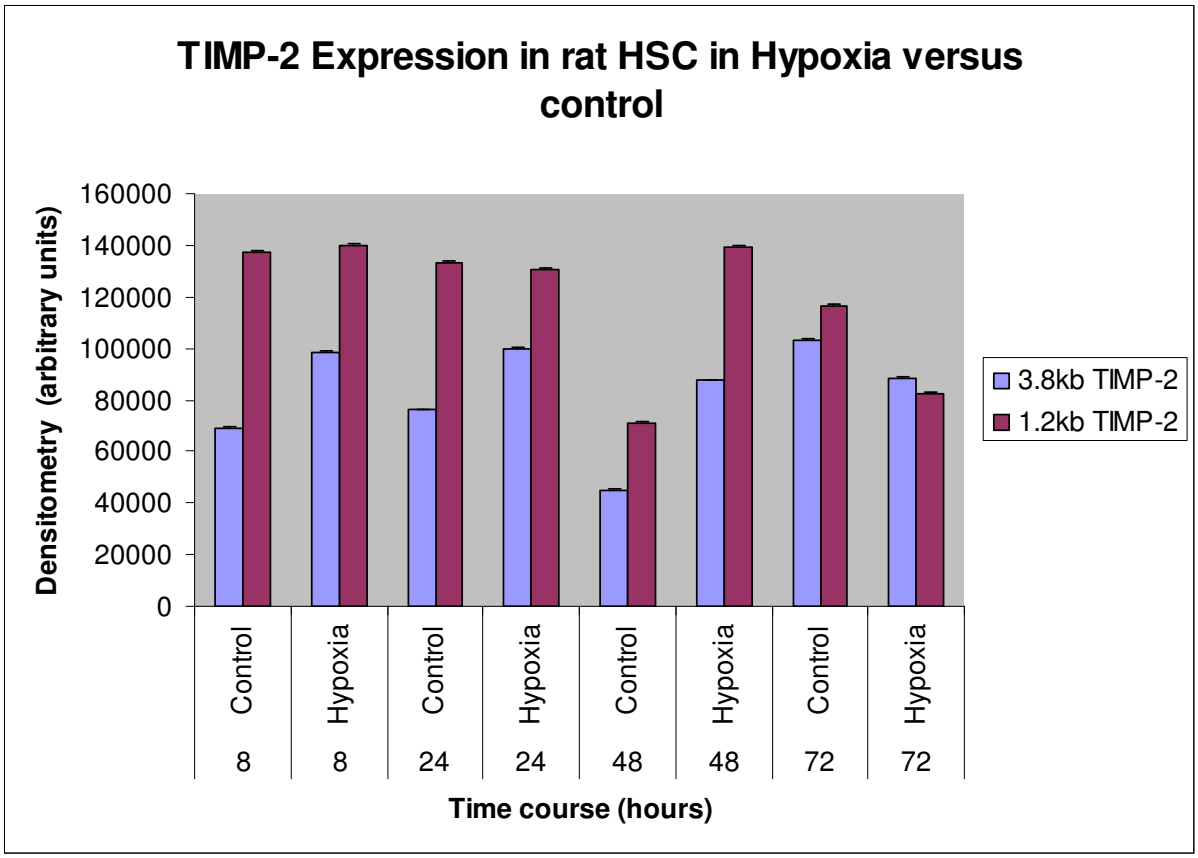

Figure 4.4 Mean of 3 experiments examining expression of TIMP-2 expression in rat HSC cultured in control and hypoxic conditions. Controls included parallel cell cultures in normoxia. Both 3.8kb and 1.2kb species of TIMP-2 are depicted with error bars demonstrating Standard error of the Mean.

4.3.2 Results

Figure 4.5 Northern Blot detecting αSMA, Procoll-1, Gel a, TIMPs -1 & -2 in activated rat pancreatic stellate cells (PSC)

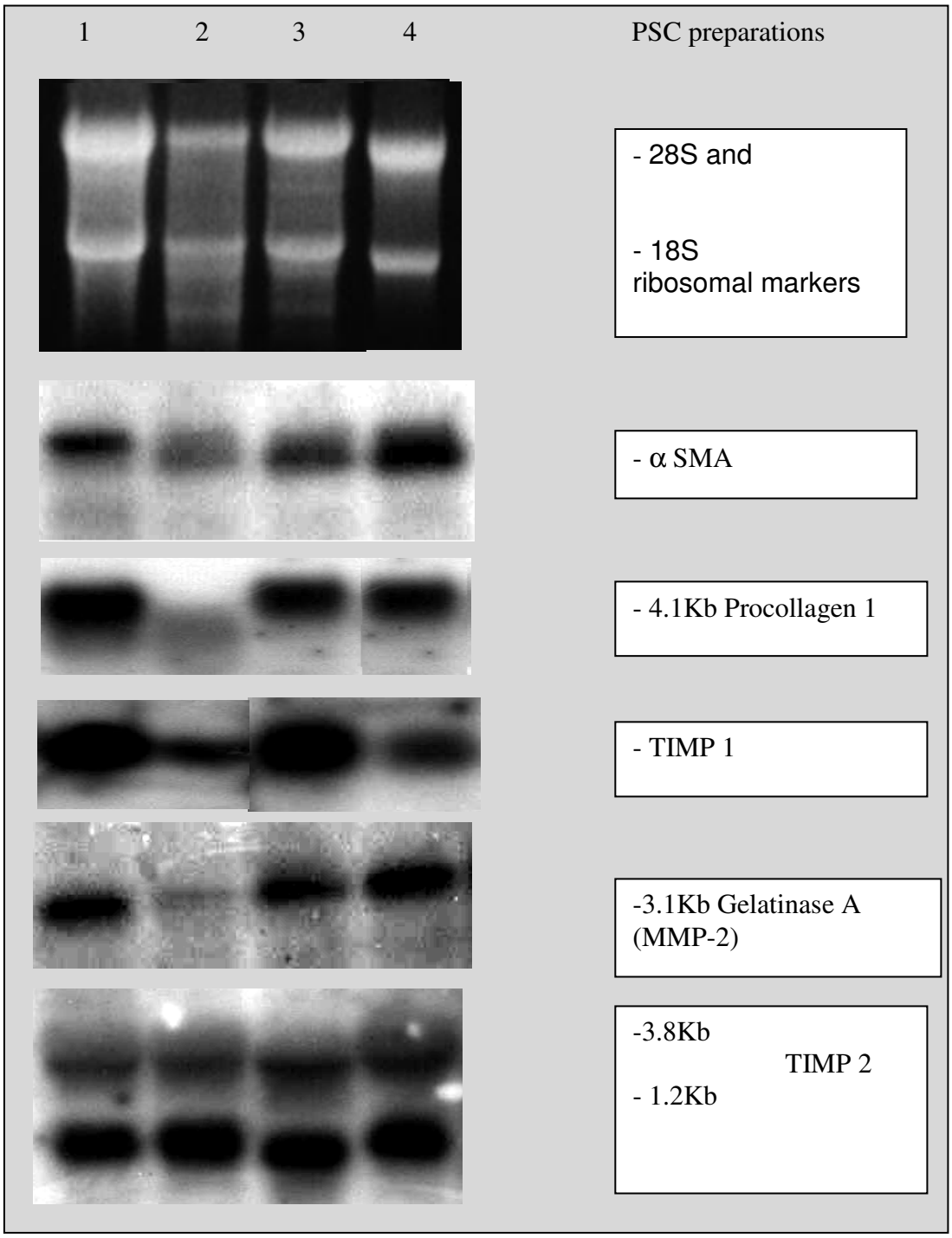

Figure 4.5 MMP / TIMP expression with activation in PSC primary cultures on uncoated tissue culture plastic with cells harvested at day 10, subjected to northern analysis, and probed with a MMP / TIMP cDNA probes. The experiment was repeated in 4 separate tissue culture experiments.

4.3.3 Results

Figure: 4.6 TIMP-2 RPA human fibrotic liver (x5) vs normal human liver (x3)

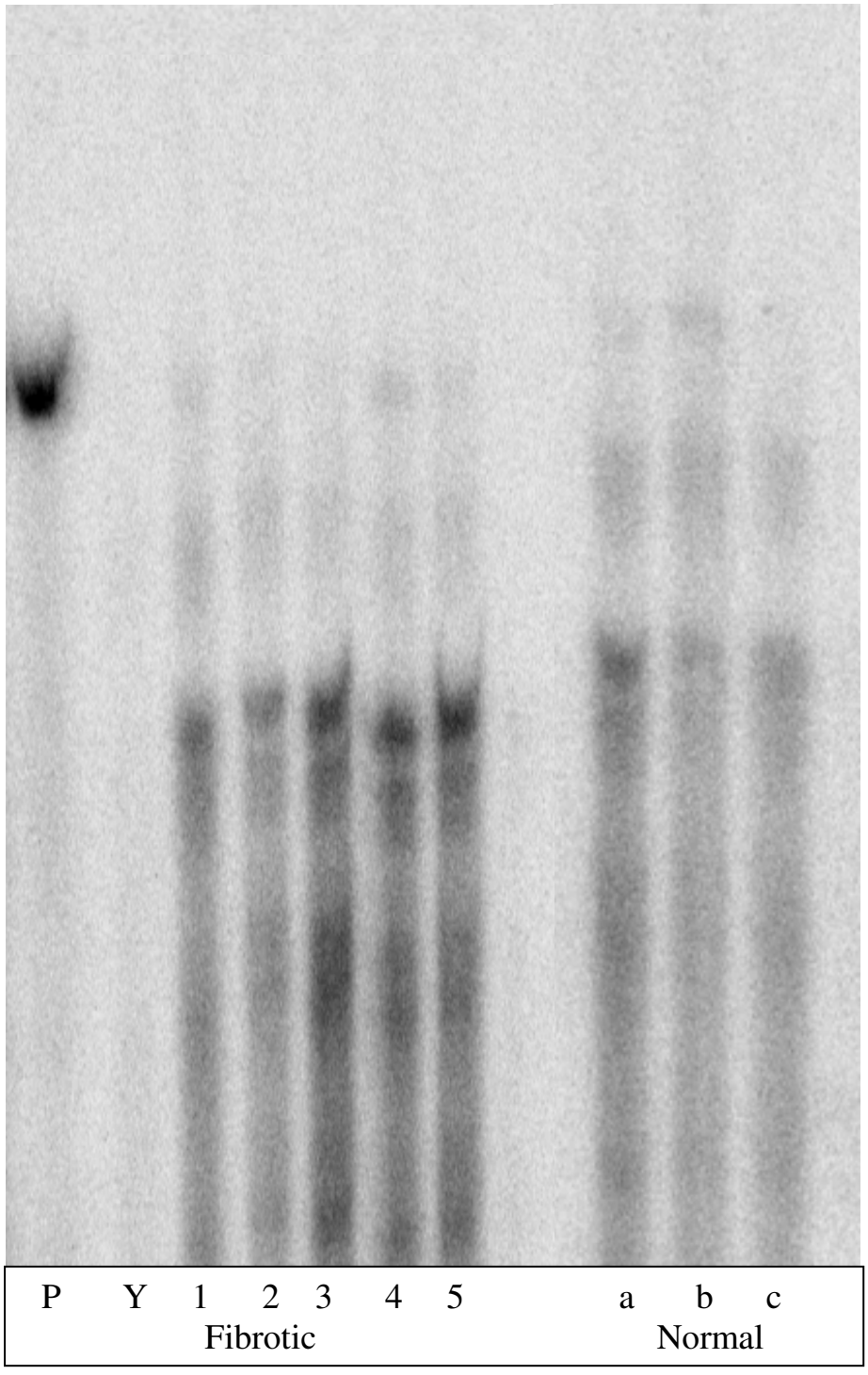

Figure 4.6 Autoradiograph of a RPA performed 5 fibrotic human liver samples and 3 normal livers. Y depicts the negative control. Samples 1-5 are from cirrhotics human livers. Samples a-c are from 3 separate human livers which were deemed clinically to be normal.

4.4 Discussion

Over 8, 24 and 48hrs there was a nominal increase in the expression of the 3.8kb TIMP-2 subspecies. In contrast the 1.2kb species was unchanged for 8 and 24hr, with a slight rise in 48hrs and then a fall at 72hr. In all this was felt to be a negative result. These results were disappointing and the collaboration with London become difficult as the cells became infected frequently with fungus due to the travel time exposure. However these experiments suggest that:

1) TIMP-2 mRNA expression was demonstrated for control and hypoxic conditions
2) TIMP-2 mRNA expression did not appear to differ in hypoxia

More recent work has demonstrated in one small study that TIMP-2 expression was shown to be enhanced in hypoxic conditions albeit the largest change was noted early at 6hr which was short-lived. It is possible that the time points here were too large and therefore the time point (6hr) that would document the largest increase in TIMP-2 mRNA expression was missed. Given the early published work on TIMP-2 mRNA expression in hypoxia this work would merit repeating and specifically to include the following:

1) Expression of TIMP-2 in primary rat and human HSC culture
2) cDNA probes could also be incorporated for the examination of beta actin, TIMP-1, procollagen 1 and gelatinase A.
3) shorter time intervals would be worth studying such as 4, 6, 8, 12 and 24hrs in early experiments both in primary and passaged rat HSC

It is possible that hypoxia has effects at the post transcriptional level therefore methods of examining TIMP-2 expression for example with ELISA should be considered. It would be interesting to repeat the experiment and introduce further variables where cells are exposed to hypoxia for a period and then returned to routine culture conditions (normoxia) for a subsequent period (a loose mimic of ischemia-reperfusion injury). In a recent study hypoxia was incorporated to examine HSC growth in low oxygen tension (1% O_2). With hypoxia the expression of HIF-1alpha and VEGF gene was induced. Western blotting was used to examine expression of alpha SMA TIMP-1 and MMP-2 – all of which were noted to increase (433). In a separate paper recently hypoxia and fibrosis was examined in the context of

chronic pancreatitis in relation to pancreatic stellate cells. Human PSCs were isolated, and cultured under normoxia (21% O2) or hypoxia (1 % O2). Hypoxia induced migration, type I collagen expression, and VEGF production in PSCs. Conditioned media of hypoxia-treated PSCs induced migration of PSCs, which was inhibited by anti-VEGF antibody, but not by antibody against hepatocyte growth factor. Conditioned media of hypoxia-treated PSCs induced endothelial cell proliferation, migration, and angiogenesis in vitro and in vivo. PSCs expressed several angiogenesis-regulating molecules including VEGF receptors, angiopoietin-1, and Tie-2. The main conclusion from the group was that hypoxia induced profibrogenic and proangiogenic responses in PSCs. In addition to their established profibrogenic roles, PSCs might play proangiogenic roles during the development of pancreatic fibrosis, where they are subjected to hypoxia (514).

In separate mRNA studies it is clear that activated rat PSC express αSMA, gelatinase-A (MMP-2), procollagen-I, TIMP-2 and TIMP-1. This was the first instance of this – there were no previous reports of this at the time in the published literature in terms of expression of TIMP-1, TIMP-2, alpha SMA, MMP-2 in rat PSC when this work was carried out in 2000. In this regard the PSCs appears to be behaving in a similar fashion to rat hepatic stellate cells (HSC) and rat renal mesangial cells. TIMP-1 & TIMP-2 mRNA are clearly expressed in pancreatic islet cells and therefore TIMP-1 and TIMP-2 may play a role in cell survival**.**

It is known in liver studies that accumulation of extracellular matrix may result not just from increased collage synthesis but also changes in degradation. Gelatinase-2 (MMP-2) degrades normal basements membrane type IV Collagen and partially degraded Collagens I, III & IV. It may also have collagen I degrading activity. MMPs including Gelatinase-A are inhibited by Tissue Inhibitors of Metalloproteinases 1 & 2. Again, in rat liver, TIMP-2 plays a specific role in the activation of Gelatinase-A (MMP-2) by linking with pro-gelatinase A and with membrane type Matrix Metalloproteinase I (MT1-MMP/MMP-14). Studies in liver and renal fibrosis suggested that it is likely that PSCs express Gelatinase-A and TIMPs-1 & -2. In this chapter there is clear evidence that this is the case, suggesting that PSCs are capable of remodeling matrix and via TIMPs may inhibit matrix degradation in chronic pancreatitis.

In the previous chapter in vivo studies examining the expression of alpha SMA, Gelatinase-A (MMP-2), MT1-MMP (MMP-14), TIMP-1 and TIMP-2 in human pancreas were carried out. The in vivo expression of these proteins together with the activation of PSCs in culure

expressing αSMA, procollagen-I, Gelatinase-A, MT1-MMP, TIMP-1 and TIMP-2 suggest that PSCs are indeed able to regulate matrix degradation in addition to synthesis and that the expression of TIMPs suggest that matrix degradation may be inhibited during chronic pancreatitis.

A ribonuclease protection assay was incorporated to study five samples of liver resection from cirrhotic liver and 3 samples from normal liver (liver resected for colorectal cancer metastases): in this setting the expression of human TIMP-2 mRNA in normal and diseased liver was studied. The results of this demonstrate that human TIMP-2 mRNA is upregulated in fibrotic liver in comparison to normal liver. This is a finding in contrast to the expected result where TIMP-2 has traditionally been conceived as constitutively expressed in a variety of cell systems.

CHAPTER 5

STUDIES OF THE TIMP-2 PROMOTER IN STELLATE CELLS

5.1 Introduction

In previous chapters the role of TIMPs and MMP expression has been examined *in vivo* through immunocytochemistry studies on rat hepatic stellate cells and pancreatic stellate cells. This chapter documents work that was intended to examine TIMP-2 expression in more detail at the molecular level using *in vitro* experiments.

The active forms of all the matrix metalloproteinases (MMPs) are inhibited by a family of specific inhibitors, the tissue inhibitors of metalloproteinases (TIMPs) (229). Inhibition represents a major level of control of MMP activity (515). A detailed knowledge of the mechanisms controlling TIMP gene expression is therefore important (213).

Previous work with the murine TIMP1 gene promoter has identified serum and phorbol ester responsive elements including an activating protein 1 (AP-1) and polyoma enhancer A3 (PEA-3) element proximal to the transcription start site. However, sequences more distal in the 5` flanking region, as well as those within intron 1, are likely to have a transcriptional role (516) (248). Recently a genomic clone of the human TIMP-1 gene has been obtained (517) enabling the transcription start points to be identified and transient transfection studies have been used to map the basal promoter.

In 1996 the human TIMP-2 gene was characterised (518). The gene is 83 kilobase pairs (Kb) long with exon-intron splicing sites located in preserved positions among the three members of the TIMP family. Work, performed on human fibroblasts isolated a 2.6 Kb genomic DNA fragment flanking the 5` end of the gene containing several regulatory elements including five SP1, two AP-2, one AP-1, and three PEA-3 binding sites (518). Our department obtained two plasmids on a collaborative basis from Prof Yves DeClerck, Professor of Paediatric and Biochemical research at the Children's Centre for Cancer and Blood diseases, Los Angles, United States of America. The first one was the 2.6 Kb segment of the promoter (full promoter), the second a 276 base pair of the promoter (short promoter), both constructs inserted upstream of the promoter-less luciferase reporter gene in the plasmid pGL3 (Promega). In commencing this work my initial aim was to transfect the vector constructs into hepatic stellate cells however the subsequent difficulties here led to a more detailed analysis of the constructs and ultimately to sub cloning the constructs into a different vector.

The pGL3 diagrams are depicted in figures 5.1a (basic negative control vector or “Mock”), figure 5.1b (positive control vector with a SV40 – simian viral promoter), figure 5.1c (full TIMP-2 2600 promoter construct) and figure 5.1d (short TIMP-2 267 promoter construct). The structure of the nucleotide sequence of the 2.6kb Pst I genomic fragment containing the human (h) TIMP-2 promoter was published in 1996 by Professor DeClerck and is depicted in figure 5.2.

The sequence includes part of the first exon. Positions of nucleotides indicated on the left are numbered from the major transcription initiation site (nt+1) shown above by an arrow (►). Consensus sequences are indicated on the diagram (underlined) and include the following binding sites:

- a TATA like motif
- five Sp1
- two AP-2
- one AP-1
- three PEA-3

The initiator ATG is shown at positions +303 to +305. Sequences extending from the 3` -end PstI site to position -519 (BamHI site) were published previously (519)

Figure 5.1a pGL-3 basic vector (negative control vector)

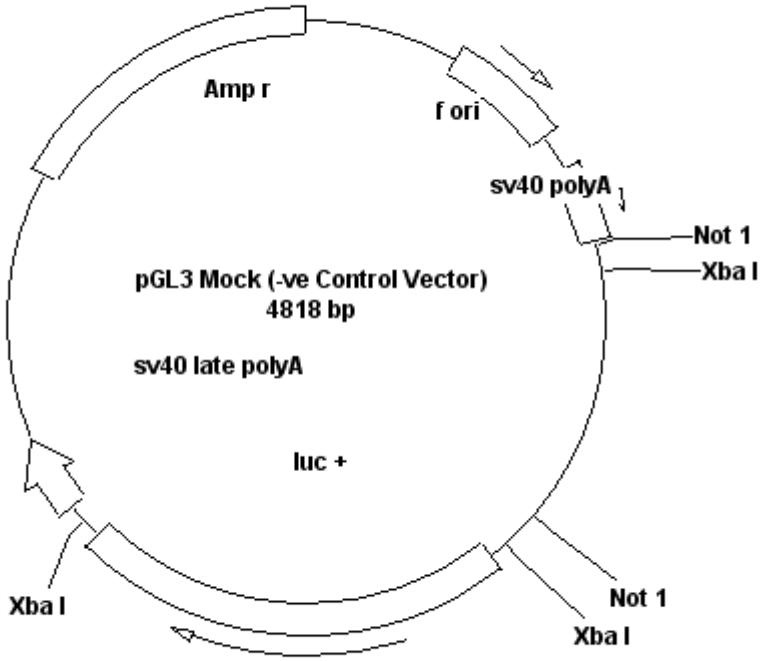

This was used in all experiments and as a negative control vector was termed “mock”.

Figure 5.1b pGL-3 basic vector with SV40 promoter

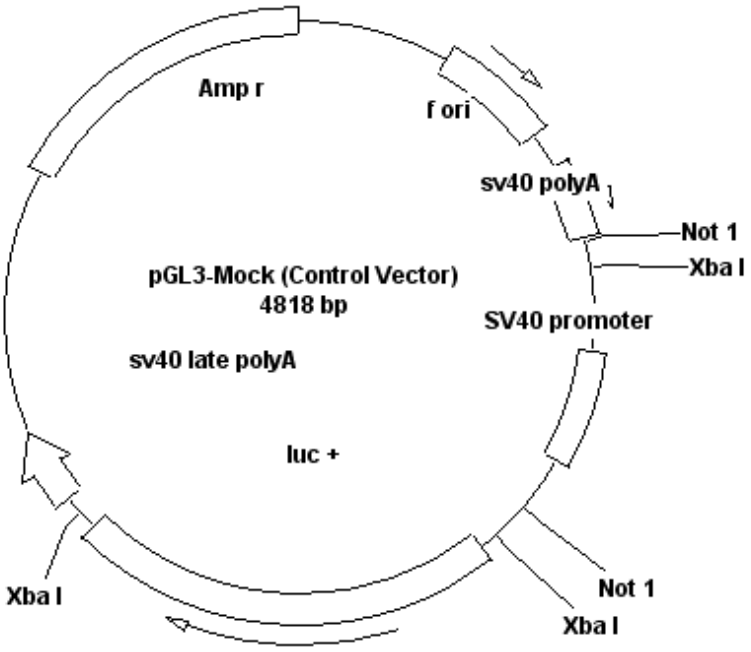

This was used in all experiments and as a positive control vector was termed positive (+ve) control.

Figure 5.1c pGL-3 basic vector with the human (h) TIMP-2 gene promoter of 2600 base pairs inserted

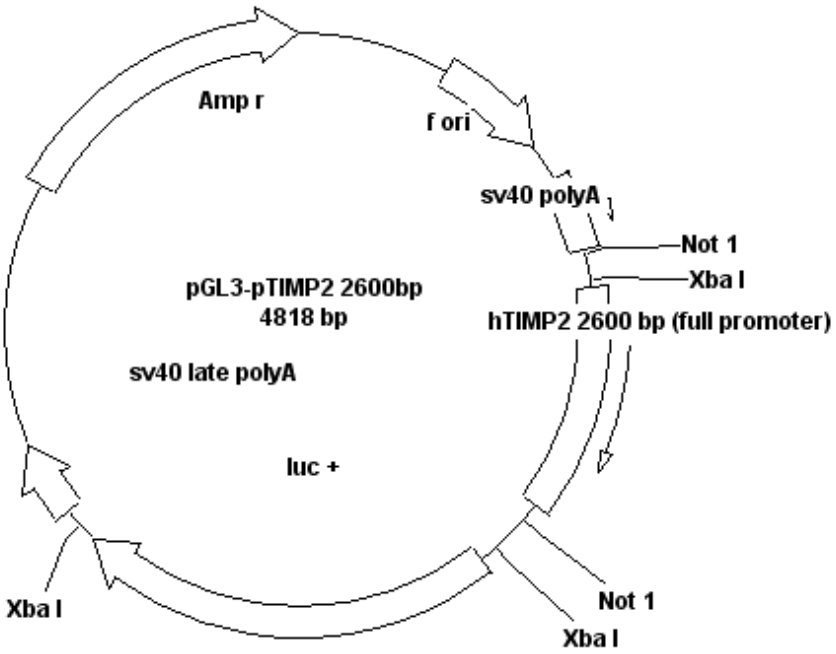

The pGL3 vector with the hTIMP-2 2600 base pair full promoter has Not-1 and Xba-1 restriction sites spanning either side of it. Downstream from the promoter is the luciferase gene itself with a sv40 late polyA gene distal to this. All of the pGL3 vectors used in this work had an ampicillin resistance gene incorporated.

Figure 5.1d pGL-3 basic vector with the human (h) TIMP-2 gene promoter of 267 base pairs inserted

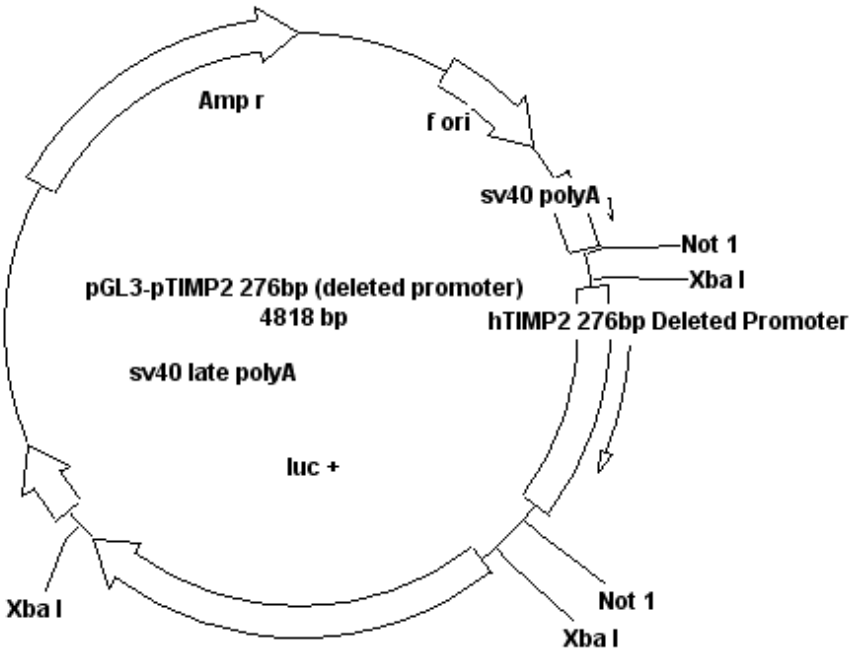

The pGL3 vector with the hTIMP-2 267 base pair short promoter has Not-1 and Xba-1 restriction sites spanning either side of it. Downstream from the promoter is the luciferase gene itself with a SV40 late polyA gene distal to this. All of the pGL3 vectors used in this work had an ampicillin resistance gene incorporated.

Figure 5.2 Nucleotide sequence of the 2.6kb Pst-1 genomic fragment containing the human (h)TIMP-2 promoter

```
-2243 CTGCAGACTCAACTTCCCCAGGCTCAAGCGATCCTCCCACCGCAGCTTCCCTGTAGCTGG

-2183 GACTACAAGTGTAGCCATCACGCCCAGCTAATTTTTTTTTTTGTAGAGATGGGGTCTCAG

-2123 TATGTTCCTCAGGCTGGTCTCAAATCCTGGCCTCAAGGTGATCCTCCCACCTTAGTTTCA

-2063 CCAAAGTGTTGGGATTACAAGCGTGAGCCACTGCACCTGGCAAGATTTCTGCTTCACTTT

-2003 TCCTGGGAGCAATTCCAGCCTGTTGTGTGCTGGTGGGGATGACTTCGGGGGAGGGCGTCA

-1943 CAGGATACAGGTGCGAGGCCTTGGGTTGGAAGTTCCAGTCTCACGCCCCCCCAACCCTGG

-1883 GCCCAGGCCCCCCTTTCCTCCCAGGTACATCCCACATTGGCCCCACCCCCTTGGCTGTCG

-1823 GCACCACAACTGCTCTAAGGTATTTATCACCCTAACATGTACCTGATCACTTATATGTAG

-1763 AGCTTGTCTAAAAGACCGAGAGCCCCTATGCTACCTGTTTTCTATCATGAACTGACAATT

-1703 GAAACACAAGTTCAACAGCATTTTGTTCCCCCTGTAACCAAAAAGAAGGAAAGAAAACAA
                                                    PEA-3
-1643 TGAAATGGCTGAAGGCAGCCAGCACATAACAATTTTCTGAATTAACTGTACTTTTAAACG

-1583 TTAGCTTCAAACATCATTTTGTGAACGACCCAACTCTATTTCACGCTAACAAAAACCAAA

-1523 AAAGTGACTTTGGATTTGTCAGGGTGCTAAAAATAACGGCATTGCTTATTTAAATCTTCT
                                  MEF-2
-1463 CAGAAACTGTCTGTTACAAAACATACACAAACAGAAAGAAGCTGTTTTTCCATTCTTTCA

-1403 TATTTTCCAAAGTTTCATACCTCAAGCTAGCACTGCTGCACAATTTAGTGGGCAATTCTT

-1343 AAAAAAAAAAAAAAACAAAAAAAACAAACAAGAGTCTTTCTCTGTCGCCCAGGCTGGAGT

-1283 GCAGTGGCGCAATCTCGGCTCACTGCAAGCTCCGCCTCCTGGGTTCATGCCATTCTCCTG
       NF-IL6                   Sp1/Rev
-1223 CCTCAGCCTCCCGAGTAGCTGGGACTACAGGCGCCCACCACCAAGCCCGGCTAATTTTTT
      Sp1/Rev
-1163 GTATTTTTAGTAGAGACGGGGTTTCACTGTCTCTACTAAATGCTAGCCAGGCTGGTCTCA

-1103 AACTCCTGGCCTCAAGTGATCCTCCTGTCGCGCCCTCCCAAAGTGCTGGGATTACAGGCT

-1043 GCAAGCACGTGCCCGCCCTGATTCTTCCTGTGTCATTTTCTGGGGCTTCCCCTCTCCCTA

-983  GCTGGACTGCAAACACTCTGGAATGCTGACCTGAGGGCTGGAGTGCTGACCTGAGTGCAG

-923  CAGTGTCCATGGAGCCCCACGGGGCACACACCAAATGTACAGGGTGGGTGCCCACAGCCG

-863  CGCACAGGCAGGTTCACAGCCAGGAAGCCGCCCTCACCACCCTACACATGTTCATCTCTT
                             PEA-3
-803  CATATGCCTGGGTCTTTCCTGGAACACAAAACTGTTTTGGGAAAAGTCCTCCGGCTCCCA
```

Figure 5.3 Nucleotide sequence of the 2.6kb Pst-1 genomic fragment containing the human (h)TIMP-2 promoter (Continued from overleaf)

```
                                  PEA-3                    NF-1
-743  CATTTGTGGACTAAGAGAGGAAACTGTGAGCGGAACCCAGCCAATGCCTCTGCTGCGATC
-683  CTACTGGCTCCTGGGCGCCTGGGCCCACCCCCGTCTCTTGTTGGCTGGTCAAAAATATGG

-623  CCAGTTTATATAAAATCCTGTTTTGTTCACAGTAACCACACCCCCCACCCCCCAACTAAA

-563  CTGGCCAGGCGCACTTAAAATTCTAAGGCCTCCATTTGAAAAAGGGATCCTGTCAGTTTC

-503  TCAATAGGCCACCCGCCCACAGAAACGGGGAGGTGGCGACAGGGAACGGCCCCTGCTCCA
                Sp1/Rev
-443  AAGGACACCCCTTGGCTCGCCCCGAGGCTGGGCTCGAAGGGACCCCGGGGTGGCGGGGGA
                                  Sp1
-383  CGGAGCAGCGTAGCCCTCCAGAGTCGAGCTGAAGGGGAAAGGGTAGCGGGTGGGTCGCCT

-323  GGTGCCCTGGAAGAACGGGCGCGAGTCCCACGCGCTGAGTCAGGGACCCCGGGCGCAGAA
                                              AP-1       AP-2
-263  GGCCACGCAGCGGGGACCGGGGTCGGGGGGGCTGGGGGCGTCCGGGCGCACCCCCGCGCGG
                                  Sp1                        AP-2
-203  GTGCGGGTCGCGGGCGCCAGGTGGTGCGGGAAGCCCCCGACTGTCCAGGCCGGGCACAAC
                                 NF-IL6
-143  AAAAGCGCGGGCTGGGGGGAGGCGCGGGCGGAGGGGGAGGAGGGGGCTGCTGGGAGCGCC

-83   CAGAGCCTGCATTGGCCGCCAGCCACCGGGAGGAGGAGCAGAAAATCCTCCGAGCGCAAT
                                  ►                          TATA
-23   AAAACTGCGGCCCGGCCCAAGCCCGCAGCAAACACATCCGTAGAAGGCAGCGCGGCCGCC
      Box                         +1
+38   GAGAGCCGCAGCGCCGCTCGCCCGCCTGCCCCCACCCCGCCGCCCCGCCCGGCGAATTGC

+98   GCCCCGCGCCCCTCCCCTCGCGCCCCCGAGACAAAGAGGAGAGAAAGTTTGCGCGGCCGA

+158  GCGGGGCAGGTGAGGAGGGTGAGCCGCGCGGGAGGGGCCCGCCTCGGCCCCGGCTCAGCC

+218  CCCGCCCGCGCCCCCAGCCCGCCGCCGCGAGCAGCGCCCGGACCCCCCAGCGGCGGCCCC

+278  CGCCCGCCCAGCCCCCCGGCCCGCCATGGGCGCCGCGGCCCGCACCCTGCGGCTGGCGCT
                                 Met
+338  CGGCCTCCTGCTGCCGCTGCTTCGCCCGGCCGAGCGCTGCAG
```

Figure 5.2 and 5.3 is shown above depicting the whole 2.6kb sequence of the human (h) TIMP-2 promoter. The sequence includes part of the first exon. Positions of nucleotides indicated on the left are numbered from the major transcription initiation site (nt+1) shown above by an arrow (►). Consensus sequences including a TATA like motif, five Sp1, two AP-2, one AP-1, and three PEA-3 binding sites in addition to other binding sites are underlined. The initiator ATG is shown at positions +303 to +305. Sequences extending from the 3` -end PstI site to position -519 (BamHI site) were published previously (519).

5.2 Methods

Isolation of rat hepatic and pancreatic stellate cells

Isolation methods are described in Chapter 2 section 2.2.1 & 2.2.7

Amplification, purification and analysis of plasmid DNA

Methods are described in detail in chapter 2 section 2.6.

This includes details on the following:

- Restriction Enzyme Analysis of Plasmid DNA (2.6.2)
- Amplification, Purification and Analysis of Plasmid DNA (2.6.4)
- Production of competent cells (DH5α *E. coli*)(2.6.5)
- Transformation and Amplification of competent *Escherichia coli (E coli)* with Plasmid DNA (2.6.6)
- Bacterial Propagation (2.6.7)
- Production of Bacterial Stock (2.6.8)
- Purification of Plasmid DNA (2.6.9)
- Restriction Enzyme analysis of Plasmid DNA (2.6.10)
- Purification of DNA or PCR products from Agarose Gels (2.6.11)

Transfection

This section is described in detail in Chapter 2 section 2.7.

This includes details of the following:

- The luciferase reporter assay system 2.7.2
- The Chloramphenicol Acetyl Transferase (CAT) Transfection Assay (2.7.4)

Systematic deletion of plasmid DNA

The methods for the Promega “Erase-a-Base” system are described in detail in 2.8.

Sequencing plasmid constructs is described in detail in section 2.9.

5.3 Results

5.3.1 Early Transfection work with the luciferase reporter assay

Transfection is discussed in detail in Chapter 2 section 2.7. Two different transfection protocols were incorporated from Promega. The first, described here, was used at the beginning of my work "Dual Luciferase Reporter Assay" and unfortunately yielded only moderate results. The luciferase enzyme used is derived from the coding sequence of the *luc* gene cloned from the firefly *'Photinus pyralis'* (491-493). The firefly luciferase enzyme catalyses a reaction using D-luciferin and ATP in the presence of oxygen and Mg^{2+} giving in light emission. The light measured in a time interval is directly proportional to that of luciferase reporter activity in the sample. This light emission was quantified using a proprietary luminometer purchased from Promega. The "Dual Luciferase Reporter Assay System" (Promega) combines two luciferase reporter enzymes. The firefly luciferase can be effectively quenched so that the second reporter – an internal control and derived from the sea pansy "Renilla reniformis" - can be assayed for its luminescence. Plasmid stocks were obtained of the pGL3 basic vector (-ve control), pGLSV40 (positive control), pGL3 TIMP-2 human 2600 (full promoter) and pGL3 TIMP-2 h276 (shortened promoter). In accordance with the current Promega protocol the stocks were defrosted over 30min. 10µg of plasmid was added to Microfuge tubes, 0.5µl of PRL (Renilla luciferase) was added for co transfection. Rat HSC in flasks were washed in serum free media for 6hrs. DNA and lipofectin/DNA were incubated for 10mins at room temperature. This was then added to the flasks of HSC. Flasks were incubated for 72hrs then the cells were harvested in order to perform the luciferase assay. Using the proprietary Promega Luminometer the light production from individual samples was measured once the Luc Assay Reagent was added. The Luciferase was then quenched with the Renilla solution and the corresponding activity was measured. The values for the firefly were divided by the renilla values. The experiment was repeated on 3 separate HSC preparations then expressed in an Excel spreadsheet chart with the standard error of the mean (SEM) applied.

Table 5.1 Transfection of pGL3 TIMP-2 2600 full promoter and 267 shortened promoter into passaged rat hepatic stellate cells

Transfection	Renilla	Firefly	Mean Renilla / Mean Firefly
1) pGL3 empty vector	0.035	0.000	
"Mock" or negative control	0.097	0.095	
	0.100	0.000	
Mean	0.077	0.032	2.41
2) pGL3 SV40	5.827	0.194	
Positive control	0.641	0.215	
	6.596	0.224	
Mean	6.28	0.211	29.76
3) hTIMP-2 276	0.032	0.008	
Short promoter	0.16	0.044	
	0.268	0.027	
Mean	0.153	0.027	5.67
4) TIMP-2 2600	0.068	0.029	
Full promoter	0.000	0.04	
	0.000	0.159	
Mean	0.023	0.076	0.303

Table 5.1: Transfection of pGL3 TIMP-2 2600 full promoter ad 267 shortened promoter into passaged rat hepatic stellate cells. Raw data example of early transfection using 'Lipofectin' (PROMEGA). Transfections carried out in single wells only on passaged rat HSC (passage 5). Each experiment required the initial incubation in serum free media for 6 hours prior to transfection. Cells were then incubated at 37°C for 72 hours. Cells were then harvested and analysed for luciferase & renilla activity.3 readings are taken for each luciferase, 3 readings for each firefly and averaged. This experiment was repeated on three occasions.

Figure 5.4 Transfection of pGL3 TIMP-2 2600 full promoter and 267 shortened promoter into passaged rat hepatic stellate cells (n=3)

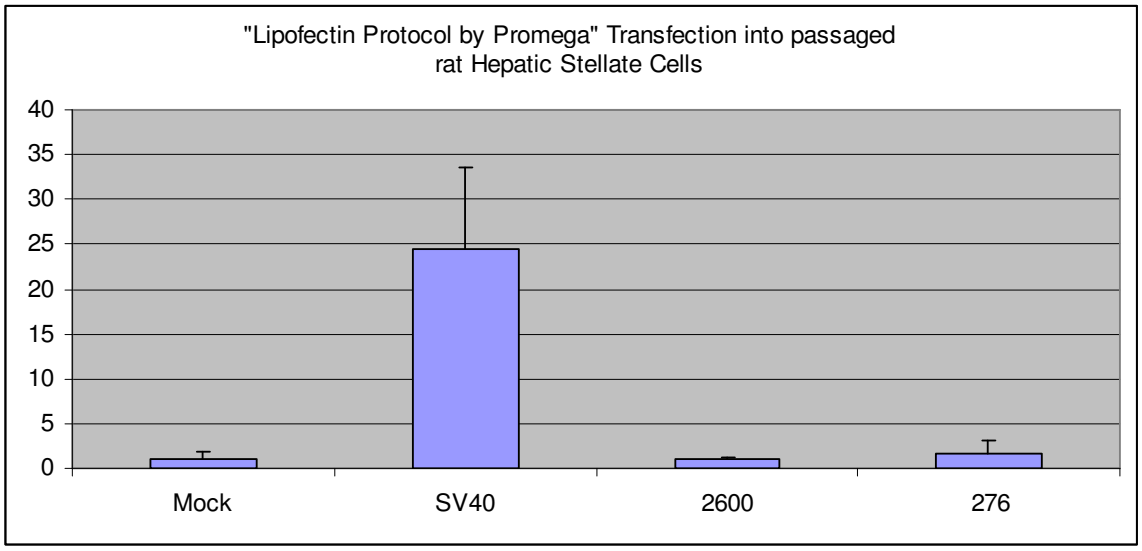

Figure 5.4 Graph depicting the mean of three experiments of transfections carried out in single wells on passaged rat HSC (passage 5). The x axis shows the 4 different constructs incorporated, the y axis depicts the relative acitivity normalised to the Mock vector with a value of 1.0. The mock depicts the negative control with a pGL3 empty vector. SV40 is the positive control. 2600 and 276 depicts the TIMP-2 long (full) and 276 (shortened) constructs transfected. Each experiment required the initial incubation in serum free media for 6 hours prior to transfection. Cells were then incubated at 37°C for 72 hours. Cells were then harvested and analysed for luciferase & renilla activity.3 readings are taken for each luciferase, 3 readings for each firefly and averaged. N=3. This data of the mean of 3 experiments was subjected to statistical analysis shown below in Table 5.2

Table 5.2 One-way Analysis of Variance (ANOVA) for data shown in Figure 5.3

Comparison	**Mean Diff**	**q**	**P value**		**95% Confidence Interval**	
					From	**To**
Mock vs SV40	-23.441	5.008	*	P<0.05	-44.639	-2.242
Mock vs 2600	-0.02788	0.005956	ns	P>0.05	-21.226	21.170
Mock vs 276	-0.5611	0.1199	ns	P>0.05	-21.759	20.637
SV40 vs 2600	23.413	5.002	*	P<0.05	2.215	44.611
SV40 vs 276	22.88	4.888	*	P<0.05	1.681	44.078
2600 vs 276	-0.5332	0.1139	ns	P>0.05	-21.731	20.665

5.4 Discussion on Early Transfection

Very little consistent activity was noted in the initial transfections. The SV40 consistently showed very positive values demonstrating its quality as a positive control. Relatively little activity was noted however for the TIMP-2 full 2.6kb and short 276bp promoters. This was disappointing given that DeClerck et al had good results in other cell systems (NIH3T3 and HT1080 cells). Their method of transfection incorporated different transfection protocols (calcium phosphate). Previous work with this transfection protocol by the liver group in previous years had produced only moderate transfection efficiencies. There are a number of possible reasons for these results. The promoters may not have been active in passaged rat HSC though it is clear in experiments demonstrating clear evidence of TIMP-2 mRNA expression that this is unlikely; equally the promoters may have only been strongly active in the early stages of passaging for example after 1-2 days. A human gene reporter may not have been as active in a rat HSC system. Further work could have been repeated here in other cells systems such has 3T3 and 1080 cells lines as well as performing the experiments on quiescent HSC cells both in rat and human HSC preparations.

A reporter system that was cumulative over time may be more appropriate and therefore the CAT assay system was chosen for the next set of transfections in hepatic stellate cells. In order to perform CAT assays the human (h)TIMP-2 2600 full promoter construct and hTIMP-2 276 short promoter construct would need to be sub cloned into a CAT reporter plasmid (pBlCAT3). This work would involve a restriction digest of the hTIMP-2 2600 and 276 constructs from the pGL3 vectors. The pBlCAT3 would then need to be linearised, treated with alkaline phosphatase and gel purified. Following ligation of the TIMP-2 inserts into pBlCAT3 the resulting plasmids would be transformed into competent cells, and plasmids subsequently amplified with the use of 'MAXIPREPS' after correct identification with 'MINIPREPS'. The resulting plasmids would need to be subjected to restriction digests to map the inserts and sequenced to confirm the orientation within the pBlCAT 3 vector. Once this was achieved only then would CAT transfections be possible.

5.5 Subcloning plasmid DNA into another plasmid vector

5.5.1 Aim: Isolation of the TIMP-2 full promoter (2600bp) insert in the pGL3 vector and subclone it into the pBlCAT3 vector

In order to subclone the plasmid DNA into another vector (from pGL3 basic to pBLCAT3) there were certain steps required in the roadmap in order to achieve this. The pGL3 TIMP-2 2600 and pGL3 TIMP-2 276 promoter constructs would need to be characterized in order to plan ahead. The key steps therefore included:

- Restriction digest of 2600/276 fragment from the PGL3 vector
- Ligation into a new vector
- Preparation of the vector: PST-1 cut/ alkaline phosphate/ gel purification
- Transformation into competent cells
- Miniprep and Maxi preps
- Mapping the new vector with restriction cuts
- Sequencing to confirm orientation
- Finally: Transfection of the new CAT vector into rat HSC

5.5.2 Method for ligating pBlCAT3

pBlCAT3 was linearised with the aid of the enzyme PST-1 (Promega): 10µl of plasmid DNA (pBlCAT3) at a concentration of 1µg/µl was incubated with 5µl of 10x buffer (Promega), 30µl of distilled water, and 5µl of PST-1 enzyme at 37^0C for two hours. To prevent vector ends from annealing immediately the linearised pBlCAT3 was treated with alkaline phosphatase: 5µl of a 10x alkaline phosphatase buffer was added with 2µl of calf intestinal alkaline phosphatase enzyme to the pBlCAT3 plasmid and incubated at 37^0C for 30 min. 1µl of phosphatase buffer was added at this stage and the linearised pBlCAT3 was incubated at the same temperature for a further thirty min. To purify the linearised plasmid it was subjected to phenol/chloroform extraction followed by ethanol precipitation. The DNA was then centrifuged at 13,000 for 5 min to obtain a pellet and after discarding the supernatant the pellet was dried. It was assumed that complete recovery was obtained and therefore distilled water was added to a final concentration of 100µg/µl.

Two sets of microfuge tubes were created for each of the three conditions

Table 5.3 Ration of plasmid to insert

	1	2	3
Ratio of Plasmid to Insert	1:1	1:3	3:1
DNA Insert	1µl	1µl	3µl
Vector	1µl	3µl	1µl
Buffer	1µl	1µl	1µl
Distilled Water	6.5µl	4.5µl	4.5µl
Ligase	0.5µl	0.5µl	0.5µl

Table 5.3: Ration of plasmid to insert. Samples of the vector/insert were transformed into competent DH5α *E. Coli* (as outlined in Chapter 2 Methods Section 2.6) and grown on agar plates overnight at 37^0C. Resultant colonies were plated and grown in CB with Ampicillin overnight at 37^0C shaking. Minipreps were prepared to isolate any resulting plasmid DNA.

Competent DH5α *E. Coli* were taken from 80^0C freezer and thawed on ice. A sample of DNA eg 5µl of TIMP 2600 insert ligated into pBlCAT3 was added to 20µl of DH5α *E. Coli* and incubated on ice for 30 min. The DH5α *E. Coli* were then heat shocked at 42^0C for 45 seconds before being returned to ice for two min. 80µl of sterile LB was added to each sample of DH5α *E. Coli* (with no ampicillin added) and incubated in a water bath at 37^0C for 30 min. The DH5α *E. Coli*/LB both was then streaked onto freshly made agar plates: one at 20µl and one at 80µl overnight at 37^0C. Colonies were then 'picked' using a sterile Pasteur pipette and inserted into LB with (no ampicillin) and incubated in an orbital shaker at 37^0C for two hours. 20µl of 25µg/ml ampicillin was then added to each and the LB/colonies were incubated shaking overnight at 37^0C.

5.5.3 Results

On the first occasion no plasmids were harvested. Therefore the experiment was repeated with the following procedures:

1. All procedures for linearizing pBlCAT3, performing a restriction digest of the human TIMP-2 2600 promoter from the vector pGL3 and ligation of this insert were carried out in one day
2. No plasmid insert was frozen
3. 1 control was run without treatment of the pBlCAT3 with alkaline phosphatase
4. The reactor: insert ratio was 1:1, 3:1, 10:1 and a control of 1:1 where the control had pBlCAT3 with no exposure to alkaline phosphatase.

Table 5.4 Results of colonies

Condition	Amount of plasmid added to agar plates	Growth / No of colonies
1. DH5 on agar plates: no growth. No pBlCAT3 or insert		No Growth
2. Control (pBlCAT3: No alkaline phosphatase)	20µl 80µl	35 colonies 246 colonies
3. 1:1 ratio of pBLCAT3 to insert	20µl 80µl	0 colonies 0 colonies
4. 10:1 ratio of pBLCAT3 to insert	20µl 80µl	1 colonies 3 colonies
5. 3:1 ratio of pBLCAT3 to insert	20µl 80µl	1 colonies 3 colonies

5.5.4 Discussion of the initial characterisation of pGL3 – TIMP2 276 Insert

The short promoter pGL3 hTIMP-2 276bp short construct was subjected to restriction enzyme analysis. Competent DH5 α *E.coli* were transformed with the pGL3 TIMP-2 276bp short construct plasmid and subsequently 'Maxipreps' were performed. 4µl of plasmid at a concentration of 1µg/µl was incubated in a Microfuge tube in a water bath at 37°C with 2µl of restriction enzyme, 2µl of buffer D (Promega) and 12µl of distilled water for two hours. Figure 5.5 shows the results on a 1% agarose gel.

With a successful restriction digest, a lower molecular weight discrete insert would be seen on the gel. With the exception of a single cut with Xba-1 on the pGL3Basic empty vector or "Mock" plasmid no restriction digest could be achieved with Xba-1 and *Not-1* on the pGL3-TIMP-2 short promoter (276bp). The same result was obtained when the experiment was repeated under new conditions (new buffers and overnight digests) and with new enzymes. The buffers for the respective enzymes were checked with the manufacturers, Promega, directly to ensure compatibility. *Not-1* was used to cut another plasmid in the laboratory to ensure that there was no intrinsic fault with the enzyme (results not shown) and a successful digest was confirmed. Figure 5.1 depicts the Promega plasmid map for pGL3 basic vector. The Promega catalogues clearly document at least two Xba-1 and NOT-1 restriction sites: one on each side of the promoter insert site, on their PGL3 vectors.

The reasons that there was only an *Xba-1* cut in the mock plasmid and no *Xba-1* and *Not-1* cut on the short hTIMP-2 276bp promoter is unclear. However there may be two possible explanations for this: one is that the sites were removed when the human TIMP-2 promoter was sub cloned into the PGL3 vector; the second is that the sites were in some way damaged at the cloning process. Prof Yves DeClerck documented himself two *Xba-1* and *Not-1* sites on his plasmid map. Despite attempts to contact Professor Yves DeClerks group I was not able to obtain any more helpful information on this.

Figure 5.5 Iinitial characterisation of pGL3 – hTIMP-2 276bp (short promoter)

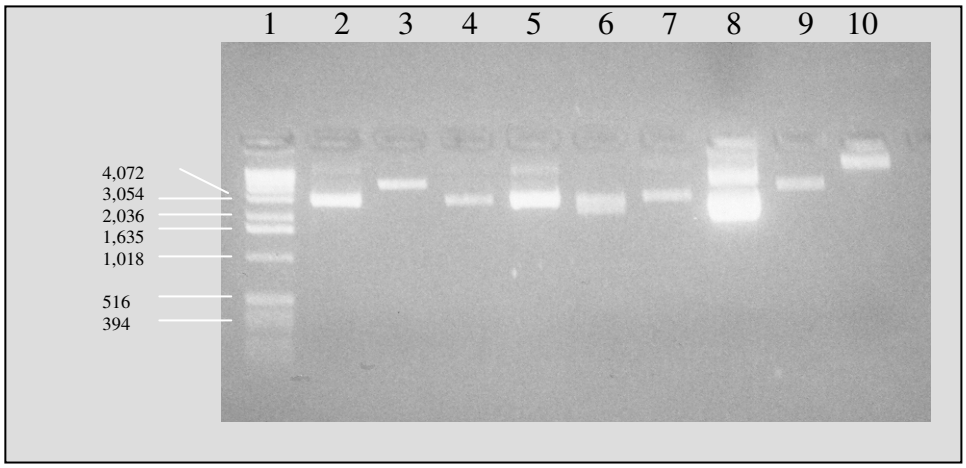

1% Agarose gel in TAE run at 30 watts 25 volts for 30 minutes. From left to right lanes 1-10 include:

1) 1kb DNA markers (Promega)

2) pGL3-Mock (uncut plasmid)

3) PGL3-Mock digest with Xba-l

4) pGL3-Mock digest with Not-1

5) pGL3 TIMP-2 short construct (276) [uncut plasmid]

6) pGL3 TIMP-2 short construct (276) digest with Xba-l

7) pGL3 TIMP-2 short construct (276) digest with Not-1

8) pBlCAT3 (uncut plasmid)

9) 1µg of linearised pBlCAT3

10) 1µg of MT1-MMP

This figure shows that whilst there is a cut with the restriction enzyme Xba-1 on the mock plasmid there is no such cut with Not-1. Similarly, no cuts are noted with Xba-1 or NOT-1, on pGL3 TIMP-2 short construct (276) plasmid.

5.5.5 Further restriction analysis

The pGL3 hTIMP-2 276bp short construct was subjected to further restriction enzyme analysis with KPN-1 and HIND III. 4µl of plasmid (1µg/µl) was incubated in a Microfuge tube in a water bath at 37^0C with 1µl of restriction enzyme (or 0.5µl of each enzyme if a double digest was performed), 2µl of buffer D (Promega) and 12µl of distilled water for two hours. Neither KPN-1 nor HIND-III linearized the Mock plasmid (-ve vector) or linearized or cut out the pGL3 TIMP-2 short 276 promoter despite the use of an image intensifier. The gel is depicted in Figure 5.6. The experimental protocol was repeated for the pGL3 TIMP-2 2600bp full promoter construct and this is shown in Figure 5.7. This plasmid mapping shows linearization of the pGL3-Mock with HIND-III and PST-1 restriction enzymes separately, and with HIND-III and PST-1 together as a double digest. Both HIND-III and PST-1 linearise the PGL3 276 plasmid separately and do the same again with a double digest. No TIMP-2 276 fragment can be seen on the pGL3-276 double digest. HIND-III appears to produce a smaller fragment in lane 11 on the PGL3 2600 vector whilst PST-1 in lane 12 and PST-1 plus HIND-III in lane 13 give a double cut: one possibility is that this may be due to PST-1 and HIND-III cutting within the 2600 site as well as pGL3 vector. However on examination of the hTIMP-2 construct sequence the restriction enzyme Pst-1 makes the following cut:

CTGCA▼G
G▲ACGTC

From the sequence described in Figure 5.2 it should in theory however only cut at the beginning and end of the sequence. See below.

-2243 **CTGCAG**ACTCAACTTCCCCAGGCTCAAGCGATCCTCCCACCGCAGCTTCCCTGTAGCTGG

+338 CGGCCTCCTGCTGCCGCTGCTTCGCCCGGCCGAGCG**CTGCAG**

Hind III makes the following cut:

A▼AGCTT
TTCGA▲A

No cut within the sequence could be noted on scanning the sequence depicted on figure 5.2.

Figure 5.6 Restriction digest of pGL3 – TIMP-2 276 short construct with KPN-1 or HIND-III

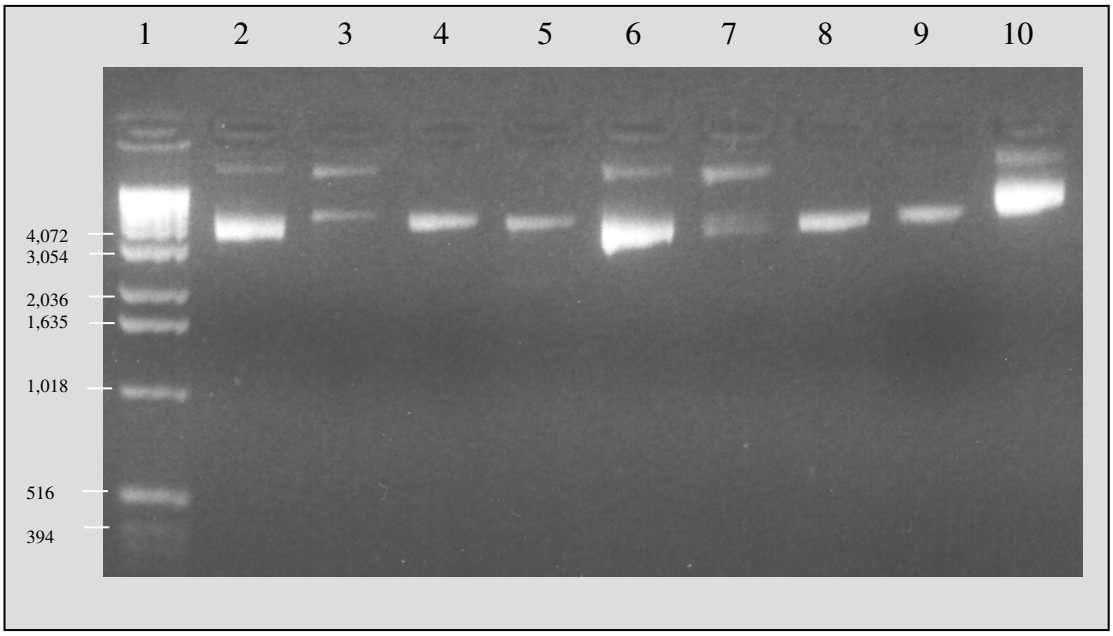

Image intensifier image of a 1% Agarose gel in TAE. Lanes 1-10 as follows:

1) 1kB DNA ladder (Promega)
2) pGL3-Mock uncut plasmid
3) pGL3-Mock digest with KPN-1
4) pGL3-Mock digest with HIND-III
5) pGL3-Mock double digest with KPN-1 and HIND III
6) pGL3 TIMP-2 short construct (276) uncut plasmid
7) pGL3 TIMP-2 short construct (276) digest with KPN-1
8) pGL3 TIMP-2 short construct (276) digest with HIND-III
9) pGL3 TIMP-2 short construct (276) double digest with KPN-1 and HIND III
10) pGL3 TIMP-2 long construct (2600) uncut plasmid

This shows that there is no cut in pGL3-Mock or pGL3 TIMP-2 276 (short promoter) vectors with KPN-1 and HIND III. An image intensifier was used to look for the TIMP-2 276 fragment.

Figure 5.7 Restriction digest of GL3 – TIMP-2 276 short construct plasmid and the pGL3 – TIMP-2 2600 long construct plasmid with PST-1 and HIND-III

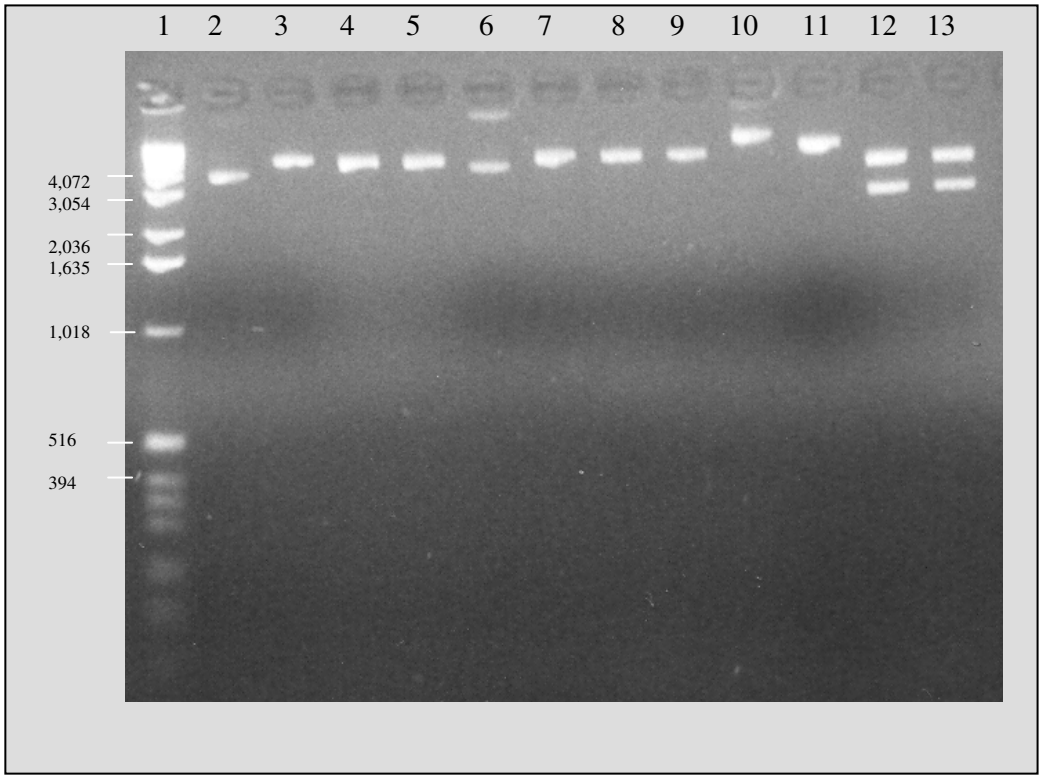

1% Agarose gel in TAE canes 1 – 13 are as follows:

1) 1kb DNA ladder (Promega)

2) pGL3-Mock (uncut plasmid)

3) pGL3-Mock digest with HIND-III

4) pGL3-Mock digest with PST-1

5) pGL3 double digest with HINDIII/PST1

6) pGL3-276 uncut plasmid

7) pGL3-276 plasmid digest with HIND-III

8) pGL3-276 plasmid digest with PST-1

9) pGL3-276 double digest with HINDIII/PST-1

10) pGL3-2600 uncut plasmid

11) pGL3-2600 digest with HIND-III

12) pGL3-plasmid digest with PST-1

13) pGL3-plasmid double digest with HIND-III and PST-1.

Figure 5.8 Purification of the pGL3 TIMP-2 2600 full promoter

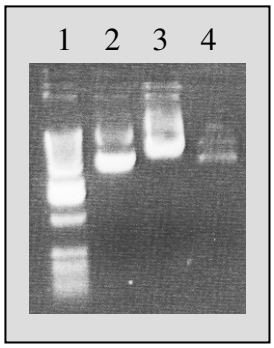

1% Agarose gel in TAE. Lanes 1-4 are as follows:

1) DNA markers

2) pGL3-Mock

3) pGL3 TIMP-2 2600bp uncut plasmid

4) pGL3 TIMP-2 2600 digest with PST-1

This shows the human pGL3 TIMP-2 2600 full promoter insert cut, purified and run on the gel.

5.5.6 Sequencing of the pGL3 TIMP-2 2600 full promoter and 276bp (short promoter)

With the anomalies encountered with the restriction digest of the human pGL3-TIMP-2 2600 full promoter and the pGL3- TIMP-2 276 short promoter constructs it was necessary to sequence them.

Methods

This was carried out by the method as described in general methods (2:1:1).

Results

The sequence is shown in figure 5.9 for the pGL3-TIMP-2 2600 full promoter construct and in more detail in figure 5.9b.

5.5.7 Discussion

Whilst I was able to do this successfully the detail on the sequencing gel was not precise enough to obtain accurate sequencing of the plasmid. The short promoter sequencing was indeed poor (not shown). I elected at this stage to have the sequencing performed professionally in an adjacent laboratory. This provided data on the full 2600 and short 276 constructs that confirmed the sequencing structure of both to be that of the published structures (518). (See Figure 5.2 for the sequence of the full human TIMP-2 2600bp promoter).

Figure 5.9a Sequencing gel of the TIMP-2 2600 and 276 constructs

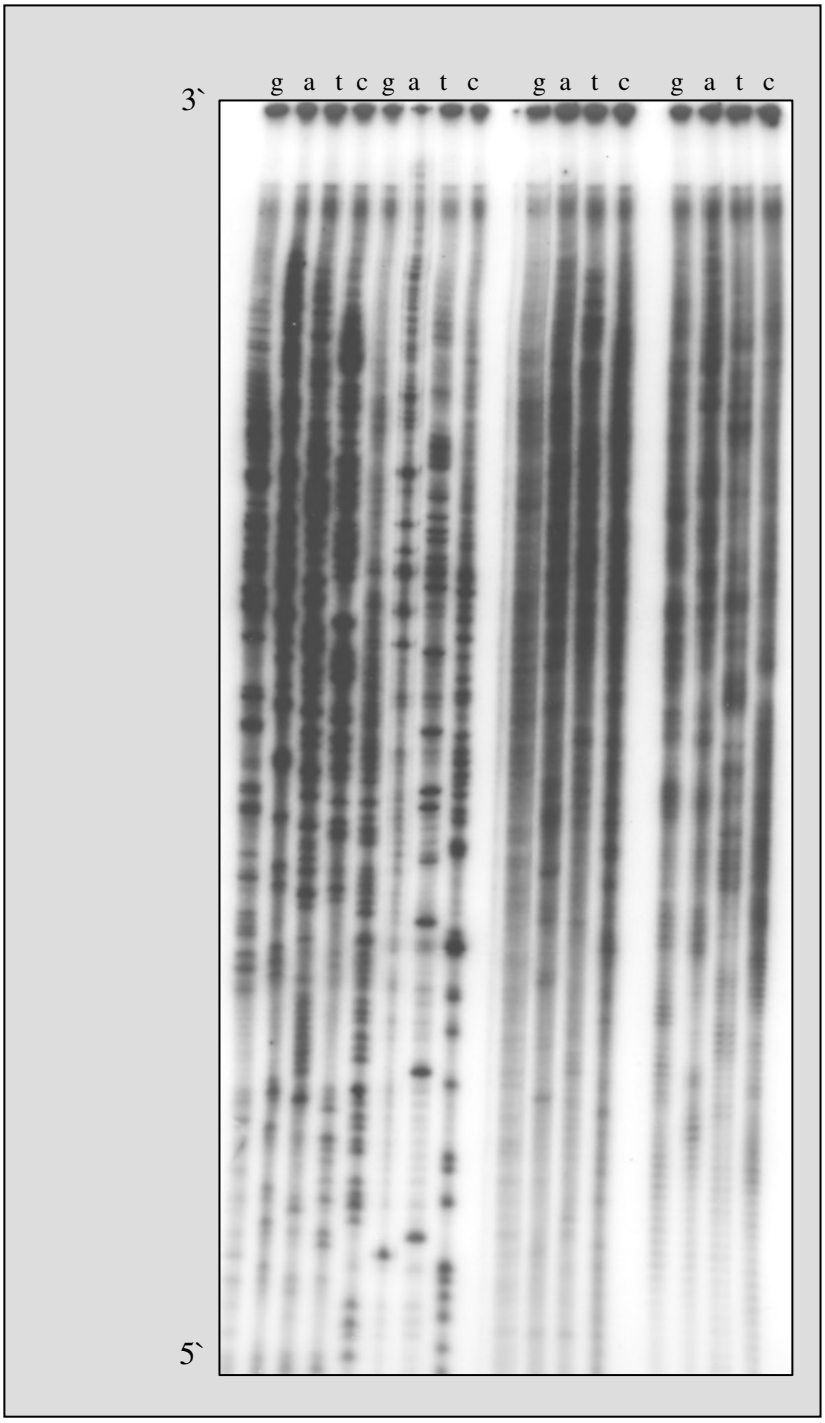

Figure 5.9a: Sequencing gel of TIMP-2 2600 and 276 Constructs. This gel shows sequencing of the pGL3 hTIMP-2 2600 and 276 inserts. Its clear that its impossible to write out the sequence based on this gel, in fact the smaller insert did not sequence as well. Both plasmids were simultaneously sequenced in a neighbouring commercial sequencing laboratory in Southampton which confirmed that the inserts were the TIMP-2 2700 and 276 as originally outlined by Dr Yves DeClerck.

Figure 5.9b Sequencing gel of the TIMP-2 2600 and 276 constructs

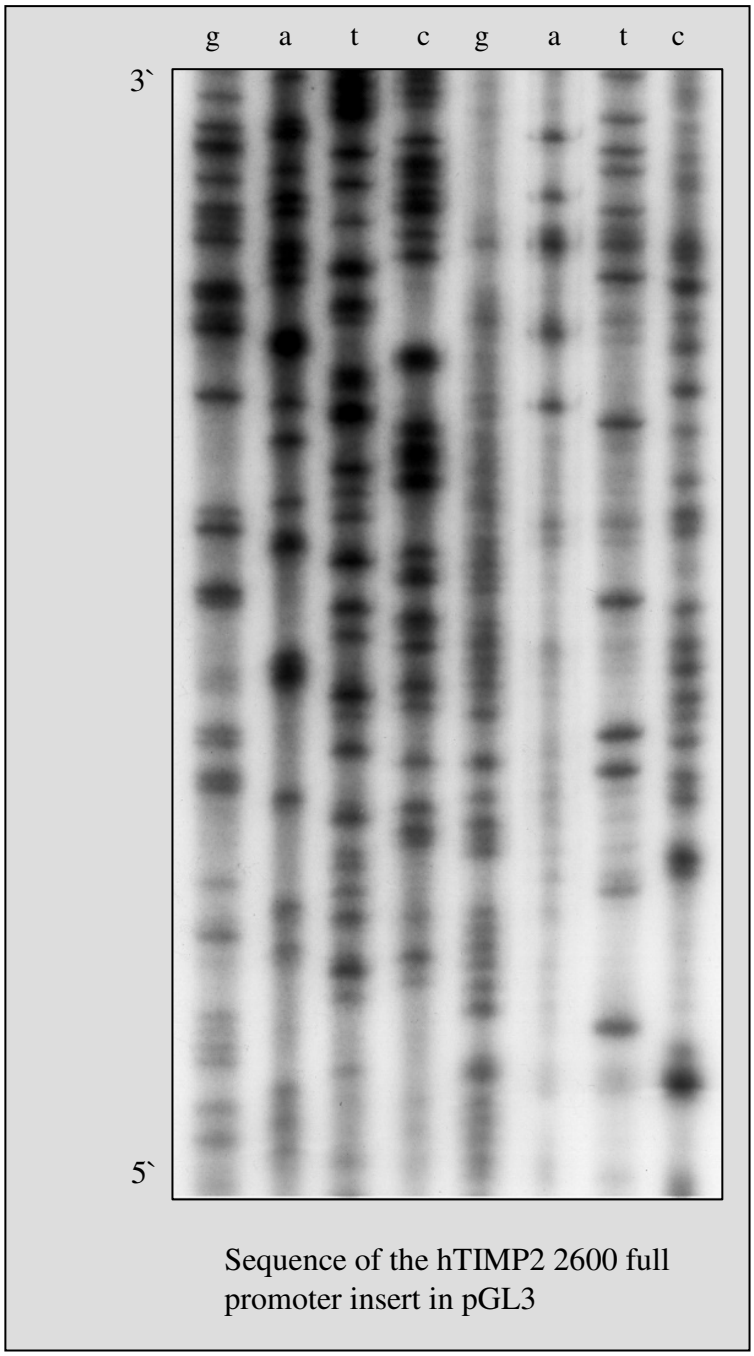

Figure 5.9b: Sequencing gel of TIMP-2 2600 in more detail

5.5.8 Subcloning the PGL3 2600 human TIMP-2 full promoter into pBLCAT3

Method

The experimental detail is provided in chapter 2 section 2.6 but is described here briefly. The following was carried out in one day:

1) The TIMP-2 2600 full promoter insert was cut out from pGL3 Basic vector with a PST1 cut: no freezing was carried out in order to minimize damage to the promoter insert.
2) pBLCAT3 vector was linearized with PST1 and treated with alkaline phosphatase.
3) A check gel was performed.
4) A phenol chloroform extraction of the TIMP-2 2600 full promoter was carried out.
5) The ligation reaction was initiated.
6) Bacterial stocks of DH5alpha were transformed and streaked out onto agar plates.
7) Following check gels minipreps of cell cultures was carried out.
8) 1 colony was picked.

Figure 5.10 Isolation of the TIMP-2600 insert

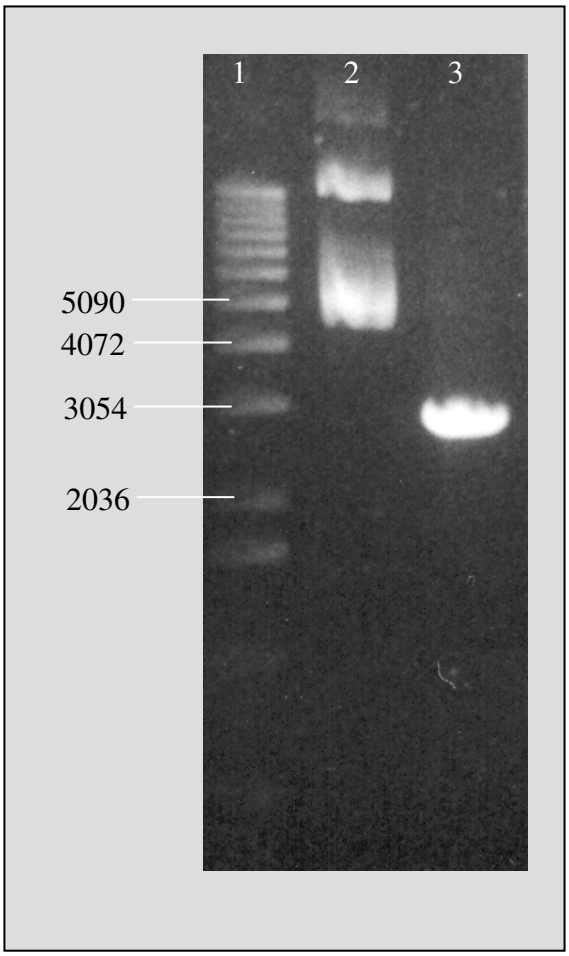

1% Agarose TAE gel lane 1-3 as follows

1) DNA ladder

2) pGL3-hTIMP2 2600kb full promoter construct (uncut plasmid)

3) hTIMP-2 2600kb full promoter insert gel purified

Figure 5.11 Isolation of the pBLCAT 3 linearised plasmid

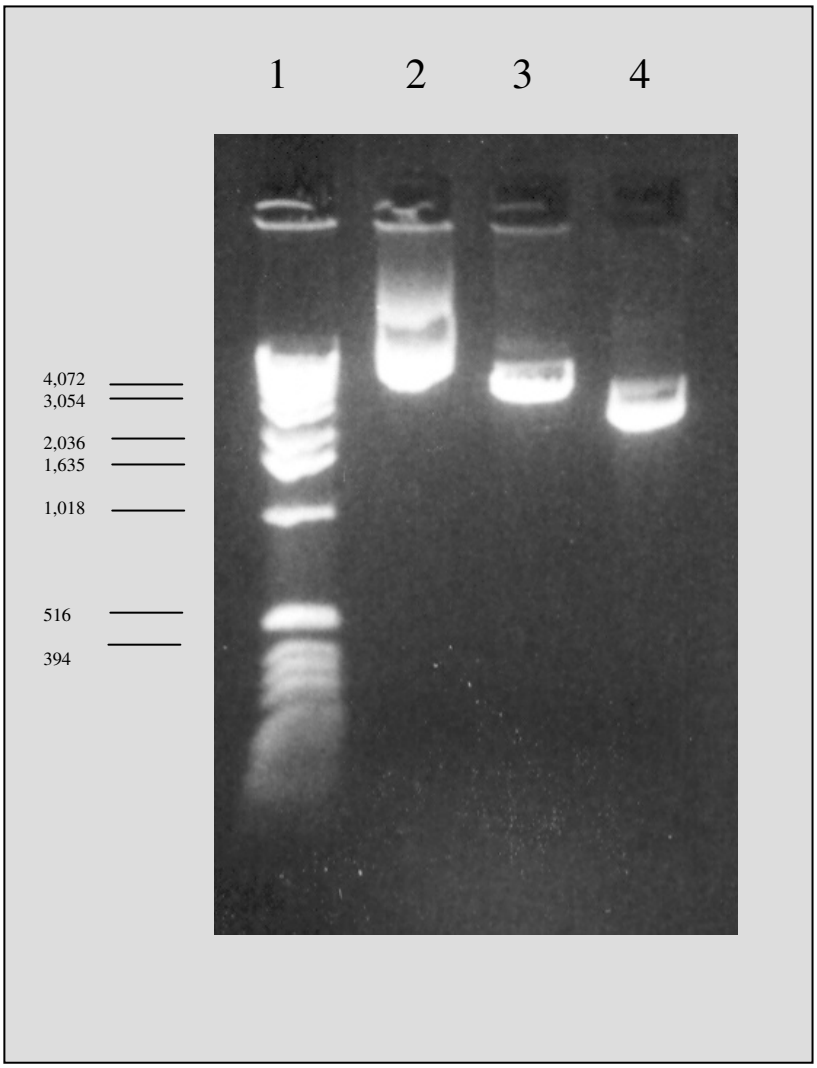

1) 1kb DNA marker (Promega)

2) pBLCAT3 uncut plasmid

3) linearised pBLCAT3 with a PST-1 cut

4) human TIMP2-2600 full promoter insert (cut from the pGL3 vector by restriction enzymes, isolated and gel purified).

Figure 5.12 Ligation of the TIMP-2 2600 insert into the pBLCAT3 vector in 7 out of 18 colonies

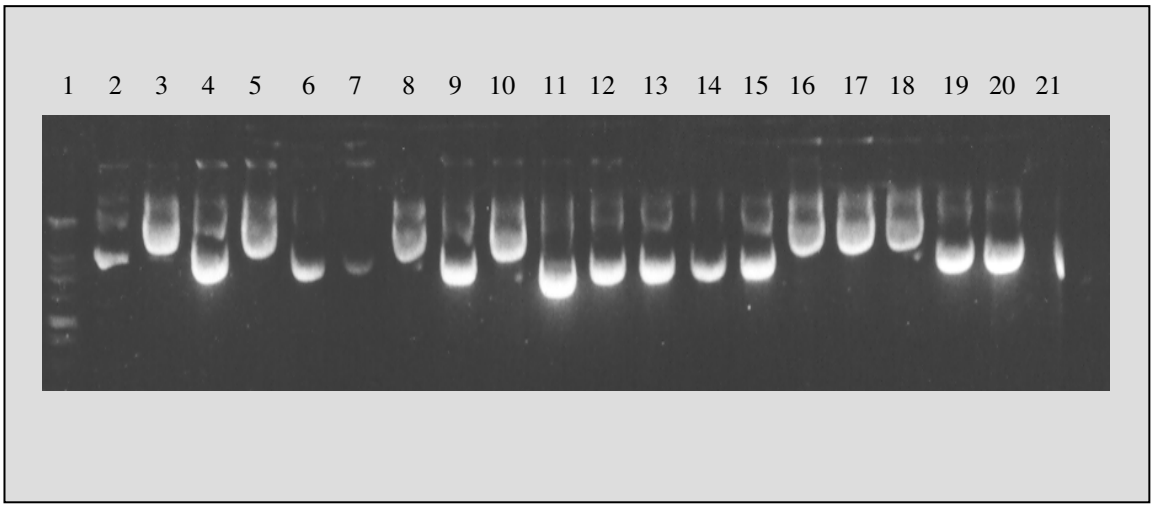

1% Agarose gel in TAE lanes 1-20 as follows:

1) 1kb DNA ladder (Promega)

2) pBlCAT3 uncut plasmid

3) – 20) samples (1-18) of minipreps performed on overnight cultures.

Conclusion: lanes 3, 5, 8, 10, 16, 17 and 18 have higher molecular weights than the other plasmids which appear to be PBLCATS (allowing for gel overloading). This suggests that the TIMP-2 2600 insert may have been sub cloned successfully into the pBLCAT3 vector.

Figure 5.13 Characterisation of the new plasmids purported to be pBLCAT3/human TIMP2-2600 insert

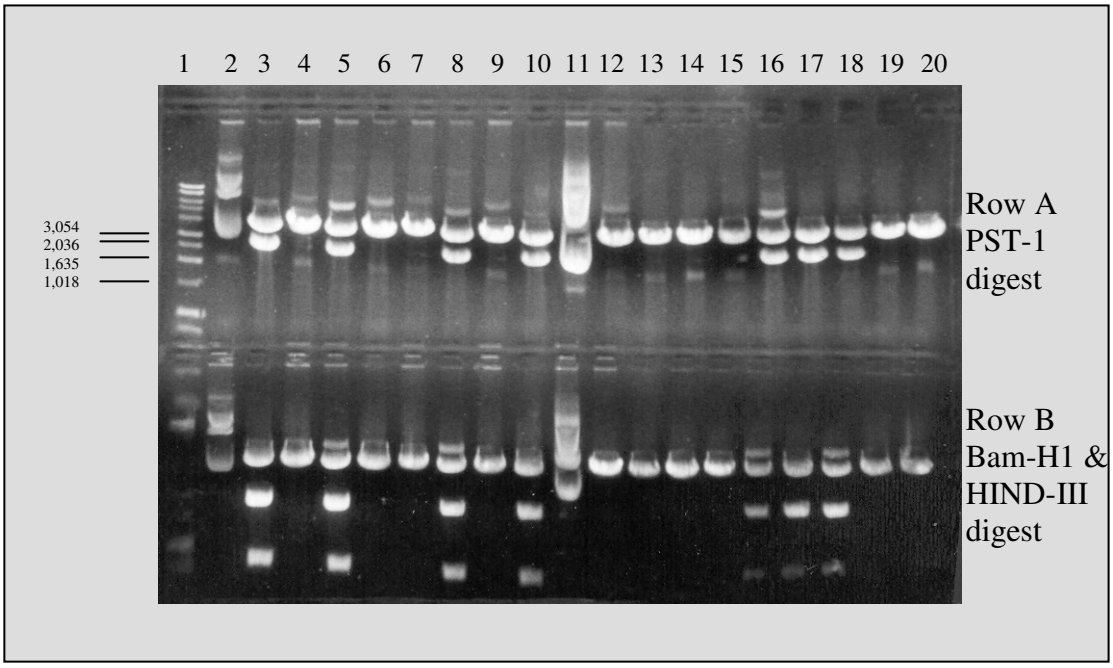

1% Agarose gel in TAE. Lanes 1 – 20 Row A are as follows

1) 1kb DNA ladder (Gibco)

2) pBlCAT3 uncut plasmid

3) – 20) 18 samples of plasmid subjected to a restriction digest with a PST-1 digest.

Lanes 1 – 20 Row B as follows

1) 1kb DNA ladder (Promega)

2) pBlCAT3 uncut plasmid

3) –20) 18 samples of plasmid subjected to a restriction digest with a BAM-H1 & HIND-III double digest.

Both Row A and Row B in the gel above appear to suggest that the human TIMP2 2600 insert has successfully been sub cloned into pBlCAT3 in samples run in lanes 3, 5, 8, 10, 16, 17 and 18.

Figure 5.14 Sequencing of pBLCAT3/TIMP2-2600 plasmid

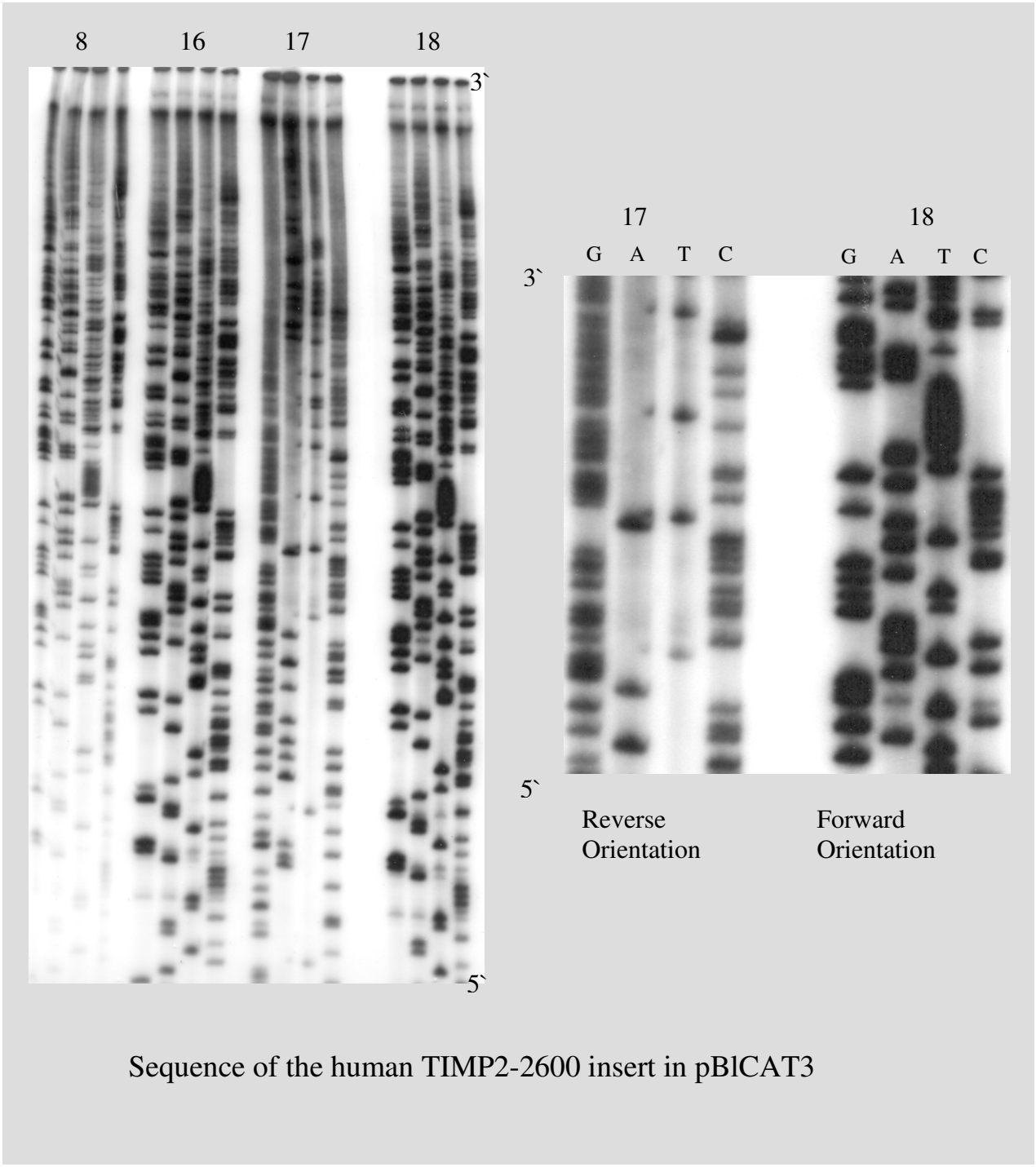

Figure 5.14: DNA sequences of 4 samples corresponding to sample numbers in previous gels. Sequencing performed to ascertain whether the TIMP-2 2600 insert was sub cloned and if so in what orientation. Samples 8, 16, and 18 have all been sub cloned in the preferred orientation, 17 has been sub cloned in the reverse orientation.

Figure 5.15 Maxi prep of TIMP2-2600 in pBLCAT3

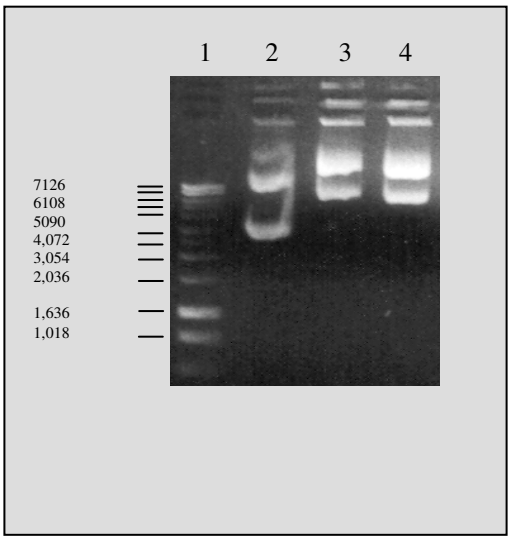

1% Agarose gel in TAE showing purified DNA from maxi preps of the human TIMP-2 2600 full promoter sub cloned in the correct orientation (forward) and incorrect orientation (reverse). Lanes are as follows:

Lane 1: 1kb DNA ladder (Gibco)
Lane 2: pBLCAT3 (uncut)

Lane 3: purified DNA from maxi preps performed in samples 18 - taken from sample outlined in Figure 5.13 - (hTIMP-2600 insert sub cloned in *forward* orientation into pBlCAT3) denoted **pBLCAT3 TIMP-2 2600$_{\text{forward}}$** Sequencing data for sample 18 is outlined in Figure 5.14.

Lane 4: purified DNA from maxi preps performed in sample 17 - taken from sample outlined in Figure 5.13 - (hTIMP-2600 insert sub cloned in *reverse* orientation into pBlCAT3 denoted as **pBLCAT3 TIMP-2 2600$_{\text{reverse}}$**. Sequencing data for sample 17 is outlined in Figure 5.14.

5.5.9 Discussion

The human TIMP-2 2600 large promoter originally donated by Professor Yves DeClerck in pGL3 basic vector was successfully sub cloned into pBlCAT3. Due to the problem of performing a digest on the PGL3 TIMP2 276 construct I elected to subclone the large promoter and then attempt to perform systematic deletions from the 5` end of this construct to obtain smaller constructs and obtain one comparable to the 276 minimal promoter provided by Prof Yves DeClerck.

I elected to use a proprietary kit from Promega, Southampton called "ERASABASE" which claims that several deletions could be obtained in only a few hours. In order to gain optimal conditions for the action of the DNA deletion with "Exonuclease III" or Exo III it is necessary to create 3` overhangs (protected from deletion) and a 5` overhang where the Exonuclease III initiates its deleting activity.

Figure 5.16 Restriction digest of pBLCAT3 and pBLCAT3/2600 TIMP-2 insert with the restriction enzymes Sph-1 and Bcl-1

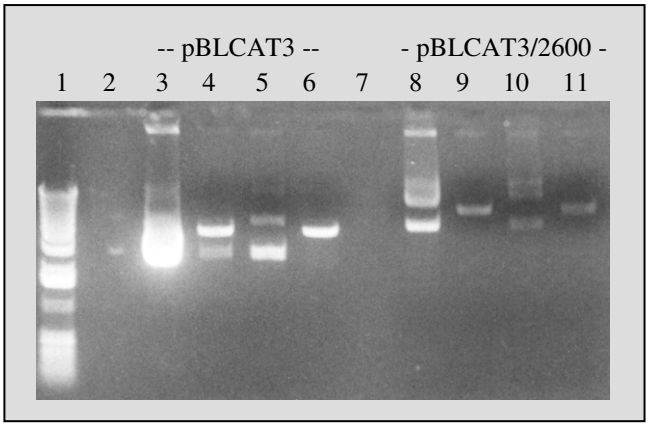

1% Agarose gel depicting restriction enzyme digests of pBlCAT3 empty vector and pBlCAT3/TIMP-2 2600 insert vector with *Sph-I* and *Bcl-1* enzymes. Lanes 2 & 7 are empty; lanes 1-9 are as follows:

1) 1kB DNA ladder
3) PBlCAT3 uncut plasmid (pBlCAT3 in lane 3 is clearly overloaded).
4) pBlCAT3 cut with *Sph-1*
5) pBlCAT3 cut with *Bcl-1*
6) pBlCAT3 double digest *Sph-l* and *Bcl-1*
8) pBlCAT3 hTIMP-2 2600 uncut plasmid
9) pBlCAT3 hTIMP-2 2600 digest with *Sph-1*
10) pBlCAT3 hTIMP-2 2600 plasmid cut with *Bcl-1*
11) pBlCAT3 hTIMP2 2600 double digest with *Sph-1* and *Bcl-1*.

5.5.10 Discussion on Bcl-1 cut of pBLCAT3

Figure 5.16 demonstrates that *Bcl-1* failed to cut either pBlCAT3 or pBlCAT3 hTIMP-2 2600bp. This experiment was repeated on 2 further occasions and finally with an overnight digest with BSA. Bcl-1 cuts at the following site:

5` T▼GATCA 3`
3`ACTAG▲T 5`

A new batch of Bcl-l enzyme was obtained from Promega and this produced the same result. On further discussion with Promega it was ascertained that *Bcl-1* does not cut methylated DNA. All plasmids had recently been produced by DH5α *E.Coli* which produces methylated DNA. DNA methylation involves the addition of a methyl group to DNA – for example, to the number 5 carbon of the cytosine pyrimidine ring –with the effect of reducing gene expression. Adenosine or cytosine methylation is part of the restriction modification system of many bacteria, in which DNAs are methylated periodically throughout the genome. A methylase is the enzyme that recognizes a specific sequence and methylates one of the bases in or near that sequence. Foreign DNAs (which are not methylated) which are introduced into the cell are degraded by sequence specific restriction enzymes. Bacterial genomic DNA is not recognized by these restriction enzymes. The methylation of native DNA acts as primitive immune system, allowing the bacteria to protect themselves from infection by bacteriophage. These restriction enzymes are the basis of the restriction fragment length polymorphisms (RFLP) testing, used to detect DNA polymorphisms.

A new bacterial stock was purchased for transformation and Mini/Maxi preparation of the pBlCAT3 TIMP-2 2600 in 'DMI *E. Coli*' bacteria (Promega). A further restriction enzyme digest of pBLCAT3 TIMP-2 plasmid was repeated after the plasmid was amplified in DM1 *E.coli* bacteria. The results are depicted in Figure 5.17 showing a successful linearization digest with *Bcl-1*. Figure 5.18 shows a successful linearization or digest with *Sph-1*.

Figure 5.17 pBLCAT3 plasmid stock grown up in 'DMI' E. coli bacteria with a digest using Bcl-1 restriction enzyme

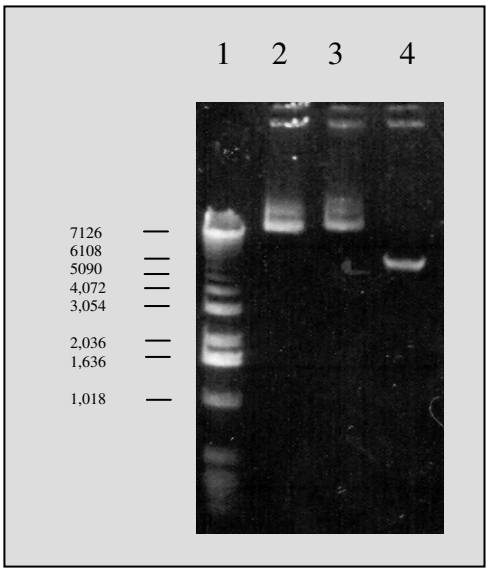

1% Agarose gel with lanes 1-4 as follows:

1) 1kB DNA ladder

2) pBlCAT3 hTIMP-2 2600 full promoter from DH5α stocks

3) pBlCAT3 hTIMP-2 2600 full promoter plasmid from DMI stocks

4) pBlCAT3 hTIMP-2 2600 full promoter plasmid from DMI stocks with a *Bcl-1* digest

This gel demonstrates successful linearisation of the pBlCAT3 hTIMP-2 2600 full promoter with *Bcl-1*. The digest is performed at 50^0C.

Figure 5.18 pBLCAT3 plasmid stock grown up in 'DMI' E. coli bacteria with a digest using Sph-1 restriction enzyme.

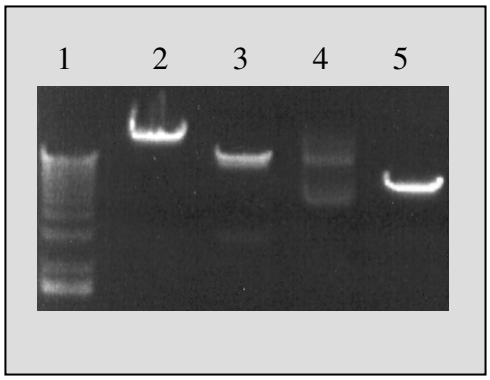

1% Agarose TAE gel. Lanes 1-5 as follows:

1) 1kB ladder

2) Lambda plasmid 1µg/1µl (used a molecular weight marker)

3) Lambda cut with Sph-1

4) DM1 stock of pBlCAT3 TIMP-2 2600 uncut plasmid

5) DMI stock of pBlCAT3 TIMP-2 2600 digest with Sph-1.

This gel shows that incubation at 37^0C with demethylated DNA with Sph-1 allows a successful digest.

5.6 Successive deletion of the pBLCAT3 hTIMP-2 2600bp insert with "Erase-a-Base"

pBLCAT3 hTIMP-2 2600 full promoter construct was restriction digested first with *Bcl-1*, then with *Sph-1* and the resulting insert was subjected to sequential digest from the 5` end by Exo III. The Erase-a-base system by Promega is designed for the rapid construction of plasmid containing progressive unidirectional deletions of any inserted DNA. This is discussed in detail in chapter 2 section 2.8. In brief an enzyme (exonuclease III or Exo III) digests insert RNA from a 5 prime (5`) protruding or blunt end restriction site. The adjacent primer binding site is protected from digestion by a 4-base 3` overhang restriction site. The 2600 base DNA fragment of the human TIMP-2 promoter provided an excellent starting point to create smaller proteins of the TIMP-2 promoter by successive deletions from the 5` prime end. The uniform rate of digestion of Exo III allows deletion of predetermined lengths to be made by removing timed aliquots from the reaction.

Conveniently the 2600 fragments inserted into pBlCAT3 had two unique restriction sites that lie between the end of the insert DNA and the sequencing primer binding sites (SP6/T7), the enzyme that cuts closest to the primary site (Bcl-I) leaves 4-base 3` overhanging ends, which are resistant to Exo III digestion. The enzyme that cuts closest to the insert DNA (SP-1) leaves blunt ends or 5` overhangs, susceptible to Exo III. Once the reaction mixture was set up, samples from the Exo III digestion were removed at timed intervals; S1 nuclease was added to remove the single stranded tails. The S1-nuclease buffer inhibits Exo III thereby inhibiting any further deletions. Klenow polymerase facilitates ligation of the inserts to circularize the deletion containing vectors. The ligation mixtures are then used directly to transform competent cells. Each successive time point yields a collection of subclones containing clustered deletions extending further into the original insert. The full hTIMP-2 2600 bp promoter was transformed and amplified in DM1 stocks purified and "gene cleaned". Successive digest were obtained with Bcl-1 to linearize then Sph-1 to obtain the 2600bp insert, see Figue 5.19 and Figure 5.20.

Figure 5.19 DMI Stock pBLCAT3 hTIMP-2 2600 insert cut with Bcl-1

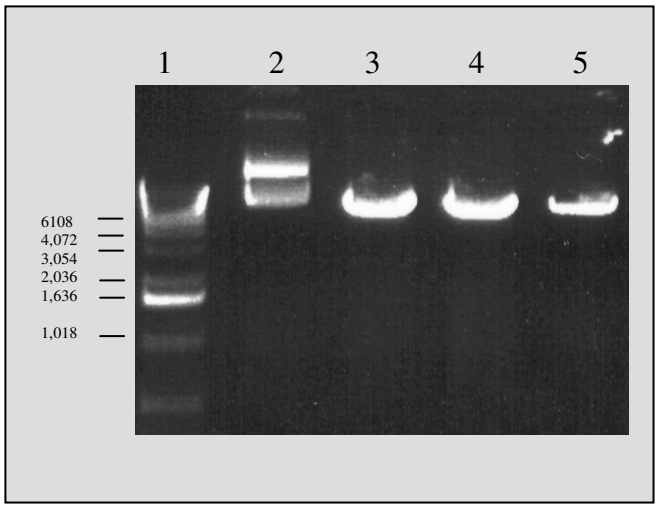

The pBlCAT3 hTIMP-2 2600bp full promoter insert was transformed and amplified in DM1 *E. coli* and purified by 'Maxipreps' and 'gene cleaned'. Purified plasmid was then cut with *Bcl-1* at 50^0C for 2 hours.

1% agarose gel; lanes 1-5 as follows:

1) 1kB DNA ladder

2) uncut plasmid DM1 pBlCAT3 hTIMP-2 2600 digest with *Bcl-1*

3)-5) 'Maxi prep' samples 1, 2 and 3 subjected to restriction digests with *Bcl-1*.

This gel demonstrates clear linearisation with *Bcl-1*.

The resulting digest was gel purified, ethanol precipitated and a further digest with *Sph-1* was carried out at 37^0C for 2 hours.

Figure 5.20 Isolation of the human TIMP-2 2600 insert with Bcl-1 and Sph-1 restriction digest

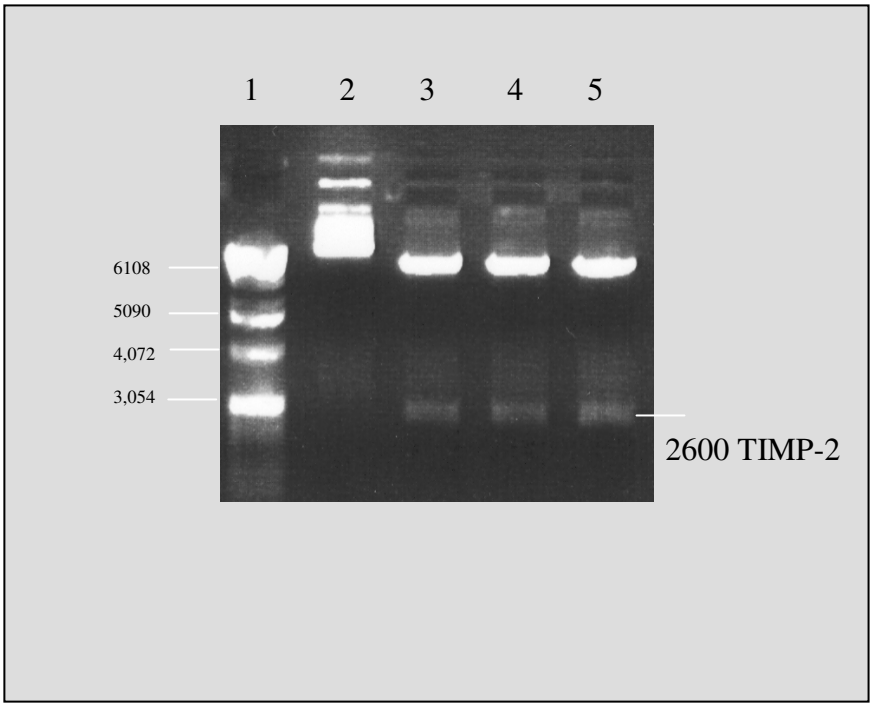

1% Agarose gel 1 – 5 as follows:

1) DNA ladder (lane overloaded)

2) DM1 plasmid stock of pBlCAT3 hTIMP-2 2600bp uncut plasmid

3)-5) samples 1, 2 and 3 of pBlCAT3 hTIMP-2 2600pb previously linearized with *Bcl-1* and now subjected to a digest with *Sph-1* at 30^0C for 2 hours.

This gel shows 3 faint signals depicting the human TIMP-2 2600 insert.

The resulting plasmid hTIMP-2 2600bp insert was gel purified and ethanol precipitated.

Figure 5.21 "Erasabase" protocol for systematic truncation of the human TIMP-2 2600 insert from the 5` end by Exonuclease III

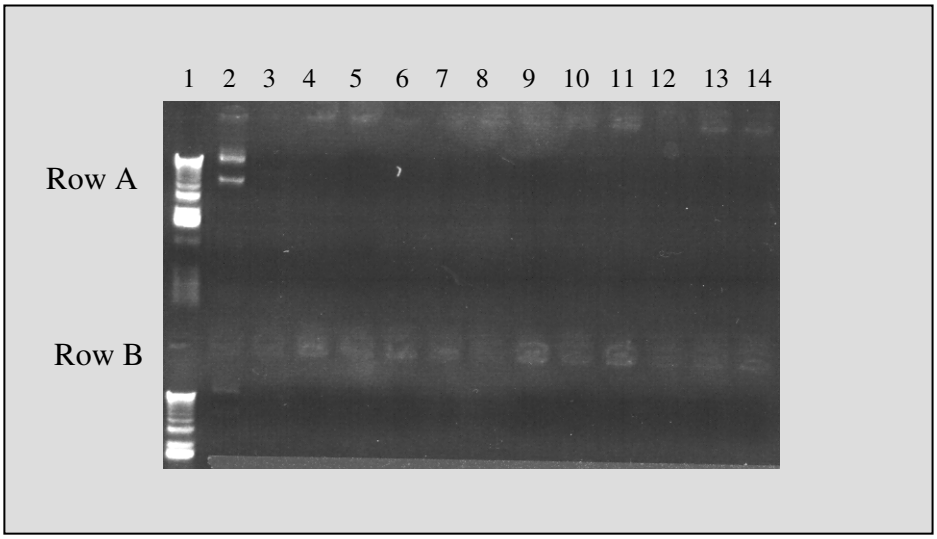

1% Agarose gel: row A includes lanes 1-14, row B includes lanes 1-14.

Row A lanes 1-14 were as follows:

1) 1kB DNA ladder

2) 1µl DM1 hTIMP-2 2600pb insert not exposed to *Exo III*

3)-14) samples 1 to 12.

Row B lanes 1-14 were as follows:

1) 1kB DNA ladder (identical to that used above)

2) 1µl DM1hTIMP-2 2600bp insert not exposed to *Exo III*

3)-14) samples 13 to 24.

This gel shows no cut was seen with Exonuclease III.

Figure 5.22 "Erasabase" protocol for systematic truncation of the control DNA (supplied by Promega) from the 5` end by Exonuclease III.

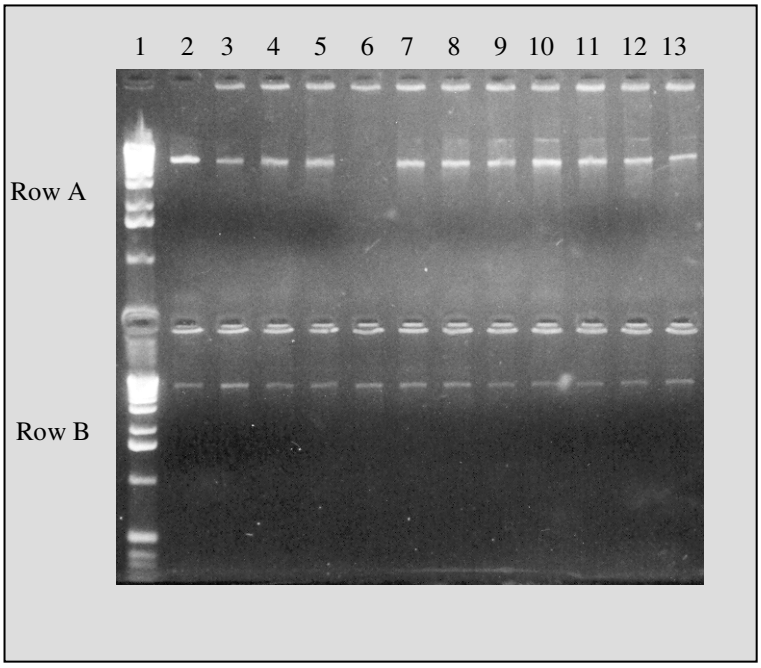

Repeat protocol for standard DNA supplied with the Erasabase kit.

Row A Lanes 1-13 as follows:

1) 1kB DNA ladder

2) Uncut control DNA

3)-13) (samples 1-11) attempted successive truncations from the 5` end with Exo III. Each sample was terminated at 30 second intervals.

4) Row B lanes 1)-13) depict samples 12-22 – again each sample was terminated at 30 seconds in sequence.

This gel shows that using the supplied DNA from Promega that the protocol gives no adequate sequential digests with *Exo-III* according to their protocol.

Figure 5.23 Erasabase protocol for systematic deletion of the human TIMP-2 2600 insert from the 5` end by Exonuclease III

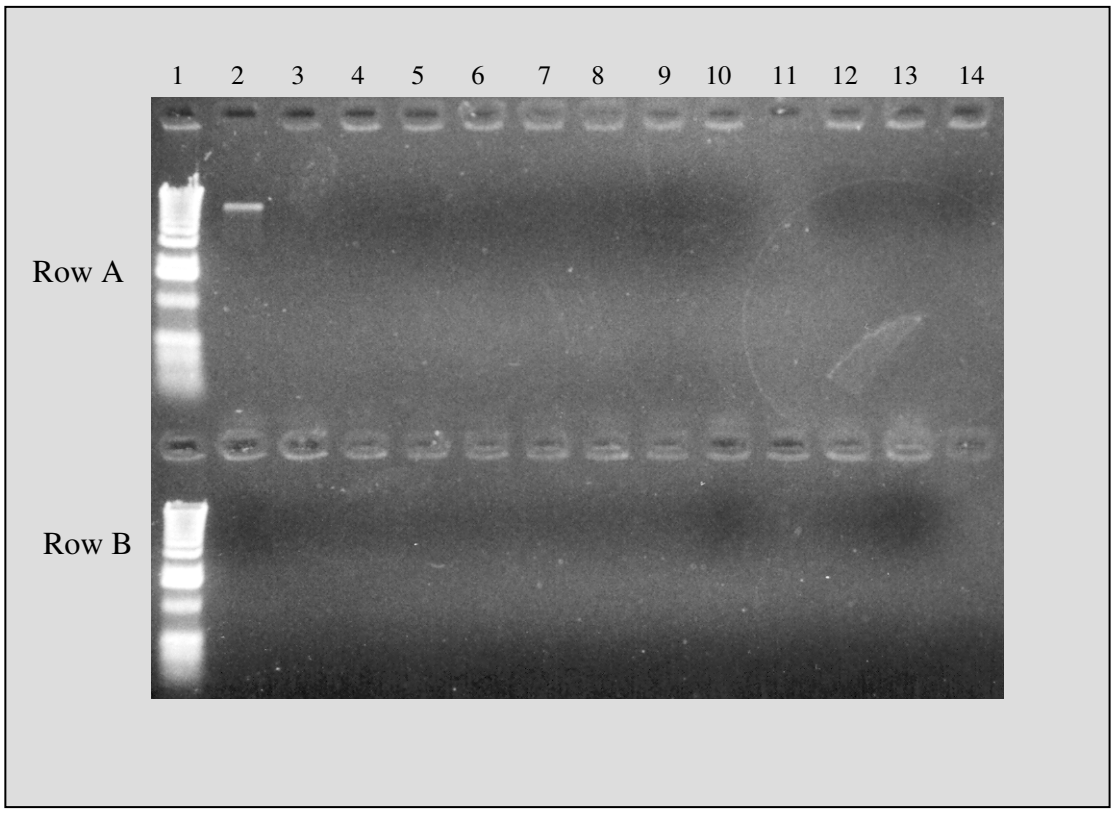

The Erasabase protocol experiment was repeated. Row A Lanes 1-14 as follows:

1) 1kB DNA ladder
2) Uncut control DNA
3)-14) (samples 1-12) successive deletions from the 5` end with Exo III. Each sample was terminated at 30 second intervals.
Row B lanes 1)-14) depict samples 13-23 – again each sample was terminated at 30 seconds in sequence.

This demonstrates no Exonuclease III digest of plasmid DNA with DM1 pBlCAT3 TIMP-2 2600 full promoter. However the recovery of DNA was poor.

5.7 Discussion

A number of explanations may account for no apparent deletion of experimental DNA when analysed by gel electrophoresis:

1) If the restriction enzymes cleaving the *Exo-III* sensitive end failed to cut completely then these singly cut molecules will remain the same size as the original starting DNA throughout the deletion time course.

2) There may not be sufficient nucleotides left near the recognition site of the second enzyme to allow cleavage.

3) If the deletion series appears to be degraded (as in this case) the original pBlCAT3 vector may contain nicked molecules ant this may allow *Exo-III* to recognise nicks within the DNA template and start to generate deletions from these nicks resulting in a smear.

4) When no DNA appears on the gel of the deletion series it may be that the loss of DNA occurred during the extraction and precipitation stage of DNA following restriction digestion, resulting in insufficient DNA being loaded on the gel for deletion; however this would not explain why control DNA continued to be present. The control DNA did not demonstrate any deletions and so the size remained the same with successive aliquots.

In summary there may have been inadequate DNA or "nicked" DNA could have been the crux of the problem due to the suggestion of smearing on one electrophoresis gel.
Nicked DNA in our lab may be caused by the following:

1) Use of ethidium bromide in the electrophoresis gels
2) High UV light exposure in the electrophoresis gel boxes
3) Shearing of DNA at any pipetting stage

The procedures were repeated therefore with the following protocols:

1) Generation of adequate quantities of DNA in the first place
2) Minimize conditions that causes 'nicked' DNA such as
    - reducing amounts of ethidium bromide,
    - low light intensity on the light box for (less than or equal to) 30 seconds,
    - reducing pipetting at any defined stage
3) I elected to create the 3` overhang first with *Bcl-1* then extract with phenol-chloroform and precipitate with ethanol followed by a *Sph-1* digest.

Figure 5.24 Restriction digest of pBLCAT3 hTIMP-2 2600bp full promoter construct with restriction digest using Bcl-1 and Sph-1

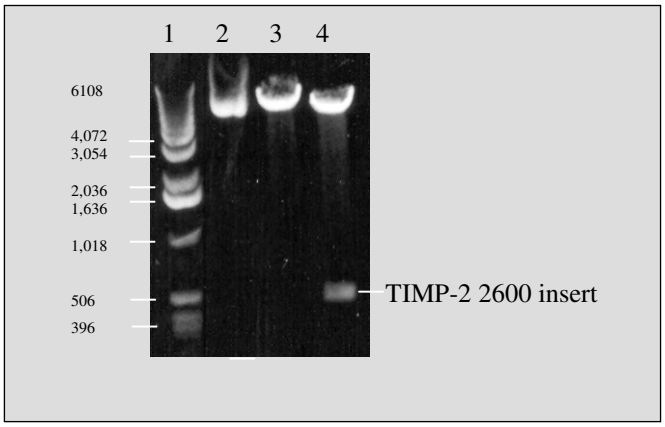

1% Agarose gel with lanes 1-4 as follows:

1) 1kB ladder

2) pBlCAT3 hTIMP-2 2600 full promoter grown up in DMI stock, uncut

3) *Sph-1* cut

4) *Bcl-1* & *Sph-1* double digest

Figure 5.25 Erasabase protocol for systematic deletion of the human TIMP-2 2600 insert from the 5` end by Exonuclease III

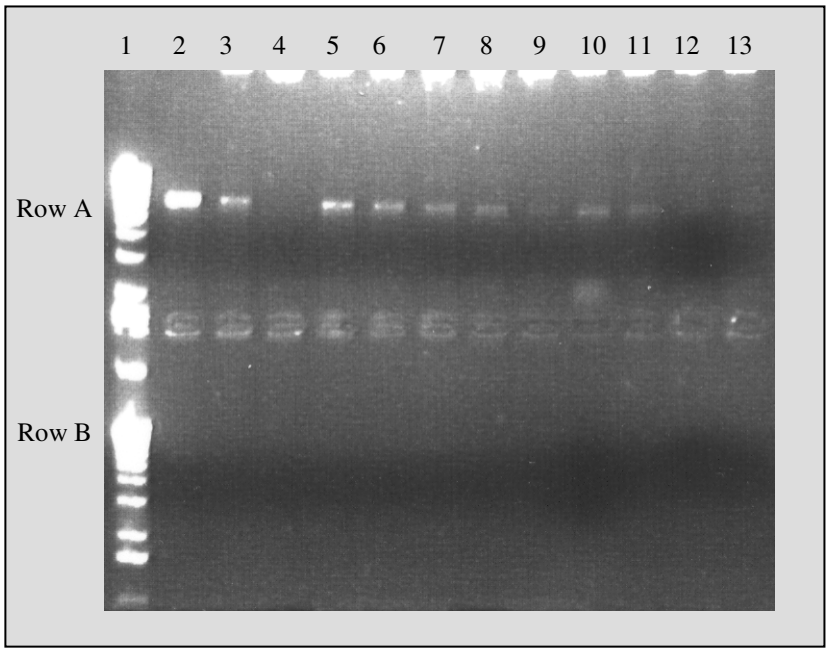

1% agarose gel in TAE. Row A Lanes 1-12 as follows:

1) 1kB DNA ladder
2) uncut plasmid pBlCAT3/2600
3)-12) denote successive DNA deletions by *Exo-III* at 30^0C (= 120 base pair cuts per 30 second intervals). 5µg of plasmid cut at 30 second intervals. Row B Lanes 1) 1kB DNA ladder, lanes 2)-12) as follows: samples 14-25 which correspond to later time points of *Exo-III* treatment.

This gel shows that there was partial success with *Exo-III* digestion but that no DNA was seen in Row B. In addition in lane 10 there is smearing suggesting that in at least 1 sample there was evidence of 'nicked' DNA. It was concluded that there were continuing problems with the 'Erasabase' protocol and subsequent work with this was abandoned.

2.7.4 The Chloramphenicol Acetyl Transferase (CAT) Transfection Assay

Methods: these are described in detail in chapter 2 section 2.7.4

The initial transfections using CAT assays were carried out with the pBlCAT3 TIMP-2 2600 insert sub cloned in the forward and reverse direction. All transfection were carried out using the 'Effectene' kit by Qiagen outlined above according to the manufacturer's instructions. After incubation in fresh media transfections were carried out over 48 hours with no serum free step. Cells were then scraped off tissue culture plates into media, and pelleted. After removing the supernatant and resuspending the cells in 5ml of PBS they pelleted again at 1000rpm for 5min; this was then repeated on two further occasions before finally resuspending the cells 50µl of 0.25M Tris buffer pH7.9. Cells were frozen in liquid nitrogen for 2 min then thawed at 37^0C for 5min followed by vortexing: this was repeated for a total of 3 occasions. The disrupted cells were then pelleted using a microfuge at 13000 rpm for 5 min. The pellet was retained and stored at -20^0C. A protein assay incorporating a proprietary kit was carried out on 2µl samples of the supernatant. Samples were then modified to 25µg in 50µl and to this a mastermix was added (the master mix represented 70µl of 1M Tris-HCl pH 7.8, 20µl of Acetyl Coenzyme A 3.25µg/µl and 1µl of 400µCi/ml [^{14}C] 35-50mCi/mmol Chloramphenicol (Amersham), for each reaction).

Sample were 'flick spun' using a microfuge at 13000rpm and incubated at 37^0C for 2 hours. To each sample 0.5 ml of ethyl acetate was added and the solution vortexed for 30 seconds then microfuged at 13000 rpm for 5mins. The top layer was removed and was speed vacuum dried; the residual precipitate was re-suspended in 15µl of ethyl acetate before being applied to a thin layer chromatography plate and allowed to dry. The plate was run in a chromatography tank containing 95% chloroform, 5% methanol. Imaging was performed by plate exposure to Blue Autoradiography X-ray film (GRI) and quantitation was determined by phosphor image analysis using a Storm scanner and an "Image Quant" software data analysis package (Molecular Dynamics).

Figure 5.26 CAT assay – transfection of TIMP-2 insert 2600$_{forward}$ and 2600$_{reverse}$ into passaged HSC

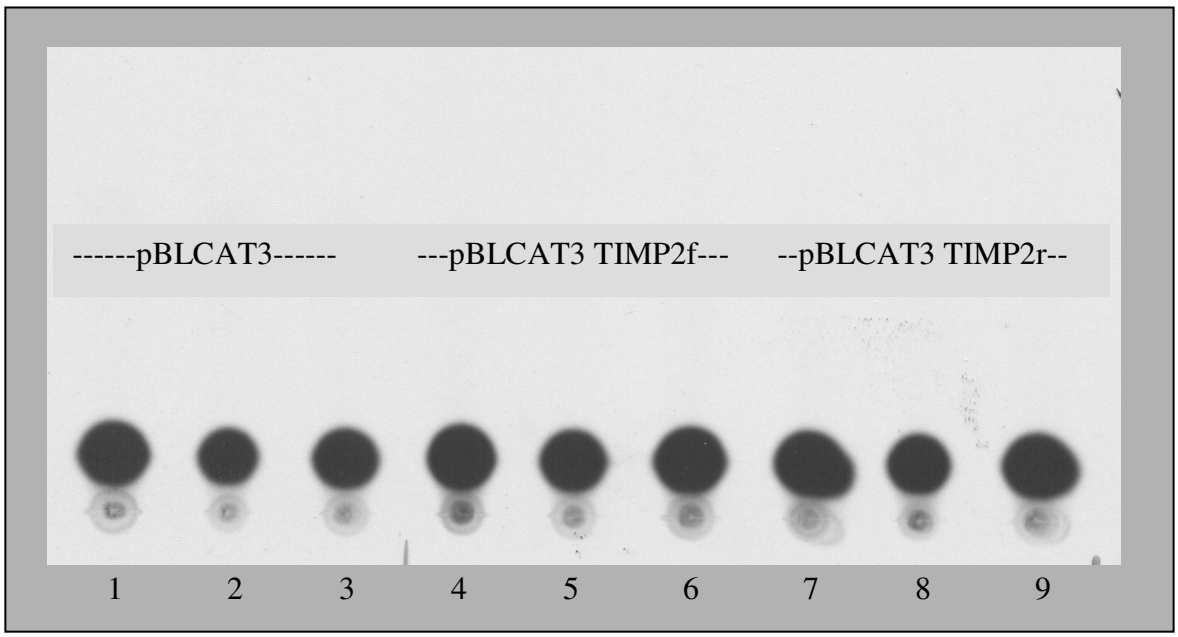

This demonstrates thin layer chromatography of CAT transfection into passaged hepatic stellate cells at 70% confluence for 72 hours. Following a CAT assay an autoradiograph was laid down for 1, 2 and 8 days. This 8 day autoradiograph shows lanes as follows

1-3) pBlCAT3 empty vector (n=3)
4-6) pBLCAT3 hTIMP-2 insert 2600$_{forward}$ vector (n=3)
7-9) pBLCAT3 hTIMP-2 insert 2600$_{reverse}$ vector (n=3)

No signal for transfection was noted. This is representative of 2 experiments.

Figure 5.27 CAT assay – transfection of TIMP-2 insert 2600$_{forward}$ and 2600$_{reverse}$ into passaged 3T3 fibroblasts

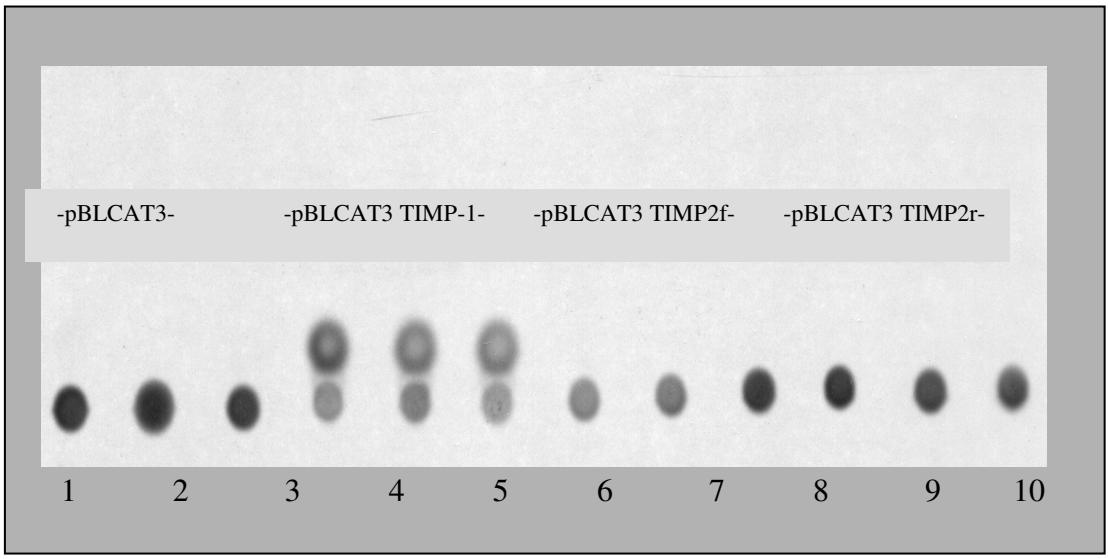

This demonstrates data from CAT transfection into passaged 3T3 fibroblasts at 70% confluence for 72 hours. Following a CAT assay an autoradiograph was laid down for 1, 2 and 8 days.

This 8 day autoradiograph shows lanes as follows

1-3) pBlCAT3 empty vector (negative control)
4-6) pBlCAT3 hTIMP-1 (positive control)
7-9) pBLCAT3 hTIMP-2 insert 2600$_{forward}$,
10-12) pBLCAT3 hTIMP-2 insert 2600$_{reverse}$ vector.

This demonstrates no activity on the part of the TIMP-2 insert 2600$_{forward}$ or TIMP-2 insert 2600$_{reverse}$ vector sub cloned into pBlCAT3. This is representative of 2 experiments in 3T3 fibroblasts and 2 experiments in 1080 human cell line.

5.75 Discussion

pBlCAT3 hTIMP-1 (positive control) showed evidence of transfection whilst CAT assays incorporating the promoters of interest showed no such activity. Clearly there are problems with the assay using the constructs though the positive control suggests that the CAT assay itself with this current protocol is viable. With problems encountered with CAT assays of the pBlCAT3 hTIMP-2 2600 full promotor construct I decided that I should return to an examination of the original constructs given to us by Prof Yves DeClerck.

Figure 5.28 Assessment of plasmid concentrations for transfections of luciferase and CAT constructs

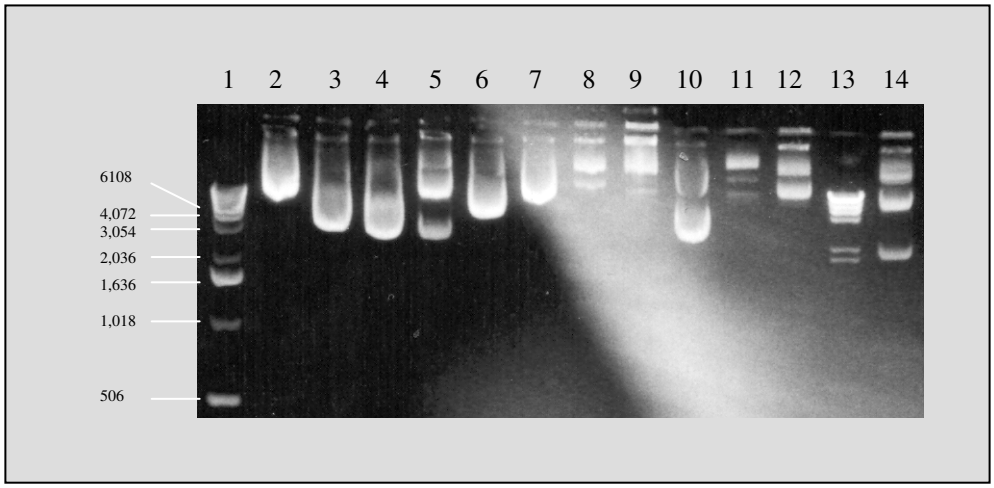

1% Agarose gel lanes 1-14 as follows:

1) 1kB DNA ladder

2) pGL3-TIMP-2 2600 construct

3) pGL3-TIMP-2 276 construct

4) pGL3 (empty vector/'mock')

5) pRL-SV40

6) 1kB Luc

7) pBlCAT3/empty vector

8) pBlCAT3/TIMP-2 $2600_{forward}$

9) pBlCAT3/TIMP-2 $2600_{reverse}$

10) pBlCAT3/TIMP-1 wild type

11) pGL3 TIMP-2 2600

13) λ-Hind-III

14) Human TIMP-2 maxi prep.

Method for "Effectene" transfection

Introduction

The method for "Effectene" transfection was as follows: freshly isolated or passaged cells were obtained and plated to achieve 70% confluence. A fresh Microfuge tube was obtained and to this 6.4µl enhancer, 91.6µl EC buffer and 1µl (= 1µg) of each plasmid was added for dual transfections. The cap was closed and the Microfuge tube vortexed briefly followed by a flick spin at 13,000g in a microfuge. 10µl Effectene was added and again a full vortex was performed for 10 seconds. Following a flick spin the mixture was incubated at room temperature for 10 minutes. Fresh media was changed (1ml to 6 well-plates). The cells were returned to the incubator. 500µl DMEM was added to the plasmid in a Microfuge tube (i.e. to a total volume of 1.6ml). This was then added to the wells. Transfections were performed in triplicate wells and took place over a 24 hour period. All plasmids were transfected at 1µg/µl to a total concentration of 1µg. Prior to cell harvesting the cells were washed once in PBS. They were then scraped off the plates and resuspended in 0.75M pH 74 and frozen at -20^0C until the luciferase assay took place.

Luciferase Assay

Samples were defrosted. 100µl of LARII buffer (firefly) was added to each sample. A 20µl was taken and inserted into a luminometer (Promega) and three sets of readings were taken. 20µl of Renilla was then added (quenching the firefly and allowing the 'Renilla' to luminesce). Again 3 readings were taken. All transfections were performed in triplicate wells.

Following the protocols described by Yves DeClerck I attempted to confirm data already documented in the original papter by Hamani et al in 1994 (518). Human 3T3 fibroblasts and *nih*1080 – a human fibrosarcoma cell line – were used in the ensuing experiments.

Table 5.5 Intitial transfections with Effectene Promega Protocol

Vector	Well	Firefly	Renilla
pGL empty vector	1)	0.105	4924
"Mock"		0.000	4164
		0.111	3682
	2)	0.069	6884
		0.000	6294
		0.96	5735
	3)	0.136	8057
		0.134	7248
		0.031	6367
pGL SV40	1)	76.11	>9999
+ve control		75.98	>9999
		75.63	>9999
	2)	28.96	>9999
		28.89	>9999
		28.39	>9999
	3)	11.32	>9999
		11.43	>9999
		11.11	>9999
pGL3 hTIMP-2 2600	1)	2.228	7318
"full promoter"		2.102	6350
		2.200	5545
	2)	0.993	3381
		0.82	3003
		0.717	2690
	3)	0.727	>9999
		0.497	>9999
		0.435	>9999
pGL3 hTIMP-2 276	1)	297.6	4312
"short promoter"		303.2	3783
		303.2	3294
	2)	7.416	3366
		7.447	2967
		7.110	2851
	3)	50.63	>9999
		51.47	9804
		53.46	8618

Table 5.5: Transfection of pGL3 basic (empty vector), pGLSV40 positive control, pGL hTIMP-2 2600 (full promoter construct), pGL3 hTIMP-2 276 (short promoter construct) transfected into passaged rat hepatic stellate cells (representative of n=3). Assays were performed on three different wells and for each well the luminometer reading was repeated on three occasions.

5.7.9 Discussion

Figure 5.1a depicts the pGL3 basic empty vector. Figure 5.1c demonstrates the pGL3 human (h)TIMP-2 2600 full promoter and Figure 5.1c the pGL3 hTIMP-2 276 short promoter.

pGL3 SV40 positive control vector

Figure 5.1b depicts the positive control pGL3 SV40 promoter. This plasmid has the firefly luciferase gene (the same gene that is driven by the TIMP-2 constructs/promoters) driven by a simian viral (SV40) promoter, acting as a positive control. The SV40 promoter luciferase genes can be transfected into cells of any type and is therefore an excellent positive control. If no firefly activity is seen in the control then the transfection has not taken place successfully.

PRL-SV40

This contains the Renilla luciferase gene under the control of the SV40 (a simian viral promoter). By co-transfecting the cultured cells e.g. 3T3 cells with both an experimental plasmid such as pGL3 hTIMP-2600 and the pRL-SV40 construct one can standardise the results of transfection efficiency. For a given assay the firefly luciferase activity is measured followed by the Renilla luciferase activity. The first value is divided by the Renilla value to standardise.

Transfections were carried out in the following co-transfections:

1) pGL3 Basic Empty vector + PRL-SV40 (“Mock” or negative control)

2) pGL3 SV40 + PRL-SV40 (positive control)

3) pGL3 TIMP2 2600 + PRL –SV40 (long construct / full promoter)

4) pGL-TIMP 267 + PRL-SV40 (short construct / shortened or truncated promoter)

All plasmids were grown into DH5α *E.coli* strain except where indicated.

The first comment to make on the first transfection above in Table 5.4 is that the Renilla values are extremely high and in many occasions were too high to be read by the luminometer. This made Firefly/Renilla calculations impossible.

Secondly there is a discrepancy between some wells transfected. This experiment was therefore repeated on two separate occasions, but this resulted in obtaining the same trend. On discussion with Promega it was indicated that the pRL-SV40 plasmid should be transfected at 1/50 – 1/100 the concentration of the co-transfected plasmid.

All transfections with pRL-SV40 renilla gene were subsequently performed at 1/50 of the previous concentration i.e. 0.2μg.

5.7.10 Results

Table 5.5 demonstrates raw data of transfecting the short and full human TIMP-2 promoters into quiescent newly harvested and activated rat hepatic stellate cells. Tables 5.6 and 5.7 depict the results normalized to the negative control. This experiment was repeated on 5 occasions and the results pooled (Table 5.7) and graphed on an Excel spread sheet with the standard error of the mean shown (Figure 5.29). There is a consistent increase in activity of the full promoter compared to the short promoter in quiescent cells. This is reversed for the activated cell phenotype.

Table 5.6 Transfection into rat Quiescent and Activated Hepatic stellate cells

QUIESCENT CELLS

	Luc	Renilla	luc/ren	Mean
B1	0.01	0.481	0.02079	0.011839
B2	0.01	0.679	0.014728	
B3	0	0.635	0	
C1	0.038	1.518	0.025033	0.025966
C2	0.083	1.57	0.052866	
C3	0	1.067	0	
2600 - 1	0	0.78	0	0.038219
2600 - 2	0	3.221	0	
2600 - 3	0.176	1.535	0.114658	
277 - 1	0	0.863	0	0.011111
277 - 2	0.06	1.8	0.033333	
277 - 3	0	0.975	0	

ACTIVATED CELLS

	Luc	Renilla	luc/ren	Mean
B1	0.066	2.503	0.026368	0.018966
B2	0.053	1.736	0.03053	
B3	0	2.385	0	
C1	0.125	1.425	0.087719	0.133806
C2	0.148	0.975	0.151795	
C3	0.221	1.365	0.161905	
2600 - 1	0.006	1.54	0.003896	0.007843
2600 - 2	0	1.214	0	
2600 - 3	0.029	1.477	0.019634	
277 - 1	0.376	5.263	0.071442	0.053436
277 - 2	0.014	2.132	0.006567	
277 - 3	0.252	3.062	0.082299	

Table 5.6 Raw data depicting transfection in primary rat hepatic stellate cells at day 0-2 (quiescent) and in the same cells when 70% confluent at day 10-12 (activated). B – negative control "Mock", C – positive control, 2600 – full human TIMP-2 promoter, 276 – human TIMP-2 short promoter. Each plasmid was co-transfected with a control vector (pRL-SV40) and results were expressed as plasmid divided by co-transfected plasmid. Results were then averaged for three wells and normalized to the negative control.

Table 5.7 Transfection into Quiescent and Activated rat Hepatic Stellate Cells

	Quiescent	**Activated**
	Value/Mean of B	Value/Mean of B
B Negative control	1	1
C +ve control	2.193258	7.055024
2600 full promoter	3.228205	0.413554
277 short promoter	0.938503	2.817446

Table 5.7 In this single experiment this table depicts data from previous table (Table 5.6) normalized with reference to the negative control.

Table 5.8 Mean of 5 experiments with data normalized to negative controls

	Quiescent	SEM	**Activated**	SEM
Negative control "Mock"	1		1	
SV40	2.359916	0.62418	113.7591	72.58506
2600	1.964803	0.385353	0.609666	0.270893
276	0.329461	0.176769	6.567827	2.620291

Table 5.8 Depicts the mean of data from 5 different experiments with data normalized to the negative control

In each of the 5 experiments the protocol was identical: transfections were carried out in primary rat hepatic stellate cells at day 0-2 (quiescent) and in the same cells when 70% confluent at day 10-12 (activated).

B – negative control "Mock"
C – positive control
2600 – full human TIMP-2 promoter
276 – human TIMP-2 short promoter

Each plasmid was co-transfected with a control vector (pRL-SV40) and results were expressed as plasmid divided by co-transfected plasmid. Results were then averaged for three wells and normalized to the negative control. Data from 5 experiments was pooled and a mean taken. SEM – standard error of the mean.

Figure 5.29 Transfection of hTIMP-2 into quiescent and activated rat HSC

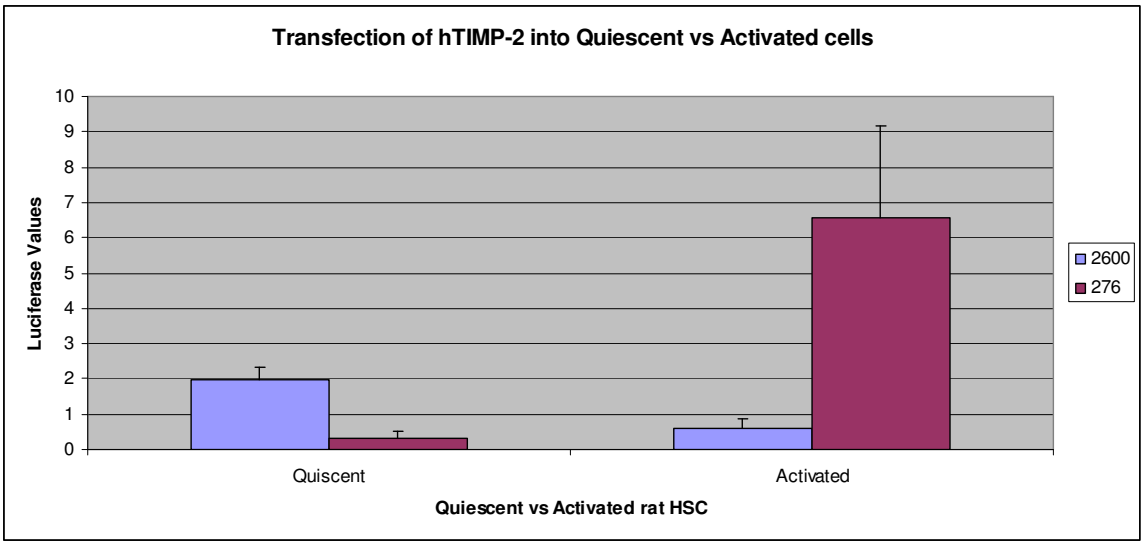

Figure 5.29 Excel spread sheet chart depicting the mean of 5 experiments for the pGL3 hTIMP-2 2600 full promoter versus the hTIMP-2 276 short/truncated promoter transfected into primary rat hepatic stellate cells at day 0-2 (quiescent) and in the same cells when 70% confluent at day 10-12 (activated).

B – pGL3 Basic "Mock" or negative control
C – pGL3 SV40 +ve / positive control
2600 – pGL3 human TIMP-2 2600 full promoter
276 – pGL3 human TIMP-2 276 short promoter.

Each plasmid was co-transfected with a control vector (pRL-SV40) and results were expressed as plasmid divided by co-transfected plasmid. Results were then averaged for three wells and normalized with the negative control.

Table 5.9 Statistical analysis (paired Student's t test) of data presented in Figure 5.29

Parameter	Quiescent	Activated	Difference
Mean	1.147	3.589	-2.442
# of points	2	2	2
Std Deviation	1.156	4.213	5.369
Std Error	0.8177	2.979	3.797
Minimum	0.3295	0.6097	-6.238
Maximum	1.965	6.568	1.355
Median	1.147	3.589	-2.442
Lower 95% CI	-9.242	-34.263	-50.683
Upper 95% CI	11.536	41.441	45.800

Table 5.9: The data shown in figure 5.29 was subjected to statistical analysis with a Student's paired t test. The two-tailed P value is 0.6362 which is not considered significant. T=0.6431 with 1 degrees of freedom. For a 95% confidence interval the Mean difference = -2.442 (Mean of paired differences) and the 95% confidence interval (CI) of the difference is: -50.683 to 45.800

5.7.11 Chapter Discussion

In this chapter the transfection of the human TIMP-2 short and full promoters obtained from Professor Yves DeClerk was examined in hepatic stellate cells. Initial work was unsuccessful and therefore the promoters were sub cloned into a new vector that may have been more suitable to the low activity of these promoters. Despite successful subcloning and sequencing the promoters I was unfortunately unable to obtain any activity with the pBLCAT hTIMP-2 promoters. On returning to the original vectors and incorporating new transfection protocols from the manufacturer (Promega) low grade activity was noted in both quiescent and activated rat HSC. Dual transfections were performed in each case with a Renilla construct linked to a SV40 promoter in pGL3-basic (Promega). Each transfection was carried out in triplicate wells with the cells harvested at 48hrs. At time 0 activity was noted with the TIMP-2 promoter (especially the full promoter) in comparison to the short promoter. In activated cells TIMP-2 activity was again noted but in this situation the short promoter was more active.

Differences in the expression of the hTIMP-2 short and full promoters may be attributable to the spatial distribution of the AP-1, PEA-3 and SP-1 motifs within each promoter construct.

CHAPTER 6

DISCUSSION

6.1 General Discussion

This work was undertaken to focus on the role of TIMP-2 in liver and pancreatic injury. The work itself was commenced in September 1997 and finished end June 2000 – around 2 years and 10 months were taken in learning techniques and carrying out the experimental work.

In the introduction I reviewed the role of the hepatic stellate cell in the liver injury process. Fibrosis and cirrhosis of the liver form a continuum of the injury process where fibrosis can be reversed and in the classical view of cirrhosis an irreversible state exists. Recent data from the liver group in Southampton challenge this view.

In liver cirrhosis there is a 3-6 fold rise in collagens type I, III and IV. This is especially seen in the space of Disse where the basement membrane components are increased and partially replaced by fibrillar collagens.

The cell central to this process is the hepatic stellate cell (HSC) located in the space of Disse. HSC in the face of liver injury undergo a change from a quiescent state of the myofibroblast like phenotype in the response to all forms of liver injury. This is characterised by phenotypic changes such as loss of vitamin A and expression of alpha SMA, proliferation and increased synthesis of collagens and other ECM proteins, release of matrix metalloproteinases and their inhibitors the so called tissue inhibitors of metalol proteinases (TIMPs).

ECM accumulation which is seen in liver injury and pancreatic injury can either be caused by excess production or decreased degradation. MMPs are responsible for ECM however. Gelatinase A (MMP-2) is capable of degrading the normal subendothelials matrix as well as fibrillar collagens. MMP-2 is activated in association with MT1-MMP and TIMP-2. Examination of TIMP2 therefore is crucial to the understainding of MMP-2 function and therefore of ECM production and turnover.

In the pancreas the corresponding cell type was the pancreatic stellate cell (PSC). In a sense whilst this was only recently described when I began my work on the thesis much of the protein expression of this cell type was not described but there was a strong belief in early work that it too had a pivotal role in ECM production and turnover both in health and fibrotic pancreatic injury..

6.2 Key Findings

Chapters I and II outline the introduction and the methods incoporated in this thesis.

6.2.1 Summary of Chapter 3

In chapter III work was undertaken to examine the expression of TIMP-1, TIMP-2, αSMA, Gelatinase-A (MMP-2) and MT1-MMP (MMP-14) both in liver and pancreatic injury using immunohistochemical techniques in archived human specimens of normal and injured liver and similarly in pancreas. 3 cases of normal human liver and 6 cases of diseased human liver were incorporated; for pancreas 6 normal archived specimens were used in addition to 6 specimens of fibrotic tissue. TIMP-1 and TIMP-2 expression was noted to be increased in liver and pancreatic injury. αSMA was noted to be slightly positive in normal liver which was unexpected and possibly may have been secondary to a liver disease process which was not documented or appreciated by the clinicians. Whilst not shown, MT1-MMP (MMP-14) expression was noted in only one or two cases with a general background in human liver and pancreas. Gel-A (MMP-2) was noted to be only weakly positive in normal liver and pancreas but strongly positive in fibrotic liver injury and fibrotic pancreas confined to fibrotic bands. In normal liver TIMP-2 was noted to be present for example in some hepatocytes and in some blood vessels with a subtle increase in background. There was however increased expression in the sinusoidal and perisinusoidal areas in fibrotic liver. In fibrotic pancreas there was some increased expression of TIMP-2 staining in pancreas injury in the periacinar stroma and fibrotic bands with marked staining in 4 out of 6 cases in the Islets (a finding that was also noted in normal pancreas specimens). In conclusion Gelatinase A (MMP-2), MT1-MMP (MMP-14), TIMP-1 and TIMP-2 are expressed in vivo in chronic pancreatitis as well as in liver injury and their expression appears to be localised to alpha SMA positive cells in pancreas as well as liver injury. The inference here is that pancreatic stellate cells in a similar fashion to hepatic stellate cells are able to regulate matrix degradation in addition to synthesis. The expression of TIMPs suggests that matrix degradation may be inhibited during chronic pancreatitis. It is possible that the PSC phenotype is similar to other “wound healing myofibroblasts” notably Hepatic stellate cells and Renal Mesangial cells.

6.2.2 Summary of Chapter 4

6.2.2.1 Hypoxia

In chapter IV the role of hypoxia was examined with regard to TIMP-2 expression in rat hepatic stellate cells. In the first instance fresh and passaged rat hepatic stellate cells were incorporated to examine and troubleshoot the hypoxic protocol. (Pancreatic stellate cell culture in hypoxic conditions was not examined). Early work in this area was unsuccessful but this may be due to the early logistical problems experienced in transferring cells to London. A nominal increase in the 3.8kb TIMP-2 subspecies was noted in comparison to the 1.2kb subspecies but this was not considered significant. The experiment did however confirm that TIMP-2 expression continues under hypoxic conditions. It is possible that by incorporating passaged cells instead of freshly isolated cells that any early subtle early rise of TIMP-2 in early activation was missed. Freshly isolated rat HSC was attempted but on two occasions unfortunately rapidly became infected with fungus during the transfer. If this experiement were to be repeated simple ways to circumvent the logistical issues that were faced would be to spend some time up in the London unit – harvest fresh rat HSC there – and perform the experiment both for primary rat (and were it to be freely available) fresh human HSC for culture. Shorter time frames in primary culture would also be appealing to study though for timepoints such as 4, 6, 8 and 12hrs would necessitate probably whole animal liver resections. The objectives therefore in chapter 3 in terms of carrying out work in both rat pancreatic tissue and human normal and fibrotic liver and pancreatic tissue were never met.

6.2.2.2 Expression of MMP and TIMP protein in activated PSC

In vitro work was undertaken to examine mRNA expression in rat PSC of αSMA, gelatinase-A (MMP-2), procollagen-I, TIMP-2 and TIMP-1. This had not been previously reported. PSC activation on uncoated tissue plastic appears to be behaving in a similar fashion to rat hepatic stellate cells (HSC) and rat renal mesangial cells. TIMP-1 & TIMP-2 mRNA are clearly expressed in pancreatic islet cells and therefore TIMP-1 and TIMP-2 may play a role in cell survival**.** Gelatinase-A (MMP02) may play a pivotal role in matrix degradation. Whilst it degrades Collagen type IV and partially degrades Collagens type I, III and V it is itself inhibited by TIMP-1 and TIMP-2. TIMP-2 as has been highlighted earlier plays a role in Gelatinase-A activity by linking in with pro-gelatinase A and with membrane type Matrix

Metalloproteinase I (MT1-MMP/MMP-14). Whilst chapter three examined the in vivo expression of alpha SMA, Gelatinase-A (MMP-2), MT1-MMP (MMP-14), TIMP-1 and TIMP-2 in human pancreas and chapter 4 the in vitro expression of αSMA, procollagen-I, Gelatinase-A, MT1-MMP, TIMP-1 and TIMP-2 there is an argument that PSCs are indeed able to regulate matrix degradation in addition to synthesis and that the expression of TIMPs suggest that matrix degradation may be inhibited during chronic pancreatitis.

6.2.2.3 Examination of TIMP-2 expression in whole human liver

In a study of human fibrotic livers (x5) compared to 3 normal controls TIMP-2 mRNA expression was examined in a ribonuclease protection assay (RPA) analysis. The results of this demonstrate that human TIMP-2 mRNA is upregulated in fibrotic liver in comparison to normal liver. This is a finding in contrast to the expected result where TIMP-2 has traditionally been conceived as constitutively expressed in a variety of cell systems. Recent research in a liver fibrosis model in rats has demonstrated an increase in TIMP-1 and TIMP-2 mRNA and protein rise over a time course of 8 weeks of injection with a fibrotic agent (520).

6.2.3 Summary of results in Chapter 5

Chapter V examined the role of TIMP-2 expression at the promoter level. Early work highlighted some technical problems with my transfection protocols which led to the promoter being sub cloned into a new plasmid vector. CAT 3 transfections however were also unsuccessful therefore I returned to the original constructs and incorporated a new protocol from Promega which yielded low grade promoter activity in quiescent and activated HSC.

6.3 Conclusions and Overall Discussion

Immunostaining of pancreas has highlighted that TIMP-1 and TIMP-2 are expressed in PSC and upregulated in tissue injury. The *in vivo* work of liver and pancreas immunostaining suggests that TIMP-2 may be upregulated during liver and pancreatic injury. In vitro work examining the expression of TIMP-2 in normal versus fibrotic human liver also suggests that TIMP-2 is upregulated which is contrary to the traditional view that TIMP-2 is a constitutively expressed protein in both normal and diseased systems when examined in liver, pancreas or renal injury. In conclusion this thesis was undertaken to examine the role of TIMP-2 in liver and pancreatic injury.

More questions arise from this work than have been answered. Further work could be undertaken examining the role of TIMP-2 in the following areas:

1) Knockout mice with an absent TIMP-2 gene
2) CCL4 rat model of liver injury and recovery
3) DNA footprinting of the promoters that I obtained from Professor Yves DeClerck

There is emerging work examining the role clinical pharmaceutical agents modifying the fibrotic process and I have no doubt that the agents and their interaction with TIMP-2 require further elucidation.

My aims in this thesis were the following:

a) Determine the key sequences of the TIMP-2 gene promoter which regulate TIMP-2 expression during hepatic stellate cell (HSC) activation and pancreatic stellate cell (PSC) activation. Whilst this was examined I conclude that I was unsuccessful in this regard. Further work on the gene promoter may elucidate this for example with DNA footprinting incorporating the short and long constructs that I obtained from Profession Yves De Clerk.

b) Determine at what level the enhanced expression of TIMP-2 mRNA observed in activated HSC and activated PSC is regulated using Nuclear Run On assays (studies of mRNA production). Again, I was unsuccessful in this regard as I was unable to show consistent successful nuclear run on assays during the nine months that I studied this experimental modality.

c) Perform studies of the TIMP-2 promoter activity in HSC and PSC in collaborative work with Dr Yves De Clerk. There is no doubt that this was carried out in the laboratory however there was clear evidence that in the transfection systems that I worked in – the TIMP-2 promoter was weak in most cases which did not allow accurate qualitative or quantitative measurements of the human TIMP-2 promoter activity in cells systems to be measured accurately.

APPENDIX I

GENERAL REAGENTS

Sterilization

All sterilization of equipment such as that used to harvest hepatic stellate cells, homogenize tissue, culture prokaryotic and eukaryotic cells and solutions such as culture media and other non-heat labile buffers was undertaken by autoclaving for 15 minutes at 121^0C. Sterilization of heat labile solutions was performed by filtration using a 0.22µm Millipore microfilter in a sterile hood.

Water

The water used for dilution of general reagents for non sterile work was obtained from a centrally operating distillation facility with reverse osmosis. Where sterility was necessary or nuclease free/high purity conditions required then bottled ultra pure water was used. For RNase free work water was initially treated with DEPC.

Chemicals

All chemicals were obtained from SIGMA unless otherwise stated.

General Solutions and Buffers

DEPC water

1 litre of DI water

Diethyl pyrocarbonate DEPC 1ml

The bottle was sealed and shaken vigorously then left overnight to allow inactivation of RNases prior to autoclaving for 2 hours to inactivate the DEPC.

GENERAL BUFFERS
All buffers were made up to volume with distilled water unless otherwise stated.

TE (Tris EDTA)

Tris Base	10mM
EDTA	1mM

HCl was used to adjust the pH to 8.0

TBE 5x (Tris Boric Acid EDTA) Electrophoresis Buffer

Tris Base	54g
Boric Acid	27.5g
EDTA 0.5M (pH 8.0)	

The volume was made up to 1 litre with DI H_2O

TAE 50x (Tris Acetate EDTA) Electrophoresis Buffer

Tris-acetate	2M
EDTA (pH 8.0)	0.1M

Gel loading buffer 6x

Ficol 400	1.8g
EDTA 0.5M pH 8.0	1.2ml
Xylene Cyanol	0.002g
Orange G	0.002g
Bromo Phenol Blue	0.002g

The volume was made up to 10ml using distilled and filter-sterilized water

Phenol/Chloroform

Phenol	50%
Chloroform	49%
Isoamyl alcohol	1%

Chloroform/isoamyl alcohol

Chloroform	96%
Isoamyl alcohol	4%

Gel extraction buffer

Ammonium Buffer	0.5M
EDTA	1mM

Volumes were adjusted with distilled water and the pH changed to pH 8.0 with acetic acid.

BACTERIAL CULTURE

Throughout the majority of this work plasmids were used which contained a gene conferring resistance to antibacterial substances. The most common gene was the *amp*^{r} gene, encoding the enzyme β-lactamase, which degrades penicillin antibiotics such as ampicillin. Ampicillin was therefore used as a method of bacterial selection. The ampicillin stock was made at a concentration of 50mg/ml in distilled water before filter sterilization. The stock was stored in aliquots at -20^0C and added to re-sterilized culture media where specified at 50μg/ml. Repeated freeze thawing of ampicillin aliquots was avoided.

Lauria Bertani (LB) medium (1 litre)

Tryptone	10.0g
Bacto Yeast	5.0g
NaCl	10.0g

The pH was adjusted to pH 7.0 with 5M NaOH (0.2mls); 1.5% w/v agar was added before autoclaving for culture plates (LB Agar).

Terrific Medium ('Terrific Broth') 200ml

Tryptone	27g
Yeast Extract	5.3g
Glycerol	0.9

The volume was adjusted with distilled water; the broth autoclaved to sterilize.

Phosphate buffer

KH_2PO_4	0.17M
K_2HPO_4	0.72M

Volumes were made up with distilled water, autoclave sterilize add 3ml to each 27ml terrific medium culture just prior to inoculation.

PRODUCTION OF COMPETENT DH5α E COLI

RF1

RbCl	100mM
$MnCl_2.4H_2O$	50mM
Potassium acetate	30mM
$CaCl_2.2H_2O$	10mM
Glycerol	15% w/v

The pH was adjusted to pH 6.8, made up to volume with distilled H_2O and filter sterilized.

RF2

MOPS	10mM
RbCl	10mM
$CaCl_2.2H_2O$	75mM
Glycerol	15% w/v

NaOH was used to adjust the pH to pH 5.8; the volume made up with distilled H_2O and filter sterilized.

PLASMID PURIFICATION

Alkaline lysis

Solution 1 (TGE)

Tris Base	25mM
EDTA	10mM
Glucose	50mM

Solution 2 (Lysis buffer)

SDS	1% w/v
NaOH	0.2M

Solution 3 (Neutralizing buffer)

Potassium acetate	3M
Glacial Acetic Acid	5M

DNA Sequencing

DNA denaturing buffer

NaOH	200mM
EDTA (pH 8.0)	200mM

Acrylamide Gel (Sequencing denaturing)

Acrylamide	8% w/v
Urea	7M
TBE	x1
Ammonium Persulphate (APS)	0.008% w/v
TEMED	0.16% v/v

Formamide loading buffer

Formamide	95%v/v
EDTA	20mM
Bromophenol Blue	0.05% w/v
Xylene Cyanol FF	0.05% w/v

Gel fixative

Methanol	10% v/v
Glacial Acetic Acid	10% v/v

Eukaryotic cell culture

Hank's Buffered Saline Solution (HBSS), (with or without Ca^{2+})

Obtained as a 10x stock (Gibco)

HBSS 10x	**100ml**
Sodium bicarbonate (7.5%)	4.6ml
HEPES (1M)	5ml

Made up to 1 litre with sterile water.

Dulbecco's Modified Eagle Medium (DMEM)

Obtained as 10x stock (Gibco)

DMEM 10x	500ml
Glutamine (200mM)	50ml
Sodium Bicarbonate (7.5%)	250ml

pH adjusted to pH 7.1 with HCL

Volume made up to 5L with sterile water and filter sterilized

Serum and Antibiotics

Fetal Calf Serum (FCS) used at 16%

Penicillin and Streptomycin used at 500u/ml

Phospate Buffered Saline

Obtained in tablet form (Sigma)

Made up to volume in distilled H_2O

Nuclear Extraction

Dignam A (Plasma membrane lysis buffer)

HEPES	10mM
$MgCl_2$	1.5mM
KCl	10mM
Dithiothreitol (DTT)	0.5mM
PMSF	0.5mM
Tergitol NP40	0.2% v/v

Dignam C (Nuclear membrane lysis buffer)

HEPES	20mM
Glycerol	25% v/v
NaCl	0.42M
$MgCl_2$	1.5mM
Dithiothreitol (DTT)	0.5mM
EDTA	0.2mM
PMSF	0.5mM

Whole cell extraction buffer

HEPES	10mM
$MgCl_2$	1.5mM
KCl	10mM
Dithiothreitol (DTT)	0.5mM
PMSF	0.5mM

Added to Dignam A/C and whole cell extraction buffers

Na_3VO_4	1mM
NaF	1mM
AEBSF	1mM
Aprotinin	2µg/ml

SDS PAGE and Western Blotting

SDS PAGE sample buffer

Tris 0.5M pH6.8	12.5% v/v
Glycerol	10% v/v
Sodium Lauryl Sulphate (SDS)	2% w/v
Bromo Phenol Blue	0.004% w/v
Dithiothreitol (DTT)	10mM

Volume adjusted with distilled water

SDS PAGE 5x Electrophoresis buffer

Tris Base	124mM
Glycine	1M
SDS	0.5% w/v

Volume adjusted with distilled water, the pH (pH 8.3) was not altered.

SDS PAGE 4% Stacking Gel

Tris 0.5M pH6.8	25% v/v
SDS	0.1% w/v
Acrylamide-Bis 37.1	4.0% w/v
APS	0.1% w/v
TEMED	0.1% v/v

SDS PAGE Running Gel 7.5%

Tris 0.5M pH 8.8	25% v/v
SDS	0.1% w/v
Acrylamide-Bis 37.1	7.5% w/v
APS	0.055 w/v
TEMED	0.1% v/v

Transfer Buffer (Western)

Tris Base	25mM
Glycine	192mM
Methanol (BDH)	20% v/v

Volume adjusted with distilled water, the pH (pH 8.3) was not altered.

Tris Buffer Saline (TBS) x20

NaCl	4M
Tris	0.4mM

The volume was made up with with distilled water and the pH adjusted to pH 7.4 HCL

Ethidium bromide 1mg/ml

Liver Homogenising buffer:

50nM	Tris HCl pH7.6
0.25%	Triton X-100
0.15M	NaCl
10mM	$CaCl_2$
0.1mM	Phenylmethylsulfonylfluoride
10µM	Leupeptin
10µM	Pepstatin A
0.1mM	Iodoacetamide
25µg/ml	Apoptonin

10x MOPS:

0.2M Morpholino propanosulfonic acid

50mM sodium acetate

10mM EDTA

0.1% DEPC adjusted to pH 7 using NaOH and autoclaved.

Trypan blue 0.05% trypan blue

ERASE-A-BASE SOLUTIONS

7.5M Ammonium acetate 100ml

57.81 ammonium acetate

Dissolve the ammonium acetate in 100ml nuclease-free water (final volume). Sterilize by filtration (0.2µm filter).

dNTP mix

0.125mM each of dATP, dCTP, dGTP and dTTP

Exo III 10x buffer

660mM Tris-HCl (pH 8.0)

6.6mM $MgCl_2$

Klenow mix

30µl Klenow 1x Buffer

3-5µl Klenow DNA polymerase

(Made fresh for each experiment).

Klenow 1x Buffer

20mM Tris-HCl (pH 8.0)

100mM $MgCl_2$

Luria Bertani (LB) medium (per litre)

10g Bacto®-tryptone

5g Bacto®-tryptone

5g NaCl

2.10.2.5 LB plates with ampicillin (per litre)

15g was added to 1 litre of LB medium and adjusted to pH 7.0 with NaOH prior to autoclaving. After the medium was allowed to cool to 55^0C, ampicillin was added (100mg/ml final concentration). 30-35ml of medium was then poured into 90mm petri dishes and where necessary, the surfaces were flamed with a Bunsen burner to eliminate bubbles. When the agar hardened it was stored at room temperature (for 1 week) or at 4^0C (for one month).

Ligase mix
790µl deionized water

100µl Ligase 10x Buffer

100µl 50% PEG

10µl 100mM DTT

5µl T4 DNA Ligase

Ligase 10x Buffer
500mM Tris-HCl (pH 7.6)

100mM $MgCl_2$

10mM ATP

2M NaCl

116.9g NaCl

Nuclease-free water was added to a final volume of 1 litre and sterilized by autoclaving.

S1 nuclease mix (for 25 time points)

172µl deionized water

27µl S1 7.4x Buffer

60u S1 nuclease

This was made fresh for each experiment.

S1 Nuclease Stop Buffer

0.3M Tris base

0.05M EDTA

S1 7.4x Buffer

0.3M potassium acetate (pH 4.6)

2.25M NaCl

16.9mM $ZnSO_4$

45% glycerol

SOC medium (per litre)

10g Bacto®-tryptone

5g Bacto®-tryptone

5g NaCl

10mM $MgSO_4$

10mM $MgCl_2$

This was adjusted to pH 7.0 with NaOH; autoclaved then had filter sterilized glucose added to a final concentration of 20mM.

2M sodium acetate (pH 4.0)

Glacial acetic acid was diluted to 2M and adjusted to a pH of 4.0 with NaOH.

3M sodium acetate (pH 5.2)

40.8g sodium acetate.$3H_20$

Sodium acetate was dissolved in 80ml of water, adjusted to a pH of 5.2 with glacial acetic acid and then water was added to a final volume of 100ml.

TE buffer

10mM Tris-HCl (pH 8.0)

1mM EDTA

TE-saturated phenol:chloroform:isoamyl alcohol (25:24:1)

Equal parts of TE buffer and phenol were mixed and the phases allowed to separate. 1 part chloroform:isoamyl alcohol (24:1) was added to 1 part lower phenol phase.

APPENDIX II

P R O C E D U R E S R U N O N T R A N S C R I P T I O N

Day 1 Prehybridisation

1. Defrost hybridisation buffer

2. Prepare hybridisation tube / hybridisation seal-bag (RNase free) with 0.5M NaOH at 45^0C

3. Wash with DEPC'd H_2O.
   Add 1x 25ml aliquot of prehybridisation buffer.

4. Wash filter / membrane with 1x SSC / 0.1% SDS

   5mls 20xSSC /0.1g SDS / 100mls DEPC'd H_20

5. Place filter in just-off-the-boil water for 1 minute
   Then plunge into ice cooled H_2O until use.

6. Prehybridise one nitrocellulose membrane overnight.

   Ensure rotisserie is on and turning

R U N O N T R A N S C R I P T I O N

Day 2 Run on transcription

PREPARATION:

Make up 5mls **Transcription Buffer**: (on ice)
Make up 10mls **Proteinase K Buffer:** (on ice)

Set up sterile screw-top/double top eppendorfs

Defrost: Intact nuclei
Acetylated BSA (-20^{0}C freezer)
Hybridisation buffer
^{32}P UTP behind screen
Nucleotides: ATP, CTP, GTP

Water bath Initially 25^{0}C for steps 1 & 2 followed by 37^{0}C

Transcription buffer: (keep on ice)

	Stock	for 5msl
50mM Hepes pH 8.0	1M	250µl
2mM MgCl2	1M	10µl
2mM MnCl2	0.5M	20µl
300mM NH_4Cl	1M	1.5ml
1µl/ml acetylated BSA	1mg/ml	5µl
Sterile H_2O		3.215mls

Proteinase K Buffer (keep on ice)

	Stock	for 10mls
10mM Tris pH 7.5	1M	100µl
100mM NaCl	4M	250µl
2mM KCL	4M	5µl
1mM EDTA	0.5M	20µl
0.5% SDS	10%	500µl
Sterile H_20	RNase free	9.125mls

Day 2 continued

R U N O N T R A N S C R I P T I O N

1. **100µl Transcription Buffer**

   50µl Nuclei (2.5×10^6 dilute with nuclei storage buffer)

   2µl RNAse inhibitor placental ribonuclease inhibitor
   (Pharmacia 39,300 u/ml / Sigma 40,000 u/ml)

   5µl ATP/GTP/CTP mix each at 10mM ⇒ 0.4mM each)
   - purchase as 100mM individual stocks

   5µl [α- ^{32}P] UTP 100µCi (800Ci/mmol ⇒ 1µM)

2. Incubate at
   25^{0}C in waterbath for 20 minutes after starting reaction with [α-^{32}P] UTP
   5µl cold UTP 100µCi (800Ci/mmol ⇒ 1µM)
   Incubate at 37^{0}C for 40 minutes.

R N A I S O L A T I O N

Chill: Absolute ethanol (freezer)
75% ethanol (freezer)
TE
Phenol / Chloroform
Pre cool cetrifuge to: -8^{0}C / -9^{0}C

3. Add:
   500µl phenol / chloroform
   50µl 2M Sodium Acetate
   Leave on ice for 15 mins.
   Centrifuge at 14000 rpm at 4^{0}C for 5 minutes.

4. Remove & keep the upper aqueous phase (contains RNA).

   Re-extract phenol/chloroform by adding:
   200µl TE buffer pH 8.0)

   Centrifuge at 14000 rpm at -8^{0}C / -9^{0}C for 5 minutes
   and keep the upper aqueous phase as above.

   (Discard radioactive material/phenol in solid radioactive bin).

5. Pool the two aqueous extracts and add:

   1 x Vol Isopropanol
   Chill at -70^{0}C for 90 mins
   Centrifuge at 14000rpm for 20 minutes at -8^{0}C / -9^{0}C.

8. Discard the supernatant (radioactive) into the sink
   (NB: the pellet may not be visible at this time)
   1/20 vol 3M NaOAc
   3 x Vol 100% Ethanol
   Chill at -70^{0}C for 90 mins
   Centrifuge at 14000rpm for 20 minutes at -8^{0}C / -9^{0}C.
   Discard the supernatant (radioactive) into the sink

9. Dissolve pellet in:
   100µl DEPC water Perform the Incorporation Test at this stage
   Pass through a Sephadex G50 spin column to get rid of residual nucleotides and very short RNA frags (this last bit is important for reducing backgrounds).

   Take 2.5-5 ml of the spin through and count in a scintillation counter. You should get somehwere between 1-5 x 106 cpm for each reaction (quiescent serum-starved cells are always less, so I often do 2 separate reactions and pool them at the end).

10. Add constant radiolabelled RNA - ideally 1-10 x 10^6 dpm - to 1ml hybridisation buffer and hybridise at 42^{0}C for 72 hours.
    Keep the vols low to incerase hybridization. Everyday or so manualy squish the contents of the bags around to mix things up even more.

    Ensure rotisserie is on and turning

-o-o-o-o-o-o-

Keep the vols low to incerase hybridization. evryday or so i would manualy squish the contents of the bags around to mix things up even more.

11. Day 5/6
    Wash filters 4 x 5 minutes of **1xSSC/0.1%SDS**
    2 x 15 minutes of **0.2x SSC/0.1% SDS 65^{0}C**

12. Expose filters to autoradiography

I N C O R P O R A T I O N T E S T

1. Take known volume of labelled RNA eg 2µl and add to 200ml 0.2M EDTA

2. Spot known volume on to 2 Whatman DE81 filter paper discs

   A = total

   B = incorporated: Wash 4x for 5minutes each

   With Na2HPO4 (100-200mls)

   Wash 2x for 1 minute H_2O

   Wash 2x for 1 minute 95% ethanol (100mls)

   Dry papers before counting

   Add 10mls scintillant

   Use a control (1 filter with nothing added)i

P R E P A R A T I O N O F N I T R O C E L L U L O S E

1. Denature DNA probe at 95^0C for five minutes after adding 0.25pmoles of probe in 100µl of 0.1M NaOH.

2. Add 2 volumes of 2M Na acetate, mix and apply 0.25pmoles/slot using manifold.

3. Wash with with 6xSSC (from a 20x SSC stock solution)

4. Mark the filters to identify the orientation: cutting the top left hand corner.

5. Bake filters for 2 hours at 80^0C and store well for use (nuclear run on studies) - in fridge.

6. Wash filters with 1x SSC / 0.1% SDS

   (5mls 20xSSC /0.1g SDS / 100mls DEPC'd H_20)

7. Place filter in just off the boil water for 1 minute
   then plunge into ice cooled H_2O until use.

S O L U T I O N S

2M Na Acetate
82.03g in 500ml sterile H_2O and autoclaved

1x SSC / 0.1% SDS
5mls 20xSSC /0.1g SDS
100mls DEPC'd H_20

0.2x SSC / 0.1% SDS
1ml 20xSSC / 0.1g SDS
100mls DEPC'd H_20

0.1M NaOH
2.0g NaOH in 250ml sterile water, then autoclave

20x SSC
175.3g NaCl
88.2g Na Citrate
1 litre of distilled sterile H_2O
pH adjust to pH 7.0 with HCl
Add 1 ml of DEPC
Leave overnight and then autoclave

TE buffer	**for 10mls**
10mM Tris (pH 8.0)	121mg
1mM EDTA	29.2mg
(free acid)	

Pre-hybridisation Solution For 200mls

55% Formamide	110mls	Stock
4x SSC	40mls	20x SSC Stock
0.1M NaH_2PO_4 pH7	20mls	1M Stock
5x Denhardts	20mls	50x Stock
0.1% SDS	2mls	10% Stock
100µg/ml Salmon Sperm DNA	4mls	5mg/ml boiled before use
H_2O	6mls	

Hybridisation Solution	for 10mls	
55% Formamide	5mls	Stock
4x SSC	2mls	20x SSC Stock
0.1M NaH_2PO_4 pH7	1ml	1M Stock
1x Denhardts	400µls	50x Stock
0.1% SDS	100µls	10% Stock
10µg/ml Salmon Sperm DNA	20µls	5mg/ml boiled before use
H_2O	1ml	Sterile

0.5M NH_4Cl
10.7g in 200mls DEPC'd H_2O
Autoclave

1M Tris
1.211g in 10mls DEPC'd H_2O

4M NaCl
2.338g in 10ml DEPC'd H_2O
Autoclave

4M KCl
2.982g in 10ml DEPC'd H_2O
Autoclave

0.5 M EDTA
1.861g in 10ml DEPC'd H_2O
Autoclave

0.2 M EDTA
0.744g in 10ml o DEPC'd H_2O
Autoclave

0.5M Na_2HPO_4
30g in 0.5litres of DEPC'd H_2O
Autoclave

REFERENCES

(1) McCrudden R, Iredale JP. Liver fibrosis, the hepatic stellate cell and tissue inhibitors of metalloproteinases. *Histol Histopathol* 2000;15(4):1159-68.

(2) Bateman AC, Turner SM, Thomas KS *et al*. Apoptosis and proliferation of acinar and islet cells in chronic pancreatitis: evidence for differential cell loss mediating preservation of islet function. *Gut* 2002;50(4):542-8.

(3) Shek FW, Benyon RC, Walker FM *et al*. Expression of transforming growth factor-beta 1 by pancreatic stellate cells and its implications for matrix secretion and turnover in chronic pancreatitis. *Am J Pathol* 2002;160(5):1787-98.

(4) Henderson NC, Iredale JP. Liver fibrosis: cellular mechanisms of progression and resolution. *Clin Sci (Lond)* 2007;112(5):265-80.

(5) Ramachandran P, Iredale JP. Reversibility of liver fibrosis. *Ann Hepatol* 2009;8(4):283-91.

(6) Brenner DA. Molecular pathogenesis of liver fibrosis. *Trans Am Clin Climatol Assoc* 2009;120:361-8.

(7) Alter MJ, Kruszon-Moran D, Nainan OV *et al*. The prevalence of hepatitis C virus infection in the United States, 1988 through 1994. *N Engl J Med* 1999;341(8):556-62.

(8) Draganov P, Toskes PP. Chronic pancreatitis: controversies in etiology, diagnosis and treatment. *Rev Esp Enferm Dig* 2004;96(9):649-54.

(9) Leon DA, McCambridge J. Liver cirrhosis mortality rates in Britain from 1950 to 2002: an analysis of routine data. *Lancet* 2006;367(9504):52-6.

(10) Geerts A. On the origin of stellate cells: mesodermal, endodermal or neuro-ectodermal? *J Hepatol* 2004;40(2):331-4.

(11) Rappaport AM. The microcirulatory hepatic unit. *Microvasc Res* 1973;6:212-28.

(12) Le Bouton AV. Relations and extent of the zone of intensified protein metabolism in the liver acinus. *Curr Mod Biol* 1969;3:4-8.

(13) Bouwens L, Baekeland M, Zanger R *et al*. Quantitation, tissue distribution and proliferation kinetics of Kupffer cells in normal rat liver. *Hepatology* 1986;6:718-22.

(14) Burt AD, Griffiths MR, Schuppan D *et al*. Ultrastructural localization of extracellular matrix proteins in liver biopsies using ultracryomicrotomy and immuno-gold labelling. *Histopathology* 1990;16:53-8.

(15) Reid LM, Fiorino AS, Sigal SH *et al*. Extracellular matrix gradients in the space of Disse: relevance to liver biology (editorial). *Hepatology* 1992;15:1198-203.

(16) Hahn EG, Wick G, Pencev D *et al*. Distribution of basement membrane proteins in normal and fibrotic human liver: collagen type IV laminin and fibronectin. *Gut* 1980;21:63-71.

(17) Martinez-Hernandez A, Delgado FM, Amenta PS. The extracellular matrix in hepatic regeneration. *Lab Invest* 1991;64:157-66.

(18) Maher JJ, Friedman SL, Roll FJ *et al*. Immunolocalization of laminin in normal rat liver and biosynthesis of laminin by hepatic lipocytes in primary culture. *Gastroenterology* 1988;94(4):1053-62.

(19) Arenson DM, Friedman SL, Bissell DM. Formation of extracellular matrix in normal rat liver: lipocytes as a major source of proteoglycan. *Gastroenterology* 1988;95(2):441-7.

(20) Lefebvre V, Peeters-Joris C, Vaes G. Production of gelatin-degrading matrix metalloproteinases ('type IV collagenases') and inhibitors by articular chondrocytes during their dedifferentiation by serial subcultures and under stimulation by interleukin-1 and tumor necrosis factor alpha. *Biochim Biophys Acta* 1991;1094:8-18.

(21) Fortunato G, Castaldo G, Oriani G *et al*. Multivariate discriminant function based on six biochemical markers in blood can predict the cirrhotic evolution of chronic hepatitis. *Clin Chem* 2001;47(9):1696-700.

(22) Wake K. Perisinusoidal fat-storing cells of the liver. In: Surrenti C, Casini A, Milani S, Pinzani M, editors. Fat-storing Cells and Liver Fibrosis. Dordrecht: Kluwer Academic Publishers, 1994: 1-12.

(23) Bissell DM. Effects of extracellular matrix on hepatocyte behaviour. In: Clement B, Guillouzo A, editors. Cellular and Molecular Aspects of Cirrhosis. Colloque INSERM/John Libbey Eurotext Ltd, 1992: 187-97.

(24) Friedman SL, Roll FJ, Boyles J *et al*. Maintenance of differentiated phenotype of cultured rat hepatic lipocytes by basement membrane matrix. *J Biol Chem* 1989;264:10756-62.

(25) McGuire RF, Bissell DM, Boyles J *et al*. Role of extracellular matrix in regulating fenestrations of sinusoidal endothelial cells isolated from normal rat liver. *Hepatology* 1992;15(6):989-97.

(26) Reid LM, Abreu SL, Montgomery K. Extracellular matrix and hormonal regulation of synthesis and abundance of messenger RNAs in cultured liver cells. In: Arias IM, Jakoby WB, Popper H et al, editors. The Liver: Biology and Pathology. New York: Raven Press Ltd, 1988: 717-37.

(27) Millward-Sadler GH, Jezequel AM. Normal histology and ultrastructure. In: Millward-Sadler GH, Wright R, Arthur MJP, editors. Wright's Liver and Biliary Disease. London: Bailliere Tindall, 1992: 12-42.

(28) Milani S. Expression of extracellular matrix components in normal and fibrotic liver. In: Surrenti C, Casini A, Milani S, Pinzani M, editors. Fat-storing Cells and Liver Fibrosis. Dordrecht: Kluwer Academic Publishers, 1994: 37-54.

(29) Schuppan D. Structure of extracellular matrix in normal and fibrotic liver: collagens and glycoproteins. *Semin Liver Dis* 1990;10:1-10.

(30) Miller EJ. The structure of fibril-forming collagens. *Annals of the New York Academy of Science* 1985;460:1-13.

(31) Prockop DJ, Kivirikko KI. Heritable diseases of collagen. *N Engl J Med* 1984;311:376-86.

(32) Rojkind M, Giambrone M-A, Biempica L. Collagen types in normal and cirrhotic liver. *Gastroenterology* 1979;76:710-9.

(33) Seyer JM, Huherson ET, Kang AH. Collagen polymorphism in normal and cirrhotic human liver. *J Clin Invest* 1977;59:241-8.

(34) Ala-Kokko L, Pihlajaniemi T, Myers JC *et al*. Gene expression of type I, III and IV collagens in hepatic fibrosis induced by dimethylnitrosamine in the rat. *Biochem J* 1987;244(1):75-9.

(35) Risteli J, Kivirikko KI. Activities of prolyl hydroxylase, lysyl hydroxylase, collagen galactosyltransferase and collagen glucosyltransferase in the liver of rats with hepatic injury. *Biochem J* 1974;144:115-22.

(36) Birk DE, Fitch JM, Babiarz JP *et al*. Collagen type I and type V are present in the same fibril in the avian corneal stroma. *J Cell Biol* 1988;106:999-1008.

(37) Birk DE, Zycband EI, Winkelmann DA *et al*. Collagen fibrillogenesis in situ. Discontinuous segmental assembly in extracellular compartments. *Annals of the New York Academy of Science* 1990;580:176-94.

(38) Miyahara M, Njieha RK, Prockop DJ. Formation of collagen fibrils in vitro by cleavage of procollagen with procollagen proteinases. *J Biol Chem* 1982;257:8442-8.

(39) Miyahara M, Hayashi K, Berger J *et al*. Formation of collagen fibrils by enzymic cleavage of precursors of type I collagen in vitro. *J Biol Chem* 1984;259:9891-8.

(40) Geerts A, Schuppan D, Lazeroms S *et al*. Collagen type I and III occur together in hybrid fibrils in the space of Disse of normal rat liver. *Hepatology* 1990;12:233-41.

(41) Ignotz RA, Endo T, Massague J. Regulation of fibronectin and type I collagen mRNA levels by transforming growth factor beta. *J Biol Chem* 1987;262:6443-6.

(42) Varga J, Rosenbloom J, Jimenez SA. Transforming growth factor beta (TGFB) causes a persistent increase in steady-state amounts of type I and type III collagen and fibronectin mRNAs in normal human dermal fibroblasts. *Biochem J* 1987;247:597-604.

(43) Ignotz RA, Massague J. Transforming growth factor beta stimulates the expression of fibronectin and collagen and their incorporation into the extracellular matrix. *J Biol Chem* 1986;261:4337-45.

(44) Penttinen RP, Kobayashi S, Bornstein P. Transforming growth factor beta increases mRNA for matrix proteins both in the presence and in the absence of changes in mRNA stability. *Proc Natl Acad Sci USA* 1988;85:1105-8.

(45) Moshage H, Casini A, Lieber CS. Acetaldehyde selectively stimulates collagen production in cultured rat liver fat-storing cells but not in hepatocytes. *Hepatology* 1990;12:511-8.

(46) Rockey DC, Maher JJ, Jarnagin WR *et al*. Inhibition of rat hepatic lipocyte activation in culture by interferon- gamma. *Hepatology* 1992;16(3):776-84.

(47) Weiner FR, Giambrone MA, Czaja MJ *et al*. Ito-cell gene expression and collagen regulation. *Hepatology* 1990;11:111-7.

(48) Weiner FR, Czaja MJ, Giambrone M-A *et al*. Transcriptional and posttranscriptional effects of dexamethasoneon albumin and procollagen messenger RNAs in murine schistosomiasis. *Biochemistry* 1987;26:1557-62.

(49) Mayne R, Wiedemann H, Dessau W *et al*. Structural and immunological characterization of type IV collagen isolated from chicken tissues. *Eur J Biochem* 1982;126(2):417-23.

(50) Mayne R, Wiedemann H, Irwin MH *et al*. Monoclonal antibodies against chicken type IV and V collagens: electron microscopic mapping of the epitopes after rotary shadowing. *J Cell Biol* 1984;98:1637-44.

(51) Siebold B, Deutzman R, Kuhn K. The arrangement of intra and intermolecular disulfide bonds in the carboxy terminal non collagenous aggregation and cross linking domain of basement membrane type IV collagen. *Eur J Biochem* 1988;176:617-24.

(52) Yurchenco PD, Schittny JC. Molecular architecture of basement membranes. *FASEB J* 1990;4:1577-90.

(53) Ramadori G, Schwogler S, Viet TH *et al*. Fat-storing (Ito) cells of the rat liver synthesize and secrete entactin (nidogen). Comparison with other hepatic and non-hepatic cells. *Gastroenterology* 1990;98:A623 (Abstr).

(54) Schuppan D, Herbst H, Milani S. Matrix, matrix synthesis, and molecular networks in hepatic fibrosis. In: Zern MA, Reid LM, editors. Extracellular Matrix. New York: Marcel Dekker, Inc., 1993: 201-54.

(55) Engvall E, Earwicker D, Haarparanta T *et al*. Distribution and isolation of four laminin variants; tissue restricted distribution of heterotrimers assembled from five differential subunits. *Cell Regul* 1990;160:731-40.

(56) Clement B, Segui-Real B, Savagner P *et al*. Hepatocyte attachment to laminin is mediated through multiple receptors. *J Cell Biol* 1990;110:185-92.

(57) Panayotou G, End P, Aumailley M *et al*. Domains of laminin with growth factor activity. *Cell* 1989;48:989-96.

(58) Schwarzbauer JE, Tamkun JW, Lemischka IR *et al*. Three different fibronectin mRNAs arise by alternative splicing within the coding region. *Cell* 1983;35:421-31.

(59) Erickson HP, Bourdon MA. Tenascin: an extracellular matrix protein prominent in specialized embryonic tissues and tumors. *Annu Rev Cell Biol* 1989;5:71-92.

(60) Weller A, Beck S, Ekblom P. Amino acid sequence of mouse tenascin and differential expression of two tenascin isoforms during embryogenesis. *J Cell Biol* 1991;112:355-62.

(61) Ramadori G, Schwogler S, Veit Th *et al*. Tenascin gene expression in rat liver and in rat liver cells. *Virchows Archiv B Cell Pathol* 1991;60:145-53.

(62) Schuppan D, Cantaluppi MC, Becker J *et al*. Undulin, an extracellular matrix glycoprotein associated with collagen fibrils. *J Biol Chem* 1990;265:8823-32.

(63) Velebny V, Kasafirek E, Kanta J. Desmosine and isodesmosine contents and elastase activity in normal and cirrhotic rat liver. *Biochem J* 1983;214:1023-5.

(64) Ramadori G. The stellate cell (Ito cell, fat-storing cell, lipocyte, perisinusoidal cell) of the liver. New insights into pathophysiology of an intriguing cell. *Virchows Archiv B Cell Pathol* 1991;61:147-58.

(65) Wake H. Perisinusoidal stellate cells (fat-storing cells, interstitial cells, lipocytes), their related structure in and around the liver sinusoids, and vitamin A-storing cells in extrahepatic organs. *Int Rev Cytol* 1980;66:303-53.

(66) Ito T, Nemoto W. Uber die Kupffersche sterzellen und die fettspeicherungszellen (fat-storing cells) in der Blutkapillarwand der menschlichen Leber. *Okajamas Folia Anatomica Japonica* 1952;24:243-58.

(67) Friedman SL. Molecular regulation of hepatic fibrosis, an integrated cellular response to tissue injury. *J Biol Chem* 2000;275(4):2247-50.

(68) Wang XD. Chronic alcohol intake interferes with retinoid metabolism and signaling. *Nutr Rev* 1999;57(2):51-9.

(69) Schuppan D, Ruehl M, Somasundaram R *et al*. Matrix as a modulator of hepatic fibrogenesis. *Semin Liver Dis* 2001;21(3):351-72.

(70) Knittel T, Kobold D, Saile B *et al*. Rat liver myofibroblasts and hepatic stellate cells: different cell populations of the fibroblast lineage with fibrogenic potential [see comments]. *Gastroenterology* 1999;117:1205-21.

(71) Geerts A. History, heterogeneity, developmental biology, and functions of quiescent hepatic stellate cells. *Semin Liver Dis* 2001;21(3):311-35.

(72) Minato Y, Hasumura Y, Takeuchi J. The role of fat-storing cells in Disse space fibrogenesis in alcoholic liver disease. *Hepatology* 1983;3(4):559-66.

(73) Pinzani M, Marra F. Cytokine receptors and signaling in hepatic stellate cells. *Semin Liver Dis* 2001;21(3):397-416.

(74) Schuppan D, Porov Y. Hepatic fibrosis: From bench to bedside. *J Gastroenterol Hepatol* 2002;17 Suppl 3:S300-S305.

(75) Rockey DC. Vascular mediators in the injured liver. *Hepatology* 2003;37(1):4-12.

(76) Milani S, Herbst H, Schuppan D *et al*. In situ hybridization for procollagen types I, III and IV mRNA in normal and fibrotic rat liver: evidence for predominant expression in nonparenchymal liver cells. *Hepatology* 1989;10(1):84-92.

(77) Abdel-Aziz G, Rescan PY, Clement B *et al*. Cellular sources of matrix proteins in experimentally induced cholestatic rat liver. *J Pathol* 1991;164(2):167-74.

(78) Geerts A, Greenwel P, Cunningham M *et al*. Identification of connective tissue gene transcripts in freshly isolated parenchymal, endothelial, Kupffer and fat-storing cells by northern hybridization analysis. *J Hepatol* 1993;19(1):148-58.

(79) Kinnman N, Francoz C, Barbu V *et al*. The myofibroblastic conversion of peribiliary fibrogenic cells distinct from hepatic stellate cells is stimulated by platelet-derived growth factor during liver fibrogenesis. *Lab Invest* 2003;83(2):163-73.

(80) Cassiman D, Libbrecht L, Desmet V *et al*. Hepatic stellate cell/myofibroblast subpopulations in fibrotic human and rat livers. *J Hepatol* 2002;36(2):200-9.

(81) Corpechot C, Barbu V, Wendum D *et al*. Hypoxia-induced VEGF and collagen I expressions are associated with angiogenesis and fibrogenesis in experimental cirrhosis. *Hepatology* 2002;35(5):1010-21.

(82) Forbes SJ, Russo FP, Rey V *et al*. A significant proportion of myofibroblasts are of bone marrow origin in human liver fibrosis. *Gastroenterology* 2004;126(4):955-63.

(83) Magness ST, Bataller R, Yang L *et al*. A dual reporter gene transgenic mouse demonstrates heterogeneity in hepatic fibrogenic cell populations. *Hepatology* 2004;40(5):1151-9.

(84) Kalluri R, Neilson EG. Epithelial-mesenchymal transition and its implications for fibrosis. *J Clin Invest* 2003;112(12):1776-84.

(85) Knittel T, Schuppan D, Meyer Zum Buschenfelde KH *et al*. Differential expression of collagen types I, III, and IV by fat-storing (Ito) cells in vitro. *Gastroenterology* 1992;102(5):1724-35.

(86) Maher JJ, Bissell DM, Friedman SL *et al*. Collagen measured in primary cultures of normal rat hepatocytes derives from lipocytes within the monolayer. *J Clin Invest* 1988;82(2):450-9.

(87) Mathew J, Geerts A, Burt AD. Pathobiology of hepatic stellate cells. *Hepatogastroenterology* 1996;43:72-91.

(88) Bronfenmajer S, Schaffner F, Popper H. Fat-storing cells (lipocytes) in human liver. *Arch Pathol* 1966;82:447-53.

(89) Sztark F, Dubroca J, Latry P *et al*. Perisinusoidal cells in patients with normal liver histology. A morphometric study. *J Hepatol* 1986;2(3):358-69.

(90) Iredale JP. Tissue inhibitors of metalloproteinases in liver fibrosis. *Int J Biochem Cell Biol* 1997;29(1):43-54.

(91) Niki T, Pekny M, Hellemans K *et al*. Class VI intermediate filament protein nestin is induced during activation of rat hepatic stellate cells. *Hepatology* 1999;29(2):520-7.

(92) Morrison SJ, White PM, Zock C *et al*. Prospective identification, isolation by flow cytometry, and in vivo self-renewal of multipotent mammalian neural crest stem cells. *Cell* 1999;96(5):737-49.

(93) vom Dahl S, Bode JG, Reinehr RM *et al*. Release of osmolytes from perfused rat liver on perivascular nerve stimulation: alpha-adrenergic control of osmolyte efflux from parenchymal and nonparenchymal liver cells. *Hepatology* 1999;29(1):195-204.

(94) Geerts A, Bouwens L, Wisse E. Ultrastructure and function of hepatic fat-storing and pit cells. *J Electron Microsc Tech* 1990;14:247-56.

(95) Ramm GA, Britton RS, Oneill R *et al*. Vitamin A-poor lipocytes: A novel desmin-negative lipocyte subpopulation, which can be activated to myofibroblasts. *Am J Physiol - Gastro Liv Physiol* 1995;32:G532-G541.

(96) Friedman SL. Seminars in medicine of the Beth Israel Hospital, Boston. The cellular basis of hepatic fibrosis. Mechanisms and treatment strategies. *N Engl J Med* 1993;328(25):1828-35.

(97) Johnson SJ, Hines E, Burt AD. Macrophage and perisinusoidal cell kinetics in acute liver injury. *J Pathol* 1992;166:351-8.

(98) Jiao J, Friedman SL, Aloman C. Hepatic fibrosis. *Curr Opin Gastroenterol* 2009;25(3):223-9.

(99) Tsukamoto H, She H, Hazra S *et al*. Anti-adipogenic regulation underlies hepatic stellate cell transdifferentiation. *J Gastroenterol Hepatol* 2006;21 Suppl 3:S102-S105.

(100) Bataller R, Schwabe RF, Choi YH *et al*. NADPH oxidase signal transduces angiotensin II in hepatic stellate cells and is critical in hepatic fibrosis. *J Clin Invest* 2003;112(9):1383-94.

(101) Tuma DJ. Role of malondialdehyde-acetaldehyde adducts in liver injury. *Free Radic Biol Med* 2002;32(4):303-8.

(102) Burt AD. Pathobiology of hepatic stellate cells. *J Gastroenterol* 1999;34(3):299-304.

(103) Geerts A, Lazou JM, De Bleser P *et al*. Tissue distribution, quantitation and proliferation kinetics of fat- storing cells in carbon tetrachloride-injured rat liver. *Hepatology* 1991;13(6):1193-202.

(104) Ogawa K, Suzuki J-I, Mukai H *et al*. Sequential changes of extracellular matrix and proliferation of Ito cells with enhanced expression of desmin and actin in focal hepatic injury. *Am J Pathol* 1986;125:611-9.

(105) Hautekeete ML, Geerts A, Seynaeve C *et al*. Contributions of light and transmission electron microscopy to the study of the human fat-storing cell. *Eur J Morphol* 1993;31(1-2):72-6.

(106) Hruban Z, Russell RM, Boyer JL *et al*. Ultrastructural changes in livers of two patients with hypervitaminosis A. *Am J Pathol* 1974;76(3):451-61.

(107) Mak KM, Lieber CS. Lipocytes and transitional cells in alcoholic liver disease: a morphometric study. *Hepatology* 1988;8(5):1027-33.

(108) Rockey DC, Boyles JK, Gabbiani G *et al*. Rat hepatic lipocytes express smooth muscle actin upon activation in vivo and in culture. *J Submicrosc Cytol Pathol* 1992;24(2):193-203.

(109) Rockey DC, Friedman SL. Cytoskeleton of liver perisinusoidal cells (lipocytes) in normal and pathological conditions. *Cell Motil Cytoskeleton* 1992;22(4):227-34.

(110) Friedman SL. Mechanisms of hepatic fibrogenesis. *Gastroenterology* 2008;134(6):1655-69.

(111) Geerts A, Vrijsen R, Rauterberg J *et al*. In vitro differentiation of fat-storing cells parallels marked increase of collagen synthesis and secretion. *J Hepatol* 1989;9:59-68.

(112) Gaca MD, Zhou X, Benyon RC. Regulation of hepatic stellate cell proliferation and collagen synthesis by proteinase-activated receptors. *J Hepatol* 2002;36(3):362-9.

(113) Friedman SL. Stellate cells: a moving target in hepatic fibrogenesis. *Hepatology* 2004;40(5):1041-3.

(114) Maher JJ. Leukocytes as modulators of stellate cell activation. *Alcohol Clin Exp Res* 1999;23:917-21.

(115) Svegliati BG, D'Ambrosio L, Ferretti G *et al*. Fibrogenic effect of oxidative stress on rat hepatic stellate cells. *Hepatology* 1998;27(3):720-6.

(116) Nieto N, Friedman SL, Greenwel P *et al*. CYP2E1-mediated oxidative stress induces collagen type I expression in rat hepatic stellate cells. *Hepatology* 1999;30:987-96.

(117) Jarnagin WR, Rockey DC, Koteliansky VE *et al*. Expression of variant fibronectins in wound healing: cellular source and biological activity of the EIIIA segment in rat hepatic fibrogenesis. *J Cell Biol* 1994;127(6 Pt 2):2037-48.

(118) Friedman SL. Cytokines and fibrogenesis. *Semin Liver Dis* 1999;19(2):129-40.

(119) Ratziu V, Lalazar A, Wong L *et al*. Zf9, a Kruppel-like transcription factor up-regulated in vivo during early hepatic fibrosis. *Proc Natl Acad Sci U S A* 1998;95(16):9500-5.

(120) Hellerbrand, Wang SC, Tsukamoto H *et al*. Expression of intracellular adhesion molecule 1 by activated hepatic stellate cells. *Hepatology* 1996;24(3):670-6.

(121) Ikeda K, Kawada N, Wang YQ *et al*. Expression of cellular prion protein in activated hepatic stellate cells. *Am J Pathol* 1998;153(6):1695-700.

(122) Philipsen S, Suske G. A tale of three fingers: the family of mammalian Sp/XKLF transcription factors. *Nucleic Acids Res* 1999;27(15):2991-3000.

(123) Rippe RA, Almounajed G, Brenner DA. Sp1 binding activity increases in activated Ito cells. *Hepatology* 1995;22(1):241-51.

(124) Chen A, Davis BH, Bissonnette M *et al*. 1,25-Dihydroxyvitamin D(3) stimulates activator protein-1-dependent caco-2 cell differentiation. *J Biol Chem* 1999;274(50):35505-13.

(125) Pinzani M, Marra F, Carloni V. Signal transduction in hepatic stellate cells. *Liver* 1998;18(1):2-13.

(126) Ankoma-Sey V, Matli M, Chang KB *et al*. Coordinated induction of VEGF receptors in mesenchymal cell types during rat hepatic wound healing. *Oncogene* 1998;17(1):115-21.

(127) Shrivastava A, Radziejewski C, Campbell E *et al*. An orphan receptor tyrosine kinase family whose members serve as nonintegrin collagen receptors. *Mol Cell* 1997;1(1):25-34.

(128) Vogel W. Discoidin domain receptors: structural relations and functional implications. *FASEB J* 1999;13 Suppl:S77-S82.

(129) Zhou X, Murphy FR, Gehdu N *et al*. Engagement of alphavbeta3 integrin regulates proliferation and apoptosis of hepatic stellate cells. *J Biol Chem* 2004;279(23):23996-4006.

(130) Friedman SL, Arthur MJ. Activation of cultured rat hepatic lipocytes by Kupffer cell conditioned medium. Direct enhancement of matrix synthesis and stimulation of cell proliferation via induction of platelet-derived growth factor receptors. *J Clin Invest* 1989;84(6):1780-5.

(131) Marra F, Grandaliano G, Valente AJ *et al*. Thrombin stimulates proliferation of liver fat-storing cells and expression of monocyte chemotactic protein-1: potential role in liver injury. *Hepatology* 1995;22:780-7.

(132) Pinzani M, Milani S, DeFranco R *et al*. Endothelin 1 is overexpressed in human cirrhotic liver and exerts multiple effects on activated hepatic stellate cells. *Gastroenterology* 1996;110:534-48.

(133) Bachem MG, Riess U, Gressner AM. Liver fat storing cell proliferation is stimulated by epidermal growth factor/transforming growth factor alpha and inhibited by transforming growth factor beta. *Biochem Biophys Res Commun* 1989;162:708-14.

(134) Matsuoka M, Pham NT, Tsukamoto H. Differential effects of interleukin 1 alpha, tumour necrosis factor alpha, and transforming growth factor beta-1 on cell proliferation and collagen formation by cultured fat storing cells. *Liver* 1989;9:71-8.

(135) Lee KS, Buck M, Houglum K *et al*. Activation of hepatic stellate cells by TGF alpha and collagen type I is mediated by oxidative stress through c-myb expression. *J Clin Invest* 1995;96(5):2461-8.

(136) Mallat A, Preaux AM, Blazejewski S *et al*. Interferon alfa and gamma inhibit proliferation and collagen synthesis of human ito cells in culture. *Hepatology* 1995;21:1003-10.

(137) Rockey DC, Chung JJ. Interferon gamma inhibits lipocyte activation and extracellular matrix mRNA expression during experimental liver injury: implications for treatment of hepatic fibrosis. *J Investig Med* 1994;42(4):660-70.

(138) Davis BH, Coll O, Beno DWA. Retinoic acid suppresses the response to platelet-derived growth factor in human hepatic ito-cell-like myofibroblasts: a post-receptor mechanism independent of raf/fos//jun/erg activation. *Biochem J* 1993;294:785-91.

(139) Marra F, Gentilini A, Pinzani M *et al*. Phosphatidylinositol 3-kinase is required for platelet-derived growth factor's actions on hepatic stellate cells. *Gastroenterology* 1997;112(4):1297-306.

(140) Marra F, De Franco R, Grappone C *et al*. Expression of monocyte chemotactic protein-1 precedes monocyte recruitment in a rat model of acute liver injury, and is modulated by vitamin E. *J Invest Med* 1999;47:66-75.

(141) Casini A, Pinzani M, Milani S *et al*. Regulation of extracellular matrix synthesis by transforming growth factor beta 1 in human fat-storing cells. *Gastroenterology* 1993;105:245-53.

(142) Bachem MG, Meyer D, Melchior R *et al*. Activation of rat liver perisinusoidal lipocytes by transforming growth factors derived from myofibroblastlike cells. *J Clin Invest* 1992;89:19-27.

(143) Imai S, Okuno M, Moriwaki H *et al*. 9,13-di-cis-retinoic acid induces the production of tPA and activation of latent TGF-beta via RAR-alpha in a human liver stellate cell line, LI90. *FEBS Lett* 1997;411:102-6.

(144) Okuno M, Moriwaki H, Imai S *et al*. Retinoids exacerbate rat liver fibrosis by inducing the activation of latent TGF-beta in liver stellate cells. *Hepatology* 1997;26(4):913-21.

(145) Friedman SL, Yamasaki G, Wong L. Modulation of transforming growth factor beta receptors of rat lipocytes during the hepatic wound healing response. Enhanced binding and reduced gene expression accompany cellular activation in culture and in vivo. *J Biol Chem* 1994;269(14):10551-8.

(146) Levy MT, McCaughan GW, Abbott CA *et al*. Fibroblast activation protein: a cell surface dipeptidyl peptidase and gelatinase expressed by stellate cells at the tissue remodelling interface in human cirrhosis. *Hepatology* 1999;29(6):1768-78.

(147) Tiggelman AM, Boers W, Linthorst C *et al*. Collagen synthesis by human liver (myo)fibroblasts in culture: evidence for a regulatory role of IL-1 beta, IL-4, TGF beta and IFN gamma. *J Hepatol* 1995;23(3):307-17.

(148) Casini A, Cunningham M, Rojkind M *et al*. Acetaldehyde increases procollagen type I and fibronectin gene transcription in cultured rat fat-storing cells through a protein synthesis-dependent mechanism. *Hepatology* 1991;13:758-65.

(149) Hernandez-Munoz I, de la TP, Sanchez-Alcazar JA *et al*. Tumor necrosis factor alpha inhibits collagen alpha 1(I) gene expression in rat hepatic stellate cells through a G protein. *Gastroenterology* 1997;113(2):625-40.

(150) Wang SC, Ohata M, Schrum L *et al*. Expression of interleukin-10 by in vitro and in vivo activated hepatic stellate cells. *J Biol Chem* 1998;273(1):302-8.

(151) Stefanovic B, Hellerbrand C, Holcik M *et al*. Posttranscriptional regulation of collagen alpha1(I) mRNA in hepatic stellate cells. *Mol Cell Biol* 1997;17(9):5201-9.

(152) Lindquist JN, Parsons CJ, Stefanovic B *et al*. Regulation of alpha1(I) collagen messenger RNA decay by interactions with alphaCP at the 3'-untranslated region. *J Biol Chem* 2004;279(22):23822-9.

(153) Schwartz DC, Parker R. Mutations in translation initiation factors lead to increased rates of deadenylation and decapping of mRNAs in Saccharomyces cerevisiae. *Mol Cell Biol* 1999;19(8):5247-56.

(154) McCarthy JE, Kollmus H. Cytoplasmic mRNA-protein interactions in eukaryotic gene expression. *Trends Biochem Sci* 1995;20(5):191-7.

(155) Jacobson A. PolyA metabolism and translation: the closed loop model. In: Hershey J, Matthews M, Sonenberg N, editors. Translational Control. New York: Cold Spring Harbor Laboratory Press, 1996: 451-80.

(156) Sachs AB, Sarnow P, Hentze MW. Starting at the beginning, middle, and end: translation initiation in eukaryotes. *Cell* 1997;89(6):831-8.

(157) Tarun SZ, Jr., Sachs AB. Association of the yeast poly(A) tail binding protein with translation initiation factor eIF-4G. *EMBO J* 1996;15(24):7168-77.

(158) Imataka H, Gradi A, Sonenberg N. A newly identified N-terminal amino acid sequence of human eIF4G binds poly(A)-binding protein and functions in poly(A)-dependent translation. *EMBO J* 1998;17(24):7480-9.

(159) Hagedorn CH, Spivak-Kroizman T, Friedland DE *et al*. Expression of functional eIF-4Ehuman: purification, detailed characterization, and its use in isolating eIF-4E binding proteins. *Protein Expr Purif* 1997;9(1):53-60.

(160) Loflin P, Chen CY, Shyu AB. Unraveling a cytoplasmic role for hnRNP D in the in vivo mRNA destabilization directed by the AU-rich element. *Genes Dev* 1999;13(14):1884-97.

(161) Lindquist JN, Marzluff WF, Stefanovic B. Fibrogenesis. III. Posttranscriptional regulation of type I collagen. *Am J Physiol Gastrointest Liver Physiol* 2000;279(3):G471-G476.

(162) Olaso E, Friedman SL. Molecular regulation of hepatic fibrogenesis. *J Hepatol* 1998;29:836-47.

(163) Lee JA, Ahmed Q, Hines JE *et al*. Disappearance of hepatic parenchymal nerves in human liver cirrhosis. *Gut* 1992;33(1):87-91.

(164) Ueno T, Sata M, Sakata R *et al*. Hepatic stellate cells and intralobular innervation in human liver cirrhosis. *Hum Pathol* 1997;28:953-9.

(165) Rockey D. The cellular pathogenesis of portal hypertension: stellate cell contractility, endothelin, and nitric oxide. *Hepatology* 1997;25(1):2-5.

(166) Shao R, Yan W, Rockey DC. Regulation of endothelin-1 synthesis by endothelin-converting enzyme-1 during wound healing. *J Biol Chem* 1999;274(5):3228-34.

(167) Rockey DC, Fouassier L, Chung JJ *et al*. Cellular localization of endothelin-1 and increased production in liver injury in the rat: potential for autocrine and paracrine effects on stellate cells. *Hepatology* 1998;27(2):472-80.

(168) Housset C, Rockey DC, Bissell DM. Endothelin receptors in rat liver: lipocytes as a contractile target for endothelin 1. *Proc Natl Acad Sci USA* 1994;90:9266-70.

(169) Ueno T, Tanikawa K. Intralobular innervation and lipocyte contractility in the liver. *Nutrition* 1997;13:141-8.

(170) Mallat A, Preaux AM, Serradeil-Le Gal C *et al*. Growth inhibitory properties of endothelin-1 in activated human hepatic stellate cells: a cyclic adenosine monophosphate-mediated pathway. Inhibition of both extracellular signal-regulated kinase and c-Jun kinase and upregulation of endothelin B receptors. *J Clin Invest* 1996;98(12):2771-8.

(171) Gressner AM. Transdifferentiation of hepatic stellate cells (Ito cells) to myofibroblasts: a key event in hepatic fibrogenesis. *Kidney Int Suppl* 1996;54:S39-S45.

(172) De Bleser PJ, Niki T, Rogiers V *et al*. Transforming growth factor-beta gene expression in normal and fibrotic rat liver. *J Hepatol* 1997;26(4):886-93.

(173) Marra F, Choudhury GG, Pinzani M *et al*. Regulation of platelet-derived growth factor secretion and gene expression in human liver fat-storing cells. *Gastroenterology* 1994;107:1110-7.

(174) Thompson K, Maltby J, Fallowfield J *et al*. Interleukin-10 expression and function in experimental murine liver inflammation and fibrosis. *Hepatology* 1998;28(6):1597-606.

(175) Hines JE, Johnson SJ, Burt AD. In vivo responses of perisinusoidal cells (lipocytes) and macrophages to cholestatic liver injury. *Am J Pathol* 1993;142:511-8.

(176) Matsuoka M, Tsukamoto H. Stimulation of hepatic lipocyte collagen production by Kupffer cell- derived transforming growth factor beta: implication for a pathogenetic role in alcoholic liver fibrogenesis. *Hepatology* 1990;11(4):599-605.

(177) Friedman SL. Stellate cell activation in alcoholic fibrosis--an overview. *Alcohol Clin Exp Res* 1999;23(5):904-10.

(178) Gressner AM, Bachem MG. Molecular mechanisms of liver fibrogenesis--a homage to the role of activated fat-storing cells. *Digestion* 1995;56(5):335-46.

(179) Leo MA, Rosman AS, Lieber CS. Differential depletion of carotenoids and tocopherol in liver disease. *Hepatology* 1993;17(6):977-86.

(180) Houglum K, Venkataramani A, Lyche K *et al*. A pilot study of the effects of d-alpha-tocopherol on hepatic stellate cell activation in chronic hepatitis C. *Gastroenterology* 1997;113(4):1069-73.

(181) Poli G, Parola M. Oxidative damage and fibrogenesis. *Free Radic Biol Med* 1997;22(1-2):287-305.

(182) Gressner AM, Lotfi S, Gressner G *et al*. Identification and partial characterization of a hepatocyte-derived factor promoting proliferation of culture fat-storing cells (parasinusoidal lipocytes). *Hepatology* 1992;16:1250-66.

(183) Baroni GS, D'Ambrosio L, Curto P *et al*. Interferon gamma decreases hepatic stellate cell activation and extracellular matrix deposition in rat liver fibrosis. *Hepatology* 1996;23(5):1189-99.

(184) Krams SM, Cao S, Hayashi M *et al*. Elevations in IFN-gamma, IL-5, and IL-10 in patients with the autoimmune disease primary biliary cirrhosis: association with autoantibodies and soluble CD30. *Clin Immunol Immunopathol* 1996;80(3 Pt 1):311-20.

(185) Thompson KC, Trowern A, Fowell A *et al*. Primary rat and mouse hepatic stellate cells express the macrophage inhibitor cytokine interleukin-10 during the course of activation In vitro. *Hepatology* 1998;28(6):1518-24.

(186) Hautekeete ML, Geerts A. The hepatic stellate (Ito) cell: its role in human liver disease. *Virchows Arch* 1997;430(3):195-207.

(187) Guarascio P, Portmann B, Visco G *et al*. Liver damage with reversible portal hypertension from vitamin A intoxication: demonstration of Ito cells. *J Clin Pathol* 1983;36(7):769-71.

(188) Kobayashi Y, Fujiyama S. Pathological study on gold impregnation of fat-storing cells in human liver. *Acta Pathol Jpn* 1981;31(1):65-74.

(189) Sztark F, Latry P, Quinton A *et al*. The sinusoidal barrier in alcoholic patients without liver fibrosis. A morphometric study. *Virchows Arch A Pathol Anat Histopathol* 1986;409(3):385-93.

(190) Yokoi Y, Namihisa T, Kuroda H *et al*. Immunocytochemical detection of desmin in fat-storing cells (Ito cells). *Hepatology* 1984;4:709-14.

(191) Gard AL, White FP, Dutton GR. Extra-neural glial fibrillary acidic protein (GFAP) immunoreactivity in perisinusoidal stellate cells of rat liver. *J Neuroimmunol* 1985;8(4-6):359-75.

(192) Neubauer K, Knittel T, Aurisch S *et al*. Glial fibrillary acidic protein - a cell type specific marker for ito cells in vivo and in vitro. *J Hepatol* 1996;24:719-30.

(193) Buniatian G, Hamprecht B, Gebhardt R. Glial fibrillary acidic protein as a marker of perisinusoidal stellate cells that can distinguish between the normal and myofibroblast-like phenotypes. *Biol Cell* 1996;87(1-2):65-73.

(194) Messing A. Nestin in the liver--lessons from the brain. *Hepatology* 1999;29(2):602-3.

(195) Knittel T, Aurisch S, Neubauer K *et al*. Cell-type-specific expression of neural cell adhesion molecule (n-cam) in ito cells of rat liver: up-regulation during in vitro activation and in hepatic tissue repair. *Am J Pathol* 1996;149:449-62.

(196) Schmitt-Graff A, Kruger S, Bochard F *et al*. Modulation of alpha smooth muscle actin and desmin expression in perisinusoidal cells of normal and diseased human livers. *Am J Pathol* 1991;138(5):1233-42.

(197) Enzan H, Himeno H, Iwamura S *et al*. Alpha-smooth muscle actin-positive perisinusoidal stromal cells in human hepatocellular carcinoma. *Hepatology* 1994;19(4):895-903.

(198) Zhou XJ. [The ultrastructural pathology of chronic hepatitis C]. *Zhonghua Bing Li Xue Za Zhi* 1993;22(3):157-9.

(199) Goddard CJ, Smith A, Hoyland JA *et al*. Localisation and semiquantitative assessment of hepatic procollagen mRNA in primary biliary cirrhosis. *Gut* 1998;43(3):433-40.

(200) Tang L, Tanaka Y, Marumo F *et al*. Phenotypic change in portal fibroblasts in biliary fibrosis. *Liver* 1994;14(2):76-82.

(201) Tuchweber B, Desmouliere A, Bochaton-Piallat ML *et al*. Proliferation and phenotypic modulation of portal fibroblasts in the early stages of cholestatic fibrosis in the rat. *Lab Invest* 1996;74(1):265-78.

(202) Somerville RP, Oblander SA, Apte SS. Matrix metalloproteinases: old dogs with new tricks. *Genome Biol* 2003;4(6):216.

(203) Younossi ZM, Gramlich T, Bacon BR *et al*. Hepatic iron and nonalcoholic fatty liver disease. *Hepatology* 1999;30(4):847-50.

(204) Iredale JP, Winwood PJ, Kawser CA *et al*. Lipocyte proliferation in the C. parvum model of macrophage-induced liver injury is associated with expression of 72kDa type IV collagenase/gelatinase. In: Knook DL, Wisse E, editors. Cells of the Hepatic Sinusoid, Vol 4. Leiden: Kupffer Cell Foundation, 1993: 105-8.

(205) Winwood PJ, Schuppan D, Iredale JP *et al*. Kupffer cell-derived 95kDa type IV collagenase/gelatinase B: Characterisation and expression in cultured cells. *Hepatology* 1995;22:304-15.

(206) Goldberg GI, Strongin A, Collier IE *et al*. Interaction of 92-kDa Type-IV Collagenase with the Tissue Inhibitor of Metalloproteinases Prevents Dimerization, Complex Formation with Interstitial Collagenase, and Activation of the Proenzyme with Stromelysin. *J Biol Chem* 1992;267:4583-91.

(207) Nagase H, Jackson RC, Brinckerhoff CE *et al*. A precursor form of latent collagenase produced in a cell free system with mRNA from rabbit synovial cells. *J Biol Chem* 1981;256:11951-4.

(208) Nagase H, Brinckerhoff CE, Vater CA *et al*. Biosynthesis and secretion of procollagenase by rabbit synovial fibroblasts. *Biochem J* 1983;214:281-8.

(209) Freije JMP, Diezitza I, Balbin M *et al*. Molecular cloning and expression of collagenase-3, a novel human matrix metalloproteinase produced by breast carcinomas. *J Biol Chem* 1994;269:16766-73.

(210) Aimes RT, Quigley JP. Matrix metalloproteinase-2 is an interstitial collagenase - Inhibitor-free enzyme catalyzes the cleavage of collagen fibrils and soluble native type I collagen generating the specific 3/4- and 1/4-length fragments. *J Biol Chem* 1995;270:5872-6.

(211) Benyon RC, Arthur MJ. Extracellular matrix degradation and the role of hepatic stellate cells. *Semin Liver Dis* 2001;21(3):373-84.

(212) Murphy G, Docherty AJP, Hembry RM *et al*. Metalloproteinases and tissue damage. *Br J Rheumatol* 1991;30 (Suppl 1):25-31.

(213) Matrisian LM. The matrix-degrading metalloproteinases. *Bioessays* 1992;14:455-63.

(214) Murphy G, Docherty AJP. The Matrix Metalloproteinases and their inhibitors. *Amer J Respir Cell Molec Biol* 1992;7:120-5.

(215) Murphy G, Atkinson S, Ward R *et al*. The Role of Plasminogen Activators in the Regulation of Connective Tissue Metalloproteinases. *Annals of the New York Academy of Science* 1992;667:1-12.

(216) Sato H, Takino T, Okada Y *et al*. A matrix metalloproteinase expressed on the surface of invasive tumour cells. *Nature* 1994;370:61-5.

(217) Takino T, Sato H, Shinagawa A *et al*. Identification of the second membrane-type matrix metalloproteinase (MT-MMP-2) gene from a human placenta cDNA library. *J Biol Chem* 1995;270:23013-20.

(218) Will H, Hinzmann B. cDNA sequence and mRNA tissue distribution of a novel human matrix metalloproteinase with a potential transmembrane segment. *Eur J Biochem* 1995;231:602-8.

(219) Murphy G, Hembry RM, Hughes CE *et al*. Role and regulation of metalloproteinases in connective tissue turnover. *Biochem Soc Trans* 1990;18:812-5.

(220) Matrisian LM. Metalloproteinases and their inhibitors in matrix remodelling. *Trend Genet* 1990;6:121-5.

(221) Murphy G, Hembry RM. Proteinases in Rheumatoid Arthritis. *J Rheumatol* 1992;19:61-4.

(222) Nakatsukasa H, Evarts RP, Hsia CC *et al*. Transforming growth factor-beta 1 and type I procollagen transcripts during regeneration and early fibrosis of rat liver. *Lab Invest* 1990;63(2):171-80.

(223) De Bleser PJ, Jannes P, van Buul-Offers SC *et al*. Insulin-like growth factor-II/mannose 6-phosphate receptor is expressed on CCl_4-exposed rat fat-storing cells and facilitates activation of latent transforming growth factor-beta in cocultures with sinusoidal endothelial cells. *Hepatology* 1995;21:1429-37.

(224) Edwards DR, Murphy G, Reynolds JJ *et al*. Transforming growth factor beta modulates the expression of collagenase and metalloproteinase inhibitor. *EMBO J* 1987;6:1899-904.

(225) Overall CM, Wrana JL, Sudek J. Independent regulation of collagenase, 72kD progelatinase, and metalloendoproteinase inhibitor expression in human fibroblasts by transforming growth factor-beta. *J Biol Chem* 1989;264:1860-9.

(226) Wahl SM, Allen JB, Weeks BS *et al*. Transforming Growth Factor-beta Enhances Integrin Expression and Type-IV Collagenase Secretion in Human Monocytes. *Proc Natl Acad Sci USA* 1993;90:4577-81.

(227) Stetler-Stevenson WG, Brown PD, Onisto M *et al*. Tissue inhibitor of metalloproteinases-2 (TIMP-2) mRNA expression in tumor cell lines and human tumor tissues. *J Biol Chem* 1990;265:13933-8.

(228) Murphy G, Cockett MI, Stephens PE *et al*. Stromelysin is an activator of procollagenase. *Biochem J* 1987;248:265-8.

(229) Denhardt DT, Feng B, Edwards DR *et al*. Tissue inhibitor of metalloproteinases (TIMP, aka EPA) - structure, control of expression and biological functions. *Pharmacol Ther* 1993;59:329-41.

(230) Docherty AJP, Lyons A, Smith BJ *et al*. Sequence of human tissue inhibitor of metalloproteinases and its identity to erythroid-potentiating activity. *Nature* 1985;318:66-9.

(231) Boone TC, Johnson MJ, De Clerck YA *et al*. cDNA cloning and expression of a metalloproteinase inhibitor related to tissue inhibitor of metalloproteinases. *Proc Natl Acad Sci USA* 1990;87:2800-4.

(232) Pavloff N, Staskus PW, Kishnani NS *et al*. A New Inhibitor of Metalloproteinases from Chicken - ChIMP- 3 - A 3rd Member of the TIMP Family. *J Biol Chem* 1992;267:17321-6.

(233) Apte SS, Mattei MG, Olsen BR. Cloning of the cDNA Encoding Human Tissue Inhibitor of Metalloproteinases-3 (Timp-3) and Mapping of the Timp3 Gene to Chromosome 22. *Genomics* 1994;19:86-90.

(234) Friedman SL. Hepatic fibrosis -- overview. *Toxicology* 2008;254(3):120-9.

(235) Murphy G, Cawston TE, Reynolds JJ. An inhibitor of collagenase from human amniotic fluid. *Biochem J* 1981;195:167-70.

(236) Cawston TE, Murphy G, Mercer E *et al*. The interaction of purified rabbit bone collagenase with pruified rabbit bone metalloproteinase inhibitor. *Biochem J* 1983;211:313-8.

(237) Murphy G, Koklitis P, Carne AF. Dissociation of tissue inhibitor of metalloproteinases (TIMP) from enzyme complexes yields fully active inhibitor. *Biochem J* 1989;261:1031-4.

(238) Weber BHF, Vogt G, Pruett RC *et al*. Mutations in the tissue inhibitor of metalloproteinases-3 (TIMP3) in patients with Sorsby's fundus dystrophy. *Nat Genet* 1994;8:352-6.

(239) Leco KJ, Khokha R, Pavloff N *et al*. Tissue Inhibitor of Metalloproteinases-3 (Timp-3) Is an Extracellular Matrix-Associated Protein with a Distinctive Pattern of Expression in Mouse Cells and Tissues. *J Biol Chem* 1994;269:9352-60.

(240) Yu WH, Yu S, Meng Q *et al*. TIMP-3 binds to sulfated glycosaminoglycans of the extracellular matrix. *J Biol Chem* 2000;275(40):31226-32.

(241) Ahonen M, Poukkula M, Baker AH *et al*. Tissue inhibitor of metalloproteinases-3 induces apoptosis in melanoma cells by stabilization of death receptors. *Oncogene* 2003;22(14):2121-34.

(242) Mohammed FF, Smookler DS, Taylor SE *et al*. Abnormal TNF activity in Timp3-/- mice leads to chronic hepatic inflammation and failure of liver regeneration. *Nat Genet* 2004;36(9):969-77.

(243) Ward RV, Atkinson SJ, Slocombe PM *et al*. Tissue inhibitor of metalloproteinases-2 inhibits the activation of 72kDa progelatinase by fibroblast membranes. *Biochim Biophys Acta* 1991;1079:242-6.

(244) Howard EW, Banda MJ. Binding of tissue inhibitor of metalloproteinases 2 to two distinct sites on human 72-kDa gelatinase. *J Biol Chem* 1991;266:17972-7.

(245) Howard EW, Bullen EC, Banda MJ. Regulation of the autoactivation of human 72-kDa progelatinase by tissue inhibitor of metalloproteinases-2. *J Biol Chem* 1991;266:13064-9.

(246) Fridman R, Fuerst TR, Bird RE *et al*. Domain Structure of Human 72-kDa Gelatinase Type-IV Collagenase Characterization of Proteolytic Activity and Identification of the Tissue Inhibitor of Metalloproteinase-2 (TIMP-2) Binding Regions. *J Biol Chem* 1992;267:15398-405.

(247) De Clerck YA, Yean T-S, Lu HS *et al*. Inhibition of autoproteolytic activation of interstitial procollagenase by recombinant metalloproteinase inhibitor MI/TIMP-2. *J Biol Chem* 1991;266:3893-9.

(248) Edwards DR, Rocheleau H, Sharma RR *et al*. Involvement of AP-1 and PEA-3 binding sites in the regulation of murine tissue inhibitor of metalloproteinase-1 (TIMP-1) transcription. *Biochem Biophys Acta* 1992;171:41-55.

(249) Overall CM, Wrana JL, Sodek J. Transcriptional and post-transcriptional regulation of 72-kDa gelatinase/type IV collagenase by transforming growth factor-beta1 in human fibroblasts. *J Biol Chem* 1991;266:14064-71.

(250) Marshall BC, Santana A, Xu QP *et al*. Metalloproteinases and Tissue Inhibitor of Metalloproteinases in Mesothelial Cells - Cellular Differentiation Influences Expression. *J Clin Invest* 1993;91:1792-9.

(251) Schorpp M, Mattei M-G, Herr I *et al*. Structural organization and chromosomal localization of the mouse collagenase type I gene. *Biochem J* 1995;308:211-7.

(252) De Clerck YA, Darville MI, Eeckhout Y *et al*. Characterization of the promoter of the gene encoding human tissue inhibitor of metalloprpteomases-2 (TIMP-2). *Gene* 1994;139(2):185-91.

(253) Wick M, Haronen R, Mumberg D *et al*. Structure of the human TIMP-3 gene and its cell cycle-regulated promoter. *Biochem J* 1995;311:549-54.

(254) Okazaki I, Maruyama K. Collagenase activity in experimental hepatic fibrosis. *Nature* 1974;252(5478):49-50.

(255) Perez-Tamayo R, Montfort I, Gonzalez E. Collagenolytic activity in experimental cirrhosis of the liver. *Exp Mol Pathol* 1987;47:300-8.

(256) Maruyama K, Feinman L, Okazaki I *et al*. Direct measurement of neutral collagenase activity in homogenates from baboon and human liver. *Biochim Biophys Acta* 1981;658:121-31.

(257) Maruyama K, Feinman L, Fainsilber Z *et al*. Mammalian collagenase increases in early alcoholic liver disease and decreases with cirrhosis. *Life Sci* 1982;30(16):1379-84.

(258) Gieling RG, Burt AD, Mann DA. Fibrosis and cirrhosis reversibility - molecular mechanisms. *Clin Liver Dis* 2008;12(4):915-37, xi.

(259) Vyas SK, Leyland H, Gentry J *et al*. Rat hepatic lipocytes synthesize and secrete transin (stromelysin) in early primary culture. *Gastroenterology* 1995;109(3):889-98.

(260) Arthur MJ, Friedman SL, Roll FJ *et al*. Lipocytes from normal rat liver release a neutral metalloproteinase that degrades basement membrane (type IV) collagen. *J Clin Invest* 1989;84(4):1076-85.

(261) Arthur MJ, Stanley A, Iredale JP *et al*. Secretion of 72 kDa type IV collagenase/gelatinase by cultured human lipocytes. Analysis of gene expression, protein synthesis and proteinase activity. *Biochem J* 1992;287 (Pt 3):701-7.

(262) Iredale JP, Benyon RC, Arthur MJ *et al*. Tissue inhibitor of metalloproteinase-1 messenger RNA expression is enhanced relative to interstitial collagenase messenger RNA in experimental liver injury and fibrosis. *Hepatology* 1996;24(1):176-84.

(263) Herbst H, Heinrichs O, Schuppan D *et al*. Temporal and spatial patterns of transin/stromelysin RNA expression following toxic injury in rat liver. *Virchows Arch B Cell Pathol Incl Mol Pathol* 1991;60(5):295-300.

(264) Arthur MJP. Matrix degradation in the liver. In: Surrenti C, Casini A, Milani S, Pinzani M, editors. Fat-Storing Cells and Liver Fibrosis. Dordrecht: Kluwer Academic Publishers, 1994: 110-27.

(265) Emonard H, Guillouzo A, Lapiere CM *et al*. Human liver fibroblast capacity for synthesizing interstitial collagenase in vitro. *Cell Mol Biol* 1990;36(4):461-7.

(266) Iredale JP, Goddard S, Murphy G *et al*. Tissue inhibitor of metalloproteinase-I and interstitial collagenase expression in autoimmune chronic active hepatitis and activated human hepatic lipocytes. *Clin Sci (Colch)* 1995;89(1):75-81.

(267) Li JJ, Kim CI, Leo MA *et al*. Polyunsaturated Lecithin Prevents Acetaldehyde-Mediated Hepatic Collagen Accumulation by Stimulating Collagenase Activity in Cultured Lipocytes. *Hepatology* 1992;15:373-81.

(268) Iredale JP, Murphy G, Hembry RM *et al*. Human hepatic lipocytes synthesize tissue inhibitor of metalloproteinases-1. Implications for regulation of matrix degradation in liver. *J Clin Invest* 1992;90(1):282-7.

(269) Benyon RC, Iredale JP, Goddard S *et al*. Expression of tissue inhibitor of metalloproteinases 1 and 2 is increased in fibrotic human liver. *Gastroenterology* 1996;110(3):821-31.

(270) Kordula T, Guttgemann I, Rosejohn S *et al*. Synthesis of Tissue Inhibitor of Metalloproteinase-1 (TIMP- 1) in Human Hepatoma Cells (HepG2) - Up-Regulation by Interleukin-6 and Transforming Growth Factor-beta1. *FEBS Lett* 1992;313:143-7.

(271) Roeb E, Graeve L, Hoffmann R *et al*. Regulation of tissue inhibitor of metalloproteinases-1 gene expression by cytokines and dexamethasone in rat hepatocyte primary cultures. *Hepatology* 1993;18(6):1437-42.

(272) Takahashi S, Dunn MA, Seifter S. Liver collagenase in murine schistosomiasis. *Gastroenterology* 1980;78(6):1425-31.

(273) Takahashi S, Simpser E. Granuloma collagenase and EDTA-sensitive neutral protease production in hepatic murine schistosomiasis. *Hepatology* 1981;1(3):211-20.

(274) Truden JL, Boros DL. Detection of alpha 2-macroglobulin, alpha 1-protease inhibitor, and neutral protease-antiprotease complexes within liver granulomas of Schistosoma mansoni-infected mice. *Am J Pathol* 1988;130(2):281-8.

(275) Murawaki Y, Koda M, Yamada S *et al*. Serum collagenase activity in patients with chronic liver disease. *J Hepatol* 1993;18(3):328-34.

(276) Murawaki Y, Yamamoto H, Koda M *et al*. Serum collagenase activity reflects the amount of liver collagenase in chronic carbon tetrachloride-treated rats. *Res Commun Chem Pathol Pharmacol* 1994;84(1):63-72.

(277) Muzzillo DA, Imoto M, Fukuda Y *et al*. Clinical evaluation of serum tissue inhibitor of metalloproteinases-1 levels in patients with liver diseases. *J Gastroenterol Hepatol* 1993;8(5):437-41.

(278) Bissell DM, Caron JM, Babiss LE *et al*. Transcriptional regulation of the albumin gene in cultured rat hepatocytes. Role of basement-membrane matrix. *Mol Biol Med* 1990;7:187-97.

(279) Bissell DM, Arenson DM, Maher JJ *et al*. Support of cultured hepatocytes by a laminin-rich gel: evidence for a functionally significant subendothelial matrix in normal rat liver. *J Clin Invest* 1987;79:801-12.

(280) Dufour JF, DeLellis R, Kaplan MM. Regression of hepatic fibrosis in hepatitis C with long-term interferon treatment. *Dig Dis Sci* 1998;43(12):2573-6.

(281) Dufour JF, DeLellis R, Kaplan MM. Reversibility of hepatic fibrosis in autoimmune hepatitis. *Ann Intern Med* 1997;127(11):981-5.

(282) Niederau C, Fischer R, Sonnenberg A *et al*. Survival and causes of death in cirrhotic and in noncirrhotic patients with primary hemochromatosis. *N Engl J Med* 1985;313(20):1256-62.

(283) Sobesky R, Mathurin P, Charlotte F *et al*. Modeling the impact of interferon alfa treatment on liver fibrosis progression in chronic hepatitis C: a dynamic view. The Multivirc Group. *Gastroenterology* 1999;116(2):378-86.

(284) Abdel-Aziz G, Lebeau G, Rescan PY *et al*. Reversibility of hepatic fibrosis in experimentally induced cholestasis in rat. *Am J Pathol* 1990;137(6):1333-42.

(285) Iredale JP. Models of liver fibrosis: exploring the dynamic nature of inflammation and repair in a solid organ. *J Clin Invest* 2007;117(3):539-48.

(286) Iredale JP, Benyon RC, Pickering J *et al*. Mechanisms of spontaneous resolution of rat liver fibrosis. Hepatic stellate cell apoptosis and reduced hepatic expression of metalloproteinase inhibitors. *J Clin Invest* 1998;102(3):538-49.

(287) Desmouliere A, Redard M, Darby I *et al*. Apoptosis mediates the decrease in cellularity during the transition between granulation tissue and scar. *Am J Pathol* 1995;146:56-66.

(288) Saile B, Knittel T, Matthes N *et al*. CD95/CD95L-mediated apoptosis of the hepatic stellate cell. *Am J Pathol* 1997;151:1265-72.

(289) Gong W, Pecci A, Roth S *et al*. Transformation-dependent susceptibility of rat hepatic stellate cells to apoptosis induced by soluble Fas ligand. *Hepatology* 1998;28(2):492-502.

(290) Nilsson G, Forsberg-Nilsson K, Xiang Z *et al*. Human mast cells express functional TrkA and are a source of nerve growth factor. *Eur J Immunol* 1997;27(9):2295-301.

(291) Frisch SM, Francis H. Disruption of epithelial cell-matrix interactions induces apoptosis. *J Cell Biol* 1994;124(4):619-26.

(292) Iwamoto H, Sakai H, Tada S *et al*. Induction of apoptosis in rat hepatic stellate cells by disruption of integrin-mediated cell adhesion. *J Lab Clin Med* 1999;134:83-9.

(293) Mirza A, Liu SL, Frizell E *et al*. A role for tissue transglutaminase in hepatic injury and fibrogenesis, and its regulation by NF-kappaB. *Am J Physiol* 1997;272(2 Pt 1):G281-G288.

(294) Ricard-Blum S, Bresson-Hadni S, Guerret S *et al*. Mechanism of collagen network stabilization in human irreversible granulomatous liver fibrosis. *Gastroenterology* 1996;111(1):172-82.

(295) Carter EA, McCarron MJ, Alpert E *et al*. Lysyl oxidase and collagenase in experimental acute and chronic liver injury. *Gastroenterology* 1982;82(3):526-34.

(296) Issa R, Zhou X, Constandinou CM *et al*. Spontaneous recovery from micronodular cirrhosis: evidence for incomplete resolution associated with matrix cross-linking. *Gastroenterology* 2004;126(7):1795-808.

(297) Vater CA, Harris EDJr, Siegel RC. Native cross-links in collagen fibrils induce resistance to human synovial collagenase. *Biochem J* 1979;181:639-45.

(298) Piacentini M, Autuori F, Dini L *et al*. "Tissue" transglutaminase is specifically expressed in neonatal rat liver cells undergoing apoptosis upon epidermal growth factor- stimulation. *Cell Tissue Res* 1991;263(2):227-35.

(299) Montfort I, Perez-Tamayo R. Collagenase in experimental carbon tetrachloride cirrhosis of the liver. *Am J Pathol* 1978;92:411-20.

(300) Watari N, Hotta Y, Mabuchi Y. Morphological studies on a vitamin A-storing cell and its complex with macrophage observed in mouse pancreatic tissues following excess vitamin A administration. *Okajimas Folia Anat Jpn* 1982;58(4-6):837-58.

(301) Ikejiri N. The vitamin A-storing cells in the human and rat pancreas. *Kurume Med J* 1990;37(2):67-81.

(302) Apte MV, Haber PS, Applegate TL *et al*. Periacinar stellate shaped cells in rat pancreas: identification, isolation, and culture. *Gut* 1998;43(1):128-33.

(303) Bachem MG, Schneider E, Gross H *et al*. Identification, culture, and characterization of pancreatic stellate cells in rats and humans. *Gastroenterology* 1998;115:421-32.

(304) Whitcomb DC. Inflammation and Cancer V. Chronic pancreatitis and pancreatic cancer. *Am J Physiol Gastrointest Liver Physiol* 2004;287(2):G315-G319.

(305) Neuschwander-Tetri BA, Bridle KR, Wells LD *et al*. Repetitive acute pancreatic injury in the mouse induces procollagen alpha1(I) expression colocalized to pancreatic stellate cells. *Lab Invest* 2000;80(2):143-50.

(306) DiMagno MJ, Dimagno EP. Chronic pancreatitis. *Curr Opin Gastroenterol* 2005;21(5):544-54.

(307) Weiss FU, Simon P, Mayerle J *et al*. Germline mutations and gene polymorphism associated with human pancreatitis. *Endocrinol Metab Clin North Am* 2006;35(2):289-ix.

(308) Finkelberg DL, Sahani D, Deshpande V *et al*. Autoimmune pancreatitis. *N Engl J Med* 2006;355(25):2670-6.

(309) Lowenfels AB, Maisonneuve P, Cavallini G *et al*. Pancreatitis and the risk of pancreatic cancer. International Pancreatitis Study Group. *N Engl J Med* 1993;328(20):1433-7.

(310) Go VL, Gukovskaya A, Pandol SJ. Alcohol and pancreatic cancer. *Alcohol* 2005;35(3):205-11.

(311) Mathurin P, Xiong S, Kharbanda KK *et al*. IL-10 receptor and coreceptor expression in quiescent and activated hepatic stellate cells. *Am J Physiol Gastrointest Liver Physiol* 2002;282(6):G981-G990.

(312) Yen TW, Aardal NP, Bronner MP *et al*. Myofibroblasts are responsible for the desmoplastic reaction surrounding human pancreatic carcinomas. *Surgery* 2002;131(2):129-34.

(313) Logsdon CD, Simeone DM, Binkley C *et al*. Molecular profiling of pancreatic adenocarcinoma and chronic pancreatitis identifies multiple genes differentially regulated in pancreatic cancer. *Cancer Res* 2003;63(10):2649-57.

(314) Apte MV, Park S, Phillips PA *et al*. Desmoplastic reaction in pancreatic cancer: role of pancreatic stellate cells. *Pancreas* 2004;29(3):179-87.

(315) Schneider G, Siveke JT, Eckel F *et al*. Pancreatic cancer: basic and clinical aspects. *Gastroenterology* 2005;128(6):1606-25.

(316) Omary MB, Coulombe PA, McLean WH. Intermediate filament proteins and their associated diseases. *N Engl J Med* 2004;351(20):2087-100.

(317) Haber PS, Keogh GW, Apte MV *et al*. Activation of pancreatic stellate cells in human and experimental pancreatic fibrosis. *Am J Pathol* 1999;155:1087-95.

(318) Casini A, Galli A, Pignalosa P *et al*. Collagen type I synthesized by pancreatic periacinar stellate cells (PSC) co-localizes with lipid peroxidation-derived aldehydes in chronic alcoholic pancreatitis. *J Pathol* 2000;192(1):81-9.

(319) Lenzi HL, Romanha WS, Santos RM *et al*. Four whole-istic aspects of schistosome granuloma biology: fractal arrangement, internal regulation, autopoietic component and closure. *Mem Inst Oswaldo Cruz* 2006;101 Suppl 1:219-31.

(320) Saotome T, Inoue H, Fujimiya M *et al*. Morphological and immunocytochemical identification of periacinar fibroblast-like cells derived from human pancreatic acini. *Pancreas* 1997;14(4):373-82.

(321) Lardon J, Rooman I, Bouwens L. Nestin expression in pancreatic stellate cells and angiogenic endothelial cells. *Histochem Cell Biol* 2002;117(6):535-40.

(322) Pandol SJ. Are we studying the correct state of the stellate cell to elucidate mechanisms of chronic pancreatitis? *Gut* 2005;54(6):744-5.

(323) Manapov F, Muller P, Rychly J. Translocation of p21(Cip1/WAF1) from the nucleus to the cytoplasm correlates with pancreatic myofibroblast to fibroblast cell conversion. *Gut* 2005;54(6):814-22.

(324) Masamune A, Satoh M, Kikuta K *et al*. Establishment and characterization of a rat pancreatic stellate cell line by spontaneous immortalization. *World J Gastroenterol* 2003;9(12):2751-8.

(325) Sparmann G, Hohenadl C, Tornoe J *et al*. Generation and characterization of immortalized rat pancreatic stellate cells. *Am J Physiol Gastrointest Liver Physiol* 2004;287(1):G211-G219.

(326) Jesnowski R, Furst D, Ringel J *et al*. Immortalization of pancreatic stellate cells as an in vitro model of pancreatic fibrosis: deactivation is induced by matrigel and N-acetylcysteine. *Lab Invest* 2005;85(10):1276-91.

(327) Jaster R, Lichte P, Fitzner B *et al*. Peroxisome proliferator-activated receptor gamma overexpression inhibits pro-fibrogenic activities of immortalised rat pancreatic stellate cells. *J Cell Mol Med* 2005;9(3):670-82.

(328) Hassan Z, Mohan V, Ali L *et al*. SPINK1 is a susceptibility gene for fibrocalculous pancreatic diabetes in subjects from the Indian subcontinent. *Am J Hum Genet* 2002;71(4):964-8.

(329) Apte MV, Haber PS, Darby SJ *et al*. Pancreatic stellate cells are activated by proinflammatory cytokines: implications for pancreatic fibrogenesis. *Gut* 1999;44(4):534-41.

(330) Luttenberger T, Schmid-Kotsas A, Menke A *et al*. Platelet-derived growth factors stimulate proliferation and extracellular matrix synthesis of pancreatic stellate cells: implications in pathogenesis of pancreas fibrosis. *Lab Invest* 2000;80(1):47-55.

(331) Schneider E, Schmid-Kotsas A, Zhao J *et al*. Identification of mediators stimulating proliferation and matrix synthesis of rat pancreatic stellate cells. *Am J Physiol Cell Physiol* 2001;281(2):C532-C543.

(332) Mews P, Phillips P, Fahmy R *et al*. Pancreatic stellate cells respond to inflammatory cytokines: potential role in chronic pancreatitis. *Gut* 2002;50(4):535-41.

(333) Phillips PA, Wu MJ, Kumar RK *et al*. Cell migration: a novel aspect of pancreatic stellate cell biology. *Gut* 2003;52(5):677-82.

(334) Iwamoto H, Sakai H, Nawata H. Inhibition of integrin signaling with Arg-Gly-Asp motifs in rat hepatic stellate cells. *J Hepatol* 1998;29(5):752-9.

(335) Whitcomb D. Legal interventions for child victims. *J Trauma Stress* 2003;16(2):149-57.

(336) Nguyen TD, Wolfe MS, Heintz GG *et al*. High affinity binding proteins for pancreatic polypeptide on rat liver membranes. *J Biol Chem* 1992;267(13):9416-21.

(337) Xu J, Lee G, Wang H *et al*. Limited role for CXC chemokines in the pathogenesis of alpha-naphthylisothiocyanate-induced liver injury. *Am J Physiol Gastrointest Liver Physiol* 2004;287(3):G734-G741.

(338) Whitcomb DC. Genetic predispositions to acute and chronic pancreatitis. *Med Clin North Am* 2000;84(3):531-47, vii.

(339) Gao R, Brigstock DR. Connective tissue growth factor (CCN2) in rat pancreatic stellate cell function: integrin alpha5beta1 as a novel CCN2 receptor. *Gastroenterology* 2005;129(3):1019-30.

(340) Aoki H, Ohnishi H, Hama K *et al*. Cyclooxygenase-2 is required for activated pancreatic stellate cells to respond to proinflammatory cytokines. *Am J Physiol Cell Physiol* 2007;292(1):C259-C268.

(341) Ohnishi N, Miyata T, Ohnishi H *et al*. Activin A is an autocrine activator of rat pancreatic stellate cells: potential therapeutic role of follistatin for pancreatic fibrosis. *Gut* 2003;52(10):1487-93.

(342) Masamune A, Satoh M, Kikuta K *et al*. Endothelin-1 stimulates contraction and migration of rat pancreatic stellate cells. *World J Gastroenterol* 2005;11(39):6144-51.

(343) Menke A, Adler G. TGFbeta-induced fibrogenesis of the pancreas. *Int J Gastrointest Cancer* 2002;31(1-3):41-6.

(344) Jaster R. Molecular regulation of pancreatic stellate cell function. *Mol Cancer* 2004;3:26.

(345) Apte MV, Wilson JS. Mechanisms of pancreatic fibrosis. *Dig Dis* 2004;22(3):273-9.

(346) Apte MV, Pirola RC, Wilson JS. Battle-scarred pancreas: role of alcohol and pancreatic stellate cells in pancreatic fibrosis. *J Gastroenterol Hepatol* 2006;21 Suppl 3:S97-S101.

(347) Pandol S. Alcohol, reactive oxygen species, pancreatitis and pancreatic cancer. In: Cho C, Purohit V, editors. Alcohol, Tobacco, and Cancer. Basil, Switzerland: Karger, 2006: 109-18.

(348) Hama K, Ohnishi H, Aoki H *et al*. Angiotensin II promotes the proliferation of activated pancreatic stellate cells by Smad7 induction through a protein kinase C pathway. *Biochem Biophys Res Commun* 2006;340(3):742-50.

(349) Kuno A, Yamada T, Masuda K *et al*. Angiotensin-converting enzyme inhibitor attenuates pancreatic inflammation and fibrosis in male Wistar Bonn/Kobori rats. *Gastroenterology* 2003;124(4):1010-9.

(350) Ohnishi H, Miyata T, Yasuda H *et al*. Distinct roles of Smad2-, Smad3-, and ERK-dependent pathways in transforming growth factor-beta1 regulation of pancreatic stellate cellular functions. *J Biol Chem* 2004;279(10):8873-8.

(351) Kikuta K, Masamune A, Satoh M *et al*. Hydrogen peroxide activates activator protein-1 and mitogen-activated protein kinases in pancreatic stellate cells. *Mol Cell Biochem* 2006;291(1-2):11-20.

(352) Masamune A, Kikuta K, Suzuki N *et al*. A c-Jun NH2-terminal kinase inhibitor SP600125 (anthra[1,9-cd]pyrazole-6 (2H)-one) blocks activation of pancreatic stellate cells. *J Pharmacol Exp Ther* 2004;310(2):520-7.

(353) Stevens T, Conwell DL, Zuccaro G. Pathogenesis of chronic pancreatitis: an evidence-based review of past theories and recent developments. *Am J Gastroenterol* 2004;99(11):2256-70.

(354) Ruthenburger M, Mayerle J, Lerch MM. Cell biology of pancreatic proteases. *Endocrinol Metab Clin North Am* 2006;35(2):313-31, ix.

(355) Apte MV, Wilson JS. Stellate cell activation in alcoholic pancreatitis. *Pancreas* 2003;27(4):316-20.

(356) Bentrem DJ, Joehl RJ. Pancreas: healing response in critical illness. *Crit Care Med* 2003;31(8 Suppl):S582-S589.

(357) Kloppel G, Detlefsen S, Feyerabend B. Fibrosis of the pancreas: the initial tissue damage and the resulting pattern. *Virchows Arch* 2004;445(1):1-8.

(358) Yokota T, Denham W, Murayama K *et al*. Pancreatic stellate cell activation and MMP production in experimental pancreatic fibrosis. *J Surg Res* 2002;104(2):106-11.

(359) Zimmermann A, Gloor B, Kappeler A *et al*. Pancreatic stellate cells contribute to regeneration early after acute necrotising pancreatitis in humans. *Gut* 2002;51(4):574-8.

(360) Lugea A, Nan L, French SW *et al*. Pancreas recovery following cerulein-induced pancreatitis is impaired in plasminogen-deficient mice. *Gastroenterology* 2006;131(3):885-99.

(361) Gibo J, Ito T, Kawabe K *et al*. Camostat mesilate attenuates pancreatic fibrosis via inhibition of monocytes and pancreatic stellate cells activity. *Lab Invest* 2005;85(1):75-89.

(362) Nagashio Y, Asaumi H, Watanabe S *et al*. Angiotensin II type 1 receptor interaction is an important regulator for the development of pancreatic fibrosis in mice. *Am J Physiol Gastrointest Liver Physiol* 2004;287(1):G170-G177.

(363) Andoh A, Takaya H, Saotome T *et al*. Cytokine regulation of chemokine (IL-8, MCP-1, and RANTES) gene expression in human pancreatic periacinar myofibroblasts. *Gastroenterology* 2000;119(1):211-9.

(364) Masamune A, Kikuta K, Satoh M *et al*. Alcohol activates activator protein-1 and mitogen-activated protein kinases in rat pancreatic stellate cells. *J Pharmacol Exp Ther* 2002;302(1):36-42.

(365) Sparmann G, Glass A, Brock P *et al*. Inhibition of lymphocyte apoptosis by pancreatic stellate cells: impact of interleukin-15. *Am J Physiol Gastrointest Liver Physiol* 2005;289(5):G842-G851.

(366) Aoki H, Ohnishi H, Hama K *et al*. Autocrine loop between TGF-beta1 and IL-1beta through Smad3- and ERK-dependent pathways in rat pancreatic stellate cells. *Am J Physiol Cell Physiol* 2006;290(4):C1100-C1108.

(367) Shimizu K, Kobayashi M, Tahara J *et al*. Cytokines and peroxisome proliferator-activated receptor gamma ligand regulate phagocytosis by pancreatic stellate cells. *Gastroenterology* 2005;128(7):2105-18.

(368) Kishi S, Takeyama Y, Ueda T *et al*. Pancreatic duct obstruction itself induces expression of alpha smooth muscle actin in pancreatic stellate cells. *J Surg Res* 2003;114(1):6-14.

(369) Demols A, Van Laethem JL, Quertinmont E *et al*. Endogenous interleukin-10 modulates fibrosis and regeneration in experimental chronic pancreatitis. *Am J Physiol Gastrointest Liver Physiol* 2002;282(6):G1105-G1112.

(370) Phillips PA, McCarroll JA, Park S *et al*. Rat pancreatic stellate cells secrete matrix metalloproteinases: implications for extracellular matrix turnover. *Gut* 2003;52(2):275-82.

(371) Bissell DM. Hepatic fibrosis as wound repair: a progress report. *J Gastroenterol* 1998;33(2):295-302.

(372) Friedman SL, Bansal MB. Reversal of hepatic fibrosis -- fact or fantasy? *Hepatology* 2006;43(2 Suppl 1):S82-S88.

(373) Perides G, Tao X, West N *et al*. A mouse model of ethanol dependent pancreatic fibrosis. *Gut* 2005;54(10):1461-7.

(374) Whitcomb DC. Mechanisms of disease: Advances in understanding the mechanisms leading to chronic pancreatitis. *Nat Clin Pract Gastroenterol Hepatol* 2004;1(1):46-52.

(375) Masamune A, Kikuta K, Satoh M *et al*. Protease-activated receptor-2-mediated proliferation and collagen production of rat pancreatic stellate cells. *J Pharmacol Exp Ther* 2005;312(2):651-8.

(376) Amann ST, Gates LK, Aston CE *et al*. Expression and penetrance of the hereditary pancreatitis phenotype in monozygotic twins. *Gut* 2001;48(4):542-7.

(377) Jemal A, Siegel R, Ward E *et al*. Cancer statistics, 2006. *CA Cancer J Clin* 2006;56(2):106-30.

(378) Mollenhauer J, Roether I, Kern HF. Distribution of extracellular matrix proteins in pancreatic ductal adenocarcinoma and its influence on tumor cell proliferation in vitro. *Pancreas* 1987;2(1):14-24.

(379) Armstrong T, Packham G, Murphy LB *et al*. Type I collagen promotes the malignant phenotype of pancreatic ductal adenocarcinoma. *Clin Cancer Res* 2004;10(21):7427-37.

(380) Binkley CE, Zhang L, Greenson JK *et al*. The molecular basis of pancreatic fibrosis: common stromal gene expression in chronic pancreatitis and pancreatic adenocarcinoma. *Pancreas* 2004;29(4):254-63.

(381) Koninger J, Giese T, di Mola FF *et al*. Pancreatic tumor cells influence the composition of the extracellular matrix. *Biochem Biophys Res Commun* 2004;322(3):943-9.

(382) Yoshida S, Yokota T, Ujiki M *et al*. Pancreatic cancer stimulates pancreatic stellate cell proliferation and TIMP-1 production through the MAP kinase pathway. *Biochem Biophys Res Commun* 2004;323(4):1241-5.

(383) Bachem MG, Schunemann M, Ramadani M *et al*. Pancreatic carcinoma cells induce fibrosis by stimulating proliferation and matrix synthesis of stellate cells. *Gastroenterology* 2005;128(4):907-21.

(384) Li G, Xie Q, Shi Y *et al*. Inhibition of connective tissue growth factor by siRNA prevents liver fibrosis in rats. *J Gene Med* 2006;8(7):889-900.

(385) Watanabe I, Hasebe T, Sasaki S *et al*. Advanced pancreatic ductal cancer: fibrotic focus and beta-catenin expression correlate with outcome. *Pancreas* 2003;26(4):326-33.

(386) Hartel M, di Mola FF, Gardini A *et al*. Desmoplastic reaction influences pancreatic cancer growth behavior. *World J Surg* 2004;28(8):818-25.

(387) Vaquero EC, Edderkaoui M, Nam KJ *et al*. Extracellular matrix proteins protect pancreatic cancer cells from death via mitochondrial and nonmitochondrial pathways. *Gastroenterology* 2003;125(4):1188-202.

(388) Edderkaoui M, Hong P, Vaquero EC *et al*. Extracellular matrix stimulates reactive oxygen species production and increases pancreatic cancer cell survival through 5-lipoxygenase and NADPH oxidase. *Am J Physiol Gastrointest Liver Physiol* 2005;289(6):G1137-G1147.

(389) Vaquero EC, Edderkaoui M, Pandol SJ *et al*. Reactive oxygen species produced by NAD(P)H oxidase inhibit apoptosis in pancreatic cancer cells. *J Biol Chem* 2004;279(33):34643-54.

(390) Munshi HG, Stack MS. Reciprocal interactions between adhesion receptor signaling and MMP regulation. *Cancer Metastasis Rev* 2006;25(1):45-56.

(391) Yamamoto H, Itoh F, Adachi Y *et al*. Relation of enhanced secretion of active matrix metalloproteinases with tumor spread in human hepatocellular carcinoma. *Gastroenterology* 1997;112(4):1290-6.

(392) Sternlicht MD, Werb Z. How matrix metalloproteinases regulate cell behavior. *Annu Rev Cell Dev Biol* 2001;17:463-516.

(393) Liotta LA, Kohn EC. The microenvironment of the tumour-host interface. *Nature* 2001;411(6835):375-9.

(394) Buchholz M, Kestler HA, Holzmann K *et al*. Transcriptome analysis of human hepatic and pancreatic stellate cells: organ-specific variations of a common transcriptional phenotype. *J Mol Med* 2005;83(10):795-805.

(395) Russo FP, Alison MR, Bigger BW *et al*. The bone marrow functionally contributes to liver fibrosis. *Gastroenterology* 2006;130(6):1807-21.

(396) Knittel T, Kobold D, Piscaglia F *et al*. Localization of liver myofibroblasts and hepatic stellate cells in normal and diseased rat livers: distinct roles of (myo-)fibroblast subpopulations in hepatic tissue repair. *Histochem Cell Biol* 1999;112(5):387-401.

(397) Uchio K, Tuchweber B, Manabe N *et al*. Cellular retinol-binding protein-1 expression and modulation during in vivo and in vitro myofibroblastic differentiation of rat hepatic stellate cells and portal fibroblasts. *Lab Invest* 2002;82(5):619-28.

(398) Baba S, Fujii H, Hirose T *et al*. Commitment of bone marrow cells to hepatic stellate cells in mouse. *J Hepatol* 2004;40(2):255-60.

(399) Panasiuk A, Prokopowicz D, Zak J *et al*. Activation of blood platelets in chronic hepatitis and liver cirrhosis P-selectin expression on blood platelets and secretory activity of beta- thromboglobulin and platelet factor-4. *Hepatogastroenterology* 2001;48(39):818-22.

(400) Waechter FL, Sampaio JA, Pinto RD *et al*. The role of liver transplantation in patients with Caroli's disease. *Hepatogastroenterology* 2001;48(39):672-4.

(401) Vleggaar FP, van Buuren HR, Zondervan PE *et al*. Jaundice in non-cirrhotic primary biliary cirrhosis: the premature ductopenic variant. *Gut* 2001;49(2):276-81.

(402) Tsukamoto H. Adipogenic phenotype of hepatic stellate cells. *Alcohol Clin Exp Res* 2005;29(11 Suppl):132S-3S.

(403) Ong JP, Younossi ZM, Speer C *et al*. Chronic hepatitis C and superimposed nonalcoholic fatty liver disease. *Liver* 2001;21(4):266-71.

(404) Herold C, Heinz R, Niedobitek G *et al*. Quantitative testing of liver function in relation to fibrosis in patients with chronic hepatitis B and C. *Liver* 2001;21(4):260-5.

(405) Yeo AE, Ghany M, Conry-Cantilena C *et al*. Stability of HCV-RNA level and its lack of correlation with disease severity in asymptomatic chronic hepatitis C virus carriers. *J Viral Hepat* 2001;8(4):256-63.

(406) Myers RP, Hilsden RJ, Lee SS. Historical features are poor predictors of liver fibrosis in Canadian patients with chronic hepatitis C. *J Viral Hepat* 2001;8(4):249-55.

(407) Pugh CW. Oxygen and genes in health and disease. *QJM* 1997;90(5):307-10.

(408) Goldberg MA, Glass GA, Cunningham JM *et al*. The regulated expression of erythropoietin by two human hepatoma cell lines. *Proc Natl Acad Sci U S A* 1987;84(22):7972-6.

(409) Beck I, Ramirez S, Weinmann R *et al*. Enhancer element at the 3'-flanking region controls transcriptional response to hypoxia in the human erythropoietin gene. *J Biol Chem* 1991;266(24):15563-6.

(410) Olsson R, Bliding A, Jagenburg R *et al*. Gilbert's syndrome - does it exist? A study of the prevalence of symptoms in Gilbert's syndrome. *Acta Med Scand* 1988;224:485-90.

(411) Semenza GL, Nejfelt MK, Chi SM *et al*. Hypoxia-inducible nuclear factors bind to an enhancer element located 3' to the human erythropoietin gene. *Proc Natl Acad Sci U S A* 1991;88(13):5680-4.

(412) Pugh CW, Ebert BL, Ebrahim O *et al*. Analysis of cis-acting sequences required for operation of the erythropoietin 3' enhancer in different cell lines. *Ann N Y Acad Sci* 1994;718:31-9.

(413) Maxwell PH, Pugh CW, Ratcliffe PJ. Inducible operation of the erythropoietin 3' enhancer in multiple cell lines: evidence for a widespread oxygen-sensing mechanism. *Proc Natl Acad Sci U S A* 1993;90(6):2423-7.

(414) Wang GL, Semenza GL. General involvement of hypoxia-inducible factor 1 in transcriptional response to hypoxia. *Proc Natl Acad Sci U S A* 1993;90(9):4304-8.

(415) Firth JD, Ebert BL, Pugh CW *et al*. Oxygen-regulated control elements in the phosphoglycerate kinase 1 and lactate dehydrogenase A genes: similarities with the erythropoietin 3' enhancer. *Proc Natl Acad Sci U S A* 1994;91(14):6496-500.

(416) Bunn HF, Poyton RO. Oxygen sensing and molecular adaptation to hypoxia. *Physiol Rev* 1996;76(3):839-85.

(417) Ebert BL, Firth JD, Ratcliffe PJ. Hypoxia and mitochondrial inhibitors regulate expression of glucose transporter-1 via distinct Cis-acting sequences. *J Biol Chem* 1995;270(49):29083-9.

(418) O'Rourke JF, Pugh CW, Bartlett SM *et al*. Identification of hypoxically inducible mRNAs in HeLa cells using differential-display PCR. Role of hypoxia-inducible factor-1. *Eur J Biochem* 1996;241(2):403-10.

(419) Nauck M, Wolfle D, Katz N *et al*. Modulation of the glucagon-dependent induction of phosphoenolpyruvate carboxykinase and tyrosine aminotransferase by arterial and venous oxygen concentrations in hepatocyte cultures. *Eur J Biochem* 1981;119(3):657-61.

(420) Goldberg MA, Schneider TJ. Similarities between the oxygen-sensing mechanisms regulating the expression of vascular endothelial growth factor and erythropoietin. *J Biol Chem* 1994;269(6):4355-9.

(421) Melillo G, Musso T, Sica A *et al*. A hypoxia-responsive element mediates a novel pathway of activation of the inducible nitric oxide synthase promoter. *J Exp Med* 1995;182(6):1683-93.

(422) Kourembanas S, Marsden PA, McQuillan LP *et al*. Hypoxia induces endothelin gene expression and secretion in cultured human endothelium. *J Clin Invest* 1991;88(3):1054-7.

(423) Estes SD, Stoler DL, Anderson GR. Anoxic induction of a sarcoma virus-related VL30 retrotransposon is mediated by a cis-acting element which binds hypoxia-inducible factor 1 and an anoxia-inducible factor. *J Virol* 1995;69(10):6335-41.

(424) Czyzyk-Krzeska MF, Bendixen AC. Identification of the poly(C) binding protein in the complex associated with the 3' untranslated region of erythropoietin messenger RNA. *Blood* 1999;93(6):2111-20.

(425) Wang GL, Jiang BH, Rue EA *et al*. Hypoxia-inducible factor 1 is a basic-helix-loop-helix-PAS heterodimer regulated by cellular O2 tension. *Proc Natl Acad Sci U S A* 1995;92(12):5510-4.

(426) Taylor DR, Shi ST, Romano PR *et al*. Inhibition of the interferon-inducible protein kinase PKR by HCV E2 protein. *Science* 1999;285:107-10.

(427) Tian H, McKnight SL, Russell DW. Endothelial PAS domain protein 1 (EPAS1), a transcription factor selectively expressed in endothelial cells. *Genes Dev* 1997;11(1):72-82.

(428) Huang LE, Arany Z, Livingston DM *et al*. Activation of hypoxia-inducible transcription factor depends primarily upon redox-sensitive stabilization of its alpha subunit. *J Biol Chem* 1996;271(50):32253-9.

(429) Pugh CW, O'Rourke JF, Nagao M *et al*. Activation of hypoxia-inducible factor-1; definition of regulatory domains within the alpha subunit. *J Biol Chem* 1997;272(17):11205-14.

(430) Arany Z, Huang LE, Eckner R *et al*. An essential role for p300/CBP in the cellular response to hypoxia. *Proc Natl Acad Sci U S A* 1996;93(23):12969-73.

(431) Kvietikova I, Wenger RH, Marti HH *et al*. The transcription factors ATF-1 and CREB-1 bind constitutively to the hypoxia-inducible factor-1 (HIF-1) DNA recognition site. *Nucleic Acids Res* 1995;23(22):4542-50.

(432) Goldberg MA, Dunning SP, Bunn HF. Regulation of the erythropoietin gene: evidence that the oxygen sensor is a heme protein. *Science* 1988;242(4884):1412-5.

(433) Shi YF, Fong CC, Zhang Q *et al*. Hypoxia induces the activation of human hepatic stellate cells LX-2 through TGF-beta signaling pathway. *FEBS Lett* 2007;581(2):203-10.

(434) Siegmund SV, Brenner DA. Molecular pathogenesis of alcohol-induced hepatic fibrosis. *Alcohol Clin Exp Res* 2005;29(11 Suppl):102S-9S.

(435) Siegmund SV, Dooley S, Brenner DA. Molecular mechanisms of alcohol-induced hepatic fibrosis. *Dig Dis* 2005;23(3-4):264-74.

(436) Ankoma-Sey V, Wang Y, Dai Z. Hypoxic stimulation of vascular endothelial growth factor expression in activated rat hepatic stellate cells. *Hepatology* 2000;31:141-8.

(437) Chen P, Zhai W, Zhang Y *et al*. [Effects of hypoxia on expression and activity of matrix metalloproteinase-2 in hepatic stellate cell]. *Zhonghua Gan Zang Bing Za Zhi* 2000;8(5):276-8.

(438) Chen P, Zhai W, Zhang Y *et al*. [Effects of hypoxia and hyperoxia on the regulation of the expression and activity of matrix metalloproteinase-2 in hepatic stellate cell]. *Zhonghua Bing Li Xue Za Zhi* 2002;31(4):337-41.

(439) Benyon RC, Arthur MJ. Mechanisms of hepatic fibrosis. *J Pediatr Gastroenterol Nutr* 1998;27(1):75-85.

(440) Hovell CJ, Benyon RC, Pawley S *et al*. Membrane-type I matrix metalloproteinase in rat hepatic stellate cells and fibrotic liver: temporal correlation with gelatinase A activation. *Hepatology* 1997;Submitted.

(441) Shi SR, Key ME, Kalra KL. Antigen retrieval in formalin-fixed, paraffin-embedded tissues: an enhancement method for immunohistochemical staining based on microwave oven heating of tissue sections. *J Histochem Cytochem* 1991;39(6):741-8.

(442) Cattoretti G. Standardization and reproducibility in diagnostic immunohistochemistry. *Hum Pathol* 1994;25(10):1107-9.

(443) Iczkowski KA, Cheng L, Crawford BG *et al*. Steam heat with an EDTA buffer and protease digestion optimizes immunohistochemical expression of basal cell-specific antikeratin 34betaE12 to discriminate cancer in prostatic epithelium. *Mod Pathol* 1999;12(1):1-4.

(444) Prooijen-Knegt AC, Raap AK, van der Burg MJ *et al*. Spreading and staining of human metaphase chromosomes on aminoalkylsilane-treated glass slides. *Histochem J* 1982;14(2):333-44.

(445) Cattoretti G, Pileri S, Parravicini C *et al*. Antigen unmasking on formalin-fixed, paraffin-embedded tissue sections. *J Pathol* 1993;171(2):83-98.

(446) Norton AJ, Jordan S, Yeomans P. Brief, high-temperature heat denaturation (pressure cooking): a simple and effective method of antigen retrieval for routinely processed tissues. *J Pathol* 1994;173(4):371-9.

(447) Brooks DA, Zola H, McNamara PJ *et al*. Membrane antigens of human cells of the monocyte/macrophage lineage studied with monoclonal antibodies. *Pathology* 1983;15(1):45-52.

(448) Mepham BL, Britten KJM. Immunostaining methods for frozen and paraffin sections. In: Jones DB, Wright DH, editors. Lymphoproliferative diseases. London: Kluwer Academic Publishers, 1990: 187-211.

(449) Bonis PA, Friedman SL, Kaplan MM. Is liver fibrosis reversible? *N Engl J Med* 2001;344(6):452-4.

(450) Hammel P, Couvelard A, O'Toole D *et al*. Regression of liver fibrosis after biliary drainage in patients with chronic pancreatitis and stenosis of the common bile duct. *N Engl J Med* 2001;344(6):418-23.

(451) Castaldo G, Fuccio A, Salvatore D *et al*. Liver expression in cystic fibrosis could be modulated by genetic factors different from the cystic fibrosis transmembrane regulator genotype. *Am J Med Genet* 2001;98(4):294-7.

(452) Achiron R, Hegesh J, Yagel S *et al*. Abnormalities of the fetal central veins and umbilico-portal system: prenatal ultrasonographic diagnosis and proposed classification. *Ultrasound Obstet Gynecol* 2000;16(6):539-48.

(453) Gordon SC. Extrahepatic manifestations of hepatitis C. *Dig Dis* 1996;14(3):157-68.

(454) Zen Y, Katayanagi K, Tsuneyama K *et al*. Hepatocellular carcinoma arising in non-alcoholic steatohepatitis. *Pathol Int* 2001;51(2):127-31.

(455) Chatterjee S, Van Marck E. The role of somatostatin in schistosomiasis: a basis for immunomodulation in host-parasite interactions? *Trop Med Int Health* 2001;6(8):578-81.

(456) Svegliati-Baroni G, Saccomanno S, van Goor H *et al*. Involvement of reactive oxygen species and nitric oxide radicals in activation and proliferation of rat hepatic stellate cells. *Liver* 2001;21(1):1-12.

(457) Nakamura I, Imawari M. [Interferon-treated hepatitis C virus(HCV) patients with sustained biochemical response without eradication of HCV(asymptomatic HCV carrier)]. *Nippon Rinsho* 2001;59(7):1284-8.

(458) Donohue TM, Jr., Clemens DL, Galli A *et al*. Use of cultured cells in assessing ethanol toxicity and ethanol-related metabolism. *Alcohol Clin Exp Res* 2001;25(5 Suppl ISBRA):87S-93S.

(459) Hohler T, Leininger S, Kohler HH *et al*. Heterozygosity for the hemochromatosis gene in liver diseases-- prevalence and effects on liver histology. *Liver* 2000;20(6):482-6.

(460) Zachariae H, Heickendorff L, Sogaard H. The value of amino-terminal propeptide of type III procollagen in routine screening for methotrexate-induced liver fibrosis: a 10-year follow-up. *Br J Dermatol* 2001;144(1):100-3.

(461) Wali M, Lewis S, Hubscher S *et al*. Histological progression during short-term follow-up of patients with chronic hepatitis C virus infection. *J Viral Hepat* 1999;6(6):445-52.

(462) Valls C, Andia E, Sanchez A *et al*. Hepatic metastases from colorectal cancer: preoperative detection and assessment of resectability with helical CT. *Radiology* 2001;218(1):55-60.

(463) Cipolli M, D'Orazio C, Delmarco A *et al*. Shwachman's syndrome: pathomorphosis and long-term outcome. *J Pediatr Gastroenterol Nutr* 1999;29(3):265-72.

(464) Tamiolakis D, Papadopoulos N, Karamanidis D *et al*. The immunophenotypic profile of hepatic hemopoiesis in fetuses with Down's syndrome during the second trimester of development. *Clin Exp Obstet Gynecol* 2001;28(3):153-6.

(465) Li L, Tao J, Davaille J *et al*. 15-deoxy-delta 12,14-prostaglandin J2 induces apoptosis of human hepatic myofibroblasts. A pathway involving oxidative stress independently of peroxisome-proliferator-activated receptors. *J Biol Chem* 2001.

(466) Koehler DR, Hannam V, Belcastro R *et al*. Targeting transgene expression for cystic fibrosis gene therapy. *Mol Ther* 2001;4(1):58-65.

(467) Fabris C, Toniutto P, Scott CA *et al*. Serum iron indices as a measure of iron deposits in chronic hepatitis C. *Clin Chim Acta* 2001;304(1-2):49-55.

(468) Santra A, Maiti A, Das S *et al*. Hepatic damage caused by chronic arsenic toxicity in experimental animals. *J Toxicol Clin Toxicol* 2000;38(4):395-405.

(469) Hasegawa T, Sasaki T, Kimura T *et al*. Measurement of serum hyaluronic acid as a sensitive marker of liver fibrosis in biliary atresia. *J Pediatr Surg* 2000;35(11):1643-6.

(470) Saile B, Matthes N, El Armouche H *et al*. The bcl, NFkappaB and p53/p21WAF1 systems are involved in spontaneous apoptosis and in the anti-apoptotic effect of TGF-beta or TNF-alpha on activated hepatic stellate cells. *Eur J Cell Biol* 2001;80(8):554-61.

(471) Ozaki K, Mahler JF, Haseman JK *et al*. Unique renal tubule changes induced in rats and mice by the peroxisome proliferators 2,4-dichlorophenoxyacetic acid (2,4-D) and WY-14643. *Toxicol Pathol* 2001;29(4):440-50.

(472) Williams EJ, Benyon RC, Trim N *et al*. Relaxin inhibits effective collagen deposition by cultured hepatic stellate cells and decreases rat liver fibrosis in vivo. *Gut* 2001;49(4):577-83.

(473) Abina MA, Tulliez M, Lacout C *et al*. Major effects of TPO delivered by a single injection of a recombinant adenovirus on prevention of septicemia and anemia associated with myelosuppression in mice: risk of sustained expression inducing myelofibrosis due to immunosuppression. *Gene Ther* 1998;5(4):497-506.

(474) Melgert BN, Olinga P, Weert B *et al*. Cellular distribution and handling of liver-targeting preparations in human livers studied by a liver lobe perfusion. *Drug Metab Dispos* 2001;29(4 Pt 1):361-7.

(475) Montes S, Alcaraz-Zubeldia M, Muriel P *et al*. Striatal manganese accumulation induces changes in dopamine metabolism in the cirrhotic rat. *Brain Res* 2001;891(1-2):123-9.

(476) George J, Rao KR, Stern R *et al*. Dimethylnitrosamine-induced liver injury in rats: the early deposition of collagen. *Toxicology* 2001;156(2-3):129-38.

(477) Munoz dB, Ibarrola C, Colina F *et al*. Fibrosing cholestatic hepatitis in hepatitis C virus-infected renal transplant recipients. *J Am Soc Nephrol* 1998;9(6):1109-13.

(478) Gorka W, Lewall DB. Value of Doppler sonography in the assessment of patients with Caroli's disease. *J Clin Ultrasound* 1998;26(6):283-7.

(479) Bendayan M, Duhr M-A, Gingras D. Studies on pancreatic acinar cells in tissue culture: basal lamina (basement membrane) matrix promotes three-dimensional reorganization. *Eur J Cell Biol* 1986;42:60-7.

(480) Fedorcsak I, Ehrenberg L, Solymosy F. Diethyl pyrocarbonate does not degrade RNA. *Biochem Biophys Res Commun* 1975;65(2):490-6.

(481) Chomczynski P, Sacchi N. Single-step method of RNA isolation by acid guanidinium thiocyanate-phenol-chloroform extraction. *Anal Biochem* 1987;162:156-9.

(482) Zinn K, DiMaio D, Maniatis T. Identification of two distinct regulatory regions adjacent to the human beta-interferon gene. *Cell* 1983;34(3):865-79.

(483) Anderson L, Seilhamer J. A comparison of selected mRNA and protein abundances in human liver. *Electrophoresis* 1997;18(3-4):533-7.

(484) Lee JJ, Costlow NA. A molecular titration assay to measure transcript prevalence levels. *Methods Enzymol* 1987;152:633-48.

(485) Birnboim HC, Doly J. A rapid alkaline extraction procedure for screening recombinant plasmid DNA. *Nucleic Acids Res* 1979;7(6):1513-23.

(486) Birnboim HC. A rapid alkaline extraction method for the isolation of plasmid DNA. *Methods Enzymol* 1983;100:243-55.

(487) Vaheri A, Pagano JS. Infectious poliovirus RNA: a sensitive method of assay. *Virology* 1965;27(3):434-6.

(488) Graham FL, van der Eb AJ. A new technique for the assay of infectivity of human adenovirus 5 DNA. *Virology* 1973;52(2):456-67.

(489) Gorman CM, Moffat LF, Howard BH. Recombinant genomes which express chloramphenicol acetyltransferase in mammalian cells. *Mol Cell Biol* 1982;2:1044-51.

(490) Hollon T, Yoshimura FK. Variation in enzymatic transient gene expression assays. *Anal Biochem* 1989;182(2):411-8.

(491) Wood KV. Marker proteins for gene expression. *Curr Opin Biotechnol* 1995;6(1):50-8.

(492) de Wet JR, Wood KV, Helinski DR *et al*. Cloning of firefly luciferase cDNA and the expression of active luciferase in Escherichia coli. *Proc Natl Acad Sci U S A* 1985;82(23):7870-3.

(493) de Wet JR, Wood KV, DeLuca M *et al*. Firefly luciferase gene: structure and expression in mammalian cells. *Mol Cell Biol* 1987;7(2):725-37.

(494) Alton NK, Vapnek D. Nucleotide sequence analysis of the chloramphenicol resistance transposon Tn9. *Nature* 1979;282(5741):864-9.

(495) Leslie AG, Moody PC, Shaw WV. Structure of chloramphenicol acetyltransferase at 1.75-A resolution. *Proc Natl Acad Sci U S A* 1988;85(12):4133-7.

(496) Thompson JF, Hayes LS, Lloyd DB. Modulation of firefly luciferase stability and impact on studies of gene regulation. *Gene* 1991;103(2):171-7.

(497) Seed B, Sheen JY. A simple phase-extraction assay for chloramphenicol acyltransferase activity. *Gene* 1988;67(2):271-7.

(498) Schenborn E, Groskreutz D. Reporter gene vectors and assays. *Mol Biotechnol* 1999;13(1):29-44.

(499) Groskreutz D, Schenborn ET. Reporter systems. *Methods Mol Biol* 1997;63:11-30.

(500) Henikoff S. Unidirectional digestion with exonuclease III creates targeted breakpoints for DNA sequencing. *Gene* 1984;28(3):351-9.

(501) Sanger F, Nicklen S, Coulson AR. DNA sequencing with chain-terminating inhibitors. *Proc Natl Acad Sci U S A* 1977;74(12):5463-7.

(502) Tabor S, Richardson CC. DNA sequence analysis with a modified bacteriophage T7 DNA polymerase. *Proc Natl Acad Sci U S A* 1987;84(14):4767-71.

(503) Fallowfield JA, Mizuno M, Kendall TJ *et al*. Scar-associated macrophages are a major source of hepatic matrix metalloproteinase-13 and facilitate the resolution of murine hepatic fibrosis. *J Immunol* 2007;178(8):5288-95.

(504) Hu YB, Li DG, Lu HM. Modified synthetic siRNA targeting tissue inhibitor of metalloproteinase-2 inhibits hepatic fibrogenesis in rats. *J Gene Med* 2007;9(3):217-29.

(505) Zhou X, Hovell CJ, Pawley S *et al*. Expression of matrix metalloproteinase-2 and -14 persists during early resolution of experimental liver fibrosis and might contribute to fibrolysis. *Liver Int* 2004;24(5):492-501.

(506) Medina J, Arroyo AG, Sanchez-Madrid F *et al*. Angiogenesis in chronic inflammatory liver disease. *Hepatology* 2004;39(5):1185-95.

(507) Pugh CW, Ratcliffe PJ. Regulation of angiogenesis by hypoxia: role of the HIF system. *Nat Med* 2003;9(6):677-84.

(508) Lau KW, Tian YM, Raval RR *et al*. Target gene selectivity of hypoxia-inducible factor-alpha in renal cancer cells is conveyed by post-DNA-binding mechanisms. *Br J Cancer* 2007;96(8):1284-92.

(509) Novo E, Cannito S, Zamara E *et al*. Proangiogenic Cytokines as Hypoxia-Dependent Factors Stimulating Migration of Human Hepatic Stellate Cells. *Am J Pathol* 2007.

(510) Janczewska-Kazek E, Marek B, Pisula A *et al*. [Serum levels of vascular endothelial growth factor in chronic hepatitis C patients treated with interferon alpha and ribavirin]. *Wiad Lek* 2007;60(3-4):120-3.

(511) Norman JT, Fine LG. Intrarenal oxygenation in chronic renal failure. *Clin Exp Pharmacol Physiol* 2006;33(10):989-96.

(512) Orphanides C, Fine LG, Norman JT. Hypoxia stimulates proximal tubular cell matrix production via a TGF-beta1-independent mechanism. *Kidney Int* 1997;52(3):637-47.

(513) Norman JT, Clark IM, Garcia PL. Hypoxia promotes fibrogenesis in human renal fibroblasts. *Kidney Int* 2000;58(6):2351-66.

(514) Masamune A, Kikuta K, Watanabe T *et al*. Hypoxia stimulates pancreatic stellate cells to induce fibrosis and angiogenesis in pancreatic cancer. *Am J Physiol Gastrointest Liver Physiol* 2008.

(515) Vincenti MP, Clark IM, Brinckerhoff CE. Using inhibitors of metalloproteinases to treat arthritis. Easier said than done? *Arthritis Rheum* 1994;37(8):1115-26.

(516) Campbell CE, Flenniken AM, Skup D *et al*. Identification of a serum- and phorbol-ester responsive element in the murine tissue inhibitor of metalloproteinase gene. *J Biol Chem* 1991;266:7199-206.

(517) Clark IM, Rowan AD, Edwards DR *et al*. Transcriptional activity of the human tissue inhibitor of metalloproteinases 1 (TIMP-1) gene in fibroblasts involves elements in the promoter, exon 1 and intron 1. *Biochem J* 1997;324 (Pt 2):611-7.

(518) Hammani K, Blakis A, Morsette D *et al*. Structure and characterization of the human tissue inhibitor of metalloproteinases-2 gene. *J Biol Chem* 1996;271:25498-505.

(519) Declerck YA, Darville MI, Eeckhout Y *et al*. Characterization of the Promoter of the Gene Encoding Human Tissue Inhibitor of Metalloproteinases-2 (TIMP-2). *Gene* 1994;139:185-91.

(520) Hasegawa-Baba Y, Doi K. Changes in TIMP-1 and -2 expression in the early stage of porcine serum-induced liver fibrosis in rats. *Exp Toxicol Pathol* 2010.